School of Pharmacy and Biomedical Sciences

Protein phosphorylation and glycosylation of the ER Translocation Machinery in *Saccharomyces cerevisiae* are differentially regulated in response to ER stress.

Kofi Lewis Paul Stevens

This thesis is presented for the Degree of

Doctor of Philosophy – Biomedical Science

of

Curtin University

November 2019

Declaration

To the best of my knowledge and belief this thesis contains no material previously published by any other person except where due acknowledgment has been made. This thesis contains no material which has been accepted for the award of any other degree or diploma in any university.

Signature: [redacted]

Date: 29/11/2019.....

Abstract

Protein translocation into the endoplasmic reticulum (ER) is a process conserved among all Eukaryotes. Approximately one third of all proteins are translocated into the ER, thus making it a robust site of protein synthesis, folding and modification. As such, multiple signal inputs are required to maintain the ER in a competent state, requiring the coordination of a variety of protein complexes and activities. If disequilibrium occurs in the ER, it can lead to widespread cellular effects, ultimately leading to cell death. It is for this reason that many ER dysfunctions are responsible for exacerbated progression of cancers, and a central to the pathology of many neuropathies. Because of this, a greater understanding of the complex nature of the ER and how it is regulated is required. For this, the yeast Saccharomyces cerevisiae is a formidable tool in which to conduct these investigations having been used as a model organism to study in high detail the exact nature of how cells work. While distantly related to humans, the core machinery and processes are conserved throughout all eukaryotes. For these reasons, I have utilised this system to better understand the role of various stressors on ER function.

This study is focused on understanding the function of two proteins whose activities are intimately linked, Sec63 and Sil1. The first, Sec63, is a major component of the ER translocation machinery, involved in the translocation of nascent polypeptides into the lumen of the ER, while also coordinating the activity of the major ER Hsp70 protein Kar2 (BiP in Mammalia). The Second, Sil1, also regulates Kar2, whereby it functions as a nucleotide exchange factor (NEF) that modulates its ATPase activity in response to changes in the ER environment.

My initial investigations focused on the essential Sec63, which sits at the centre of the ER translocon, coordinating both co and posttranslational translocation. Its essential role in regulating multiple aspects of ER activity provided the rationale for my primary hypothesis; is Sec63, and in extension the ER regulated

through TOR dependent phosphorylation? As TOR (Target of Rapamycin) is the major signalling nexus controlling anabolic processes, and with the ER being a highly anabolic organelle, it is an attractive proposal. For this, I utilised mass spectrometry for the identification of phosphorylation sites, which then informed site directed mutagenesis and genetic manipulation of various strains of yeast. I also utilised well characterised translocation substrates to determine if mutation of Sec63 had any major effect on the translocation machinery, through the monitoring of proteins by western blot. My investigations were able to confirm Sec63 is phosphorylated in a TOR dependent manner, yet the implications this phosphorylation event has on Sec63 function is less clear. However we have identified a region of Sec63 located proximately to a TOR sensitive phosphorylation site that is important for functionality.

During this initial investigation I noted several anomalies in the maturation of the Sil1 NEF, a non-essential glycosylated resident ER protein. This observation led us to investigate the nature of these phenotypes. This investigation exemplifies the power of model systems like *Saccharomyces cerevisiae.* As the nature of these observations alone were difficult to reason, a combination of gene knock out strains, and genetically modified vector systems were utilised to accurately identify the pathways that were perturbed under redox conditions. Again, western blotting was an invaluable tool, as were protease protection and cyclohexamide chase assays in characterising protein landscape of the ER. With this, I demonstrated that N-glycosylation of Sil1 is regulated in a REDOX dependent manner to better control Kar2 and protein folding during ER stress. Specifically the accumulation of unglycosylated Sil1 (uSIl) is beneficial in reductive stress. Conversely, accumulation of uSil1 in oxidative conditions is extremely deleterious resulting in loss of viability. Additionally, I found several conserved elements of Sil1, previously identified to possess thioredoxin activity, that also coordinate Sil1 degradation, with Sil1 degradation occurring in a non-conventional manner. This is the further regulation of SIl1, and likely used to control its accumulation following the changes to the redox environment of the ER.

Together this work highlights the complex nature in which multiple aspects of ER activity are regulated, and further exemplifies the power of yeast cell biology in being able to decipher these exquisite protein regulation pathways. This study provides the groundwork for future investigations into the TOR dependent regulation of the ER translocon, a subject which I believe will have greater relevance and importance than can be demonstrated in a single study. Finally, we have identified a novel mode of protein activity regulation through the coordination of ER glycosylation dynamics, and the ER associated degradation network. Together these systems modulate the activity of Sil1 (and likely many more proteins) in response to the redox status of the ER. These findings may prove instrumental in understanding the role of Sil1 in the context of disease, with Sil1 associated with many pathologies in humans, and ER folding dynamics and fundamentally important process yet to be fully characterised.

Acknowledgements

Firstly, I would like to acknowledge Curtin University, The School of Pharmacy and Biomedical Sciences, and CHIRI for providing me with the funding, facilities and opportunity to pursue this research. Additionally, I wish to pay respect to the Aboriginal and Torres Strait Islander members of our community by acknowledging the traditional owners of the land on which the Bentley Campus is located, the Wadjuk people of the Nyungar Nation.

Over the course of my PhD I have been privileged to meet and form relationships with a diverse group of people, which I am truly thankful of, as I believe this to be the most enriching, and rewarding experience I had during this time. While impossible to name everyone who has influenced me during my time here, I would like to pay a special mention to the following people.

To Mailys Vergnolle, I both thank and blame you for my now, impossible love of all things small, complex, and yeasty, and thank you for starting me off on this journey, you taught me more than science.

In a similar vein, I would like to thank Carl Mousley, whom is responsible for developing my skills, and shaping me into the scientist I hope to one day be. His wealth of knowledge, passion and scientific integrity encapsulate everything I aspire to maintain.

To Rob Steuart, I wish to thank you for being a constant companion and mentor since my first days at Curtin, and for all things fermented and fun.

To Adrian Paxman, Elizabeth Watkin, and David Townsend, I am thankful to have had such great lecturers and people to guide me through the early years and beyond.

I could not have completed this work without the support and friendship of the fantastic group of people in my lab group, past and present, particularly Chris Witham for all his assistance in the lab.

To Jordan Rowlands, his support and ever constant presence during the long nights, kept me sane and helped push me to the finish line.

As for Joshua Ravensface, I'd love to say it was your role as assistant homebrewer that I'm most thankful for, but in truth it was your encouragement and belief in me, your friendship and of course, our numerous tavern debates.

I'd like to pay a special mention to my favourite caffeination station, Higher Grounds, for all the fantastic coffee and for all the lovely faces/beaks ever happy to chat.

As for my Cellarbrations Carlisle family, for all the beers over the years, for keeping me afloat, and being so understanding, thank you.

To Bev, Pippo, Michelle, Steven, and the entire Randazzo clan, thank you for making me a part of your family, bringing me in on the traditions and teaching me about the simplest pleasures in life.

To my parents, thank you for affording me the many opportunities I've had, particularly the life I have in this amazing place, for instilling in me the importance of education, and loving me no matter what.

And for everyone, family and friend, who has helped me over the last 7 years, no matter how small, thank you, I could not have reached this point without it.

Finally, to my best friend, and life companion, Dr Samantha Randazzo,
I dedicate this thesis to you.

Ever by my side, you have supported me, loved and cared for me, endured the lonely nights and believed in me since the beginning. I cannot begin to thank you enough, but I have the rest of my lives to try.

Here's to the rest of our life, I cannot wait for it to truly commence.

Attributions

During the course of this research, the majority of the work presented in chapters 4 and 5 was prepared into a manuscript, submitted and accepted by the Proceedings for the National Academy of Sciences (Appendix 1)

Reference: Stevens, K. L. P., et al. (2017). "Diminished Ost3-dependent N-glycosylation of the BiP nucleotide exchange factor Sil1 is an adaptive response to reductive ER stress." Proceedings of the National Academy of Sciences **114**(47): 12489-12494.

Several co-authors were included within this study, and below is the information regarding their contributions.

Kofi L. P. Stevens – 50%
Conducted and critically analysed all experiments, co-wrote manuscript.
Amy L. Black – 4%
Technical assistance of experiments, proofing final document.
Kelsi M. Wells – 4%
Technical assistance of experiments, proofing final document.
K. Y. Benjamin Yeo – 4%
Generated vectors used in study.
Robert F. L. Steuart – 6%
Supervisor, helped the design and critical analysis of experiments, proofing final document.
Colin J. Stirling – 2%
Involved in the early genesis of the work, and the generation of many in house reagents.
Benjamin L. Schulz – 5%
Provided expertise in the field, critical analysis, proofing final document.
Carl J. Mousley – 25%
Primary supervisor, co-designed, conducted and critically analysed all experiments, co-wrote manuscript.

Approved by Carl Mousley

Table of contents

Table of Figures.

Table of Tables.

Abbreviations

AA: Amino acid

BME: 2-mercaptoethanol

CHX: Cyclohexamide

DNA: Deoxyribonucleic acid

DTT: Dithiothreitol

MM: Minimal media (yeast nitrogen base)

nt: Nucleotide

OD: Optical density (often OD_{600} -600nm)

ORF: Open reading frame

PCR: Polymerase chain reaction

PTM: Post-translational modification

RNA: Ribonucleic acid

SDM: Site directed mutagenesis

SEC: Secretory

Tm: Tunicamycin

TOR: Target of Rapamycin

YNB: Yeast nitrogen base

YP: Yeast extract Peptone (rich growth media)

Introduction

1.1. The Endoplasmic Reticulum and Secretory Pathway

A fundamental feature of eukaryotic cells is the compartmentalisation of specific activities into lipid bilayer encased compartments known as organelles, each enriched with a specific subset of proteins, lipids and small molecules. The endoplasmic reticulum (ER) is a highly organised network of interconnected ribbon like structures surrounding the nuclear envelope that extend throughout the cytosol and is the entry point to the secretory pathway. While protein secretion is the central function of the ER, it is also a major site of lipid biogenesis and modification, synthesising the bulk mass of membranes lipids and precursors to many specialised lipids, and is thus responsible for driving cellular and organellular growth. Dysfunction in any of these activities can therefore have severe consequences on the cell, ultimately leading to cell death. As such the environment within this organelle is highly regulated to ensure the efficient folding and post-translational modification of the newly synthesised proteins. Following maturation, secretory proteins are targeted to their appropriate locations within the secretory pathway, first traversing the Golgi before being secreted, delivered to the cell surface, or sorted to the endosomes/lysosomes. With approximately one third of the proteome being targeted to the secretory pathway the ER represents a major site of protein synthesis. As the ER membrane is impermeable, preventing the free flow of cytosolic components into the lumen, the translocation of proteins across this lipid bilayer requires specialised machinery. The recognition and efficient targeting of substrates to this machinery therefore designates the first step in the secretory pathway.

1.2. Signal Sequence

Substrates destined for the secretory pathway contain short degenerative N-terminal signal sequences (Blobel and Dobberstein 1975; Milstein et al. 1972; Ng, Brown and Walter 1996; von Heijne 1985). Structurally signal sequences tripartite and contain a hydrophobic core that is flanked by a positively charged N-terminal region and a polar C-terminal region (Figure 1.1) (von Heijne 1985). Signal sequence length varies, with an average length of 15-30 amino acids (AA), however they can be as large as 50 AA. The signal sequence is used both to identify substrates and direct them to one of two main translocation pathways (detailed in sections 1.3 and 1.4). Signal sequences containing larger and more hydrophobic cores are recognised during translation and are targeted to the ER by the signal recognition particle (SRP). Signal sequences containing weaker hydrophobic cores are not initially recognised, with translocation occurring posttranslationally (Sec62-dependent translocation). While N-terminal hydrophobicity initially identifies translocation substrates, N-terminal processing of methionine is a key determinant for translocation competency. Bioinformatic analysis of 277 open reading frames (ORFs) from *Saccharomyces cerevisiae* identified 72% of cytosolic proteins to be substrates for N-terminal methionine cleavage, in contrast only 23% of proteins containing signal sequences are predicted to be processed (Forte, Pool and Stirling 2011). Interestingly, N-terminal acetylation was found to block the translocation of secretory precursor proteins (Forte, Pool and Stirling 2011). This is of particular importance in distinguishing posttranslational substrates from cytosolic proteins, with greater than 99% of signal sequences predicted to not be acetylated or be sufficiently hydrophobic to be co-translationally targeted. Thus, N-acetylation status is an early determinant in the sorting of nascent polypeptides.

As previously stated, there exist two main translocation pathways, the SRP-dependent (Co-translational translocation) and Sec62-dependent (Posttranslational translocation) translocation. While the targeting methods are mechanistically distinct, both pathways converge on the heterotrimeric Sec61 translocon, which

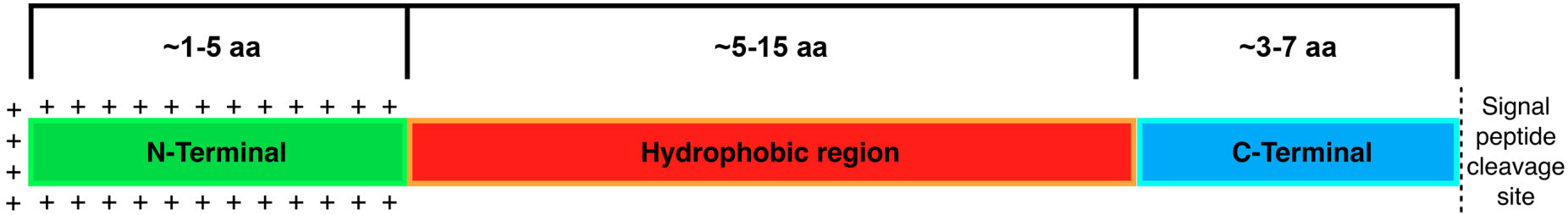

Figure 1.1 General structure of the signal peptide.

Signal sequences typically possess a short N-terminal domain, followed by a glycine rich hydrophobic core, followed by a polar region that contains the site of cleavage for the signal peptidase. The average length of each domain is shown here, with larger and more hydrophobic cores directing peptides for SRP-dependent translocation.

forms a protein conducting channel that allows for the transport of polypeptides across the lipid bilayer.

1.3. SRP-dependent pathway

Of the two pathways, the SRP-dependent is the better studied, likely due to it being the dominant mode of polypeptide targeting to the ER, particularly for higher eukaryotes. The SRP-dependent pathway is often referred to as cotranslational translocation, as recognition, targeting and transport across the ER membrane, as the name suggests, occur during protein synthesis (Figure 1.2). Facilitating this process is a ribonucleoprotein complex termed SRP, which is responsible for the identification of secretory proteins that possess a signal sequence of sufficient hydrophobicity (Kurzchalia et al. 1986). The ability of SRP to identify preproteins for export is an evolutionarily conserved process identified in all domains of life, however an increased structural complexity is observed in higher eukaryotes (Poritz et al. 1990; Pool 2005; Althoff, Selinger and Wise 1994). At the core of mammalian SRP is an approximately 300 nucleotide (nt) RNA molecule, termed 7S which has a forked appearance. Bound to the 7S are six protein subunits; SRP9, 14, 19, 54, 68, and 72, named in respect to their masses in kDa (Gundelfinger et al. 1983). Structurally SRP can be divided into two domains: the Alu and S-domains (Gundelfinger et al. 1983). In contrast, bacterial SRP such as the *Escherichia coli* SRP complex consists simply of a 4.5S RNA and the SRP54 homologue Ffh (Fifty four homologue), lacking the Alu-domain completely (Poritz et al. 1990).

1.3.1. S- and Alu-domains

It is evident that evolution has led to an increasingly complex SRP, with the functional orthologues of 7S and SRP54 found in all forms of self-replicative life (Pool 2005). SPR54 functions to recognise and bind to the signal sequence of nascent polypeptides once they emerge from the exit tunnel of a translating ribosome (Kurzchalia et al. 1986; Siegel and Walter 1988b). Structurally, SRP54 is

divided into two domains; the NG domain that displays Ras-like GTPase activity, and the M-domain which is responsible for binding the protein to the helix-8 region of the 7S RNA (Freymann et al. 1997; Zheng and Gierasch 1997). Within the M-domain is a hydrophobic groove rich in methionine residues that accommodates a wide variety of hydrophobic signal sequences and hence responsible for the recognition of substrates suitable for export (High and Dobberstein 1991; Keenan et al. 1998; Zopf et al. 1990). Connecting the S-domain to the Alu-domain is the SRP68/72 heterodimer (Halic et al. 2004; Siegel and Walter 1988a). Removing both SRP68/72 from the SRP molecule inactivates the translocation and elongation arrest activities of SRP (Siegel and Walter 1985).

The remaining section of the 7S RNA and the SRP 9/14 heterodimer form the Alu-domain of SRP. Selective biochemical inactivation of the protein subunits of SRP identified the Alu-domain coordinates SRPs elongation arrest activity(Siegel and Walter 1988b). It was determined through cryo-electron microscopy (cryo-EM) that the Alu-domain interacts with several conserved regions of the ribosome. Specifically, these regions are the binding site for eEF-2 (eukaryotic elongation factor 2) which co-ordinates the shuttling of tRNAs from the A and P sites, thus allowing the subsequent tRNA to be loaded (Zhou et al. 2014). Therefore the competitive binding of this site by the Alu domain severely reduces the translation efficiency (Halic et al. 2004). The main function of SRP is the binding of signal sequences and the subsequent targeting of the ribosome to the ER associated translocon. This function is dependent on the retardation of chain elongation, which provides the translating ribosome sufficient time to bind to the ER (Walter and Blobel 1981). Taken together this demonstrates that the essential role of SRP is to co-ordinate the recognition and binding of the signal peptide with a temporal retardation of translation so as to allow for interaction of the ribosome with the ER membrane, thus ensuring efficient translocation.

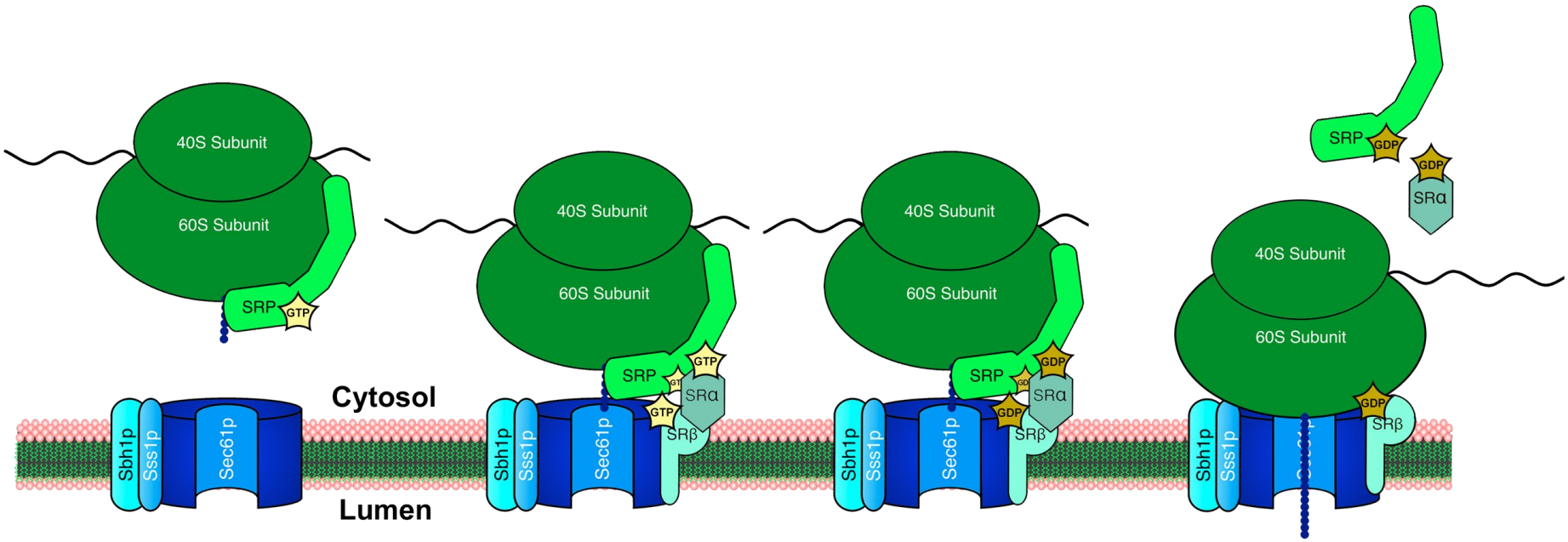

Figure 1.2 SRP-dependent translocation machinery.

As the name implies, SRP-dependent translocation requires the SRP molecule to direct the nascent polypeptide to the translocon, whereby translation generates the driving force for translocation. When GTP bound, SRP efficiently binds the ribosome, inhibiting chain elongation. Also GTP bound, SRα brings the ribosome to the translocon as it interacts with its membrane spanning partner SRβ. Coordinated GTP hydrolysis initiates the dissociation of the SRP-SR-ribosome complex, allowing chain elongation and translocation to proceed.

1.3.2. SRP-SR interaction

In eukaryotes, once the nascent polypeptide has been recognised by SRP, the ribosome is directed to the ER membrane through the association with its cognate receptor. The SRP receptor (SR) is composed of two subunits, SRα and SRβ (Lauffer et al. 1985). SRα is a GTPase similar in structure to SRP54's NG domain (Miller et al. 1993; Connolly, Rapiejko and Gilmore 1991; Connolly and Gilmore 1989). The second subunit, SRβ contains a single transmembrane domain, allowing it to both interact with the major ER ribosome receptor (Sec61) and recruit SRα to the ER membrane (Lauffer et al. 1985). SRα is then able to bind to SRP54s NG domain in a GTP dependent manner, thus tethering the ribosome to the ER allowing for its interaction with Sec61. The initial association with the Sec61 complex promotes GTP hydrolysis by SRP54 and SRα (Song et al. 2000). This is followed by the dismantling of the SRP/SR/Ribosome complex, allowing for elongation of the peptide to continue directly into the ER lumen. The prokaryotic SR is a single protein, FtsY, which displays GTPase activity like its eukaryotic counterpart (Luirink et al. 1994). Whilst the prokaryotic SRP and SR are more simplistic, the conserved nature of protein translocation is exemplified by Ffh and FtsY. *In vitro*, they are able to replace both SRP and SR and successfully translocate secretory peptides to mammalian microsomal membranes even though they lack the elongation arrest activity (Powers and Walter 1997).

1.4. Sec62-dependent translocation pathway

Secretory proteins lacking sufficiently hydrophobic signal sequences or those which complete translation prior to emerging from the ribosomal exit tunnel are directed for post-translational translocation. During protein synthesis the nascent polypeptide chain is bound by several molecular chaperones that prevent folding, and maintain the pre-protein in a translocation competent state (Plath and Rapoport 2000). Two of the involved chaperones, Ssa1 and Ssa2, belong to the

HSP70 (Heat Shock Protein) family, a property of this group of proteins is their affinity for ATP and its subsequent hydrolysis. The Hsp70 family of proteins undergo multiple cycles of protein binding and release through the coordinated hydrolysis of ATP. Hydrolysis of ATP is stimulated by J-domain proteins, and elicits a conformational change in the Hsp70 protein, allowing for the binding of misfolded/unfolded proteins. The release of ADP and reloading of ATP by Nucleotide exchange factors triggers the release of the bound peptide, and reprimes the Hsp70, allowing the cycle to repeat. The two molecular chaperones Ssa1 and Ssa2 share 98% identity and are both involved in the binding and subsequent transport of the nascent chain complex to the ER (Deshaies et al. 1988). The J-domain protein Ydj1p activates the ATPase activity of the chaperones, causing a conformational change in their structure that enables Ssa1 and Ssa2 to bind to the polypeptide chain (Chirico, Waters and Blobel 1988; Deshaies et al. 1988). The localisation of Ydj1p directs post-translational precursors to the translocon, with this activity potentially coordinated through farnesylation, which is the posttranslational addition of lipid soluble farnesyl-groups (Caplan, Cyr and Douglas 1992). The attachment of the 15-carbon farnesol to the protein is thought to drive the interaction and stable association of Ydj1p with the ER membrane, and the Sec62 complex (Caplan et al. 1992).

Following recruitment to the ER membrane, these secretory proteins are directed to the *SEC61* complex (see below) for transport into the ER lumen. The chaperone-nascent chain complex is presented to Sec61 by the Sec63 complex. The Sec63 complex is formed by two essential genes *SEC62* and *SEC63*, and two non-essential genes *SEC71* and *SEC72* (Brodsky and Schekman 1993; Deshaies et al. 1991; Feldheim and Schekman 1994). The recognition and binding of signal sequences is conducted in most part by Sec62, with Sec72 assisting the process through its interaction with Ssa1, thus recruiting the chaperone/nascent polypeptide complex (Feldheim and Schekman 1994; Wittke, Dünnwald and Johnsson 2000) (Figure 1.3). The complex is stabilised by the Sec63 protein which is bound to Sec61, 62 and 71 (Deshaies et al. 1991). Spanning the ER membrane three times Sec63 has two domains of importance. The C-terminal cytoplasmic domain,

which interacts with Sec62, and a luminal domain that is homologous to DnaJ (A HSP40 protein) of *E.coli* and is required to activate the ATPase activity of Kar2 (BiP in mammalian cells) (Sadler et al. 1989). Recently, the entire heptatrimeric complex was purified and visualised via cryo-EM, elucidating the nature of this complex (Wu, Cabanos and Rapoport 2019). It was confirmed that Sec63 is pivotal in anchoring the complex to the Sec61 translocon. Additionally, Sec63 was found to be partially responsible for opening the lateral gate of the translocon, while part of Sec63s C-terminal domain was found to prevent ribosome binding, thus priming the translocon for posttranslational translocation (Wu, Cabanos and Rapoport 2019). Whereas SRP-dependent substrates are translocated utilizing the force provided through chain elongation, posttranslational precursors require an alternative mechanism. Thusly it has been modelled that Brownian motion is the driving force for post-translational translocation. Here, following looped insertion of the nascent chain into the translocation channel, Kar2 binds exposed hydrophobic patches as they enter the lumen, thus preventing any backwards movement (Matlack et al. 1999b; Elston 2002). The process repeats until the entire protein passes into the ER lumen.

In mammalian cells, only small subsets of proteins have been identified that can be translocated into the ER through the SRP-independent system (Lakkaraju et al. 2012). However, in yeast the majority of proteins pass through in a Sec62-dependent manner, with a particular few specific for co-translational translocation (Brodsky and Schekman 1993; Panzner et al. 1995; Young et al. 2001; Ng, Brown and Walter 1996). While *SEC63* and *SEC62* are conserved in higher eukaryotes, to date no known gene orthologous of *SEC71* and *SEC72* have been identified in Mammalia. Furthermore, while conserved, there are several differences in the function of Sec62 and Sec63 between yeast and mammals. Sec62 of higher eukaryotes has been found to interact with the ribosome, thus further stabilising the predominant SRP-dependent translocation pathway (Müller et al. 2010). Additionally, mammalian Sec62 possesses a calcium (Ca^{2+}) binding motif, which has been shown to regulate Ca^{2+} leakage through the Sec61 translocon. The importance of this activity in mammalian Sec62 is further highlighted whereby, dysregulation of

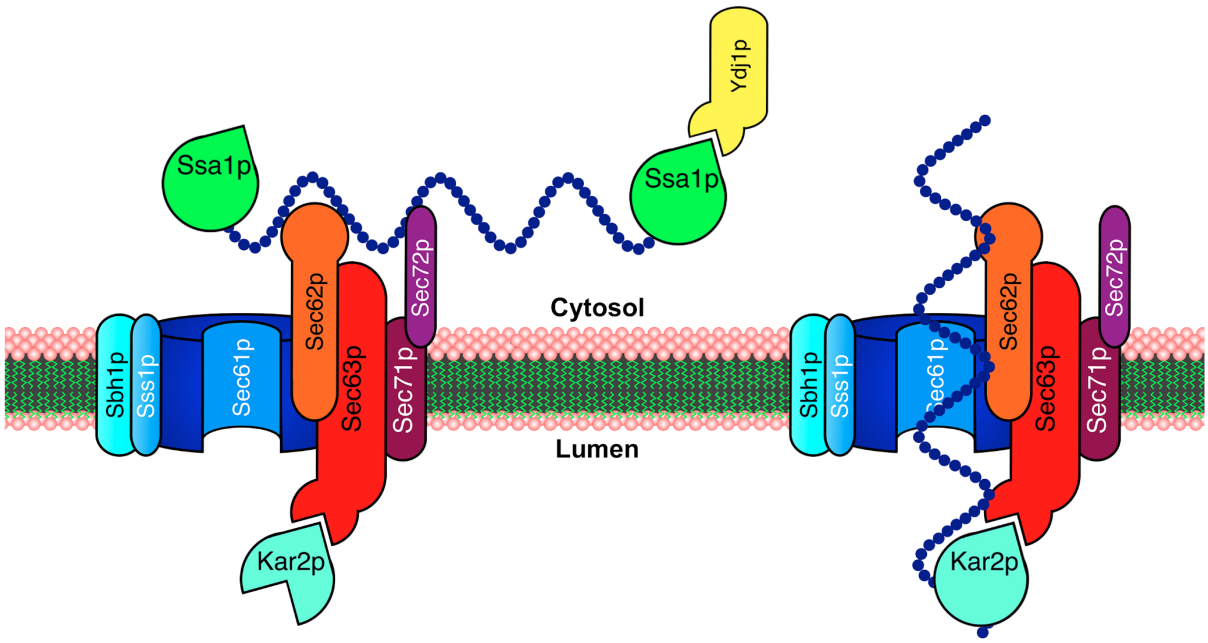

Figure 1.3 Sec62-dependent translocation machinery.

SRP-independent translocation occurs following the complete translation of the polypeptide. During translation, the precursor is recognised as a target, and the cytosolic molecular chaperones Ssa1 and Ssa2 bind, and prevent the premature folding of the peptide. Binding requires stimulation by the HSP40, Ydj1, which is also believed to direct the peptide to the translocon. The polypeptide interacts with the SRP-independent apparatus consisting Sec62, Sec63, Sec71, and Sec72, and unlike SRP-dependent translocation, requires an alternative force to drive the peptide across the membrane. It is proposed that the peptide traverses the translocon via Brownian motion, assisted by rounds of Kar2 binding and release, which also prevent its backflow.

Ca^{2+} homeostasis, through the accumulation of Sec62, can be detrimental to the prognosis, of certain cancers (Linxweiler et al. 2013). While Sec63 of mammalian cells performs a similar role to that of yeast, the additional factor Erj1 (ER J-domain protein 1), has also been found to interact with the ribosome, and recruit BiP to the translocon in a similar manner (Dudek et al. 2002).

1.5. Translocon

SRP- and Sec62-dependent translocation proceeds via a common protein conducting channel termed the translocon or the *SEC61* complex. The translocon is a heterotrimeric complex, which in *S. cerevisiae* is comprised of Sec61, Sbh1, and Sss1 (Sec61α, Sec61β, and Sec61γ in mammals) (Deshaies and Schekman 1987; Esnault et al. 1994; Finke et al. 1996a; Stirling et al. 1992). Sec61 is the largest of the three proteins, spanning the ER membrane 10 times with both the N and C-termini located in the cytosol, along with Sbh1 and Sss1 which are small C-terminally anchored proteins (Akiyama and Ito 1987; Deshaies and Schekman 1987; Stirling et al. 1992). In yeast, the Sec61 and Sss1 subunits are essential for their viability (Osborne, Rapoport and van den Berg 2005). The *SEC61* complex forms a channel that allows proteins to be translocated through the ER membrane, with Sec61 identified via photo-crosslinking experiments to be the main pore-forming component of the complex (Mothes, Prehn and Rapoport 1994). Additional to the main Sec61 complex, a secondary complex exists in eukaryotes. In yeast, the central component of this complex is Ssh1 (Sec Sixty one Homologue), with Sbh2 and once again Sss1 representing the β and γ subunits respectively (Finke et al. 1996b). This secondary complex is involved in protein translocation, however little else has been established regarding its function (Jan, Williams and Weissman 2014; Wilkinson, Tyson and Stirling 2001).

Our understanding of translocon activity has been driven primarily by structural information from the homologous archaeal and bacterial SecY complexes (Berg et al. 2004; Zimmer, Nam and Rapoport 2008). From these, it has been determined that Sec61 is split into two halves, from TM domains 1-5 and 6-10, with

a loop connecting the halves acting as a hinge. This hinge allows for the opening of the translocon, with the opening termed the lateral gate, being required for the insertion of TM-domains into the lipid bilayer of the ER. The small subunit Sss1 has been shown to clamp both halves of the translocon together, thus regulating the opening of the lateral gate, with interactions between Sec61 and a channel partner (Sec62 complex/ribosome) triggering this conformational change. The shape of the translocon resembles an hourglass, with the central constriction forming a pore ring comprised of 6 hydrophobic residues with inwardly pointing sidechains. The aqueous channel of the translocon allows for the transport of proteins into the ER lumen, but also provides a channel in which small soluble molecules such as Ca^{2+} and glutathione are able to passively diffuse (Heritage and Wonderlin 2001; Lang et al. 2011). As such, the translocon is appropriately gated, primarily by TM2a forming a plug, and Kar2 (BiP in mammalia) forming a luminal seal (Berg et al. 2004; Hamman, Hendershot and Johnson 1998; Zimmer, Nam and Rapoport 2008).

1.6. Sec63

Sec63 contains three transmembrane domains, with the functional domains located in both the cytosol and the lumen of the ER. The luminal J-domain has been demonstrated to be important in both SRP-dependent and Sec62-dependent translocation. Sec63 as a J-Domain protein, stimulates Kar2 ATP hydrolysis providing the driving force for Sec62-dependent translocation. Additionally, Sec63 dependant regulation of Kar2 activity is required for Kar2s stable interaction with the luminal face of the translocon, both for gating, and the opening of the pore (Matlack et al. 1999b; Willer et al. 2003; Wittke, Dünnwald and Johnsson 2000; Young et al. 2001).

The cytoplasmic domain of Sec63 contains two functionally important domains. The first, which comprises the majority of the C-terminus, is known as a Sec63/Brl domain located N-terminally of the acidic domain (Ponting 2000). Aside from Sec63 (from which the domain was identified), this domain is commonly found in RNA helicase proteins such as Brr2. Functionally, Brr2 is required for the stable assembly of the pre-mRNA spliceosome complex, and possesses RNA-

helicase activity (Absmeier, Santos and Wahl 2016). Deletion of 61 residues within the Sec63/Brl-domain of Sec63 leads to severe translocation defects in both SRP-dependent and Sec62-dependent translocation (Jermy et al. 2006). Mechanistically this is due to an inability to form both the SEC (Sec61, Sbh1, Sss1, Sec62, Sec63, Sec71 and Sec72) and the SEC' (as with SEC excluding Sec62) complexes (Jermy et al. 2006). The loss of functional translocon assembly observed in the truncated Sec63 is consistent with the role Brr2 plays in the co-ordination of the spliceosome complex (van Nues and Beggs 2001). Furthermore, the Sec63/Brl-domain of Brr2 interacts with specific snRNA's, this ability to bind RNA may indicate the potential for Sec63-ribosome associations critical for translocation.

The extreme C-terminus of Sec63 is also required for the assembly of the heptatrimeric SEC complex. In yeast, the final 52 residues of Sec63 are predominantly acidic, with the last 14 residues identified to specifically interact with Sec62 (Wittke, Dünnwald and Johnsson 2000). It was further determined that residues T652 and T654 are constitutively phosphorylated by the CK2 protein kinase, and phosphorylation increases the stable association of Sec62 with Sec63 (Wang and Johnsson 2005). Phosphorylation of Sec63 by CK2 is also required for the stable association of Sec63 and Sec62 in humans (Ampofo et al. 2013).

Regarding mammalian Sec63, the importance of this protein is exemplified by the numerous pathologies associated with its disruption/mutation. Mutations in Sec63 are observed as a driver of autosomal polycystic liver disease (Davila et al. 2004). Furthermore, mutations in Sec63 are observed in over 40% of gastric, colorectal, and small bowel cancers (Linxweiler, Schick and Zimmermann 2017). While in Zebrafish, mutations in Sec63 have been shown to result in defective axon myelination, and liver abnormalities, primarily due to ER stress (Monk et al. 2013).

1.7. Kar2 (BiP)

The ER is a major site of protein biogenesis and consequently protein folding. Following translocation, substrates engage various post-translational modifications (PTMs) including the addition of N-glycans and the formation of both intra and intermolecular disulfide bonds, which contribute to their folding and

maturation. The folding and modification of newly synthesised proteins are coordinated by molecular chaperones. In the ER this is predominantly performed by the resident Hsp70, Kar2 (BiP). This process of maturation is monitored by the ER quality control (ERQC) apparatus in order to prevent the accumulation of misfolded protein and maintain the specific environmental conditions of the ER. Kar2 plays an essential role in the maintenance of ER homeostasis through the regulation of translocation, protein folding, activation of the unfolded protein response (UPR), and gating of the translocon preventing the free flow of solutes.

Hsp70 chaperones are ubiquitous through all domains of life, with a high degree of evolutionary conservation (Gupta and Golding 1993). Structurally these proteins are divided into two main domains, the N-terminal nucleotide binding domain (NBD) and the C-terminal substrate binding domain (SBD), joined by a highly conserved linker. The NBD is further divided into four subdomains (IA, IB, IIA, and IIB), with the two lobes forming a deeply set hydrophilic pocket which accommodates ATP. The SBD is composed of two subdomains, SBDβ containing the hydrophobic pocket, and SBDα which forms the lid (Yang et al. 2015).

1.7.1. ATPase cycle and folding

Hsp70s interact with a wide variety of substrates including: unfolded protein intermediates, either during translation or translocation; and misfolded or aggregated polypeptides. While the range of substrates is diverse, the binding motif for Hsp70 substrates consists of a hydrophobic core ~5 amino acids in length, flanked by a region enriched in basic amino acids (Rüdiger et al. 1997). On average, this motif occurs in proteins every 36 amino acids, typically located in the hydrophobic cores of folded proteins. In the case of misfolded proteins, the normally buried hydrophobic motifs become accessible to interaction by Hsp70s, differentiating them from successfully folded proteins. The coordinated binding and

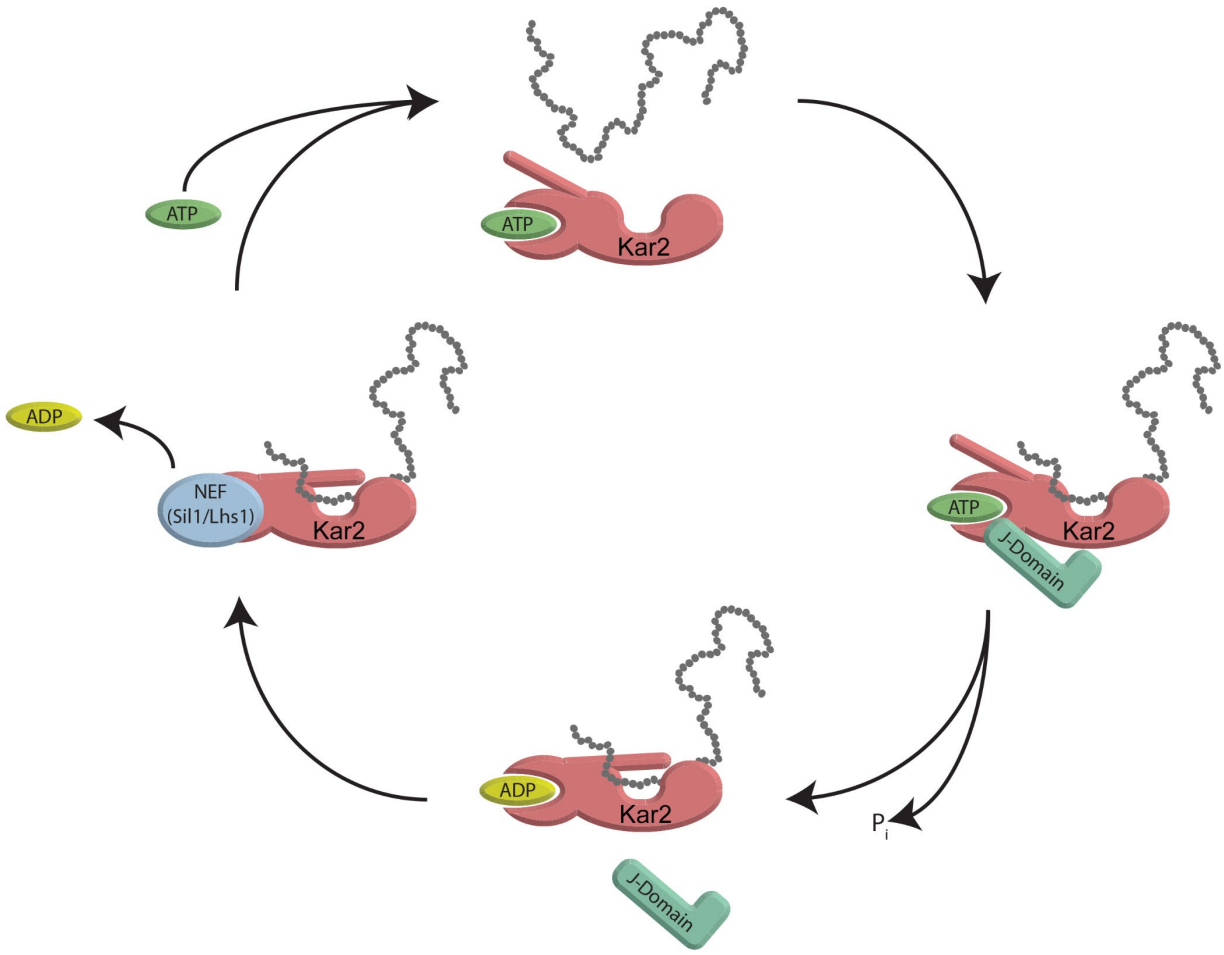

Figure 1.4 ATPase cycle of HSP70 chaperones.

Protein folding in the ER is co-ordinated by the HSP70 Kar2/BiP (Shown in red) in conjunction with J-domain proteins (Sec63) and Nucleotide Exchange Factors (Lhs1/Sil1). When ATP bound, Kar2s substrate binding domain (SBD) is open. Upon substrate binding, J-domain proteins stimulate ATP hydrolysis locking the SBD and securing the peptide. Opening of the SBD requires nucleotide exchange, co-ordinated by either Lhs1 or Sil1, release of ADP from the nucleotide binding domain (NBD) allows for ATP to be reloaded, and the cycle continues.

release of polypeptides by Hsp70s requires the assistance of two groups of co-chaperones, J-domain proteins (JDPs) which stimulate ATP hydrolysis, and nucleotide exchange factors (NEFs) which facilitate the release of ADP (Figure 1.4). Simplistically, once a peptide enters the SBD, ATP hydrolysis is stimulated via JDPs, resulting in a conformational change of SBD increasing the affinity for the bound peptide. To complete the cycle, NEFs facilitate the release of ADP from the NBD allowing the reloading of ATP and the subsequent release of the peptide from the SBD (Hartl and Hayer-Hartl 2002).

As such Hsp70s like Kar2 exist in two main conformational states. When ATP bound, the SBD is in the open state, with SBDα and SBDβ bound to different regions of the NBD(Yang et al. 2015). The intrinsic ATPase activity of Hsp70s is low, with approximately one molecule of ATP hydrolysed every 20-30 minutes. This results in high rates of association and disassociation between polypeptides and the SBD. Both substrate interaction and JDP binding are required to stimulate ATP hydrolysis, with the rate of hydrolysis increasing >1000 fold (Liberek et al. 1991; Alderson, Kim and Markley 2016). The interaction of JDPs stimulates hydrolysis through a conformational change in the NBD, which allosterically regulates the peptide binding affinity of the NBD. When in the closed state (ADP bound), the SBDα closes over the peptide located with the hydrophobic groove of SBDβ, increasing the affinity up to 400-fold (Mayer et al. 2000; Schmid et al. 1994). The final step in the cycle is the coordinated release of ADP by NEFs and reloading of ATP, which stimulates the release of the peptide, allowing the Hsp70 to reengage with substrate (Hartl and Hayer-Hartl 2002).

1.7.2. Nucleotide Exchange factors

There are two resident NEFs in the lumen of the ER representing two of the three families of NEFs; Lhs1/Grp170 (Hsp110 family) and Sil1/Bap1 (HspBP1 family). While both Lhs1 and Sil1 exhibit nucleotide exchange activity, their mode of action is distinct, which likely accounts for the differences in directing specific Kar2/BiP activities. Sls1 was the first NEF identified for Kar2. Sls1 was identified in the yeast

Yarrowia lipolytica in a synthetic lethal screen to identify interactors of a temperature sensitive variant of SCR2, which encodes the 7S RNA of SRP (Boisramé, Beckerich and Gaillardin 1996). The function of Sls1 at this point was unknown, however, it was known to interact with Sec61 and Kar2 and deletion of Sls1 resulted in cotranslational translocation defects (Boisramé, Beckerich and Gaillardin 1996; Boisramé et al. 1998). Independently a homologue of Sls1 was identified in *S. cerevisiae* while trying to dissect the function of Lhs1. Deletion of *LHS1* is viable but results in two main phenotypes; a partial defect in posttranslational translocation, and the constitutive induction of the UPR (Tyson and Stirling 2000). Preventing the induction of the UPR through the deletion of *IRE1* (Ire1 is essential for UPR activation) in *lhs1Δ* cells resulted in a severe growth defect, indicating that constitutive induction of the UPR was essential for the viability of *lhs1Δ.* A multicopy suppressor screen performed in the *ire1Δ lhs1Δ* double mutant identified a single gene that was able to rescue the severe growth defect observed in this strain, *SIL1* (Suppressor of the *IRE1*/*LHS1* double mutant) (Tyson and Stirling 2000). As with *LHS1*, deletion of *SIL1* is viable, but deletion of both results in synthetic lethality, indicating a conserved functionality. While both Sil1 and Lhs1 act as NEFs for Kar2/BiP, their interaction is mutually exclusive, furthermore Lhs1 displays a greater activity of nucleotide exchange than Sil1. Additional to its role as a NEF, Lhs1 being a large member of the Hsp70 family also exhibits chaperone activity (Saris et al. 1997). This activity is thought to be tailored to more of a holdase, preventing the aggregation of unfolded/misfolded protein (Saris et al. 1997). Unlike Kar2, it has been determined that Lhs1 ATPase activity is independent of both J-domain and NEF activity. Instead, Lhs1 mediated hydrolysis of ATP first requires interaction with Kar2 and is intimately coupled to Kar2 ATP hydrolysis (Steel et al. 2004). This may explain the much greater rate of hydrolysis experienced with Lhs1 vs Sil1 in ATP hydrolysis experiments, as Lhs1 ATPase activity would be stimulated in congruence with Kar2. Thereby, upon the hydrolysis of ATP by Kar2, and the subsequent reloading of ATP by Lhs1, the newly released peptide is able to be bound by Lhs1, preventing the formation of aggregates.

Although the functional overlap of Sil1 and Lhs1 is evident, the two are not completely interchangeable, null mutants display different phenotypes which are not fully rescued through cross complementation, and both Lhs1 and Sil1 have distinct genetic interactions. Furthermore, loss of *LHS1* in *S. cerevisiae* is tolerated but is embryonic lethal in mice, while mutations in Sil1 of humans is attributed to over half of all Marinesco-Sjögren syndrome (MSS) cases (Kitao et al. 2001; Senderek et al. 2005). Disruption of Sil1 in mice results in the 'woozy' phenotype, which phenocopies many of the pathologies associated with MSS including cerebellar ataxia and progressive myopathy (Zhao et al. 2005). These differences indicate that our understanding of the specific roles Sil1 and Lhs1 play is limited and requires further investigation.

1.8. Protein folding and post translational modification

Newly synthesised polypeptides entering the ER require a diverse group of proteins to assist in their folding to ensure successful maturation. As previously mentioned, the resident HSP70, Kar2 plays an essential role in the folding of immature substrates. However, the ER is home to additional chaperone networks, such as the lectin chaperones (Calnexin and Calreticulin), and folding enzymes that coordinate disulfide bond formation (PDI and Oxidoreductase). In addition to folding, the majority of proteins traversing the secretory pathway undergo PTM, including signal sequence cleavage and N-linked glycosylation, both of which occur predominately during translocation. Protein quality control in the ER is closely monitored to prevent abhorrent protein misfolding, as is the environment within the ER lumen, which provides the optimal conditions for efficient protein folding/maturation. Proteins that fail to adopt their native conformation are targeted for degradation via the ERAD pathway. Accumulation of misfolded/unfolded proteins and prolonged perturbations to the environment of the ER induces the UPR. This process upregulates a subset of genes aimed at increasing the folding capacity of the ER and the ERAD machinery, ultimately restoring ER homeostasis (Acosta-Alvear et al. 2018).

1.8.1. *N*-Linked Glycosylation

The addition of carbohydrates to protein is ubiquitous in life, serving a variety of functions. In eukaryotes the majority of glycosylated proteins reside within the ER, with *N*-linked glycosylation in particular and to a lesser extent, *O*-linked mannosylation representing the most commonly observed form of PTM (Apweiler, Hermjakob and Sharon 1999; Spiro 2002). The addition of N-linked glycans to Asn residues occurs specifically at a consensus motif Asn-X-Ser/Thr (where X can be any amino acid except proline) termed a sequon. The core glycan is composed of 3 glucose residues, 9 mannose residues, and 2 N-acetyl glucosamine residues (Glc3Man9GlcNAc2). The covalent attachment of the core glycan to the amide group of Asn residues typically occurs cotranslocationally once the sequon is 12-14 amino acids within the ER lumen (Nilsson and von Heijne 1993). Recognition and transfer of N-glycans to proteins is coordinated by the oligosaccharyltransferase complex (OST) which is juxtaposed to the translocon (Chavan, Yan and Lennarz 2005). In yeast, OST is composed of 9 protein subunits: Ost1, Ost2, Ost3, Ost4, Ost5, Ost6, Stt3, Swp1, and Wbp1 (Figure 1.5). However, the hetero oligomeric complex only contains 8 subunits at any time, with Ost3 and Ost6 present in sub-stoichiometric levels. Structural analysis of the OSTase complexes in yeast and mammals determined that Ost3 and DC2 are responsible for interactions with the translocon respectively, and thus provide the mechanistic evidence for co-translocational N-glycosylation (Braunger et al. 2018; Wild et al. 2018). Although homologues, there is little sequence identity between Ost3 and Ost6, conversely they possess near identical hydropathy plots (Knauer and Lehle 1999). Deletion of either Ost3 or Ost6 has no effect on growth, although minor disruptions to N-glycosylation are observed, deletion of both results in a severe defect in the glycosylation of both membrane and soluble proteins (Knauer and Lehle 1999). Interestingly deletion of Ost6 and not Ost3, results in sensitivity to agents that effect cell wall biogenesis, however the sensitivity is greatly increased in the double knockout, indicating both a degree of functional overlap and specialised activity for each (Knauer and Lehle 1999).

N-glycosylation of proteins serves a wide variety of biological functions including, increasing the stability and dictating the conformation of proteins, recruitment of proteins involved in folding and quality control, and serving as markers for maturation as the protein traverses the secretory pathway (Spiro 2002). Regarding protein folding and stability, the intrinsic role N-glycans play is multifaceted. The addition of these relatively large carbohydrate molecules to the protein backbone is thought to stabilise the residues in close proximity, due in part to C-H-π interactions (Chen et al. 2013). Additionally, N-Glycans are hydrophilic in nature, this property promotes a more solvent accessible fold of the surrounding peptide chain while increasing the relative solubility of the folding protein (Lee, Qi and Im 2015). Individually the intrinsic effects on protein folding and stability by N-glycans are minimal, however collectively they represent a significant increase in the free energy, thereby promoting the native folding capacity.

The major extrinsic role of N-glycans directs the protein through a specific ER chaperone system termed the 'Calnexin-Calreticulin cycle' (Williams 2006). Both Calnexin and Calreticulin are lectin binding proteins which specifically recognise glycosylated precursors, assisting in their folding, and directing them for degradation if terminally misfolded. Additionally, both proteins have the ability to bind calcium (Ca^{2+}), with Calreticulin having a significant role in ER calcium flux (Llewelyn Roderick et al. 1998; Corbett et al. 2000). The membrane protein Calnexin and its soluble homologue Calreticulin function in the same manner in regards to glycoprotein chaperoning, however it has been determined that each interacts with a unique subset of glycoproteins (Zhang and Salter 1998). In contrast, *S. cerevisiae* encodes a single ER lectin chaperone homologous to the membrane variant Calnexin, which lacks the Ca^{2+} binding activity its mammalian equivalent, likely a result of the ER not being the primary storage site of calcium for *S. cerevisiae* (Parlati et al. 1995).Following the transfer of N-glycans to the translocating peptide, glucosidases 1 and 2 remove two of the three terminal glucose molecules from the core glycan (Williams 2006).

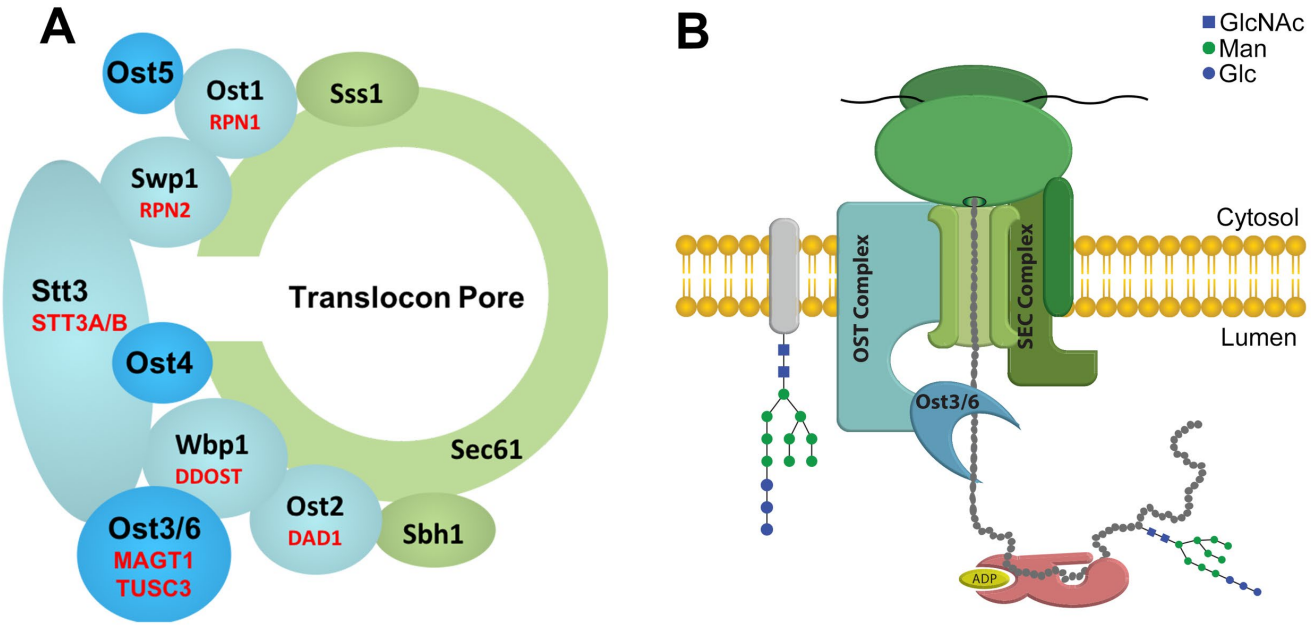

Figure 1.5 The Oligosaccharyltransferase complex.

The oligosaccharyltransferase complex (OST) is located next to the translocon. A) Depicts the nine proteins that constitute OST, however only 8 are found within the complex at any one time with Ost3 and Ost6 represented in a stoichiometric amounts, the mammalian homologues are shown in red. B) is representative of the cotranslocational nature of protein N-glycosylation, with transfer of the glycan from the dolichol precursor to the translocating peptide occurring once ~15 residues have passed into the lumen of the ER. Recognition of peptides requiring N-glycans is further specialised by Ost3/6 interactions with the translocating peptide, and its proximity to the translocon allows efficient targeting.

This ‘trimming’ event is required for Calnexin/Calreticulin to recognise the newly synthesised peptide through direct interaction of the modified glycan and their lectin binding domain. The interaction of unfolded peptides with either Calnexin or Calreticulin assists in their folding through stabilisation of the peptide, thereby: preventing aggregation; reducing the speed in which folding occurs; the recruitment of protein disulfide isomerases (PDI’s – disulfide bond formation); and the retention of unfolded/misfolded proteins in the ER. This final step is co-ordinated through the removal of the remaining terminal glucose by glucosidase 2 (Williams 2006). If the peptide has successfully folded it is directed for anterograde trafficking, however, misfolded/unfolded proteins are recognised by the quality control sensor Ugt1 (UDP-glucose: glycoprotein glucosyltransferase 1), which upon recognition of exposed hydrophobic patches transfers a single glucose molecule back onto the glycan (Williams 2006). Thus, the protein is again a substrate for Calnexin/Calreticulin re-entering the cycle to attempt refolding. Repeated failure to achieve a native fold results in the targeting of the protein to the ER-associated degradation (ERAD) machinery.

1.8.2. Disulfide bonding

The formation of intra- and inter-molecular disulfide bonds is an important stage in the biogenesis of natively folded proteins and protein complexes stabilising both tertiary and quaternary structures. Disulfide bonds can occur within proteins which are not part of their native fold (e.g. misfolded proteins) or are required transiently to achieve their native conformation (e.g. cysteine knot proteins). Like with glycosylation, disulfide bond formation is a highly regulated process requiring the co-ordination of several groups of proteins, however this process is largely dependent on the environmental conditions within the ER. Oxidative folding (i.e. disulfide bond formation), as the name suggests, requires a source of ‘oxidative power’ and as such the ER is maintained in a more highly oxidised state. Generally, the redox potential within a cell is determined by measuring the ratio between the reduced (GSH) and oxidised states (GSSG) of the tripeptide glutathione (Glu-Cys-

Gly). To what degree the ER is 'oxidised' has been a controversial topic, with initial reports determining the ratio of GSH/GSSG to be 1-3:1 in the secretory pathway, conversely total cellular GSH/GSSG ratios of 30-100:1 indicate a predominantly reduced cellular state (Hwang, Sinskey and Lodish 1992). One caveat with these early works was the potential for exogenous oxidation during the extraction process, with the use of thiol modification inhibitors a ratio ~5:1 GSH/GSSG was determined for the ER (Dixon et al. 2008). Furthermore, the use of GFP and YFP redox sensitive probes has allowed for more accurate and compartment specific measurements, with cytosolic GSH/GSSG ratios of 10,000-50,000:1, orders of magnitude higher than previously believed (Dardalhon et al. 2012; Marcus et al. 2008; Morgan et al. 2013). Regardless of the method used, what can be seen is that glutathione is a major determinant of the ERs oxidising potential and essential to maintain the specific conditions needed.

Oxidative folding is a critical step in the folding and secretion of proteins targeted to the ER, particularly as the cysteine content of targeted proteins is significantly higher than cytosolic proteins (Fahey, Hunt and Windham 1977). As such both the oxidative environment and the enzymes responsible for disulfide bond formation (Protein Disulfide Isomerase – PDI) are intimately linked. PDI family proteins are characterised in containing 4 thioredoxin like domains (Trx) comprised of Cys-X-X-Cys, 2 of which are active, while the other 2 are considered to be involved in substrate recruitment (Kozlov et al. 2010).

Functionally, PDI is able to interact with and catalyse the formation/removal of disulfide bridges with cysteine pairs depending on the oxidation state of its own Trx domains (Hatahet and Ruddock 2009). While PDIs are conserved amongst eukaryotes, their observed oxidation states differ, in yeast Pdi1 is found in a predominantly oxidised state, whereas mammalian PDI is in a semi-reduced state (Frand and Kaiser 1999; Mezghrani et al. 2001). Potential reasons for this difference may be due to the complex arrangement of disulfide bonds within mammalian cells requiring more extensive remodelling than those in yeast.

Although PDI is the enzyme responsible for the direct isomerisation of disulfide bonds, much of its functionality is attributed to the regulatory role of the

ER oxidoreductin Ero1 (Sevier and Kaiser 2008). Simplistically, Ero1 is responsible for transferring disulfide bonds to PDI, thus priming PDI to actively target and transfer those disulfides to the required substrates. However, this process requires the reduction of small molecule intermediates, rounds of inter-cysteine shuttling of disulfides, and finally transfer to PDI, all of which is regulated by the redox state of two sets of regulatory cysteine pairs (Gross et al. 2004; Sevier and Kaiser 2008). Two catalytically active cysteine pairs within Ero1 are responsible for generating oxidised PDI. The first pair, termed the 'active site', are located adjacent to the binding site of flavin adenine dinucleotide (FAD)(Gross et al. 2004). This site is able to reduce FAD, oxidising the cysteine pair, and generating H_2O_2. The now oxidised active site performs a dithiol-disulfide exchange with the 'shuttle' cysteine pair, which in turn oxidise PDI. The ability of Ero1 to exchange the oxidised state between the active site and the shuttle cysteines is controlled by two pairs of 'regulatory' cysteines. Upon oxidation, these cysteines restrict the flexibility required for the two catalytical pairs to interact, ultimately preventing oxidation of PDI and reducing the rate at which disulfides are formed (Gross et al. 2004). This regulation in times of hyper-oxidation both prevents PDI forming non-native disulfides and allows for reduced PDI to remodel disulfides produced by free radicals in the form of H_2O_2 or GSSG.

1.8.3. ER Associated Degradation

The processes outlined above constitute the critical role of protein folding and how PTMs are able to both assist in the successful folding and identify proteins unable to adopt their native conformations. Complementing the highly regulated protein folding processes are the ER quality control (ERQC) systems in which protein folding is monitored, and in the case of misfolded/unfolded proteins are recognised and targeted for retrotranslocation/dislocation and subsequent degradation by 26S proteasome (Nishikawa, Brodsky and Nakatsukasa 2005). This activity, broadly termed ER associated degradation (ERAD), is a multifaceted approach to the removal of protein from both the lumen and the membrane of the

ER, achieved through two main protein complexes each targeting a unique subset of substrates (Ruggiano, Foresti and Carvalho 2014) (Figure 1.6). Once recognised as a misfolded substrate, the protein is polyubiquitinated 'marking' it for degradation. This process requires the co-ordination of several classes of protein, both resident ER and cytosolic factors, to efficiently recognise and transfer misfolded protein to the proteasome.

The first evidence of ER specific degradation pathways came from the observations that misfolded/unassembled viral proteins were recognised and retained, through their interactions with BiP, in the ER (Desilva, Balch and Helenius 1990; Gething, McCammon and Sambrook 1986; Stella et al. 1989). In 1993, the first 'bona fide' ERAD component and substrate was identified, through the observation that a loss of function mutant of *UBC6* (UBiquitin Conjugating) restored growth in a temperature sensitive mutant of *SEC61* (Thomas and Stefan 1993). Additional work also identified Sss1 to be degraded via the same route, while work in mammalian cells showed that CFTR (Cystic Fibrosis Transmembrane conductance Regulator), the most commonly mutated gene in cystic fibrosis, was degraded by the 26S proteasome following ubiquitination (Biederer, Volkwein and Sommer 1996; Ward, Omura and Kopito 1995). Subsequent work in yeast furthered the number of substrates targeted for degradation, one in particular, HMG-CoA reductase (HMGR), was utilised in a genetic screen to identify three new ERAD genes *HRD1-3* (HMG-CoA Reductase Degradation) (Hampton, Gardner and Rine 1996; Hampton and Rine 1994). Two more substrates, CPY* and PrA*(Carboxypetidase Y and Proteinase yscA, * denotes the misfolded ERAD variants), were crucial in the understanding of ERAD and were utilised to identify two new genes required for ERAD, *DER1* and *DER2* (Degradation in the ER) (Bordallo et al. 1998; Knop et al. 1996). The screen also identified a third gene, *DER3*, which was determined to be identical to the previously discovered *HRD1*. Both screens identified components of the HRD1 complex, however the substrates differed in their ER localisation, HMGR is an integral membrane protein, while CPY* and PrA* are soluble. All the identified substrates required the activity of Hrd1/Der3 while only CPY* and PrA* required

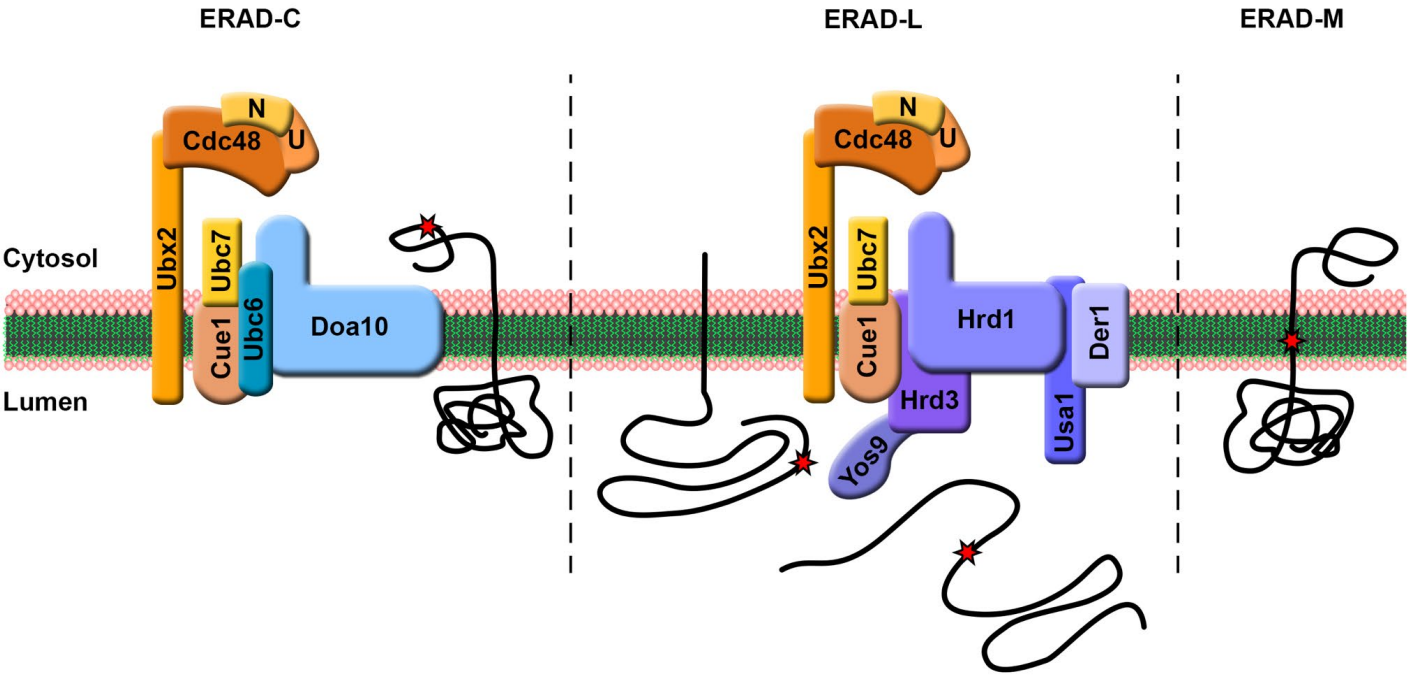

Figure 1.6 The ERAD machinery of yeast.

ERAD in general utilises one of two main pathways, represented by a unique E3 ligase, Doa10 and Hrd1. Each pathway is responsible for the recognition of a specific range of substrates. The Doa10 E3 ligase is responsible for the degradation of ER membrane proteins with misfoldings within the cytosol, termed ERAD-C. While Hrd1 is responsible for the degradation of luminally misfolded proteins including those, which are glycosylated (ERAD-L) and proteins misfolded within their membrane spanning domains (ERAD-M). Aside from the core E3 ubiquitin ligase, several proteins are conserved between the two, including the Cdc48 complex containing the co-factors Ufd1 and Npl4, responsible for pulling the ubiquitinated protein out of the ER.

*Protein misfoldings, also termed degrons, are denoted by red stars.

Der1, indicating mechanistic differences. Characterisation of new substrates revealed an alternative to the HRD1 pathway existed. Mutant variants of the multispanning membrane protein Ste6 were identified to be degraded in a ubiquitin dependant manner (Loayza et al. 1998). However it was revealed that its degradation, unlike CPY*, was independent of the HRD1 complex, instead requiring the multispanning membrane protein Doa10 (Huyer et al. 2004). Doa10 had previously been implicated in the degradation of the soluble transcription factor Mat2α (Swanson, Locher and Hochstrasser 2001). Combined these reports elucidated that ERAD is not one defined pathway, rather it is comprised of multiple components, each responsible for the targeting and degradation of a unique subset of proteins. Simplistically, ERAD is characterised by two main pathways, the Doa10 and Hrd1 complexes. Doa10 is responsible for degrading membrane proteins misfolded in their Cytosolic domains (ERAD-C), whereas Hrd1 targets proteins misfolded in the Membrane spanning domains and Luminally misfolded proteins (ERAD-M and ERAD-L respectively) (Carvalho, Goder and Rapoport 2006).

At the core of each complex are the E3 ubiquitin ligases Doa10 and Hrd1, which are partially responsible for substrate recognition and the transfer of ubiquitin to the misfolded substrate. While each pathway is distinct in its role, several components are shared between the DOA10 and HRD1 complexes (Ruggiano, Foresti and Carvalho 2014). Common to the pair is the CDC48 complex (comprised of Cdc48, Ufd1 and Npl4), which provides the mechanic force to extract the ERAD substrate from the ER. Also shared between the two complexes is the E2 ubiquitin conjugating enzyme Ubc7, which delivers ubiquitin to the E3 ligase. The final two proteins common to both are the recruitment factors Cue1 (recruits Ubc7), and Ubx2 (recruits the CDC48 complex). Of the two, Doa10 is the simpler, primarily comprised of Doa10 and the shared components. Unique to the Hrd1 complex are several proteins that recognise luminal substrates including Der1 and Usa1 (recruits Der1), with Der1 also proposed to facilitate transfer into and across the membrane. The major effector of luminal lesions is Hrd3, which is able to recognise glycosylated and unglycosylated proteins, furthermore it's responsible for the recruitment of the luminal protein Yos9, which specifically targets glycosylated

proteins for degradation (Ruggiano, Foresti and Carvalho 2014). Described above are the central components of the multiple ERAD pathways present in yeast and metazoans, with increasing complexity and additional machineries found in higher eukaryotes (Ruggiano, Foresti and Carvalho 2014). The ERAD pathway coordinates essential activities in maintaining ER proteostasis through regulated degradation of functional proteins and removal of misfolded substrates even more so under conditions of ER stress in which large scale protein misfolding occurs.

1.8.4. UPR

ER functionality is dependent on the maintenance of specific environmental conditions, with perturbations to this homeostasis detrimental to ER function, and cell survival. While ERAD is able to degrade misfolded proteins, under conditions of high stress such as changes to the redox environment, the large accumulation of misfolded proteins requires an additional pathway, the UPR. As the name suggest, the UPR is activated upon the accumulation of misfolded proteins in the ER, and in response to changes in the lipid environment. In *S. cerevisiae,* the activation of the UPR induces the upregulation of ~380 genes which collectively are involved in activities such as protein folding, disulphide bonding, N-glycosylation, ERAD and lipid biosynthesis (Travers et al. 2000). Thus, activation of the UPR increases the biosynthetic capacity of the ER both through an increased folding capacity and reestablishment of ER homeostasis.

The UPR is highly conserved with the IRE-dependent pathway conserved throughout eukaryotes. In metazoans, the PERK and ATF6 pathways are also involved, however our focus will be on the *IRE1* pathway in *S. cerevisiae* (Walter and Ron 2011). At the core of this pathway is the type-1 membrane protein Ire1, which both recognises the ER stress (either misfolded protein or lipid disequilibrium) and generates the transcription factor responsible for upregulating UPR targets (Figure 1.7). The luminal domain of Ire1 is responsible for the detection of misfolded proteins, causing its self-association and subsequent activation. Two

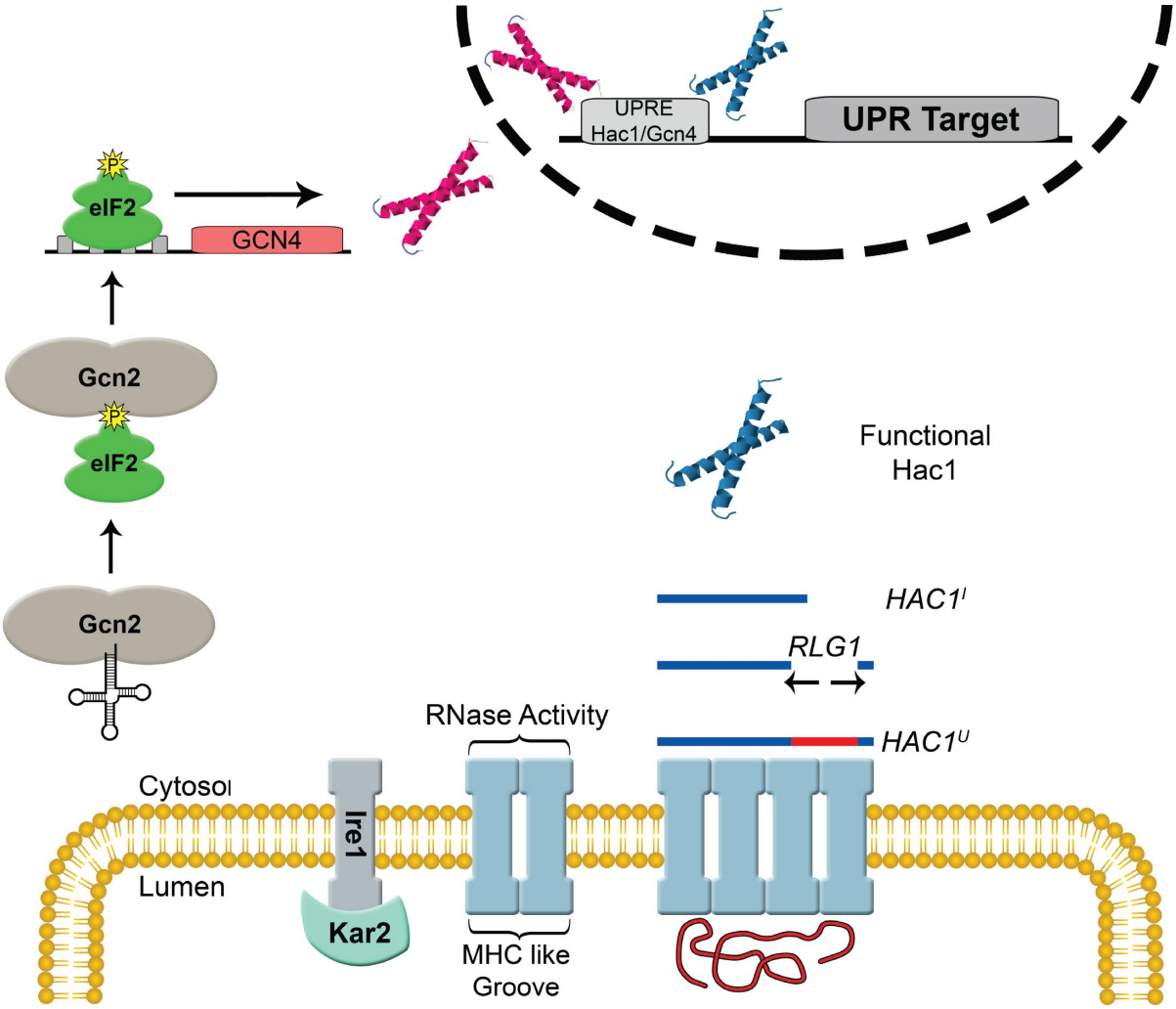

Figure 1.7 Activation of the UPR in yeast.

Depicted here are the two arms of the UPR in yeast. Primarily Ire1, the main progenitor of the UPR is maintained in a monomeric form by Kar2 under normal conditions. Upon the accumulation of misfolded proteins, Kar2 disassociates from Ire1, whereby it directly recognises misfolded proteins resulting in its oligomerisation. This triggers trans-autophosphorylation, resulting in a conformational change activating the C-terminal RNase domain. The constitutively produced $HAC1^{U}$ mRNA is then spliced, producing $HAC1^{I}$, the mRNA responsible for producing the active Hac1 transcription factor, where is then upregulates the expression of UPR target genes. The second transcription factor Gcn4 is regulated in response to changes in free amino acids, communicated by tRNA molecules. When uncharged, tRNAs are recognised by Gcn2 which in turn phosphorylates eIF2, which allows for the efficient translation and production of Gcn4.

main mechanisms have been suggested for how this is accomplished, the first suggests that at steady state, Kar2 interacts with the Ire1 luminal domain preventing its self-association. As misfolded proteins increase, Kar2 disassociates allowing for dimerisation of Ire1. The second, and better supported mechanism involves the direct binding of misfolded protein by the luminal domain of Ire1, and its subsequent self-association. Structural analysis of the luminal domain revealed it shares homology with the major histocompatibility complex (MHC) peptide binding grooves, further supporting this model of direct interaction. Activation of the UPR following dimerisation requires the cytosolic domain, comprised of a kinase domain, and RNase domain. Following oligomerisation, the kinase domain undergoes trans-autophosphorylation resulting in a confirmation change which in turn activates the RNase domain located C-terminally. The RNase domain is unique in that it specifically targets a single mRNA, that of the transcription factor Hac1 (Xbp1 in humans). Constitutively transcribed, the Hac1 mRNA contains a 252-nucleotide intron which prevents the production of the active transcription factor. The endoribonuclease activity of Ire1 excises the intron and the resulting mRNA is ligated, allowing for the production of the functional Hac1 transcription factor. Hac1 then translocates into the nucleus, upregulating the expression of UPR target genes, specified by the presence of a UPRE (UPR element). In yeast, this signal transduction pathway represents the main potentiator of the UPR. However, it has been demonstrated that the general amino acid control (GAAC) transcription factor Gcn4, is also able to further stimulate the UPR along with Hac1, and independently activate a subset of UPR targets. How UPR stimuli are communicated and regulate Gcn4 activity is not known. Its activation during amino acid starvation is tightly regulated, first requiring the recognition of the uncharged tRNA molecules by Gcn2, which in turn phosphorylates eIF2α allowing it to bind the upstream portion of the GCN4 mRNA. This portion on GCN4 mRNA contains 4 short ORFs (uORF) which under normal conditions prevent the translating ribosome from reaching the start codon of GCN4, instead reading the first and fourth uORF, terminating its translation. Therefore, binding by eIF2α to the uORFs of GCN4 allows for its efficient translation.

The UPR is an efficient signal transduction pathway able to rapidly communicate perturbations in protein folding to the nucleus. While it is now accepted that Ire1 directly senses misfolded proteins, Kar2 bound to Ire1 stabilises the monomeric/inactive form, thus dampening the threshold required for activation of the UPR. The remainder of the ERQC network is able to mitigate smaller disturbances, preventing the inappropriate activation and energy consumption of the UPR. While the specifics of Gcn4s involvement have yet to be uncovered, its role in nutrient signalling would suggest that the UPR is responsive to the environmental conditions and nutritional requirements of the cell. As the ER is a primary site of autophagosome production, thus responsible for metabolic recycling, this interconnected signalling between nutrient availability and the biosynthetic capacity of the ER would further allow for the response to be regulated to changes at a cellular level.

1.8.5. Autophagy

Protein synthesis, modification, and secretion are all anabolic processes, requiring the input of energy and the production of larger molecules from smaller. The ER, as a major site of all of these processes is a highly anabolic organelle, requiring multiple regulatory pathways to ensure it functions efficiently. Under conditions of extended stress, or nutritional depletion, anabolic processes are downregulated, with catabolic recycling of cytosolic material, and specific targeting of organellular material. This process termed autophagy (self-eating) is responsible for recycling cellular material, allowing for the continued production of various essential cellular components that the current environmental conditions demand. While a highly anabolic organelle, the ER is also involved in the supplying the double membraned vesicles that engulf the material to be recycled. These membranes form a phagophore, which following engulfment of cellular material, close forming autophagosomes which eventually fuse with the lysosome (vacuole in yeast) where the cargo is degraded. Not only are the majority of membranes

derived from the ER, but many of the protein and lipid factors required also reside within the ER.

While important in assisting the general autophagic pathway (macrophagy), the ER is also subject to specific autophagic processes targeting the ER for recycling, known as ER-phagy. This process can be dissected into two distinct pathways, micro and macro ER-phagy with the latter akin to the general macrophagy response. Unlike macrophagy and macro ER-phagy, micro ER-phagy occurs independently of the core autophagy related genes. Instead, micro ER-phagy occurs through direct invagination of ER material by the vacuole. How this process occurs has yet to be elucidated, however it requires the formation of 'ER whorls' which are then selectively removed by the vacuole. The process of micro ER-phagy is fundamentally important in regulating ER volume, specifically during and following ER stress and UPR induction, which itself can account for a 5-fold increase in volume. Together with macro ER-phagy (macrophagy), the ER volume and components can undergo large scale recycling depending on the environmental conditions and constitute part of the ERQC-pathway. In coordination with the UPR and ERAD, ER-phagy can also regulate excess membrane proteins, both as a general housekeeping mechanism and following ER stress.

Macrophagy and macro ER-phagy are highly upregulated upon nutrient deprivation or inhibition of TOR (Target of Rapamycin), the master regulator of anabolism and proliferation. In general, autophagy requires the repression of anabolic processes (i.e. inhibition of TOR) and vice versa. This relationship between anabolism and catabolism, and the involvement of the ER in both, situates the secretory pathway in a unique position, one in which the numerous and often opposing signalling pathways intersect.

1.9. Aims

Together, the production, targeting and delivery of proteins through the secretory pathway requires the coordinated input of multiple pathways and processes under 'normal' conditions. Further complications arise due to various

stresses, both exogenous and those experienced as part of vegetative growth, requiring the input of yet more pathways to ensure the continued function of the ER and the secretory pathway as a whole. Maintaining and folding the large protein load of the ER is energetically costly, and if poorly regulated, highly detrimental to cellular physiology with end stage ER stress resulting in cell death, and strongly associated with a multitude of pathologies. With this in mind, our understanding of how many of the processes are regulated, is still limited.

As previously stated, the ER is both fundamentally important in both anabolism and catabolism, yet to date there is a paucity of data directly linking the ER and TOR. As a central component of the cell, with multiple signal transduction pathways able to alter gene expression, contact sites with multiple organelles such as the mitochondria, and responsible for the secretion of factors that sequester the numerous exogenous nutritional requirements of the cell, the ER is poised to communicate the various needs of the cell. I therefore hypothesise that a link between the ER and TOR exists and is likely communicated through the phosphorylation of a central component of the translocon, Sec63. Supporting this, is the identification of a TOR sensitive phosphorylation site in Sec63 of the fission yeast *Schizosaccharomyces pombe* (Dr Janni Petersen, Flinders University, Personal Communication). As such I aim to establish if such a site exists with *S. cerevisiae,* and subsequently characterise any changes to regular ER function that occur following mutational disruption of the site.

As Sec63 in part regulates the molecular chaperone activity of Kar2, I aim to better understand the relationship between the major Hsp70 of the ER, Kar2, and the NEF Sil1. To date, the role of Sil1 has been overlooked. However recent findings have attributed Sil1 to several diseases, as such I wish to better characterise the role of Sil1, and how its activity is regulated under various stresses which perturb ER function, and thus lead to pathological outcomes (Liu et al. 2016; Senderek et al. 2005; Xu et al. 2018; Zhao et al. 2005).

Thus the primary aims of this study are as follows:

I. **To identify and characterise phosphorylation sites in the c-terminal domain of Sec63 which are regulated in a TOR dependent manner.**

II. **Investigate the consequences reductive stress has on the glycosylation of the nucleotide exchange factor Sil1 and characterise the role glycosylation has on the activity of Sil1.**

III. **Further investigate the nature in which the abundance and activity of Sil1 are regulated in response to changes in REDOX.**

Materials and methods

All chemicals and reagents were of analytical grade or higher and purchased from Astral Scientific, Amresco or Sigma Aldrich unless otherwise stated. DNA modifying enzymes were purchased from New England Biolabs. Media and growth supplements were purchased from Becton Dickinson, Oxoid and Sigma Aldrich. All other materials will have the manufacturers listed.

2.1. Microbiological techniques

Table 1.1 ***S. cerevisiae*** **strains used in this study**

Name	Genotype	Original Source
BY4742	*MATα his3Δ1 leu2Δ0 lys2Δ0 ura3Δ0*	(Brachmann et al. 1998)
BYY5	*MATα leu2-3,112 trp1-1 can1-100 ura3-1 ade2-1 his3-11 KanMX4-pMET3-SEC63 [phi+]*	(Jermy et al. 2006)
BWY780	BY4742 *sec63Δ::KanMX4* [pJKR2 (*SEC63, URA3)*]	Barry Wilkinson
ire1Δ	BY4742 *ire1Δ::KanMX4*	(Winzeler et al. 1999)
ost3Δ	BY4742 *ost3Δ::KanMX4*	(Winzeler et al. 1999)
ost6Δ	BY4742 *ost6Δ::KanMX4*	(Winzeler et al. 1999)
sil1Δ	BY4742 *sil1Δ::KanMX4*	(Winzeler et al. 1999)
JTY62	*ire1Δ::kanMX4 lhs1Δ::kanMX4 [pJT40 (LHS1, ADE3, URA3)]*	(Tyson and Stirling 2000)
JTY65	*sil1Δ::kanMX4 lhs1Δ::kanMX4 [pRC43 (LHS1, URA3)]*	(Tyson and Stirling 2000)
KSY1	*MATa ade2 ade3 his3 leu2 trp1 ura3 ire1Δ::kanMX4 lhs1Δ::kanMX4 SIL1N181Q::LEU2*	This study
lhs1Δ	*BY4742 lhs1Δ::KanMX4*	(Winzeler et al. 1999)
doa10Δ	*BY4742 doa10Δ::KanMX4*	(Winzeler et al. 1999)
hrd1Δ	*BY4742 hrd1Δ::KanMX4*	(Winzeler et al. 1999)
hrd3Δ	*BY4742 hrd3Δ::KanMX4*	(Winzeler et al. 1999)

Table 1.2 Plasmids used in this study

Plasmid	Description	Source
pRS315	Yeast centromeric *LEU2* vector	(Sikorski and Hieter 1989)
pRS316	Yeast centromeric *URA3* vector	(Sikorski and Hieter 1989)
pRS313	Yeast centromeric *HIS3* vector	(Sikorski and Hieter 1989)
pJKR2	pRS316-*SEC63*	(Jermy et al. 2006)
pUH7	*URA3* to *HIS3* marker swap vector	(Voth, Wei Jiang and Stillman 2003)
YCp *sec63*^{467AA}	pJKR2:: *sec63*^{467AA}	This study
YCp *sec63*^{467DD}	pJKR2:: *sec63*^{467DD}	This study
YCp *sec63*^{467EE}	pJKR2:: *sec63*^{467EE}	This study
YCp *sec63*^{512A}	pJKR2:: *sec63*	This study
YCp *sec63*^{512D}	pJKR2:: *sec63*^{512D}	This study
YCp *sec63*^{512E}	pJKR2:: *sec63*^{512E}	This study
YCp *sec63*^{528A}	pJKR2:: *sec63*^{528A}	This study
YCp *sec63*^{528D}	pJKR2:: *sec63*^{528D}	This study
YCp *sec63*^{528E}	pJKR2:: *sec63*^{528E}	This study
YCp *sec63*$^{467/568\text{-}AA\text{-}Trunc}$	pJKR2:: *sec63*$^{467/568\text{-}AA\text{-}Trunc}$ Marker swapped with pUH7	This study
YCp *sec63*$^{467/468\text{-}EE\text{-}MS}$	pJKR2:: *sec63*$^{467/468\text{-}EE}$ Marker swapped with pUH7	This study
YCp *sec63*$^{467/468\text{-}AA\text{-}HIS3}$	pRS313:: *sec63*^{467AA}	This study
YCp *sec63*$^{467/468/512\text{-}AAA\text{-}HIS3}$	pRS313:: *sec63*^{467AA}	This study
YCp *SEC63*^{MS}	pJKR2 Maker swapped with pUH7	This study
YCp *SEC63* ^{HIS3}	pRS313-*SEC63*	This study
pRC43	Constitutive Hac1I expression	(Chapman and Walter 1997)
p*OST3*	Low copy expression of *OST3*	(Schulz et al. 2009)
p*ost3*$^{C\rightarrow S}$	Low copy expression of *ost3* $^{C73S\ C76S}$	(Schulz et al. 2009)
YEp *SIL1*	Overexpression of *SIL1*	This study
YEp *sil1*$^{C52S\ C57S}$	Overexpression of *sil1*$^{C52S\ C57S}$	This study
YEp *sil1*^{C203S}	Overexpression of *sil1*^{C203S}	This study
YEp *sil1*^{C373A}	Overexpression of *sil1*^{C373A}	This study
YEp *sil1*^{N105Q}	Overexpression of *sil1*^{N105Q}	This study
YEp *sil1*^{N181Q}	Overexpression of *sil1*^{N181Q}	This study
YEp *sil1*^{N215Q}	Overexpression of *sil1*^{N215Q}	This study
YEp *sil1*^{N233Q}	Overexpression of *sil1*^{N233Q}	This study
YEp *sil1*^{N315Q}	Overexpression of *sil1*^{N315Q}	This study
YEp *sil1*^{N333Q}	Overexpression of *sil1*^{N333Q}	This study
YCp *SIL1*	Low copy expression of *SIL1*	This study
YCp *sil1*^{N181Q}	Low copy expression of *sil1*^{N181Q}	This study
YEp *OPT1*	Overexpression of *OPT1*	This Lab

2.1.1. Growth and maintenance of *Escherichia coli*

Escherichia coli strains were grown in lysogeny broth (LB): 1% (w/v) Tryptone, 0.5% (w/v) Yeast Extract, 1% (w/v) NaCl, pH 7.5 (NaOH), 1.5% (w/v) bacteriological agar was added prior to autoclaving if solid medium was required. If blue/white screening was needed, IPTG was added to a final concentration of 0.1 mM and X-gal to a final concentration of 40ug. Growth was at 37°C, with shaking at 180rpm. Maintenance of plasmids was performed in LB supplemented with filter sterilised ampicillin (100 µg/ml). *E. coli* strains and plasmids were prepared for long term storage by the addition of 15% (v/v) sterile glycerol, followed by snap freezing in liquid nitrogen with storage at -80°C.

2.1.2. Preparation and transformation of highly chemical competent *E. coli*

A starter culture of *E. coli* was grown overnight with vigorous shaking (250rpm) in 25 ml of SOB medium: 2% Tryptone (w/v), 0.5% (w/v) Yeast Extract, 2.5 mM KCl, 10 mM $MgCl_2$, 10 mM $MgSO_4$ and 10 mM NaCl ($MgCl_2$ and $MgSO_4$ were added after autoclaving), pH 7.0 (NaOH). Using 1-2ml, the overnight culture was subbed into 250ml of fresh SOB in a 2L flask and incubated at 16°C until reaching an OD_{600} of 0.55-0.6. Cells were placed in an ice water bath for 10 minutes before being harvested at 2500g's and 4°C for 10 minutes. The cells were then resuspended in 80ml of transformation buffer (TB): 10 mM $CaCl_2$, 250 mM KCl, 55 mM $MnCl_2$ and 10 mM PIPES, pH 6.7 (using KOH prior to the addition of $MnCl_2$). Cell were again harvested at 2500g's and 4°C for 10minutes. The pellet was resuspended in 20ml of TB supplemented with 1.5ml of DMSO before being snap frozen and stored at -80°C in 200 µl aliquots.

Transformations were carried out by adding 1-2 µl of plasmid DNA to 50 µl of cells. The mixture was placed on ice for a minimum of 30 minutes then placed at 42°C for 45 seconds before being placed back on ice. The mixture was plated out onto LB containing the appropriate antibiotic and incubated overnight at 37°C.

2.1.3. Isolation of plasmid DNA from *E. coli*

A single colony was placed in 5-10ml of LB supplemented with the appropriate antibiotics and grown overnight at 37°C. Cells were harvested at 10,000g's for 1 minute. Plasmid DNA was extracted using the Bioline Isolate II Plasmid Mini Kit following manufacturer's instructions. Following extraction, the DNA was eluted in 50 µl of ddH_2O and stored at -20°C.

2.1.4. Growth and maintenance of *Saccharomyces cerevisiae*

S. cerevisiae strains not requiring auxotrophic selection were grown in YPD: 1% (w/v) Yeast Extract, 2% (w/v) Peptone, 2% (w/v) glucose (added after autoclaving). For plasmid selection strains were grown YNB: 0.17% (w/v) Yeast Nitrogen Base without amino acids and ammonium sulfate, 0.5% (w/v) ammonium sulfate, 2% (w/v) glucose (added after autoclaving) and supplemented with amino acids (Ade, His, Leu, Lys, Trp, Ura at 0.002% (w/v) and Met at 2 mM) added after autoclaving. For solid medium Bacto bacteriological agar was added to 2% (w/v) before autoclaving. *S. cerevisiae* strains were grown at 30°C unless otherwise stated. *S. cerevisiae* strains were prepared for long term storage by the addition of 15% (v/v) sterile glycerol to log phase cultures, followed by snap freezing in liquid nitrogen then stored at -80°C.

2.1.5. High efficiency transformation of *S. cerevisiae*

S. cerevisiae cells were grown overnight in 15ml of the appropriate medium. Culture were harvested by centrifugation at 3000g's for 5 minutes and resuspended in ddH_2O, cells were again harvested at 3000g's for 5 minutes. The cell pellet was resuspended in 1ml of 1xLiOAC/TE (100 mM Lithium Acetate, 10 mM Tris-HCL pH 7.5 (using Acetic acid) and 1 mM EDTA) and incubated at 30°C with shaking for 1 hour. Cells were harvested by centrifugation at 3000g's and resuspended in 200 µl of 1x LiOAC/TE. The transformation reaction contained the following: 34 µl of cells,

6 µl of ssDNA (salmon sperm DNA boiled at 95°C for 5 minutes), 2 µl of DNA (plasmid or single stranded) and 200 µl of 1x LiOAC/TE containing 40% (w/v) PEG4000. The mixture was vortexed and held at room temperature for 30 minutes before incubation at 42°C for 15-30 minutes. The mixture was then plated out on the appropriate selective media and grown at 30°C for 3-4 days.

2.1.6. Isolation of Genomic DNA from cerevisiae

Genomic DNA was prepared from approximately 5-10ml of an overnight culture with cells being harvested by centrifugation at 3000g's for 5 minutes. The cell pellet was washed once in ddH_20 then resuspended in 1ml of Sorbitol Buffer (1M Sorbitol, 0.1M EDTA pH 7.5). The cell suspension was incubated with 50 µl of lyticase (5U/µl) at 30°C with shaking for 1 hour. The resulting spheroplasts where harvested by centrifugation at 3000g's for 5 minutes. The cell pellet was resuspended in 500 µl of yeast resuspension buffer (50 mM Tris-HCL pH 7.4, 20 mM EDTA pH 7.5) and transferred to a microfuge tube containing 50 µl of 10% SDS and placed at 65°C for 30 minutes. Following the incubation, 200 µl of a 5 M potassium acetate solution was added and placed on ice for 1 hour to precipitate SDS bound protein. The resulting precipitate was separated by centrifugation at 16,000g's at 4°C for 5 minutes. The supernatant was then transferred to a clean microfuge tube and an equal volume of isopropanol was added and mixed by inversion. Nucleic acids were recovered by centrifugation at maximum speed for 10 seconds, the liquid removed and the pellet allowed to dry. The pellet was dissolved in 300 µl of TE buffer pH8 containing 20 µg/ml of RNase and incubated at 37°C for 30 minutes. DNA was precipitated by the addition of 30 µl of 3M sodium acetate (pH7) and 200 µl of isopropanol. DNA was recovered by centrifugation at max speed for 20 seconds, the liquid was removed and the pellet allowed to dry before dissolving in 100 µl of TE pH7.4.

2.2. Nucleic Acid Techniques

Table 1.3 List of primers used in this study

Name	Forward Primer	Reverse Primer
SIL1 N105Q SDM	GTCGGTGATCAAGGTAGCCATGAG	ATTCTTCTCATCATTTAGTTTTGCC
SIL1 N181Q SDM	CGCCCTCTTGGCCCAACTTAGTCTC	AATTCATGGGTAATAATTTTGTAGCC
SIL1 N215Q SDM	CCTGTAGTCGAGTTCATTCAAGAAA GTTTTCC	AGGATTGTTTCTCAAGCAGC
SIL1 N233Q SDM	GTCAAATTTGCAAGATTCTAACCACA GATCC	AGAGCGGCCATGATTTTGC
SIL1 N315Q SDM	GAAATGCTGAGCAATGGTCGTCAAA TCTG	TTTTGAACAAAATTAGATTTGTATCG
SIL1 N333Q SDM	CCAAGAGATGGTCCAGCAAAAAAGT ATAGATG	AACTCGTTTGCCCACTCTTGC
SIL1 C52S C57S SDM	GGAATTCGATCAGCGTTGATAATCG TAGCTATCCTAAGATATTTG	CTGAAATTTCAAGTTCTTTAAGATCT TCTGC
SIL1 C203S SDM	CATTACCAGCAGCTTGAGAAACAATC C	ACTCTAGTACTGAGCTCTCTC
SIL1 C373A SDM	CGCAACAAGCTAAAGCCAGGC	CTAACCAATTCAAAAACCCTTTG
SIL1 LEU2 integration	SIL1 N181Q F	CTTCATTGACACAAGAATTGGCCGCC AAAATCGTTCAGCATAACTGTGGGA ATACTCAGG
SEC63 TS467AA SDM	GATACCAGCTGCCTTAATTCCTG	AATGGCTGTTTAGCAGAACG
SEC63 TS467DD SDM	GATACCAGATGACTTAATTCCTG	
SEC63 TS467EE SDM	GATACCAGAAGAGTTAATTCCTG	
SEC63 S512A SDM	CGTGGGGCTTGGTGCTGTCTGGTAA GTTCTCA	AGACAGCACCAAGCCCCACGTCTCTT TGTAGG
SEC63 S512D SDM	ACGTGGGGACTGGTGCTGTCTGGTA AGTTCTCA	AGACAGCACCAGTCCCCACGTCTCTT TGTAGG
SEC63 S512E SDM	ACGTGGGGAGTGGTGCTGTCTGGTA AGTTCTCA	AGACAGCACCACTCCCCACGTCTCTT TGTAGG
SEC63 T528A SDM	CTTCAAGCGCCAATTATCATTG	TATTTTACCATCTTTTTGAGAAC
SEC63 T528D SDM	CTTCAAGACCCAATTATCATTG	
SEC63 T528E SDM	CTTCAAGAGCCAATTATCATTG	

2.2.1. PCR

Standard PCR was conducted using NEB *Taq* DNA polymerase following manufacturers' specifications. A reaction of 25 µl would typically contain primers (manufactured by Sigma Aldrich) at a concentration of 0.2 µM, DNTP's supplemented to a final concentration of 200 µM, 50ng of template DNA and 0.75U of *Taq*. NEB Q5 high fidelity enzyme was used for all cloning and difficult to amplify targets. Reactions followed manufacturers' specifications, primer were used at a concentration of 0.5 µM and Q5 high fidelity polymerase was used at 0.5U per 25 µl reaction. PCR products were visualised on agarose gels.

2.2.2. Agarose Gel Electrophoresis

DNA fragments were separated in agarose gels (0.5-2%) made with 1x Sodium Borate buffer (50x SB - 1.8M boric acid adjusted to a pH of 8 using sodium hydroxide ~20g) supplemented with 0.1x Gel Green DNA stain. Before loading, samples were mixed with 6x loading buffer (30% glycerol, 60 mM Tris pH7.5, 0.1% (w/v) bromophenol blue) to a final concentration of 1x and electrophoresed at 60-120V until sufficient separation was achieved. DNA fragments were visualised under UV light in a BioRad Chemidoc.

2.2.3. Gel Extraction and PCR purification of DNA fragments

Following PCR or separation of DNA fragments, the products or specific band were purified using the Bioline ISOLATE II PCR and Gel Kit according to the manufacturers' specifications. DNA fragments were eluted in ddH20 to ensure downstream compatibility.

2.2.4. Poly A-Tailing of PCR products and Cloning

Prior to cloning into the preferred vector, each PCR fragment was initially cloned into the pGEM T Easy vector (Promega). PCR fragments generated from Q5 High fidelity polymerase lack a poly-A tail, therefore a PCR was set up in these cases containing, 10 µl of purified PCR product, 1U of NEB *Taq* polymerase, 200 µM dNTP's, and ddH20 up to a total volume of 20 µl. The reaction conditions were 95°C for 2 minutes, and 68°C for 5-10 minutes. Following poly A-tailing or standard PCR, the products were cleaned up and eluted in 15 µl of ddH20. A ligation reaction was conducted following the Promega pGEM T-easy vector specifications. Each 10 µl reaction consisted 5 µl of 2x ligation buffer, 1 µl of T4 DNA-ligase (Promega), 0.5 µl of pGEM T-easy vector, and 3.5 µl of PCR template. The ligation reactions were placed at 16°C overnight and 2-5 µl was transformed into XL-10 gold chemically competent *E. coli* cells. Following blue/white screening, positive clones were further screened using insert specific restriction sites, PCR, and sequencing to confirm the orientation. Once in pGEM T-Easy, the fragment could be liberated either using restriction sites incorporated in the insert during PCR or using the multi-cloning sites found within the vector. Ligations were then prepared from purified RE-digested vector and insert. A 10 µl reaction consisted of 1 µl of NEB T4 DNA-ligase (NEB), 1 µl of 10x Ligase buffer, and a ratio of vector to insert of 1:1, 1:3, or 1:7. Following ligation overnight at 16°C, 2-5 µl of the reaction was transformed into XL-10 gold chemically competent *E. coli* cells.

2.2.5. Restriction Endonuclease Digestion of DNA

Restriction endonuclease digests were performed using NEB enzymes and where possible using high fidelity enzymes. A typical 25 µl reaction would contain up to 2 µg of DNA, and 10-20U of enzyme and incubated at the recommended temperature for 1-2 hours in the appropriate buffer before being analysed by agarose gel electrophoresis.

2.2.6. Site Directed Mutagenesis

One of two techniques was employed for site directed mutagenesis (SDM). The first followed the methodologies developed by Stratagene/Agilent for the quickchange system. Primer oligos were designed with the changes incorporated into the central region of the oligo flanked either side with approximately 20 nucleotides and with a tm of 78°C, both forward and reverse primers were complimentary to one another. Each PCR contained 125ng of both forward and reverse primer, 200 µM dNTPs, and 2.5U of *pfu* high fidelity polymerase (Agilent). Cycle conditions were as follows; 1x (95°C for 30s), 16x (95°C for 30s, 55°C for 1 minute, 68°C for 1 minute per kb). Following PCR the products were treated with 10U of *dpnI* at 37°C for 1 hour before being transformed into *E. coli*.
The second technique employed the methodology developed by NEB for the Q5 Site-directed mutagenesis kit. The mutation is incorporated towards the 5' end of the forward primer with the reverse primer immediately adjacent to the 5' end of the forward primer but not overlapping. The PCR consist of the same components as described in the above Q5 reaction, with no more than 25ng of template. Cycle conditions were as follows; 1x (98°C for 30s), 25x (98°C for 10s, 50-72°C for 15s, 72°C for 20-30s per kb), and 1x (72°C for 2 minutes). Following PCR the a 10 µl reaction consisting of; 1 µl of PCR product, 10U of polynucleotide kinase, 20U of T4 DNA ligase, and 1x DNA Ligase buffer was incubated at 16°C overnight. The reaction was then treated with *dpnI* at 37°C for 1 hour and transformed into *E. coli.*

2.3. Protein Techniques

2.3.1. Total Protein Extract

Cultures of *S. cerevisiae* were grown and $5OD_{600}$ units were harvested by centrifugation at 3000g's, the resulting pellet was washed once in sterile ddH_2O and re-harvested. The pellet was then resuspended in 40 µl per OD of laemmli buffer (63 mM Tris-HCL pH 6.8, 10% glycerol, 5% β-mercaptoethanol, 2% SDS, 0.005% Bromophenol Blue) and acid washed glass beads were added up to the meniscus.

The mixture was then shaken in a MP-Bio FastPrep-24 5G (Speed-6, Time- 40 seconds) and immediately placed at 95°C for 5 minutes. The resulting lysate was isolated by piercing the lowermost end of the tube and placing it in another, the two tubes were centrifuged at 2000g's for 5 seconds to separate the liquid from the beads. The sample was then either immediately loaded or stored at -20°C for later use.

2.3.2. SDS-Poly Acrylamide Gel Electrophoresis of Protein

Following extraction, proteins were subject to SDS-PAGE in which their relative size was resolved. Typically, the resolving gel contained between 8 and 15% acrylamide subject to the size of the proteins being analysed. Resolving gels were composed of acrylamide (30% (w/v) Stock, 37.5:1 (Acrylamide:Bisacrylamide) Biorad) diluted to the required percentage in resolving buffer (375 mM Tris-HCl pH 8.8, 0.1% (w/v) SDS) and polymerised using 0.5% (v/v) of an ammonium persulfate solution (10% (w/v)), and 0.05% (v/v) of tetramethylethylenediamine (TEMED). Stacking gels were layered above the resolving gel and composed in much the same way, however the percentage of acrylamide was between 3-4.5% diluted in stacking buffer (125 mM Tris-HCl pH 6.8, 0.1% (w/v) SDS) and polymerised as above. Protein samples were loaded into the wells located in the stacking gel and the gel was placed in SDS running buffer (25 mM Tris, 192 mM glycine, 0.1% (w/v) SDS). Gels were run at 25-35mA for 1-2 hours. Following migration the gels were either stained using Coomassie stain (10% (v/v) glacial acetic acid, 40% (v/v) Methanol, 0.1% (w/v) Coomassie G250) or prepared for transfer.

2.3.3. Transfer of protein onto Nitrocellulose or PVDF membranes

Proteins were transferred onto either nitrocellulose or PVDF depending on the proteins being investigated (size) and the downstream procedures. If using PVDF the membranes were soaked in 100% methanol prior to use. To ensure an even transfer, a "sandwich" consisting of 3-5 sheets of 3MM CHR filter paper

(Whatman), one sheet of either nitrocellulose or PVDF, the gel being transferred, and a further 3-5 sheets of filter paper. The sandwich was soaked in transfer buffer (20 mM Tris-base, 150 mM glycine, 20% (v/v) methanol), and all air pockets removed using a roller. If using a semi dry approach, the sandwich was placed in a Bio-Rad Trans-Blot SD and ran at 150mA for 1.5 hours. Alternatively, a wet transfer tank kept at 4°C using 400mA for 3-4 hours, or 100mA overnight was used. In both instances, the gel was placed adjacent to the cathode.

2.3.4. Western Blotting

Following transfer membranes were placed in a blocking solution (5% (w/v) of dry skim milk powder (Diploma) dissolved in 1x TBS-T (130 mM NaCl, 2.6 mM KCl, 2 mM Tris-HCL pH7.6, 0.1% (v/v) Tween-20)) for a minimum of 30 minutes at room temperature, the solution was changed during this time. Prior to blocking, transfer efficiency could be checked on nitrocellulose but not PVDF using a Ponceau stain (0.5% (w/v) Ponceau S, 1% (v/v) Glacial acetic acid). Following blocking, the primary antibody was diluted in blocking solution and incubated on the membrane for 1-4 hours at room temperature, or at 4°C overnight, this was done with gentle agitation on a rocking platform. The primary antibody was removed, and the membrane washed at least three times in 1x TBS-T at 5-minute intervals. The appropriate secondary antibody (Horse Radish Peroxidase conjugated) again diluted in blocking solution was incubated on the membrane for 1 hour at room temperature. Again, the antibody was removed, and the membrane washed as above. The membrane was washed once in 1x TBS to remove any residual detergent and Pierce SuperSignal West Pico Chemiluminescent reagent was added to the membrane and left to incubate for 2 minutes, followed by visualisation using the Chemiluminescent protocol on a BioRad Chemidoc.

2.3.5. Preparation of *S. cerevisiae* membranes

Depending on the application *S. cerevisiae* cells were grown overnight, if requiring exponential phase, the cells were isolated between 0.5-1.0 OD_{600} units otherwise cells were isolated between 1.0-2.0 OD_{600} units. Cells were harvested at 3000g's for 5 minutes and resuspended in 100 mM Tris-SO_4 pH9.4, 10 mM β-mercaptoethanol to a concentration of 50 OD_{600} units/ml and kept at room temperature for 10 minutes. The cells were again harvested at 3000g's for 5 minutes and resuspended in spheroplast buffer (0.7M Sorbitol, 0.5% (w/v) Glucose, 50 mM Tris-HCL pH7.4) at a concentration of 100 OD_{600} units/ml, supplemented with either 1.5U of Zymolase per OD_{600} units of cells, or 3U of lyticase per OD600 per OD_{600} units of cells. Cells were incubated for a minimum of 30 minutes at 30°C with shaking. Spheroplasts were harvested at 2500g's for 5 minutes at 4°C (in pre-chilled rotors), and resuspended in Ice-cold Lysis Buffer (0.1M sorbitol, 50 mM KOAc, 20 mM HEPES, pH7.4, 2 mM EDTA, 1 mM DTT) at 200 OD_{600} units/ml and acid washed glass beads (~500 µM) were added up to 75% of the final volume. The cell/bead suspension was vortexed at least 5 times on high for 30 seconds a time, with 30 seconds on ice in-between each vortexing. The cell disruption was assessed microscopically and if sufficient 1ml of Ice-cold Lysis Buffer was added and vortexed for 10 seconds. The suspension was harvested at 1000g's for 10 minutes at 4°C (in pre-chilled rotors) and the upper soluble fraction transferred to microfuge tubes and harvested at 10,000g's for 20 minutes at 4°C. The resulting pellet was washed twice in membrane storage buffer (250 mM sorbitol, 20 mM HEPES, pH7.4, 50 mM KOAc, 1 mM DTT, 2 mM MgOAc) each time harvesting at 10,000g's for 20 minutes at 4°C. Membranes were finally resuspended in membrane storage buffer at 50 OD_{280} units/ml and snap frozen in liquid nitrogen and stored at -80°C until needed. When required, protease inhibitors and phosphatase inhibitors used. For protease inhibition a cocktail consisting : PMSF 1 mM, and 1% v/v Sigma protease inhibitor cocktail for fungi ((P8215), AEBSF 1 mM, E-64 14 µM, Pepstatin A 22 µM, 1,10-Phenanthroline 5 mM) was used. For phosphatase inhibition a cocktail consisting: Sodium Fluoride 20 mM, Sodium Orthovanadate 50mM, and

beta-glycerophosphate 50mM was used.

2.3.6. Cyclohexamide Chase

For cyclohexamide chase assays, 0.25 mg/mL chx was added to log-phase yeast cultures, and cell aliquots were removed at the indicated times after addition. Cells were harvested by centrifugation and resuspended in ice cold 10 mM NaN3 so as to ensure a halt in cellular activity through the depletion of ATP. Cells are again pelleted, with protein lysates prepared as above, and equal OD_{600} units were loaded onto SDS-PAGE gels, followed by transformation onto PVDF membranes and western blots performed as above. Band densitometry was performed using the biorad image dock software.

2.3.7. MRM Mass Spectrometry

For the identification of phosphorylation sites we chose to utilise multi reaction monitoring (MRM) mass spectrometry (MS). This approach differs significantly from standard MS approaches as only specific ions, those that possess the calculated mass/charge ratios for your peptide of interest, are isolated and used for analysis. This method is highly specific and can quantify peptides to the femtamole concentration. One aspect of this technique particularly useful for my purposes is ability to easily and accurately provide relative abundance without the use of complicated standards.

All MS work was performed by Proteomic international, Proteomics International is accredited for compliance with ISO/IEC 17025 also holds Research and Development accreditation to ISO/IEC 17025. All the information on the services can be found at https://www.proteomics.com.au/analytical-services/srms-mrm/, with all services and methods the intellectual property of proteomics International.

Investigating TOR Dependent Phosphorylation of Sec63.

3.1. Introduction

In higher eukaryotes there exists two main ER translocation pathways, co-translational and post translational. While the population of proteins that are directed to each pathway is diverse, there is a commonality to the translocation machinery. In yeast Sec63 is an essential component of both co- and post-translational translocation with phosphorylation required for its function. Specifically two C-terminal residues, T652 and T654, are phosphorylated by CK2 (Casein Kinase 2) *in vivo* (Wang and Johnsson 2005). Phosphorylation of Sec63 at these sites is constitutive and alters the ability of Sec63 to interact with Sec62. Mutation of either residue to a non-phosphorylatable alanine results in a decreased affinity for Sec62 binding by Sec63, which in turn results in post-translational translocation defects. While CK2 dependent phosphorylation of Sec63 has been documented, there is little evidence on how Sec63 activity can be co-ordinated at a more generalised level. Its central role in both co- and post-translational translocation, and the importance of Sec63s J-domain in regulating Kar2 activity places Sec63 in a unique position (Brodsky and Schekman 1993; Corsi and Schekman 1997; Jermy et al. 2006; Young et al. 2001). By specifically coordinating Sec63 activity, multiple aspects of ER function can be readily modulated.

One way in which this could be achieved is through the additional phosphorylation of Sec63. Published proteomics data has identified 4 phosphorylation sites in the C-terminal domain of Sec63 to which no function has been designated (Albuquerque et al. 2008a; Holt et al. 2009). I propose that these sites may be a target for TOR dependent phosphorylation, based primarily on the findings that a C-terminal phosphorylation site in Sec63 of *Schizosaccharomyces pombe* has the 4th greatest change globally in response to the TOR inhibitor Torin 1 (Dr Janni Petersen, Flinders University, Personal Communication). While significant differences exist between *S. cerevisiae* and *S. pombe*, this would indicate that TOR activity may possess the capacity to regulate certain aspects of the translocon and

the ER, mediated through Sec63. As the ER is a major site of protein synthesis and lipid biogenesis, it is a highly anabolic organelle, with significant energy demands. Therefore, ER activities would likely be significantly impacted by changes to TOR activity, as TOR is the master regulator of anabolic growth in response to nutritional signalling. Thus, providing the initial rationale for this proposed TOR dependent phosphorylation of Sec63.

The target of rapamycin (TOR) is a protein kinase complex which in yeast is encoded primarily by two genes, *TOR1* and *TOR2*, with both of these protein kinases the central component in TORC1 and 2 (TOR complex) protein complexes (Schmelzle and Hall 2000). While either Tor1 or Tor2 can be incorporated into TORC1, TORC2 exclusively contains the Tor2 subunit. The central components Tor1 and Tor2 possess domains homologous to phosphatidylinositol kinases (PIK), however there is little to suggest lipid kinase activity is present. Instead, like many PIK-related kinases, they specifically phosphorylate serine and threonine residues. It is this activity in which the TOR complexes are able to regulate a multitude of cellular processes. TOR activity is primarily directed through the activation of downstream effectors, which in turn are responsible for the phosphorylation of an even greater pool of substrates, thus TOR sits at the centre of this signalling network. The primary effector phosphorylated by TORC1 is Sch9 (S6-kinase in mammals), with Ypk2 being the primary target of TORC2 (Loewith and Hall 2011). Each of these intermediate kinases are responsible for the ensuing signalling cascade that is able to rapidly communicate the nutritional availability of the cell, as discerned by TOR. In regard to the activities co-ordinated by each pathway, TORC1 characterisation has identified its functions in cellular growth through the regulation of protein synthesis; ribosome biogenesis and cell size/growth (Hinnebusch 2005; Jorgensen et al. 2004; Lempiäinen and Shore 2009). The complex also inhibits the cellular responses to stress, and through the regulation of various transporter proteins, TORC1 can control the uptake of particular nutrients dependent upon their availability (Loewith and Hall 2011). TORC2 appears to be less promiscuous but is still critical for cellular development. TORC2 has been shown to regulate actin polarisation, which is crucial to all cytoskeletal functions

(Kamada et al. 2005). Furthermore, *TOR2* mutants display deficiencies in the correct organisation of actin, resulting in defective cell division, secretion of proteins and lipids to the budding daughter cell (Loewith and Hall 2011). TORC2 has also been implicated in endocytosis, a function critical for the control of cell growth (Bultynck et al. 2006). Additionally TORC2 stimulates the biosynthesis of sphingolipids, a functional and structural component of lipid bilayers (Powers, Aronova and Niles 2010).

I postulate a role for TOR dependent phosphorylation in the regulation of ER activity, specifically the modulation of Sec63 activity. As previously stated, Sec63 in *S. pombe* has previously been identified to be a TOR substrate. The interactions of Sec63 with multiple components of the ER and in particular, the various components involved in translation and translocation would make Sec63 an ideal candidate for regulation by TOR. Furthermore, as the entry point to the secretory pathway, any changes to the activity of the translocon would have far reaching consequences. For these reasons, I have investigated if there exists a link between Sec63 and TOR and attempted to ascertain any changes that occur upon its disruption.

3.2. Results

3.2.1. The C-terminal domain of Sec63 contains multiple phosphorylation sites

Several phosphorylation sites have previously been characterized in Sec63, most notable are T652 and T654 located at the extreme C-terminus of Sec63 (Wang and Johnsson 2005; Ampofo et al. 2013). Phosphorylation of these residues by CK2 is required for the tight association of Sec63 with Sec62 and is thus required for efficient posttranslational targeting to the ER. The remaining phosphorylation sites identified reside within the Brl-domain of Sec63. Whilst the precise function of this region is not known, the Brl-domain is essential for Sec63 function (Jermy et al. 2006). As such, the congregation of four phosphorylation sites within this domain indicates that its activity may be regulated by several signalling nexuses. It is suggestive that TOR activity may coordinate activity of this domain as the observed phosphorylation of residue T504 in the Brl-domain of Sec63 in *S. pombe* was found to be the 4th largest change, with phosphorylation being depleted upon inhibition of TOR activity (Dr Janni Petersen, Flinders University, Personal Communication). Its corresponding location within the BRL domain of Sec63 was used as the rationale to investigate the phosphorylation status of Sec63 in
S. cerevisiae upon inhibition of TOR. Of the four candidates in *S. cerevisiae*, Y450 is the least likely to be representative of the T504 residue in *S. pombe*, due the paucity of true tyrosine kinases in *S. cerevisiae*, with phosphor-tyrosine making up as little as 0.05% of the phosphoproteome (Chi et al. 2007). The remaining sites, T467/S468, S512, and T528 were evaluated as candidates for TOR dependent phosphorylation.

Several phosphoproteomic studies have attempted to derive consensus motifs for TOR-dependent phosphorylation, but as TOR activity is primarily conducted through downstream effectors, no single consensus motif is representative of global TOR activity (Soulard et al. 2010).However, for the purpose of determining which, if any, of the remaining candidates were potential TOR substrates, a PSSM's

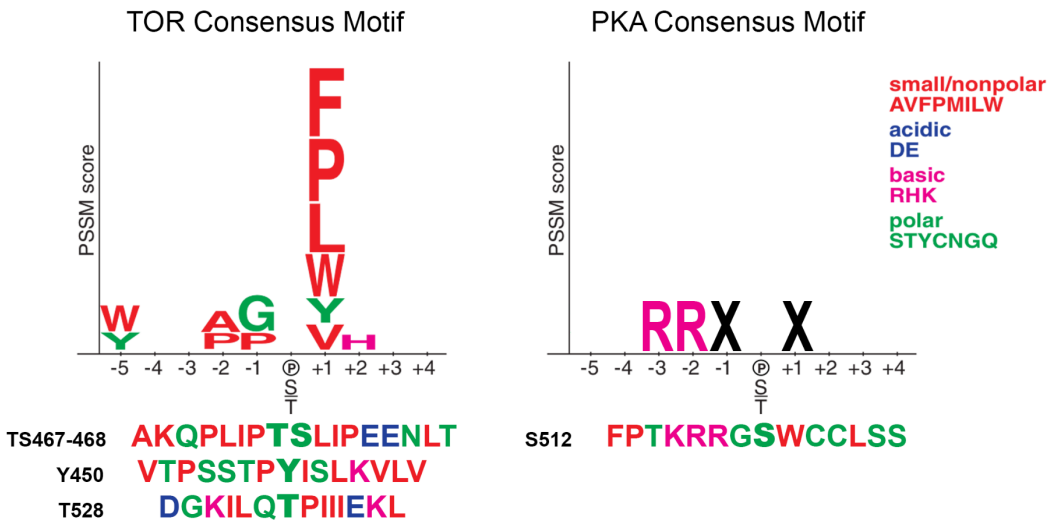

Figure 3.1 Comparison of Sec63 phosphorylation sites with the consensus motifs of TOR and PKA.

Graphical representation of the TOR and PKA consensus motifs, whereby the relative size of each amino acid correlates to the likelihood of this amino being present at a particular position. Regarding the motif for PKA, any amino acid can be present at positions -1 and +1. The sequences of the amino acids are coloured based on their amino acid properties, highlighting similarities to the consenus'. This figure has been adapted from (Hsu et al. 2011).

(Position Specific Scoring Matrix) was utilised generated form the global proteome of mTOR (mammalian TOR) (Hsu et al. 2011). As can be seen in figure 3.1, T528 has the least similarity to the motif, whereas both T467/S468 and S512 share a modest resemblance to the predicted consensus motif. Upon further investigation, it was determined that S512 conforms perfectly to a PKA consensus motif, and not TOR. However, it is also reported that significant overlap exists between TOR and PKA, with TOR identified to phosphorylate the R-R-X-**S**-X motif of PKA (Pedruzzi et al. 2003; Soulard et al. 2010). This analysis is suggestive that both T467/S468 and S512 are potential substrates for TOR phosphorylation.

3.2.2. Identification of rapamycin sensitive phosphorylation in Sec63

My initial bioinformatics analysis of the sequences surrounding the Sec63 phosphorylation sites has identified two out of the four which partially conform to consensus motif for TOR phosphorylation. The four phosphorylation sites contained within the Brl-domain of Sec63 were identified in large-scale phosphoproteomic studies under varying conditions (Holt et al. 2009; Albuquerque et al. 2008b). Most notably S512 has been identified in at least 5 studies, with one looking at the effect of TOR inhibition, although no significant change was identified (Li et al. 2007; Chi et al. 2007; Holt et al. 2009; Albuquerque et al. 2008b; Soulard et al. 2010). For my investigation, I wished only to survey the phosphorylation status of Sec63. As such a more targeted approach is required to identify those residues whose phosphorylation status is altered upon TOR inhibition. Therefore, I utilised multiple reaction monitoring (MRM) mass spectrometry to specifically and accurately measure the abundance of the four potential TOR phosphorylation sites (Mass spectrometry was performed by Proteomics International – see chapter 2.3.7).

Purification of Sec63 using antibody crosslinked beads or IgG purified TAP tagged Sec63, was assessed initially. The use of both techniques yielded insufficient protein content and were therefore dismissed. Fortunately, as MRM is able target peptides of specific mass/charge ratios for further analysis, unpurified mixtures of protein can be used. To determine the effect of TOR inhibition on Sec63

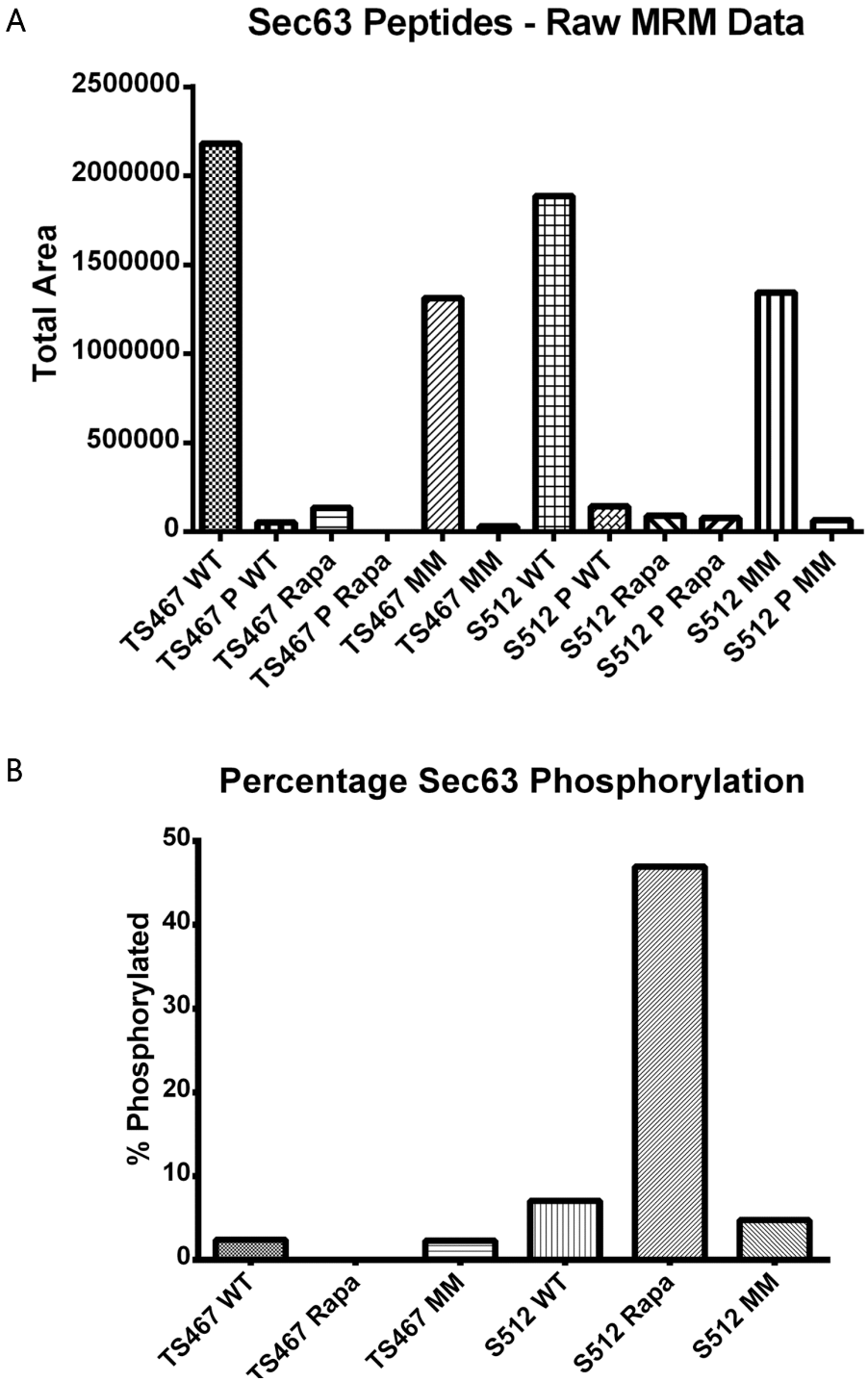

Figure 3.2 Identification of phosphorylated Sec63 using MRM mass spectrometry.

(A) Shown here are the raw values for each peptide corresponding to the phosphorylation sites TS467-468 and S512 in both their native and phosphorylated state from BY4742 cells grown in YPD (WT), YPD + rapamycin (Rapa) and yeast nitrogen base (MM). For each peptide total area under the curve values were used representing the maximum detected values. (B) Using the above data, the percentage phosphorylation for each site was calculated for each condition tested.

phosphorylation, the potent inhibitor rapamycin was used to treat wildtype cells. Early to mid-log cells were treated with 250 ng/ml of rapamycin or mock treated for 2 h (growth is severely inhibited at 10-50 ng/µl, this concentration was used to ensure near complete inhibition of TOR activity). Samples were also prepared from untreated cells grown in yeast nitrogen base (YNB) to simulate a more 'physiological' decrease in TOR activity. As YNB is a nutrient restrictive medium, it provides cells with the minimum requirements for growth, a consequence of this is a decrease in translation, corresponding with decreased TOR activity (Stracka et al. 2014). Following treatment, cells were harvested, and crude membranes isolated in the presence of several protease and phosphatase inhibitors. Once isolated, membranes were solubilised, and equivalent $OD_{260/280}$ units loaded onto SDS-PAGE gels. For each experimental condition, two technical replicates were combined prior to SDS-PAGE. Following electrophoresis, an immunoblot for Sec63 was performed on an aliquot of each sample, checking for the quality, abundance and location of Sec63, with a corresponding small portion of the gel (~10mm x 20mm) extracted and used for MRM mass spectrometry (Data not shown).

The targeted mass spectrometry approach used was able to identify all peptides containing the residues of interest. Phosphorylated versions of Y450 and T528 were undetectable and were not investigated further. In WT conditions, phosphorylation of both remaining sites was detected, with the phospho-version representing less than 10% of the total detected peptide (Figure 3.2 (A)). Upon treatment with rapamycin, phosphorylation of T467/S468 was completely ablated, demonstrating its phosphorylation to be extremely rapamycin sensitive. No significant change was observed when cells were grown in YNB, which is not unexpected as TOR activity is diminished and not abolished under these conditions. More surprising were the changes in phosphorylation of S512 upon treatment with rapamycin. In WT conditions, phospho-S512 represented ~7% of the total detected S512 containing peptides. Following treatment, a considerable increase was detected, with the phosphopeptide comprising ~47% of the total detected S512 peptides (Figure 3.2 (B)). Together this data indicates that two sites within the Brl domain of Sec63 are differentially phosphorylated depending on the activity of

TOR. As S512 phosphorylation is upregulated upon rapamycin treatment and there is a loss of T467/S468 phosphorylation I speculate if this is a compensatory mechanism. The significance of this alone is limited, however it corroborates with observations in *S. pombe*.

3.2.3. Characterisation of the TOR reactive phosphorylation sites of Sec63

My bioinformatics analysis and mass spectrometry data support the notion that Sec63 harbours TOR dependent phosphorylation sites. To determine what role these sites play, and how they affect Sec63 and ER function in general, a mutational approach was used. Specifically, site directed mutagenesis was employed to mutate residues T467/S468 and S512 and to a non-phosphorylatable form (alanine substitution) and to phospho-mimetic residues (aspartic acid and glutamic acid substitution). Mutants for the T528 phosphorylation site were also generated in the same manner, however much of the focus for this work is on the TOR reactive sites revealed by mass spectrometry. Site directed mutagenesis was performed on the pJKR2 vector, a yeast centromeric vector that harbours a functional *URA3* gene that confers uracil prototrophy to otherwise *ura3Δ* dependent uracil auxotrophs and *SEC63*. As *SEC63* is an essential gene, a functional analysis of each mutant generated was performed in two distinct systems. Initially mutants were transformed into BYY5, a W303α strain with the endogenous *SEC63* expressed via the *MET3* promoter. This system allows for the suppression of *SEC63* expression upon the addition of methionine to the growth media, and has previously been instrumental in understanding the importance of the Brl-domain of Sec63 (Jermy et al. 2006). Initial characterisation was conducted by transforming the generated mutants, vector control and pJKR2 into BYY5, and following successful transformation, cells were spotted out on YNB, with or without the addition of 2 mM methionine. As expected, the vector control is unable to support growth upon suppression of endogenous *SEC63* with the addition of methionine. The WT containing vector pJKR2 rescues the ability of BYY5 to grow in the presence of methionine, as do all vectors harbouring mutated *SEC63*. As no discernible changes

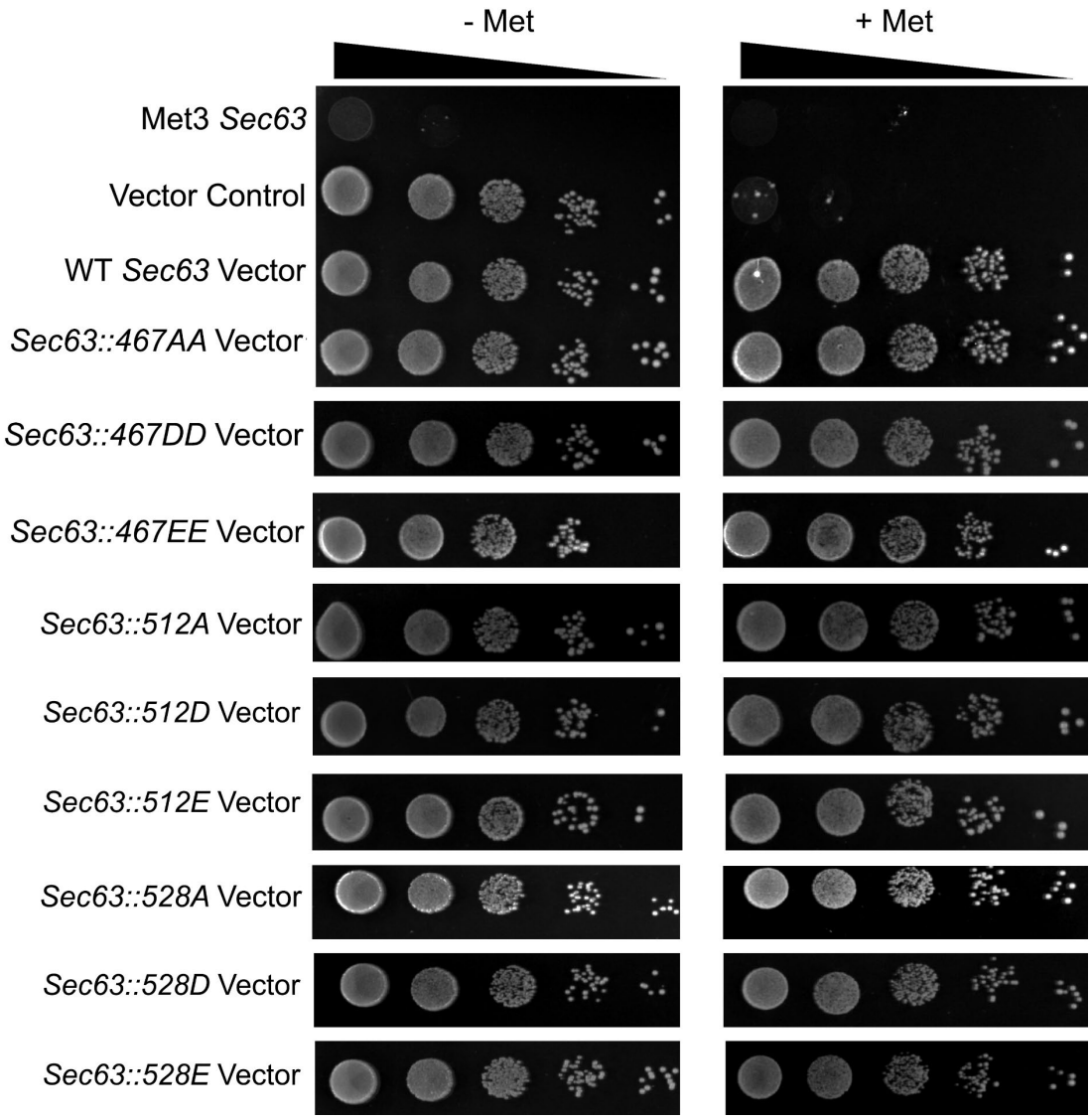

Figure 3.3 Growth of *SEC63* phosphorylation mutants in the BYY5 strain.

BYY5 cells have the endogenous *SEC63* gene under the transcriptional control of *MET3* promoter, thus in the presence of 2 mM methionine *SEC63* expression is repressed. As *SEC63* is an essential gene only cells expressing a functional copy are viable when grown in the presence of 2 mM methionine. To test the function of the mutants generated, serial dilutions of cells were spotted onto -Ura YNB with and without methionine and grown at 30^{o}C for 2d. The same procedure was carried out for cells grown at 18^{o}C and 37^{o}C, and for cells grown in the presence of 5 mM DTT and 10 µg/ml of Tm.

were observed at 30°C, spot tests were also performed at 18°C and 37°C, to determine if changes in growth temperature were able to exacerbate any defects as a result of the mutations made. As before, no changes were observed in the growth of the mutated *SEC63* bearing cells (Figure 3.3). Finally, cells were treated with the reductant DTT and the N-glycosylation inhibitor Tm, as both are known to disrupt normal ER function. Once again, no change in the growth of BYY5 harbouring the various mutants was observed. As no changes in growth were observed for any of the mutants in all conditions tested, growth at 30°C has been used to represent all conditions tested (Figure 3.3).

Disruption of translocon components like Sec63 typically leads to the defective translocation of precursors into the ER, and difficulties in maintaining appropriate N-glycosylation. As such, the translocation of several ER resident proteins into the ER were examined by immunoblot. As Sec63 is a long-lived membrane protein, tests were initially performed to determine how long cells were required to be pre-treated with methionine to sufficiently deplete the endogenously expressed Sec63. In the presence of 2 mM methionine, BYY5 cells alone were observed to have significantly reduced growth after 4 hours of treatment, but detectable levels of Sec63 remained. However, depletion of Sec63 as determined via western blot indicated that treatment for 7 hours resulted in a near total loss of Sec63, and therefore this was the preincubation time chosen for all subsequent analysis. Whole cell lysates were prepared from cells both with and without 2 mM methionine, and blots were performed for Sec63, Sec61, Lhs1, Kar2, and Sil1 (Figure 3.4). Following methionine treatment, both strain alone and vector control have Sec63 levels significantly decreased (below detection), while Sec61 levels show a marked increase (Figure 3.4 (A)). This increase is representative in several of the mutants following the addition of methionine, however to a lesser degree. This may be a result of UPR induction, or the general imbalance of the translocon due to depletion of Sec63, as such I do not regard this to be indicative of altered Sec63 activity. In regard to Sec63 levels, ectopically expressed *SEC63* appears equally abundant when compared to the strain alone without addition of methionine (Figure 3.4 (A)). The migration of Sec63 was unperturbed in all samples

except for *Sec63::467AA*, where a marginal increase in its molecular weight is observed, as to why, no conclusions have been made (Figure 3.4 (B)). The same can be said for all mutant vectors. As expected, the strain alone and vector control in which Sec63 levels are significantly depleted, accumulation of untranslocated Kar2, Lhs1 and what is likely untranslocated Sil1 is seen (Figure 3.4 (A)). Outside of the strain alone and the vector control, no discernible differences are observed in any of the ER markers tested with the exception of Sil1. Regarding changes to Sil1, the accumulation of a lower molecular weight species, which would be consistent with unglycosylated Sil1, is evident in several of the mutant vectors tested (Figure 3.4 (B-D)). This specie does not consistently accumulate in these mutants, therefore no conclusions can be made. It does however suggest that Sil1 maturation may be sensitive to various perturbations in ER homeostasis, and thus warrants further investigation. Collectively, the growth and immunoblot data would suggest that mutating each of the four phosphorylation sites in Sec63 exhibits no significant alteration to function of Sec63 and the ER in general. However this system is far from ideal, Sec63 suppression using the *MET3* promoter has several limitations, primarily suppression is likely not absolute, due to the long half-life of Sec63, thus totally depleting endogenous Sec63 is a difficult process. Furthermore, the background strain W303 is known to be genetically distinct from the primary genetic background of S288C, which the majority of laboratory strains are derived (Matheson, Parsons and Gammie 2017).

Due to the concerns above, a more rigorous system was utilised for further analysis of the two TOR responsive phosphorylation sites T467/S468 and S512. As *SEC63* is an essential gene, genetic knockouts require complementation with ectopically expressed *SEC63*. The *SEC63* shuffle strain BWY780, derived from the BY474 background, is maintained through expression of *SEC63* on a *URA3* centromeric vector while the endogenous copy is deleted. These so called ‘shuffle’ strains provide the opportunity to investigate the functionality of mutant variants of the gene, whereby the mutant is the only copy of the gene within the cell. This is accomplished through the transformation and expression of the mutant variant on

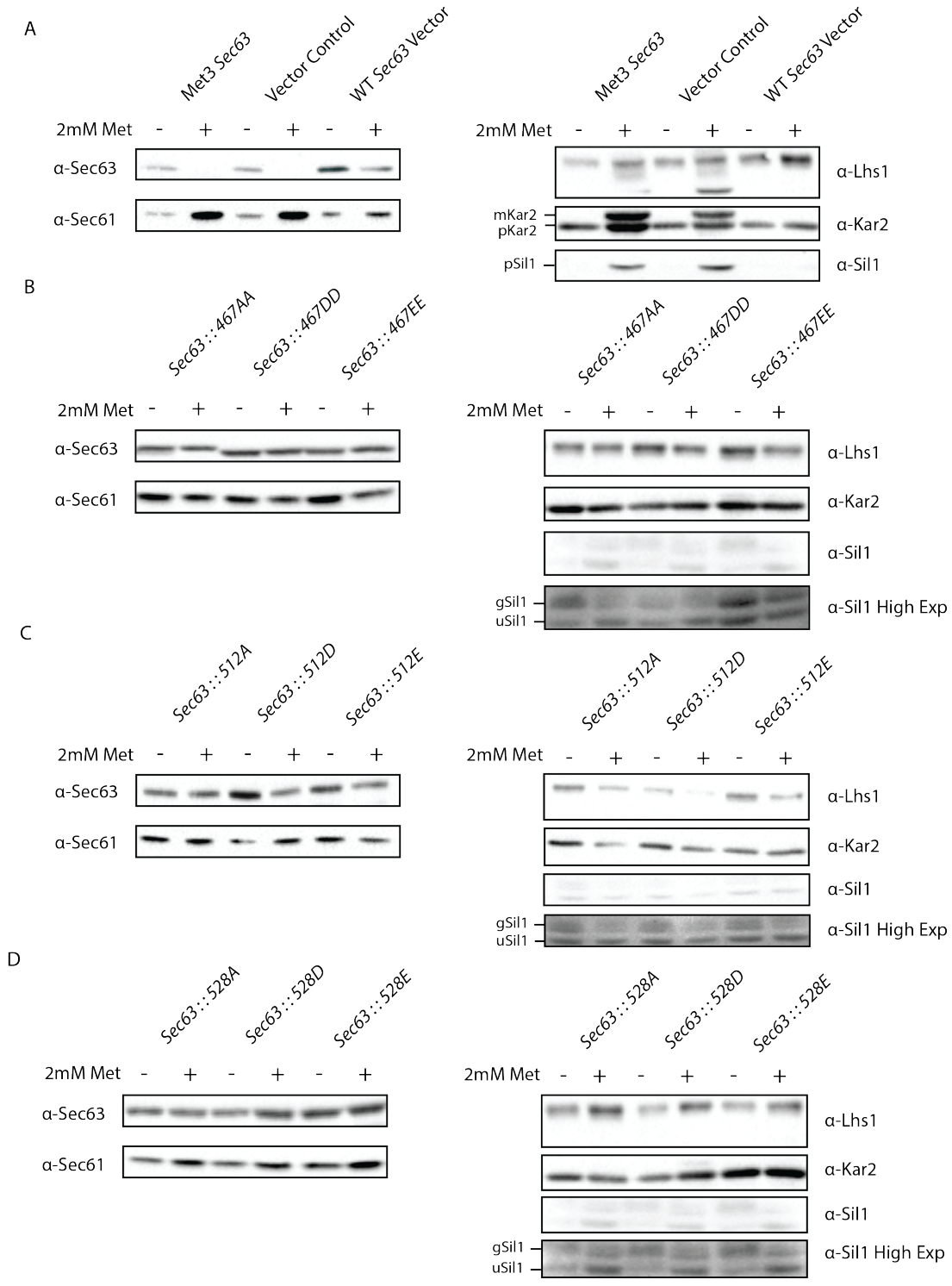

Figure 3.4 Immunoblot analysis of ER markers from cells expressing phosphorylation mutants of *SEC63.*

BYY5 cells and cells expressing vector control (pRS316), WT Sec63 Vector (pJKR2), (A) or *SEC63* mutants (B-D) were grown to mid-log in YNB alone or in the presence of 2 mM methionine. Immunoblot analysis was conducted for the prepared lysates, with Sec63, Sec61, Lhs1, Kar2, and Sil1 examined.

a plasmid containing any prototrophic marker other than *URA3* into the shuffle strain. Following transformation with the mutant, the WT ectopically expressed gene is counter selected for utilising the compound 5-Fluoroorotic acid (5FOA). 5FOA is a fluorinated precursor used by the *URA3* gene to synthesise 5-flourouracil, an acutely toxic compound. Thus, only cells that no longer propagate the *URA3* selective vector, which also harbours the wild type *SEC63*, can survive providing that the mutant *SEC63* derivative is also functional. However, cells cannot grow if the mutant derivative is non-functional. As the initial vectors were derived from a pRS316 background (*URA3*) several methods were employed to generate vectors compatible with the shuffle strain. While the obvious protocol would be simply to subclone *SEC63* from pRS316 into a compatible backbone, such as pRS315 (*LEU2*) or pRS313 (*HIS3*), difficulties in the generation of these strains resulted in alternative approaches to be employed in tandem. The alternative approach utilised the natural homologous recombination machinery of yeast to insert either the *LEU2* or *HIS3* gene into the *URA3* locus on pRS316. This was accomplished by co-transforming my *URA3* containing *SEC63* vectors with SmaI digested pUL9 or pUH7. These vectors contain the *URA3* gene disrupted internally by either *LEU2* or *HIS3*, thereby providing the sites of recombination for *URA3*, while simultaneously inserting the new selectable marker. Transformants were then plated onto YNB supplemented with the appropriate amino acids, with successful candidates screened for their loss of uracil prototrophy. Additionally, diagnostic digests were performed to confirm the insertion of either the *LEU2* or *HIS3* gene into the *URA3* locus. This method was successful in generating WT *SEC63* and $SEC63^{467/468\text{-}AA/EE}$ with *LEU2* and *HIS3* cassettes. Subsequently, routine subcloning of the WT *SEC63* gene into pRS313 was also achieved, and the regeneration of each mutant through SDM provided the entire suite of vectors for analysis.

Initially, the shuffle strain BWY780 was transformed with WT *SEC63*, $sec63^{467/468\text{-}AA}$, and $sec63^{467/468\text{-}EE}$ marker swapped vectors. Following transformation, colonies were transferred to YNB supplemented with 5x excess uracil, and 5-FOA (1g/L final concentration) in order to chase out the WT *SEC63 URA3* vector. Genetic complementation with the mutated vectors was successful

indicating that the mutations do not completely disrupt Sec63 function. As before, spot tests were used for growth at permissive (30°C) and restrictive temperatures (37°C) to identify any reduction in function of the generated mutants. Growth was as WT with the exception of *sec63*$^{A467/A468AA}$, which had a significant growth defect at 37°C (Figure 3.5(A)). Interestingly, extended maintenance at room temperature, led to a reversion in temperature sensitivity, potentially indicating a significant loss of Sec63 function at all temperatures. To address this, the strain was regenerated at regular intervals, and temperature sensitivity checked prior to further work.

As significant perturbations were observed during growth at 37°C, immunoblot analysis of Sec63 and Kar2 and Sil1 was conducted, at both 30°C and 37°C. For this, BWY780 cells expressing WT *SEC63*, *sec63*$^{467/468\text{-}AA}$, and *sec63*$^{467/468\text{-}EE}$ were grown in YPD to mid-log, and whole cell lysates prepared. Immediately of note when analysing the migration of Sec63 was the apparent decreased molecular weight of the *sec63*$^{467/468\text{-}AA}$ mutant in comparison to both WT *SEC63* and *sec63*$^{467/468\text{-}EE}$ (Figure 3.5 (B)). While the electrophoretic mobility of proteins can be altered when phosphorylated, this would not explain the observed mobility shift for the *sec63*$^{467/468\text{-}AA}$ mutant, as mutation of the same site to glutamic acid had no effect to its apparent molecular weight. Also of note was the accumulation of the untranslocated form of Kar2 at both permissive and elevated temperatures, with an obvious increase in pre-Kar2 accumulation at 37°C. Together this data would indicate that disruption of the TOR dependent phosphorylation sites T467 and T468 is detrimental to Sec63 function, and as Kar2 translocation was perturbed, results in disruption to the translocation of precursors into the ER (Figure 3.5 (B)). While this data provides support for both my mass spectrometry findings and my initial hypothesis that TOR dependent phosphorylation of Sec63 may be required for its function, the significant change in the migration of the *sec63*$^{467/468\text{-}AA}$ mutant raises concern. Particularly as the apparent molecular weight of *sec63*$^{467/468\text{-}AA}$ in BYY5 cells (MET-*SEC63*) was observed to be marginally greater than in WT Sec63 and all the mutants tested. As no differences were noted in the diagnostic restriction digests performed following marker swap, my only conclusion was that further

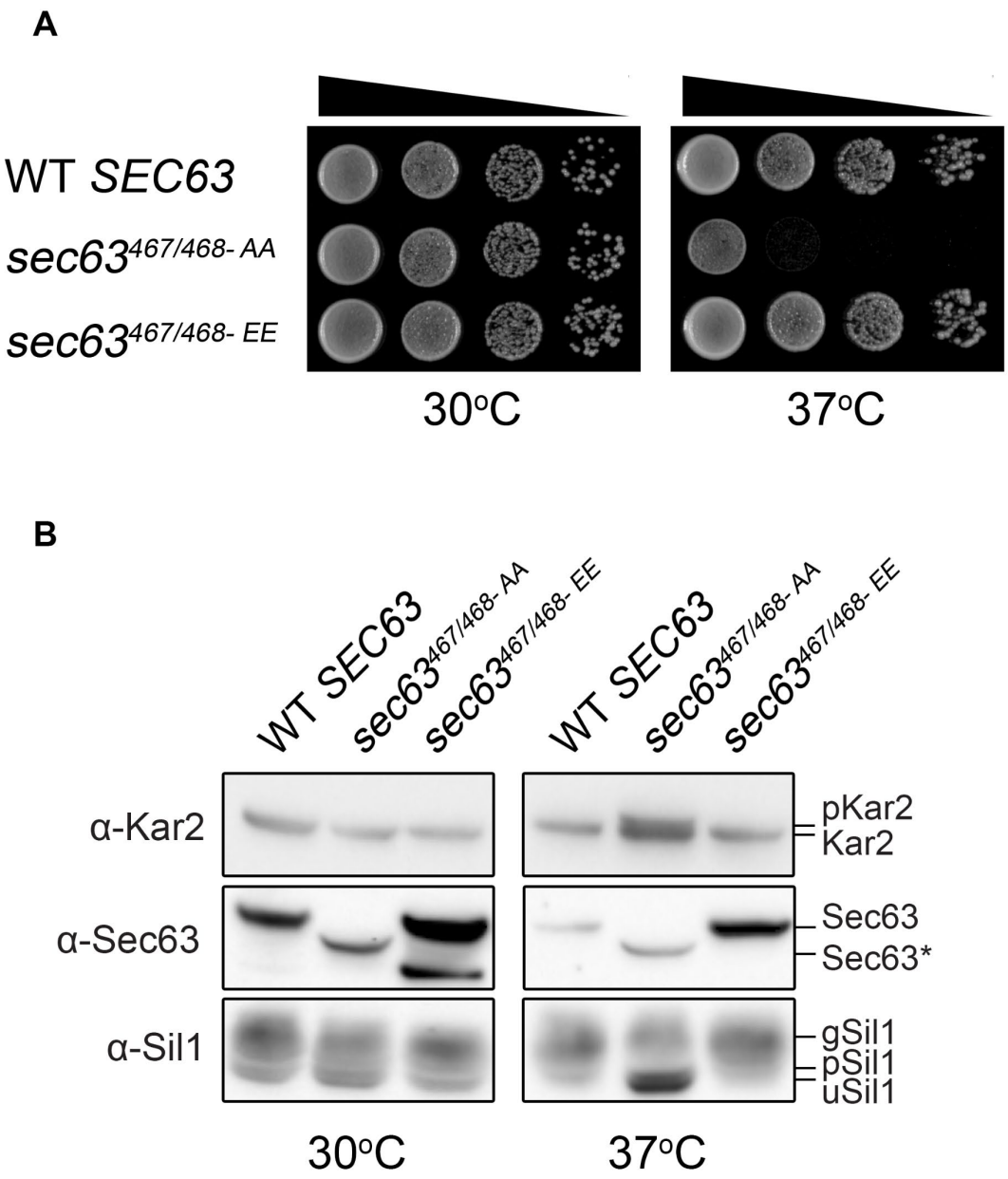

Figure 3.5 Growth and immunoblot analysis of *SEC63* mutants in the *SEC63* shuffle strain.

(A) Shown is the growth of BWY780 cells following the successful transformation of marker swapped vectors expressing *SEC63* and counterselection on 5FOA. Cells were grown to mid-log, harvested and resuspended to an OD_{600} of 1, with serial dilutions spotted onto YPD agar and grown at the indicated temperatures for 2 days. (B) Cells were generated as in (A), followed by growth in YPD to mid-log at the specified temperatures. Equivalent ODs of cells were harvested, and protein lysates ran on SDS-page gels with immunoblotting for Sec63, Kar2 and Sil1. Sec63* denotes the form migrating more rapidly than in WT.

mutational events may have occurred within *sec63*$^{467/468\text{-}AA}$. To address this, marker swapped *sec63*$^{467/468\text{-}AA}$ was sequenced to determine if any changes had occurred during the marker swap process. As suspected the sequencing data identified a 60 bp deletion 12 bp downstream of residue 1404 in the *SEC63* ORF (Serine 468). Interestingly, during the generation of this marker swapped vector, several plasmids were isolated also displaying the same molecular weight shift, which is suggestive that this locus may be a recombination hotspot. This deletion did not disrupt the mutated sites nor the reading frame of Sec63, however this does explain the observed difference in molecular weight, and potentially the decreased fitness of the mutant. As deletions in the Brl-domain of Sec63 have previously been associated with significant translocation and growth defects, this observation is not surprising. Although this deletion event does not help dissect the specific functional consequences of mutating the confirmed phosphorylation sites T467-S468, the decreased fitness of this mutant (henceforth *sec63*$^{467/468\text{-}AA\text{-}Trunc}$) provides greater insight into the role of the Brl-domain. Additionally, the close proximity of the deletion to residues T467-S468 may elucidate the role of this sub-domain and has been analysed herein.

As previously stated, successful subcloning of the *SEC63* gene into pRS313 was followed by SDM to produce the required mutations for analysis. However, as previous investigations had been inconclusive, the final analysis was conducted with only alanine mutants. Additionally, due to the observation that phosphorylation of S512 is significantly increased upon rapamycin treatment, whereby T467-S468 phosphorylation is lost, mutational analysis of S512 was performed in conjunction with T467-S468 giving rise to the mutant *sec63*$^{467/468/512\text{-}AAA}$, with the rationale that any potential compensatory mechanisms, as elicited by S512 phosphorylation, are mitigated. As before, BWY780 cells were transformed with WT *SEC63*, *sec63*$^{467/468\text{-}AA}$, *sec63*$^{467/468/512\text{-}AAA}$, and *sec63*$^{467/468\text{-}AA\text{-}Trunc}$ followed by counterselection on 5-FOA. Following the plasmid shuffle, spot tests were conducted at 18^{o}C, 30^{o}C and 37^{o}C on YPD and YNB to determine if any of the mutants are detrimental to growth. Growth was also conducted in the presence of

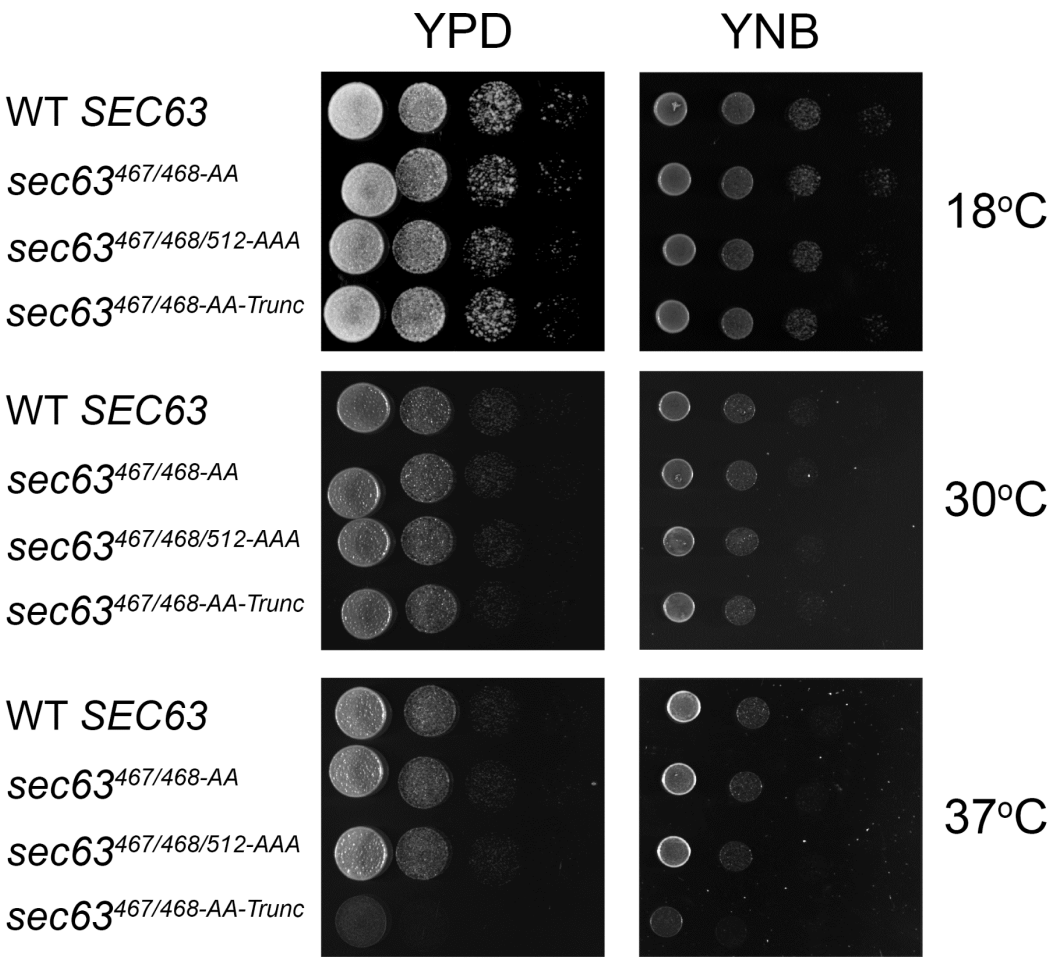

Figure 3.6 Growth of *SEC63* mutants in the *SEC63* shuffle strain

Shown is the growth of BWY780 cells following the successful transformation of subcloned *SEC63* mutants and counterselection on 5FOA. Cells were grown to mid-log, harvested and resuspended to an OD_{600} of 1, with serial dilutions spotted onto YPD agar and YNB, and grown at the indicated temperatures for 2 days.

rapamycin at both 30°C and 37°C (data not shown). As before, growth of *sec63*$^{467/468\text{- }AA\text{-}Trunc}$ was significantly reduced at 37°C, but no additional sensitivity was noted when grown in the presence of rapamycin, as such growth in the absence of rapamycin has been used as a representative. With regards to the *sec63*$^{467/468\text{- }AA}$, and *sec63*$^{467/468/512\text{-}AAA}$ mutants, no changes in growth were observed for any of the conditions tested including growth in the presence of rapamycin (Figure 3.6). It can therefore be concluded that disruption of the TOR sensitive phosphorylation sites does not grossly affect the function of Sec63, unlike the truncated version of Sec63. As such, I continued my analysis of the mutants generated by observing if there were any changes to the translation and translocation of specific ER resident proteins. To reiterate, even though mutation of the phosphorylation site has no effect, it is clear from *sec63*$^{467/468\text{- }AA\text{-}Trunc}$ that this particular region of the Sec63 Brl domain is of importance for normal function.

As before, cells were grown in YPD to mid-log at both 30°C and 37°C before being harvested, and protein lysates ran on SDS-PAGE gels. As I had previously seen changes in molecular weight of Sec63, and as loss of phosphorylation can alter its electrophoretic mobility, I looked to see if there were any changes. The *sec63*$^{467/468\text{-}AA\text{-}Trunc}$ mutant was observed to have the expected decrease in molecular weight, which corresponds to the 20 amino acid deletion in this mutant. However, the remaining mutants migrated along with the WT Sec63, and protein levels in all samples were equivalent, thus indicating the mutations have no effect on the half-life of Sec63 (Figure 3.7). Lysates were also probed for Kar2, Lhs1, and Sil1, as their translocation, protein abundance and modification provide insight into the physiological state of the ER. The translocation of the ER Hsp70 Kar2 can occur via both the co- and posttranslational pathways, thus the accumulation of pre-Kar2 (pKar2) can be indicative of a general defect in translocation. Additionally, as a fundamentally important component required for protein folding, Kar2 is greatly upregulated via the UPR, thus the accumulation of Kar2 is indicative of ER stress. No changes in the abundance of Kar2 were observed for WT *SEC63*, *sec63*$^{467/468\text{-}AA}$ and *Sec63*$^{467/468/512\text{-}AAA}$ (Figure 3.7). With regards to the *sec63*$^{467/468\text{- }AA\text{-}Trunc}$ mutant, I

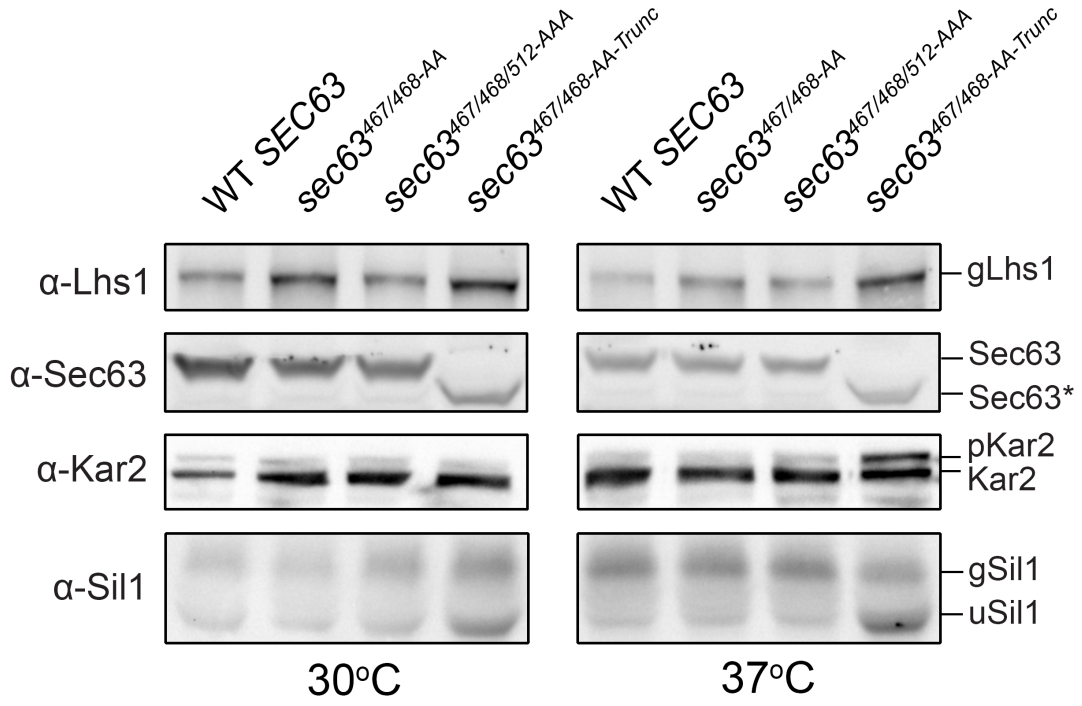

Figure 3.7 Immunoblots of *SEC63* mutants in the *SEC63* shuffle strain

Liquid cultures of BWY780 cells were prepared following the successful transformation of subcloned *SEC63* mutants and counterselection on 5FOA. Cells were grown to mid-log, harvested and whole cell lysates prepared. Lysates were probed for multiple ER makers. Sec63* indicates the truncated Sec63.

observed the accumulation of pKar2 at 37°C, but no obvious increase in its abundance at either temperature. As for Lhs1, being a glycoprotein allows not only its translocation competency to be assessed, but also observe if the mutants present any defects in glycosylation. No significant differences were noted for the translocation, modification or accumulation of Lhs1 in all mutants tested, at 30°C and 37°C respectively. This would suggest that not only is the glycosylation machinery intact, but also as a co-translocational substrate, that the *sec63*$^{467/468\text{- AA-}Trunc}$ mutant does not disrupt the co-translational translocation machinery. Furthermore, as a UPR target, the unchanged accumulation would also suggest none of these mutants activate the UPR.

I also looked at Sil1, as a glycoprotein and significant target of the UPR, any changes observed can provide insight in the general health of the ER. As before, no changes were observed for any of the mutants, except for *sec63*$^{467/468\text{- AA-}Trunc}$. It can be seen the accumulation of uSil1 at both 30°C and 37°C, with an increased accumulation at the non-permissive temperature. I have previously seen the accumulation of uSil1 in several of the mutants in the *MET3-SEC63* strain. I initially concluded this was due to general ER stress associated with the repression of the endogenous *SEC63*. However, the accumulation of uSil1 in these instances was far less pronounced than observed in *sec63*$^{467/468\text{- AA-}Trunc}$. The accumulation of uSil1 has also been observed in previous work following the chemical induction of the UPR. It would stand that as glycosylation of Lhs1 in unaffected, and that Sil1 levels appear elevated in *sec63*$^{467/468\text{- AA-}Trunc}$, that a mild UPR induction may occur in this strain at 37°C, explaining both the uSil1 accumulation and its increased abundance. Furthermore, as the molecular weight of uSil1 and pSil1 are similar, it is likely that pSil1 is also accumulating, particularly at 37°C, where a more obvious second band directly above uSil1 can be seen. As with the accumulation of pKar2, and uSil1, these deficits indicate perturbations to ER physiology, due to disrupted Sec63, and that in these cells, a post-translational translocation defect is present.

3.3. Discussion

The secretory pathway exemplifies the necessity for compartmentalisation in eukaryotes. As a major site of protein biogenesis, there are a diverse range of proteins, requiring multiple steps to achieve maturity before being targeted to their final destination. This necessity is driven by the complex nature of these steps, whereby the organisation of these activities into discrete regions allows for the processing of cargo as it traverses the secretory pathway. As the entry point to the secretory pathway, the ER is fundamentally important in regulating this entire pathway. Synthesis and translocation of proteins through the Sec61 channel is therefore the primary stage of protein secretion, with the function of this complex essential for all proceeding activities. Perturbations in translocon activity have far reaching effects, and as such mutations in the proteins associated with protein translocation are commonly observed in a multitude of disease states from cancer to diabetes (Lloyd, Wheeler and Gekakis 2010; Schonthal 2012). Protein translocation occurs through one of two main pathways, SRP-dependent and Sec62 dependent, with the Sec61 complex (Sec61, Sbh1, and Sss1) and Sec63 at the core of each pathway. The requirement of Sec63 in both SRP-dependent and Sec62-dependent translocation uniquely poises Sec63, as disruption to its function can have negative outcomes to both pathways.

Due to an essential role for Sec63 in both co- and post-translational translocation it is attractive to hypothesise that through regulating Sec63, multiple aspects of translocon activity, and in extension ER function, could be coordinated. One such way in which this could be achieved is through phosphorylation. It has previously been determined that phosphorylation of Sec63s extreme C-terminus is required for its interaction with Sec62, with Sec63 having several additional phosphorylation sites with which no function has yet been attributed (Ampofo et al. 2013; Holt et al. 2009). I was therefore interested in investigating the potential for phosphorylation regulating Sec63 activity. With the observed decrease in Sec63 phosphorylation at T504 in *S. pombe* following treatment with the TOR inhibitor Torin 1, providing the rationale for this study (Dr Janni Peterson, Flinders University,

personal communication). As previously discussed, the TOR kinases regulate a wide variety of cellular functions in response to nutrient availability. As TOR activity is responsible for ribosome biogenesis, and thus a driver of protein synthesis, TOR activity would impact the abundance of cargo being targeted to the ER, leading us to speculate if TOR dependent phosphorylation of Sec63 is important for modulating the activity of the translocon in accordance with cellular demands.

While both *S. cerevisiae* and *S. pombe* are single cell yeasts, there exists significant sequence dissimilarity. As such my initial investigation required the identification of the corresponding site of phosphorylation, if indeed Sec63 of *S. cerevisiae* possessed at TOR dependent phosphorylation site. For this I investigated four sites previously observed to be phosphorylated in high throughput proteomic studies. This was done through MRM mass spectrometry (multiple reaction monitoring) a high sensitivity technique which can selectively quantify targets within a mixed population of peptides. As with the study in *S. pombe*, I treated cells with a potent inhibitor of TOR, in this case rapamycin, to identify which of the phosphorylation sites were indeed responsive to TOR inhibition. This identified two potential phosphorylation sites to be TOR responsive, the first T467-S468 possess similarity to the predicted TOR consensus motif, while the second conforms perfectly to the PKA consensus motif. Unlike the data from *S. pombe,* in which a 100-fold decrease in T504 phosphorylation was observed, I find only ~3% of T467-S468 to be phosphorylated in WT conditions, however the phosphorylated peptide is undetectable following treatment with rapamycin. This would suggest this site is extremely sensitive to rapamycin inhibition, and likely a TOR dependent phosphorylation site. The significance of this depletion is debatable considering the low abundance of this phosphorylated site in WT conditions. However, several factors may contribute to this, one being simply that phosphorylation of this site dictates a specific activity, one that may not be required under vegetative growth. Furthermore, one factor not considered was if either T467 or S468 can be phosphorylated alone, as only the double phosphorylated state was targeted. If each site can be independently phosphorylated my initial analysis would be biased towards under representing the abundance of phosphorylation at this location. This

would also bias my observation that phosphorylation is completely ablated following rapamycin treatment, and as such future investigations will consider these factors. Also of note was the decreased abundance of all peptides targeted following rapamycin treatment. This is to be expected as inhibition of TOR greatly reduces the protein content of cells, while also decreasing the efficiency of cell lysis. A final contributing factor to this is the difficulty in efficiently getting phosphorylated peptides to fly and be detected, exacerbated by the fact two sites are found on a single peptide. Again, further analysis of these phosphorylation sites will factor in these considerations.

The observation that phosphorylation of S512 increases by ~50% following rapamycin treatment provides further support for my hypothesis that Sec63 function is regulated in a TOR dependent manner. I envisage two scenarios regarding this result; S512 is phosphorylated in response to the loss of phosphorylation at T467-S468, or that phosphorylation of S512 is an independent event and coordinates a separate activity required following repression of TOR. Of the two, I consider the first scenario to be the more likely for several reasons. The relatively close proximity of the two sites suggest the potential to maintain any activity attributed to their phosphorylation or provide a reciprocal response following downregulation of TOR. Supporting this are observations that the TOR and PKA pathways are able to work synergistically with both kinases regulated in response to the nutritional status of the cell (Pedruzzi et al. 2003; Soulard et al. 2010). The differences in abundance for each phosphorylation site is suggestive that phosphorylation of S512 has a greater requirement following downregulation of TOR. Alternatively, the half-lives of each phosphorylation site may be significantly different, thus providing a potential explanation for the accumulation of phospho-S512 following TOR inhibition. As S512 conforms perfectly to the PKA phosphorylation motif, investigations following inhibition of PKA would prove beneficial in understanding the regulation of both sites. While changes to the phosphorylation status of Sec63 were observed, this primary investigation of these sites is limited, and may not be wholly representative of the situation, specifically regarding the exact quantification and detection of the different peptides due to

the limitations of Mass Spec, and the limited number of samples used. Again, further work is required to better understand the phosphorylation kinetics of Sec63.

Following the confirmation that Sec63 is indeed phosphorylated in *S. cerevisiae* in a TOR responsive manner, I aimed to characterise the physiological consequences of this. To do this, mutants were generated to ablate (alanine substitution) or mimic phosphorylation (aspartic acid/glutamic acid substitution) at each site, with two methods employed for this characterisation. The first utilised a methionine repressible promoter to knock down endogenous expression of *SEC63*, with ectopically expressed *SEC63* then being the predominant source. The second, and more rigorous method employed the use of a *SEC63* shuffle strain in which only a single copy of the *SEC63* gene was present. In each case, cells were transformed with WT and mutant variants of *SEC63*, thus ensuring any changes observed were attributed to the mutations generated, and not due to differences in their mode of expression. In the initial testing both non-phosphorylatable and phosphomimetic mutants were investigated in BYY5 (*MET3-SEC63*). No changes were observed to the growth of the generated mutants in all conditions tested. As with growth, no conclusions could be made regarding the functionality of the mutants following immunoblot analysis. A range of ER proteins were investigated for their translocation status, abundance, and modification with no differences observed between WT and mutant variants of Sec63. However, it was consistently observed that multiple forms of Sil1 accumulated during these investigations. Specifically, I observed the accumulation of unglycosylated Sil1 (uSil1) following repression of the endogenous *SEC63*. This was observed in WT expressing cells and in all the mutants tested. The amount of uSil1 found to accumulate was inconsistent, with no trend towards increased accumulation in any specific mutant. I attributed this increase in uSil1 to a low-level ER stress as indicated by subtle changes to the protein abundance of several of the markers tested. Furthermore, following the addition of methionine, growth was seen to be decreased in all cases, likely due to a preference for endogenously expressed *SEC63*, again suggestive of a disrupted

cellular physiology. While I cannot attribute the differences in Sil1 glycosylation to any functional deficits in Sec63 activity, the occurrence of this warrants further investigation.

As the initial characterisations provided no evidence to altered activity of Sec63, and as neither aspartic acid nor glutamic acid can always re-capitulate the bulky and more negative charge that phosphorylation sites bring to proteins, I chose to focus on non-phosphorylatable variants of Sec63. Additionally, as phosphorylation of T467-S468 in WT conditions is minimal, I reasoned that a more substantial difference in function may be observed if both TOR responsive sites were substituted to alanine. This time the analysis was conducted whereby the mutants represent the only source of *SEC63*, thereby eliminating the possibility that low-level endogenous expression in BYY5 cells may be mitigating the effect of my mutations. As with my previous characterisations, I found no changes to growth, even in the presence of rapamycin. The same can be said for my panel of ER markers, with no differences observed. While disappointing, this strongly suggests that these sites are not required for the general function of Sec63. It may be that additional compensatory mechanisms exist, or that phosphorylation of these sites is required for a highly specific activity under conditions not considered during this investigation. As this represents the first direct characterisation of these sites, there is little in which to direct my investigations. There are several ways in which the functionality of these sites could be further investigated. One approach would be to test the functionality of these mutants in a genetic knock-out library. While my mutations alone display no gross alterations to the activity of Sec63, there may be synthetic interactions that would assist in identifying certain proteins/pathways in which Sec63 is involved. The same could be said for a chemogenomic screen, again to help identify potential targets for further testing.

While unable to characterise the role of these phosphorylation sites, I do not believe them to be functionless for several reasons. Firstly, the observation that a TOR dependent phosphorylation site also exists in *S. pombe* is suggestive this site is

conserved, potentially constituting a conserved function. The reciprocal nature in which S512 is phosphorylated following TOR inhibition would also allude to phosphorylation of Sec63s Brl-domain being required to maintain this function. The only biological data I have in support of this would be the deficits seen in the *sec63*$^{467/468\text{- AA-Trunc}}$ mutant, which highlights the functional importance of this region. Unlike my phospho-mutants alone, I find *sec63*$^{467/468\text{- AA-Trunc}}$ to have significant growth perturbations at 37^{o}C, but not at permissive temperatures. Upon further investigation I observed the accumulation of pKar2 and pSil1 at 37^{o}C, suggestive of translocation defects. However, no other translocation defects were noted, and as both Sil1 and Kar2 are posttranslational substrates I would also expect to see translocation defects in Lhs1. I do not find Lhs1 translocation to be compromised, nor are there any defects to its apparent maturation with a single glycosylated specie accumulating. I therefore surmise that this truncation does not elicit gross defects to translocation, as only the accumulation of untranslocated Kar2 and Sil1 are observed. Of more note is the abundance of uSil1 in this mutant. Unlike previous experiments in BYY5 cells, significantly more uSil1 was found to accumulate in the *sec63*$^{467/468\text{- AA-Trunc}}$ mutant. At permissive temperatures, I see a subtle accumulation of uSil1, with a substantial increase in its abundance at 37^{o}C. As before, I was unable to justify the occurrence of this specie. One potential reason for this could be that *sec63*$^{467/468\text{- AA-Trunc}}$ disrupts the glycosylation machinery, however the fact that Lhs1 glycosylation appears to be intact would suggest otherwise. Again, this phenotype warrants further investigation, and is suggestive that Sil1 modification may be extremely sensitive to changes in ER physiology. As the 20 amino acid truncation in *sec63*$^{467/468\text{- AA-Trunc}}$ is directly adjacent to the TOR dependent phosphorylation site, I propose that phosphorylation of T467-S468 may in some way coordinate this specific domain. A more detailed examination into the mechanistic implications of this mutant would therefore help guide future work into the nature of these phosphorylation sites. A recently published structure of the posttranslational translocation machinery may be of use in understanding the consequences of this truncation and in extension phosphorylation of this region. Here it was reported that several residues located

within a β-sheet and lasso-loop of the Brl-domain are in close proximity to the cytosolic loops of TM6-TM7 and TM8-TM9 of Sec61 (Wu, Cabanos and Rapoport 2019). This interaction was predicted to be important for opening the lateral gate of the translocon, and structural analysis would indicate this interaction blocks ribosome binding, thus priming the translocon for posttranslational translocation. The residues in question, T444, S447 and E482 were experimentally confirmed to be required for Sec63 function through the simultaneous mutation of each site (Wu, Cabanos and Rapoport 2019). The 20 AA truncation within *sec63*$^{467/468\text{- AA-Trunc}}$ is proximally located to these established Sec61 interacting residues, thus potentially helpful in understanding the defective nature of this truncation. Moreover, the role of this specific domain as understood from the structural analysis of the posttranslational translocon will be informative in guiding further work into the role of Sec63 phosphorylation. With the knowledge that this region anchors Sec63 to the Sec61 translocon preventing ribosome interaction and as TOR is a driver of translation and ribosome dynamics, it is attractive to speculate that TOR dependent phosphorylation of T467-S468 may be of importance in regulating this interaction.

Here I report the existence of two sites, whose phosphorylation status is modified in response to TOR inactivation. While the characterisation of these sites through SDM was unsuccessful in determining their exact role, it did provide several avenues for further investigation. The first was the identification of a truncation mutant, *sec63*$^{467/468\text{- AA-Trunc}}$, in which protein and growth deficits were noted, providing insight into the importance of this region for Sec63 activity. This observation is supported by a recent structural characterisation of the posttranslational translocon, which again will help direct future work into the role of these phosphorylation sites. The second, being the observed accumulation of a variant species of the nucleotide exchange factor Sil1. I repeatedly detected the accumulation of uSil1 throughout my characterisations of the various Sec63 mutants. In particular, the *sec63*$^{467/468\text{- AA-Trunc}}$ mutant was found to accumulate substantially more uSil1, the consequences of which are unknown. As this was the

only protein whose maturation was observed to be disrupted, I am interested in understanding the specific circumstances that generate this phenotype. While possible that Sil1 glycosylation is sensitive to generalised ER stress, I believe it to be a specific ER stress, potentially elicited by disrupted translocon physiology. As such, a more detailed characterisation of Sil1 dynamics may provide a useful marker of ER dysfunction. Furthermore, as I do not observe a general deficit in glycosylation, the accumulation of uSil1 may provide novel insight into the regulation and mechanics of glycosylation.

Characterisation of Sil1 Glycosylation Dynamics and Function in Reductive Stress.

4.1. Introduction

Cells possess several compensatory mechanism in order to buffer against fluctuations in the ER folding capacity. These mechanisms are critical for ER homeostasis, as they regulate essential molecular chaperones such as the Hsp70 orthologue Kar2 (BiP in mammals) (Brodsky et al. 1999; Corsi and Schekman 1997; Matlack et al. 1999a; Nishikawa et al. 2001; Simons et al. 1995). Kar2 activity is regulated by two classes of co-regulators; Hsp40/DnaJ-like proteins stimulate ATP hydrolysis, whereas nucleotide exchange factors (NEFs) promote ADP release and ATP reloading (Liberek et al. 1991; Szabo et al. 1994). Together they promote Kar2 to undergo multiple cycles of substrate binding and release to facilitate function. Together these mechanisms function either to bolster or down-regulate Kar2 activity in order to deal with the pending ER stress.

Two main processes have been demonstrated to regulate BiP activity, ADP-ribosylation/and or phosphorylation, and oxidation of a conserved cysteine within the ATPase domain of BiP. In mammals, ADP-ribosylated BiP is observed in response to a decrease in the burden of unfolded proteins in the ER lumen and following depletion of cellular glucose or amino acids (Chambers et al. 2012; Ledford and Leno 1994). Similarly, phosphorylation of BiP has been identified under similar conditions (Hendershot, Ting and Lee 1988; Freiden, Gaut and Hendershot 1992). Both ADP-ribosylation and phosphorylation are needed under these conditions as they have been shown to diminish the substrate binding capacity of BiP, which in turn interferes with the allosteric co-ordination of the nucleotide binding domain (NBD) and the substrate binding domain (SBD). Together this greatly reduces the activity of BiP in an efficient manner, while allowing for its rapid reactivation when required.

The oxidation of BiP, unlike ADP-ribosylation, appears to be conserved amongst eukaryotes and was recently identified exploiting the yeast ER HSP70 Kar2. In overly oxidizing conditions, such as the hyperactivation of Ero1, a highly conserved cysteine residue of Kar2, C63 (C41 in mammals), is oxidized directly by the resulting H_2O_2 produced (Wang et al. 2014). Oxidation of this key residue in Kar2 results in significantly diminished ATPase activity, conversely oxidized Kar2 appears to have an equal to or greater ability to bind peptides through its SBD. This data taken together provides a model in which oxidation of C63 under conditions of oxidative stress increases the ability of Kar2 to bind substrates, preventing their aggregation and their potential unchecked disulfide bond formation, while minimizing consumption of ATP within the ER. Thus, altering Kar2 activity from a 'foldase' to a 'holdase', restricting the potential detrimental effects of oxidative stress (Wang et al. 2014). As can be seen, regulation of Kar2/BiP activity is critical for maintaining ER homeostasis and consequently the viability of the cell. While a plethora of work has revealed the complex mechanistic, and regulatory factors coordinating the ERs HSP70 chaperone system, very little is understood regarding the NEFs that interact with Kar2/BiP. As such, I have characterized the role and glycosylation dynamics of the Kar2 NEF, Sil1 under conditions of ER stress to determine both their direct effect on Sil1, and the consequences this may have on Kar2 and ER homeostasis.

4.2. Results

4.2.1. N-linked glycosylation of the Sil1 nucleotide exchange factor, but not of Lhs1, is diminished by reductive stress.

Sil1 is synthesised and translocated into the ER lumen whereby its signal sequence is cleaved, and subsequently undergoes N-glycosylation. Additionally, upon ER stress a significant increase in the abundance of Sil1 is observed as it is highly upregulated by the UPR. The processes in which these variants manifest is well understood and thus make Sil1 a useful diagnostic tool in evaluating cellular homeostasis. However, under certain conditions, as reported previously, there is an increase in the presence of a lower molecular weight species of Sil1, an unglycosylated variant. The conditions that lead to this perturbation of glycosylation of Sil1 are varied and uncharacterised. As they are all in some way a stress response implies that the glycosylation status of Sil1 may have some effect on its function, however whether this is a positive or negative affect is unknown. I therefore sought to determine the underlying mechanism behind the observed glycosylation changes and the effect that glycosylation has on the function of Sil1. First, to replicate this effect, WT cells (BY4742) were treated with 10 mM of the potent reductant DTT for 2 h before whole cell lysates were prepared and probed with antisera targeting both of Kar2 NEFs, Sil1 and Lhs1. As Sil1 has no ER homologues, Lhs1 shares several properties that make it useful as a control. Primarily, both Sil1 and Lhs1 are glycoproteins and both are upregulated upon UPR induction. Therefore, WT cells were also treated with 10 µg/ml of the N-glycosylation inhibitor Tm and whole cell lysates were prepared. Untreated cell lysates reveal both Sil1 and Lhs1 are predominantly glycosylated during vegetative growth conditions (Figure 4.1 (A)). Following treatment with Tm the accumulation of a smaller specie can be seen migrating in both Sil1 and Lhs1 probed membranes corresponding to the unglycosylated forms of each respectively (Figure 4.1 (A)). Additionally, there is a marked increase in the abundance of both Sil1 and Lhs1, as expected with *SIL1* and *LHS1* being upregulated upon the induction of the UPR.

Treatment with DTT had no effect on glycosylation status of Lhs1. However, it can be seen that efficient glycosylation of Sil1 is compromised under this condition owing to the presence of similarly sized adduct, as observed in Tm treated cells (Figure 4.1 (A)).

As the migration of unglycosylated Sil1 (uSil1) can be difficult to resolve from that of untranslocated Sil1 (~2kDa difference), a protease protection assay was conducted to better resolve the identity of this specie. The phospholipid bilayer of the ER membrane provides a sufficient barrier that protects ER luminal proteins from proteinase K following incubation with membranes. Only protein domains exposed to the cytosol are sensitive to exogenous proteinase K, thus confirming the physical location of the proteins (Sil1) investigated. To perform the protease protection assay, membranes were isolated from cells either treated with DTT or untreated and lysates were ran on SDS-PAGE gels, probed with antisera specific for Sil1, in addition to Kar2 and Sec63. As expected, incubation of membranes with proteinase K depleted the Sec63 signal, as the antisera used is specific for the C-terminal cytoplasmic domain of Sec63, confirming the activity of my proteinase K (Figure 4.1 (B)). Conversely, there was no reduction in protein levels observed for Kar2 which is located in the lumen of the ER. Signal for Kar2 was only lost upon treatment with a combination of proteinase K and Triton X-100 (Figure 4.1 (B)). As with Kar2, signal for either band corresponding to glycosylated Sil1 (gSil1) and the suspected unglycosylated Sil1 (uSil1) was unaffected with proteinase K treatment alone requiring the solubilisation of the membranes before any loss was observed (Figure 4.1 (B)). This confirms that the specie that accumulates upon treatment with DTT is that of uSil1 and not the precursor unable to be efficiently translocated. The use of DTT to potently induce the UPR is common practice, as a strong reductant it elicits wide spread protein misfolding due to the production of an environment that is not conducive with the formation of disulphide bonds, during oxidative protein folding in the ER lumen. Alternative reductants such as β-mercaptoethanol (BME) are also used to disrupt protein folding. Its use here would help discern if the observed changes are due to the reduction of the ER or an

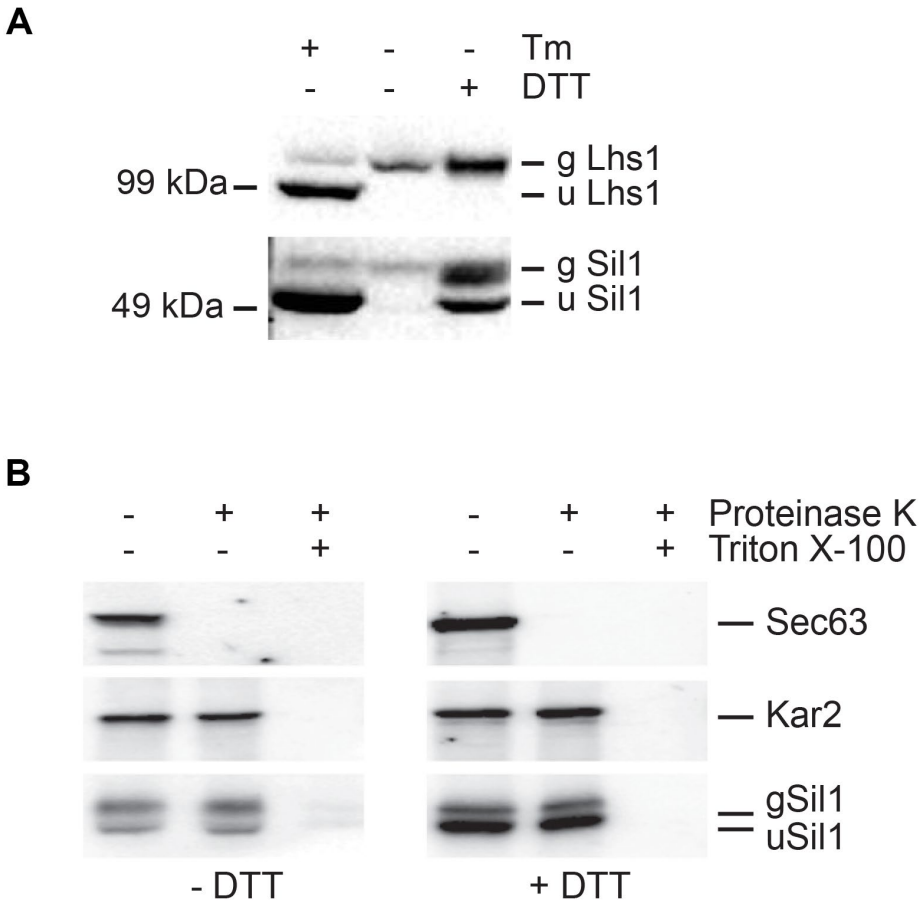

Figure 4.1 Treatment of WT cells with DTT perturbs Sil1 glycosylation.

(A) BY4742 cells were grown in YPD to mid-log, at which time cells were treated with either 10 µg/ml of Tm or 10 mM DTT for 2h. Cells were isolated and whole cell lysates probed for Lhs1 and Sil1 following SDS-PAGE and transfer onto PVDF. (B) BY4742 cells were grown to mid-log in YPD in the presence or absence of 10 mM DTT and membrane extracts prepared. Membranes were left untreated or treated with a 1% (v/v) solution of Triton X-100 then digested with proteinase K. Samples were immunoblotted for Sec63, Kar2 and Sil1.

unexpected effect of DTT. As such the glycosylation status of Sil1 was investigated in cells treated with increasing concentrations of BME, with DTT used as a control for uSil1 accumulation. Treating cells with 5 mM BME gave rise to a mild increase in protein load of Lhs1, less than observed in cells treated with the similar concentration of DTT (Figure 4.2 (A)). Protein levels for gSil1 are comparable to untreated cells, however even at this low concentration of BME, accumulation of uSil1 can be seen (Figure 4.2 (A)). As BME concentrations increase, so do the protein levels for both Lhs1 and Sil1, indicating a stronger UPR induction, with uSil1 levels increasing respectively. Again, no changes are observed for Lhs1 glycosylation, suggestive that the glycosylation machinery is still functional and that Sil1 glycosylation may be sensitive to the redox potential of the cell (Figure 4.2 (A)).

It is still unclear if Sil1 glycosylation is compromised in response to wide spread reductive stress, as elicited by the chemical reductants DTT and BME, or specifically ER reductive stress. Additionally, these effects may be the result of indirect effects of the reductants used. With this in mind, a more physiologically relevant method was employed in which Ero1, the predominant regulator of the oxidising potential of the ER, was inhibited. It has previously been demonstrated that Ero1 activity can be modulated through mutation of several key cysteine pairs, directly altering the redox homeostasis of the ER (Sevier et al. 2007; Wang et al. 2014). Therefore, inhibition of Ero1 would specifically reduce the ER and not the entire cell, without the use of a chemical reductant. The chemical inhibitor Bromo-5-methoxy-2,4-dinitrobenzene (Erodoxin) is specific for yeast Ero1 (decreased affinity for mouse Ero1α) and was utilised to determine if Sil1 glycosylation is specifically sensitive to a reduced ER environment. Cells were treated with increasing concentrations (25 µM-100 µM) of Erodoxin with Tm and DTT treatments used as controls. Again, whole cell lysates were isolated and analysed by western blots probing Sil1 and Lhs1. As with all previous experiments, no alteration in the glycosylation state of Lhs1 was observed. In corroboration with DTT and BME treatments, inhibition of Ero1 resulted in the accumulation of uSil1 in a dose dependent manner, albeit to a lesser degree than the chemical reductants (Figure 4.2 (B)).

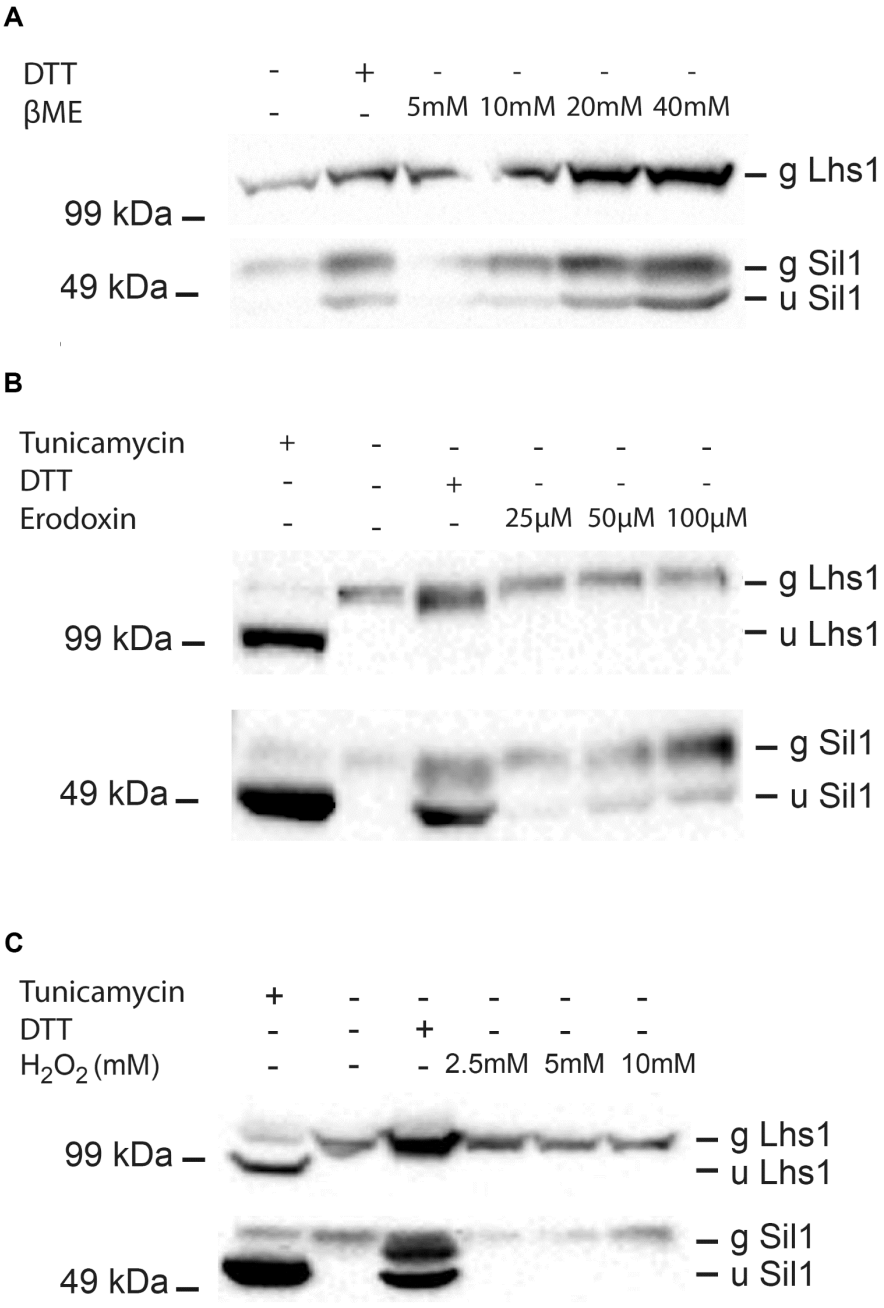

Figure 4.2 Cells accumulate unglycosylated Sil1 in reductive stress but not oxidative stress.

(A) BY4742 cells were treated with 5 mM DTT for 2h, or the indicated concentration of BME. Whole cell lysates were prepared and immunoblots of Lhs1 and Sil1 performed. (B) BY4742 cells were treated with the Ero1 inhibitor Erodoxin at the indicated concentrations for 2h, with Tm and DTT treatments used as controls and whole cell lysates were immunoblotted for Lhs1 and Sil1. (C) BY4742 cells were treated with increasing concentrations H_2O_2 for 2h, with DTT and Tm used as controls, and analysed as above.

Ero1 is responsible for maintaining an appropriate redox balance within the ER, disruption of which can have significant knock-on effects. As such, the observed alterations in Sil1 glycosylation may be due to the redox imbalance imparted by either DTT/BME or Erodoxin and not specifically reductive stress. To address this, chemical oxidants were used to emulate the accumulation of ROS within the cell, thus disrupting the redox balance of the ER, generating an increased oxidising potential. Initially, WT cells were treated with increasing concentrations (2.5 mM-10 mM) of the oxidizing agent H_2O_2, with whole cell lysates probed with anti-Sil1 and anti-Lhs1 antisera. Conversely to reductive stress, no change in glycosylation was observed for either Sil1 or Lhs1 (Figure 4.2 (C)). However, protein levels of Sil1 but not Lhs1 are reduced when exposed to 2.5 mM H_2O_2 in comparison to untreated WT cells. Furthermore, it would appear that as the concentration of H_2O_2 increases, so too does the abundance of Sil1, albeit not to the level as untreated cells (Figure 4.2 (C)). Several lines of evidence have shown that oxidative stress, specifically the increase in oxidising potential of the ER engage a mild UPR response (Ramming et al., 2014) which may be responsible for the increased levels of Sil1 observed in these conditions.

While it is clear that reductive stress has an inhibitory effect on Sil1 N-glycosylation, as stated throughout, reductive stress is a potent activator of the UPR. It is therefore not clear if this is a direct result of a reduced ER, or if the alteration in Sil1 N-glycosylation requires an active UPR. As such I investigated if the observed changes may be a consequence of UPR induction, independent of reductive stress. Excluding the use of reductants and Tm, several alternatives of UPR induction are available. Inositol depletion is an effective activator of the UPR as *IRE1* (Inositol Requiring Enzyme), the primary activator of the UPR in yeast, is exquisitely sensitive to inositol depletion. I therefore grew WT cells in inositol free media supplemented with or without of 100 µM inositol. Cells were grown to mid-log, whole cell lysates were prepared and investigated using antisera for Sil1 and compared to cells treated with either DTT or Tm. No change to the glycosylation status of Sil1 was observed in inositol free media, with or without supplementation of inositol (Figure 4.3 (A)). As a final control for UPR induction the

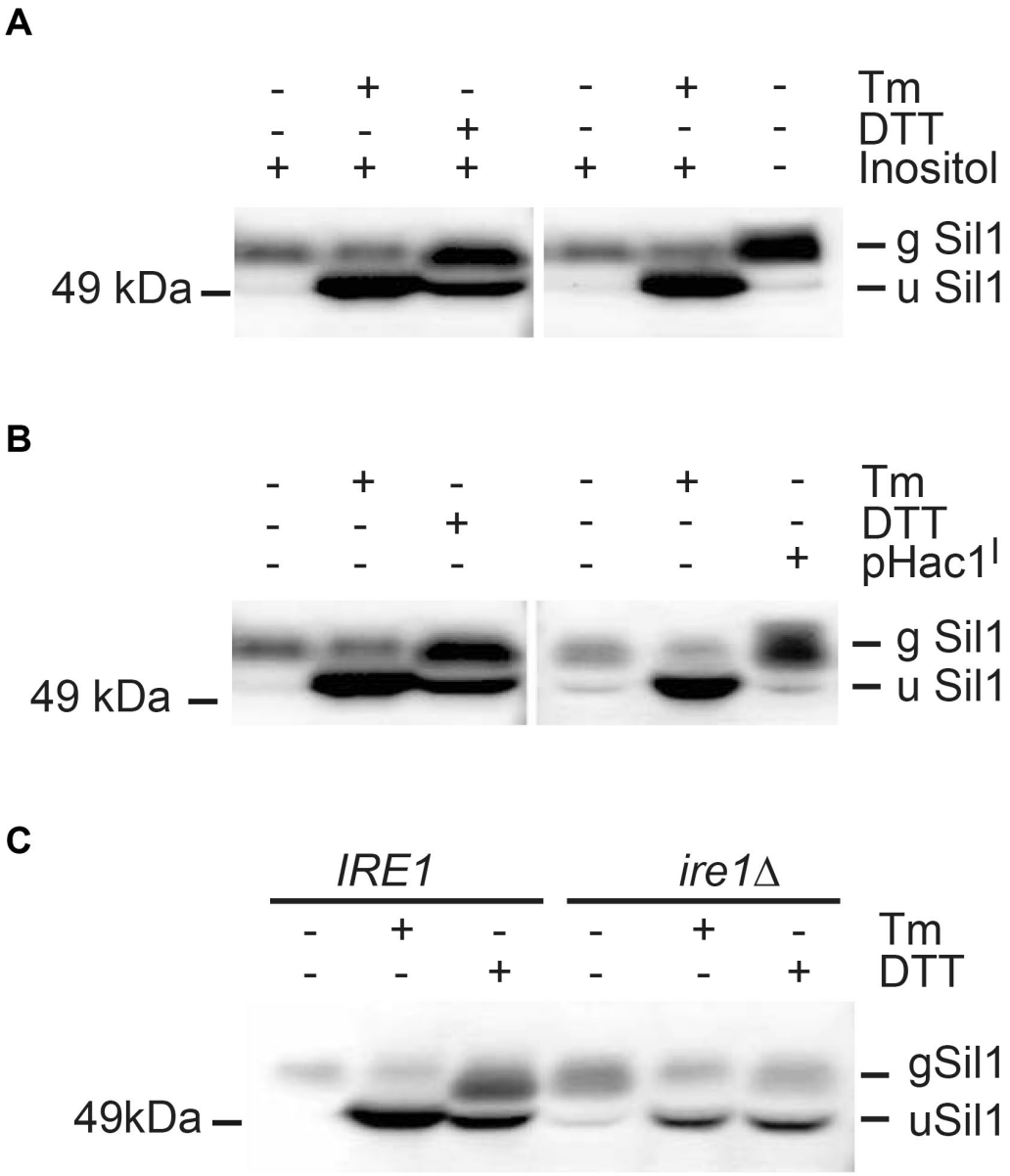

Figure 4.3 Glycosylation defects in Sil1 are independent of UPR induction.

(A) BY4742 cells were grown in inositol free YNB supplemented with the required amino acids, with or without the addition of inositol, DTT and Tm were used as controls for N-glycosylation. Whole cell lysates were processed and α-Sil1 serum used for immunoblotting. (B) BY4742 cell were transformed with pHac1^{I} or vector control, with cells grown to mid-log before harvesting and whole cell lysate prepared and analysed as in (A). (C) Whole cell lysates were prepared from BY4742 cells and *ire1Δ* cells, with or without the addition of Tm or DTT for 2h, samples were processed as in (A).

experiments were repeated in strains with a constitutively activated UPR. This was accomplished by first transforming WT cells with the pHac1^{I} vector. The pHac1^{I} vector encodes for the active form of the transcription factor Hac1, thus circumventing the requirement for Ire1 dependent splicing of HAC1 mRNA. As with inositol depleted media, no changes to Sil1 glycosylation were observed, however in both instances protein load was significantly increased, as expected upon induction of the UPR (Figure 4.3 (B)). To ensure that the observed changes were truly independent of the UPR, whole cell lysates were prepared from cells devoid of *IRE1* (*ire1Δ),* with or without DTT. Protein accumulation of Sil1 probed western blots were consistent with DTT treatments in the WT background, albeit with reduced protein load due to the inability to activate the UPR in this strain (Figure 4.3 (C)). As such, glycosylation of Sil1 and not Lhs1, is perturbed in response to reductive stress. This change in glycosylation status is specific to reductive stress and not a general response to permeations in the redox homeostasis of the ER or dependent on a functional UPR.

4.2.2. N-Glycosylation of Sil1 is Ost3 dependent.

Both Sil1 and Lhs1 stimulate nucleotide exchange in Kar2, however only Sil1 is differentially glycosylated in response to reductive stress. I have shown these changes are independent of the UPR, indicating the observed differences between Sil1 and Lhs1 may reflect distinctions in the machinery required for their efficient glycosylation. Oligosaccharyltransferase (OST) is the complex responsible for the transfer of glycans to newly synthesised proteins as they enter the lumen of the ER. OST exists in two main isoforms containing either Ost3 or Ost6. It has been described that the Ost3 and Ost6 subunits exhibit unique substrate specificities, and that these are partially dependent on a thioredoxin-like-motif located within their peptide binding pockets (Schulz et al. 2009). Furthermore, this thioredoxin-like-motif exhibits redox-dependent peptide binding properties, the reduction of which has been shown to alter the glycosylation efficiency of particular substrates. I postulate that the distinctions observed are a result of their affinity for a particular

isoform of OST and therefore aimed to determine the specific OST dependence of both Sil1 and Lhs1. Whole cell lysates were prepared from both *ost3Δ* and *ost6Δ* cell lines, with Tm and DTT treatments as controls. Neither Sil1 nor Lhs1 glycosylation was perturbed in *ost6Δ* cells, indicating both proteins are glycosylated independently of the Ost6 subunit (Figure 4.4). In contrast, the electrophoretic mobility of both NEFs was altered in whole cell lysates derived from *ost3Δ* mutants. Analysis of Lhs1 blots reveal a band intermediate of its unglycosylated and glycosylated forms, suspected to indicate that at least one N-glycosylation site is Ost3 dependent, however this modification is impartial to alterations in the redox potential of the ER. However, N-glycosylation of Sil1 is primarily Ost3 dependent, with uSil1 representing the major form in *ost3Δ* cells (Figure 4.4).

4.2.3. N-glycosylation of Sil1 requires a functional Ost3 thioredoxin-like-motif

Both Ost3 and Ost6 containing OST complexes exhibit different substrate specificities. This is further influenced by their thioredoxin-like folds, which harbor an active thioredoxin-like motif (CxxC). Oxidation of this motif is required to from a substrate recognition motif for a subset of proteins that are glycosylated in an Ost3/Ost6 dependent manner. The binding can be either non-covalent, requiring only the peptide-binding groove, or in approximately 10% of cases, require the formation of mixed disulfides between substrate, and the CxxC motif of Ost3/6 (Mohd Yusuf et al. 2013). As glycosylation of Sil1 appears to be entirely Ost3 dependent and is redox sensitive, I hypothesized that disruption of the CxxC motif in Ost3 would be detrimental to Sil1 N-glycosylation. To confirm that Sil1 requires an intact CxxC motif for efficient N-glycosylation, *ost3Δ* cells were transformed with a vector control (pRS316), a vector containing OST3 (YCp *OST3*), and a vector containing a mutant of OST3, in which both cysteines within the CxxC motif were mutated to serine (YCp $ost3^{C\text{-}S}$). The YCp $ost3^{C\text{-}S}$ vector expresses a functional Ost3 subunit, albeit with a non-functional thioredoxin motif, and has

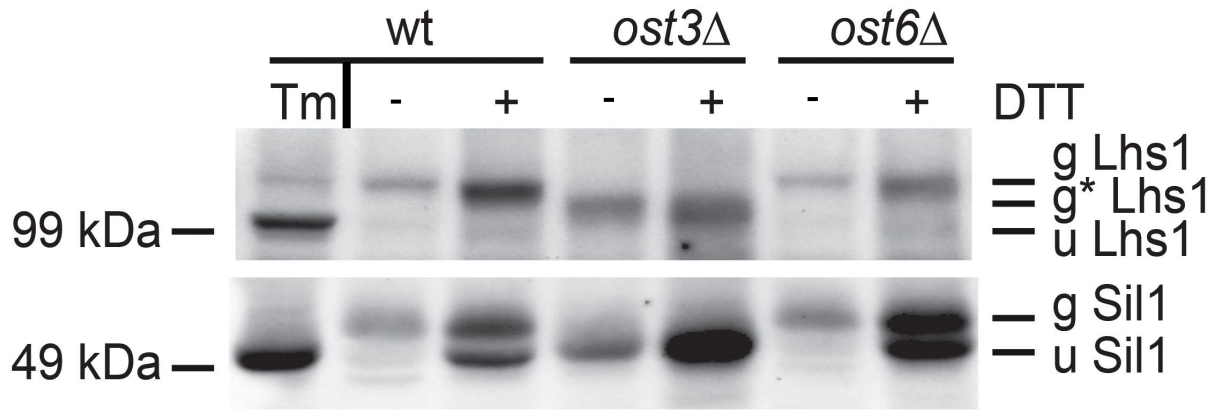

Figure 4.4 Sil1 N-glycosylation is Ost3-dependent.

Whole cell extracts were analysed by immunoblot from BY4742, *ost3Δ* and *ost6Δ* cell lines. Cells were grown in YPD to mid-log, then either treated or untreated with 10 µg/ml of Tm or 10 mM DTT for 2 hours.
(g* indicates an intermediate glycosylated form of Lhs1)

previously been shown to have defects in glycosylating particular substrates (Schulz et al. 2009). Cells containing either vector were grown to mid-log and isolated, and cell lysates produced. Glycosylation of Lhs1 was compromised in the vector only isolates, with restoration of N-glycosylation in cells transformed with either *OST3 or ost3*$^{C\text{-}S}$ (Figure 4.5). In contrast, Sil1 N-glycosylation was only partially restored by expression of both *OST3* and *ost3*$^{C\text{-}S}$, with a larger accumulation of uSil1 in the thioredoxin mutant (Figure 4.5). This indicates that Sil1, unlike Lhs1, requires a functional thioredoxin-like motif for its efficient glycosylation *in vivo*, and this process in acutely sensitive to the redox status of the ER. Further support of this is evident as Sil1 N-glycosylation is unable to be completely restored with either vector, unlike Lhs1. As such Sil1 N-glycosylation appears perceptive to minor changes in the OST complex, specifically alterations to the Ost3 subunit.

4.2.4. Identification of the sites required for N-glycosylation of Sil1

Loss of Ost3 or disruption of its CxxC motif leads to the accumulation of uSil1, as does an increased reductive environment in the ER. One explanation connecting these observations is that Sil1 N-glycosylation requires the formation of mixed disulfides with the CxxC motif of Ost3, and under reductive stress, these interactions are severely hindered. Consequently, if Sil1 does form mixed disulfides with Ost3, then mutation of the critical cysteines within Sil1 would mimic the effects of reductive stress, potentially abolishing N-glycosylation. The Sil1 protein contains four cysteine residues (C52, C57, C203, C373), two of which constitute a potential thioredoxin-like motif (C52-C57) and are more likely to be involved in the formation of mixed disulfides with Ost3. Loss of the *SIL1* gene is not associated with any major phenotype allowing for stable episomal expression of *SIL1* to be utilized for mutational studies. To determine the role of the cysteines within Sil1, SDM of each residue was performed, with substitution to serine in all cases except for C373, with alanine substituted instead (as I was unable to generate the Serine mutant, alanine was chosen for its well tolerated substitution). Following SDM, the vector YEp*SIL1* was sequenced to confirm only the desired mutation had been

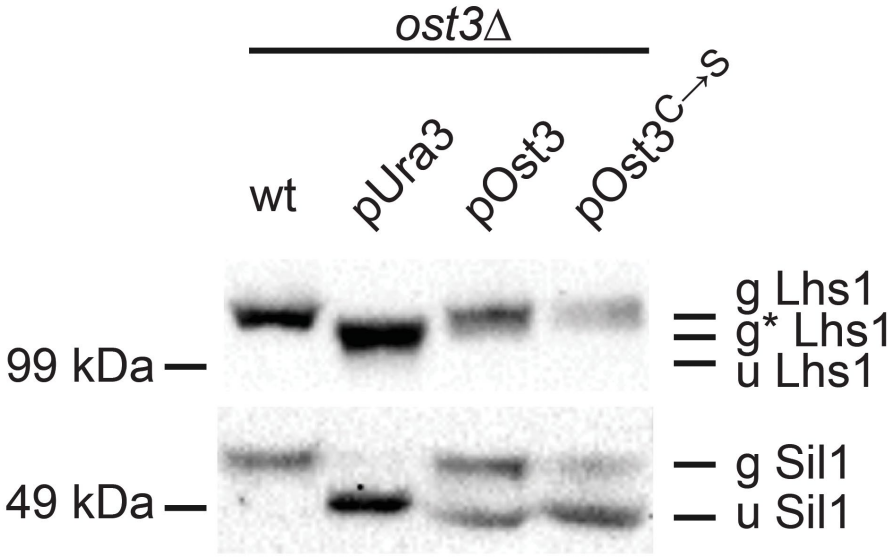

Figure 4.5 N-glycosylation of Sil1 requires the functional thioredoxin motif of Ost3.

WT BY4742 cells and *ost3Δ* cells transformed with pUra3 (vector control), pOst3 and pOst3$^{C\text{-}S}$ were grown to mid-log. Whole cell lysates were extracted and ran on SDS-PAGE gels before transfer onto PVDF and immunoblot analysis for Lhs1 and Sil1.
(g* indicates an intermediate glycosylated form of Lhs1)

incorporated, before transformation into *sil1Δ* cells, and collection of whole cell lysates. Mutation of cysteine residues within Sil1 had no discernible effects on its N-glycosylation as compared to WT *SIL1*, indicating that Sil1 N-glycosylation occurs independently of cysteine-cysteine interactions between Sil1 and Ost3 (Figure 4.6 (A)). Furthermore, the treatment of all cysteine mutants with DTT led to the same accumulation of uSil1 as observed in WT *SIL1* (Figure 4.6 (B)). While it is evident that Sil1 glycosylation does not require internal cysteine residues, the increased accumulation of uSil1 in cells expressing Ost3 with a disrupted thioredoxin domain would suggest it plays a significant role in the efficient glycosylation likely due to the specific fold adopted by Ost3's thioredoxin domain when functional.

As disruption of cysteine residues in Sil1 had no effect on glycosylation, to be able to understand and characterise the role that N-glycosylation has on the protein, the primary site of attachment is required. The covalent attachment of N-linked glycans occurs within the sequence motif N-X-S/T (X not Pro) that is referred to as a sequon. Bioinformatics analysis of the *SIL1* ORF identified 6 potential sequons, with 5 of these located within the armadillo-repeats responsible for nucleotide exchange activity of Sil1. To determine the specific sequon that undergoes glycosylation, glutathione scanning mutagenesis of the identified sites was conducted. As before, YEp *SIL1* was mutaganised, followed by confirmatory sequencing and subsequent transformation into *sil1Δ* cells. Western blot analysis of the 6 mutated sequons identified that disruption of Sil1 N-glycosylation was only perturbed upon substitution of N181. Although N-glycosylation of Sil1 is abolished in $sil1^{N181Q}$, the observed smearing above the band representative of uSil1, potentially indicative that the protein still undergoes extensive modification, potentially through mannosylation (Figure 4.7). It is also worth noting that the attachment of N-glycans is typically associated with folding and is required for either stability or as a 'marker' for maturation, however the protein load appears consistent with all other mutants and WT Sil1. Furthermore, no obvious signs of degradation are present such as ubiquitin laddering, suggestive that the protein is able to adopt its native state and produces no adverse effects.

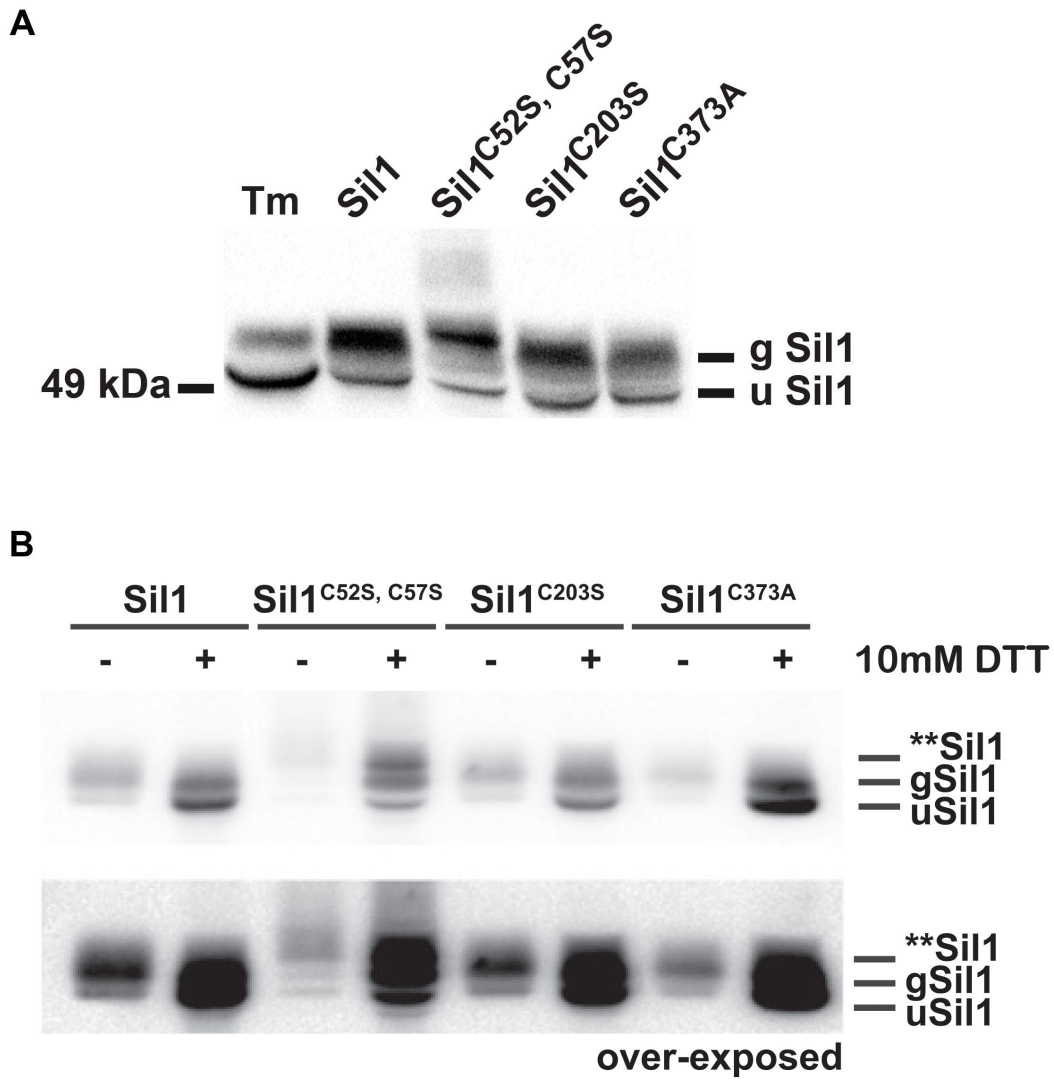

Figure 4.6 Sil1 N-glycosylation is independent of cysteines within Sil1.

(A) *sil1Δ* cells were first transformed with YEp *SIL1*, YEp *sil1*$^{C52S, C57S}$, YEp *sil1*^{C203S,} and YEp *sil1*^{C373A}. Cells were then grown to mid-log and a 2hr Tm treatment of BY4742 cells was used as a control. Whole cell lysates were prepared and immunoblot analysis of Sil1 performed. (B) *sil1Δ* cells transformed with YEp *SIL1*, YEp *sil1*$^{C52S, C57S}$, YEp *sil1*^{C203S,} and YEp *sil1*^{C373A} were grown either in the presence of 10 mM DTT or mock treated for 2h. Whole cell lysates were then extracted and Sil1 investigated by immunoblot.
(**Sil1 denotes an unknown form of posttranslationally modified Sil1)

4.2.5. Unglycosylated Sil1 is a functional NEF

The successful identification of the primary site of N-glycosylation in Sil1 provides us a useful tool in understanding the function, if any, imparted by the glycan. Utilising the 'unglycosylatable' *sil1*^{N181Q} allows all analyses to be conducted without the use of OST KO strains or chemical treatment, thus eliminating any off-target effects. Single deletions of either *SIL1* (*sil1Δ*) or *LHS1* (*lhs1Δ*) are viable in yeast, and result in a small number of mild phenotypes, with loss of *LHS1* the more severe of the two. However, deletion of both is synthetically lethal, indicating that the ER requires the Kar2 specific nucleotide exchange activity provided by either NEF, with Lhs1 regarded to be the dominant NEF. The use of the double KO offers a convenient genetic tool to determine the functionality of both NEFs, and in this case allows us to test the functionality of the unglycosylatable *sil1*^{N181Q}. The strain JTY65 has genomic deletions of both *SIL1* and *LHS1*, with growth maintained through expression of *LHS1* on a *URA3* vector (pRC43). The expression of WT *SIL1* and *sil1*^{N181Q} in JTY65 was enabled through the use of a single copy centromeric vector (pRS315), providing a closer mimic of endogenous expression levels. Following transformation, cells were struck onto selective media containing 5-FOA to drive the loss of pRC43 plasmid. After the loss of the pRC43 plasmid only cells expressing a functional Sil1 will be able to grow. As expected, cells transformed with vector alone were unable to grow, whereas those transformed with WT *SIL1* and *sil1*^{N181Q} produced viable colonies. This indicates 'unglycosylatable' Sil1 is functional (Figure 4.8 (A)). While this confirms uSil1 is functional, I wanted to investigate whether N-glycosylation affects any aspect of Sil1 function. Initially Sil1 was identified due to its ability to suppress the severe growth defects observed in the *ire1Δ lhs1Δ* mutant strain when overexpressed. This strain provides a more stringent test of functionality than loss of *LHS1* alone, as significantly more Sil1 is required to supress this growth defect, thereby highlighting any deficiency in functionality that may occur due to a loss of Sil1 N-glycosylation. Therefore, is *sil1*^{N181Q} able to suppress the growth defect in *ire1Δ lhs1Δ* like its glycosylatable cognate? The strain JTY62 contains genomic deletions of both *IRE1* and *LHS1*, with

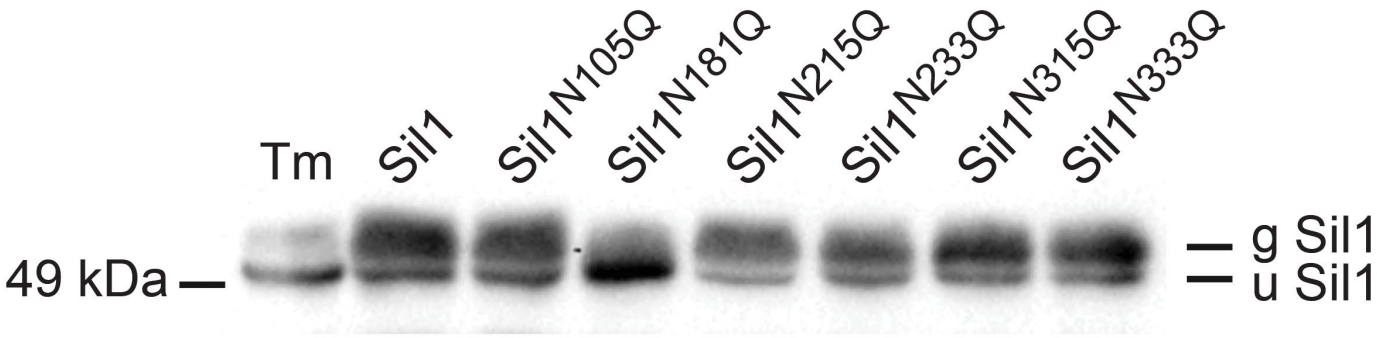

Figure 4.7 Sil1 asparagine 181 is the site of Ost3 dependent glycosylation.

Immunoblot analysis of whole cell lysates derived from *sil1Δ* cells expressing either YEp *SIL1*, YEp *sil1*^{N105Q}, YEp *sil1*^{N181Q}, YEp *sil1*^{N215Q}, YEp *sil1*^{N233Q}, YEp *sil1*^{N315Q}, or YEp *sil1*^{N333Q}. For control, cells were treated with 10 µg/ml Tm.

viability maintained through expression of pJT40 (*LHS1, ADE3, URA3*). The JTY62 strain was transformed with either YEp *SIL1* or YEp *sil1*^{N181Q}, and viability was tested upon loss of pJT40 through growth on 5-FOA media. As before, vector alone was unable to grow upon loss of *LHS1*, whereas overexpression of *SIL1* allowed for suppression of the growth defect (Figure 4.8 (B)). However, I observed the suppressive effects of WT *SIL1* to be non-uniform as I routinely observed the growth of small and large colonies. This implies that even overexpression of Sil1 is not able to completely supress the phenotype produced following the loss of *LHS1*. Interestingly, upon further phenotypic analysis the large colonies isolated were viable at 37^{o}C, while the small colonies only grew at permissive temperatures (Figure 4.8 (C)). Remarkably, when assayed by western blot the Sil1 signature differed between the large and small colonies. Significantly more unglycosylated Sil1 was found to accumulate in the larger of these dimorphic colonies (Figure 4.8 (D)). Conversely, overexpression of the unglycosylated *sil1*^{N181Q} mutant was able to provide robust suppression of *ire1Δ lhs1Δ* double mutants upon loss of pJT40 with all colonies uniform in size and viable at 37^{o}C (Figure 4.8 (B)). This not only confirms that uSil1 is functional but suggests that it provides greater activity in the context of the *ire1Δ lhs1Δ* double mutant than gSil1. Bolstering this claim is the bias towards accumulation of uSil1 in the larger, more robust suppressors isolated from cells transformed with WT Sil1. While the mechanism generating this change is not known, it demonstrates that accumulation of uSil1 is a rapid adaptation allowing suppression of the detrimental phenotypes as a result of loss of *IRE1* and *LHS1*.

Since overexpression *sil1*^{N181Q} allows robust growth in the *ire1Δ lhs1Δ* double mutant whereas WT Sil1 does not, I examined if a modest increase in expression was sufficient to suppress the growth defect. JTY62 cells were again transformed, this time with YCp *SIL1* and YCp *sil1*^{N181Q} and growth analysed following counter selection of pJT40 on 5-FOA media.

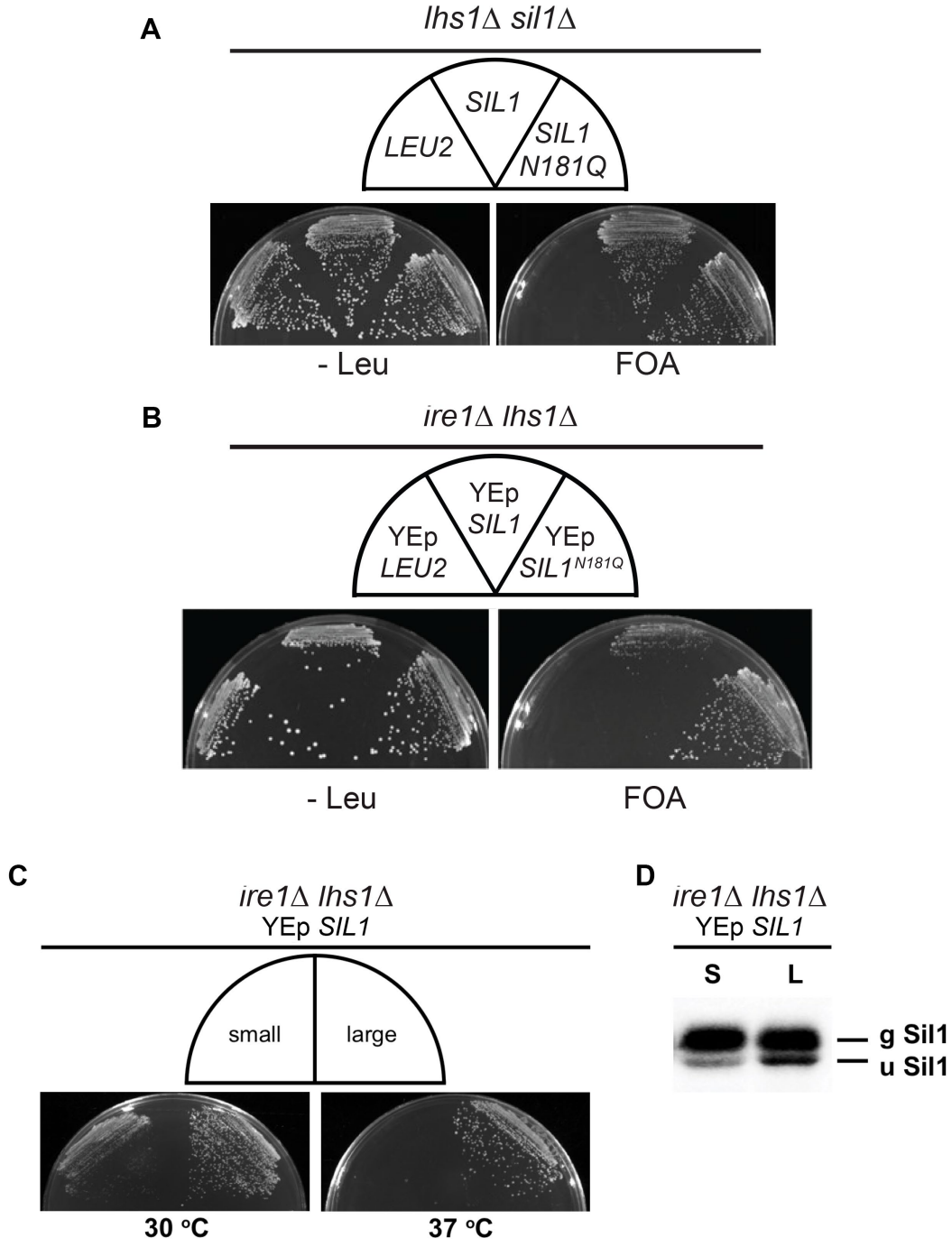

Figure 4.8 Unglycosylated Sil1 functionally compensates for loss of Lhs1 better than glycosylated Sil1.

(A) JTY65 yeast harbouring either YCp *LEU2*, YCp *SIL1*, or YCp *sil1*^{N181Q} cells were streaked onto –Leu selective medium and medium containing FOA and incubated at 30 °C for 2 d. (B) JTY62 yeast harbouring either YEp *LEU2*, YEp *SIL1*, or YEp *sil1*^{N181Q} were streaked onto –Leu selective medium and medium containing FOA and incubated at 30 °C for 2 d. (C) JTY62 yeast harbouring YEp *SIL1* produce large and small colonies following FOA. Small and large colonies were struck out onto YPD and incubated at both 30°C and 37°C for 2 d. (D) Small and large colonies obtained from JTY62 cells expressing YEp *SIL1* were grown to mid-log with whole cell lysates prepared and analysed by immunoblot.

Surprisingly, expression using a single copy vector containing *sil1*^{N181Q} again promoted substantially more growth when compared to *SIL1* expression in the same system. Evidently, uSil1 is far more competent than its glycosylated cognate, with a ~2-fold increase in expression of *sil1*^{N181Q} allowing for growth of JTY62 (Data not shown, see supplementary data in (Stevens et al. 2017)).

With *ire1Δ lhs1Δ* cells unable to grow with only a single copy of endogenous *SIL1*, I investigated if substitution of the *SIL1* ORF with *sil1*^{N181Q} would be sufficient to rescue the growth defect. To examine this, an integration construct for *sil1*^{N181Q} was generated utilizing *leu2* prototrophy as selection. The construct was amplified from YCp *sil1*^{N181Q} with a forward primer specific for the 3' end of the *SIL1* ORF, and a reverse primer targeting the 5'UTR of *LEU2* containing a 40bp overhang specific for the 5' UTR of *SIL1* (Figure 4.9 (A)). Successful integration of the *sil1*^{N181Q}*::LEU2* construct into the *SIL1* genetic locus via homologous recombination was confirmed by sequencing, and a Sil1 immunoblot (Figure 4.9 (B)). Genomic substitution of *SIL1* with *sil1*^{N181Q}*::LEU2* was able to support growth upon the 5-FOA dependent loss of pJT40, unlike endogenous *SIL1* alone. Collectively, this data confirms that uSil1 is functionally able to compensate for the loss of Lhs1 more adequately than gSil1 (Figure 4.9 (C)).

4.2.6. Unglycosylated Sil1 is beneficial in reductive stress

Under conditions of reductive stress I have shown Sil1 N-glycosylation to be compromised resulting in the accumulation of uSil1. I have further demonstrated that uSil1 is more able to complement the loss of *LHS1* than its glycosylated cognate. I therefore hypothesise that the accumulation of unglycosylated Sil1 upon reductive stress may be rapid adaptation to protect cells from this deleterious stress. This was investigated by expressing YCp *sil1*^{N181Q} in *ire1Δ* and assessing growth in a range of concentrations of DTT. Cells lacking *IRE1* are hypersensitive to low concentrations of DTT, therefore does expression of *sil1*^{N181Q} alleviate the growth sensitivity of *ire1Δ* under these conditions? The utilisation of *ire1Δ* allows UPR induction to be bypassed, eliminating any benefits

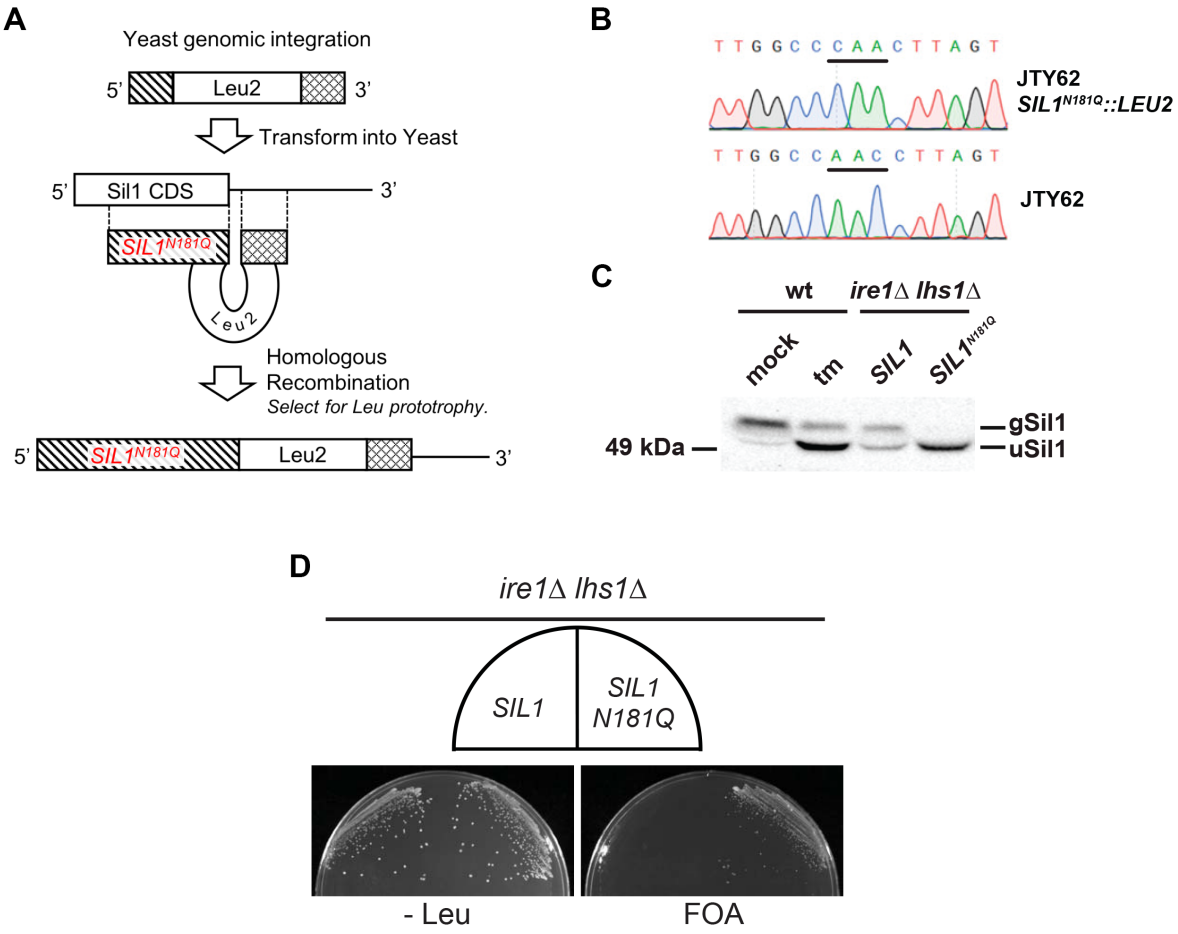

Figure 4.9 A single copy of uSil1 is able to suppress *ireΔ lhs1Δ*.

(A) Diagrammatic representation of the method used for integration of *sil1*^{N181Q} into the *SIL1* locus of JTY62. (B) Sequencing chromatogram confirming the integration of *sil1*^{N181Q} into JTY62, WT JTY62 used as comparison. (C) Immunoblot analysis of Sil1 in lysates prepared from WT BY4742 cells either mock or Tm treated for 2h, WT JTY62, and JTY62 *sil1*^{N181Q}*::LEU2.* (D) WT JTY62 and JTY62 *sil1*^{N181Q}*::LEU2* were streaked onto -Leu and FOA media and incubated at 30°C for 2 days.

endowed by its induction. Furthermore, *SIL1* expression is significantly increased following induction of the UPR, thus using *ire1Δ* mutants prevents the upregulation of *SIL1* to be a confounding factor. The relative growth of *ire1Δ* cells expressing either YCp *SIL1* or YCp *sil1*^{N181Q} was evaluated in liquid growth medium supplemented with increasing concentrations of DTT (0.05 – 1 mM). A modest suppression of the *ire1Δ* sensitivity to DTT was elicited by YCp *SIL1*^{N181Q} compared to YCp *SIL1*, with an approximate 1.5x increase in growth for cells exposed to 0.25-0.5 mM DTT (Figure 4.10 (A)). While the difference in growth is only moderate, it demonstrates that uSil1 constitutes a gain of function, particularly in times of significant ER stress, with the effect likely bolstered in WT cells following UPR induction of Sil1. Furthermore, it provides evidence for a Sil1 function unable to be replicated by the dominant ER NEF, Lhs1.

If true, coupled with the fact that *lhs1Δ* cells are also sensitive to DTT, and that uSil1 is demonstrably better able to compensate for the loss of Lhs1, can *sil1*^{N181Q} reduce *lhs1Δ* sensitivity to DTT? Fortunately, *lhs1Δ* is sensitive to concentrations of DTT that negligibly effect Sil1 glycosylation, thus limiting the bias of this assay. It was observed that across all concentrations tested (0.1-1.6 mM) that *sil1*^{N181Q} was once again better able to restore growth than WT Sil1 (Figure 4.10 (B)).

One tempting explanation for the 'gain of function' observed in cells accumulating uSil1 is that, contrary to dogma that N-glycans help to stabilise a proteins fold, uSil1 is more stable than gSil1. For cells under reductive stress, the production of uSil1 would benefit their overall fitness as more would be able to accumulate until such time that ER homeostasis is restored. To test this hypothesis a cycloheximide chase analysis was conducted on cells. Treatment of cells with cycloheximide induces a potent and rapid translation break, thus endowing investigation of the half-life of the various Sil1 species. For this particular investigation, cells were treated to an acute challenge with DTT, used to generate near equal levels of gSil1 and uSil1. Cells were then treated with cycloheximide, providing a window in which the relative degradation rates of each specie could be the

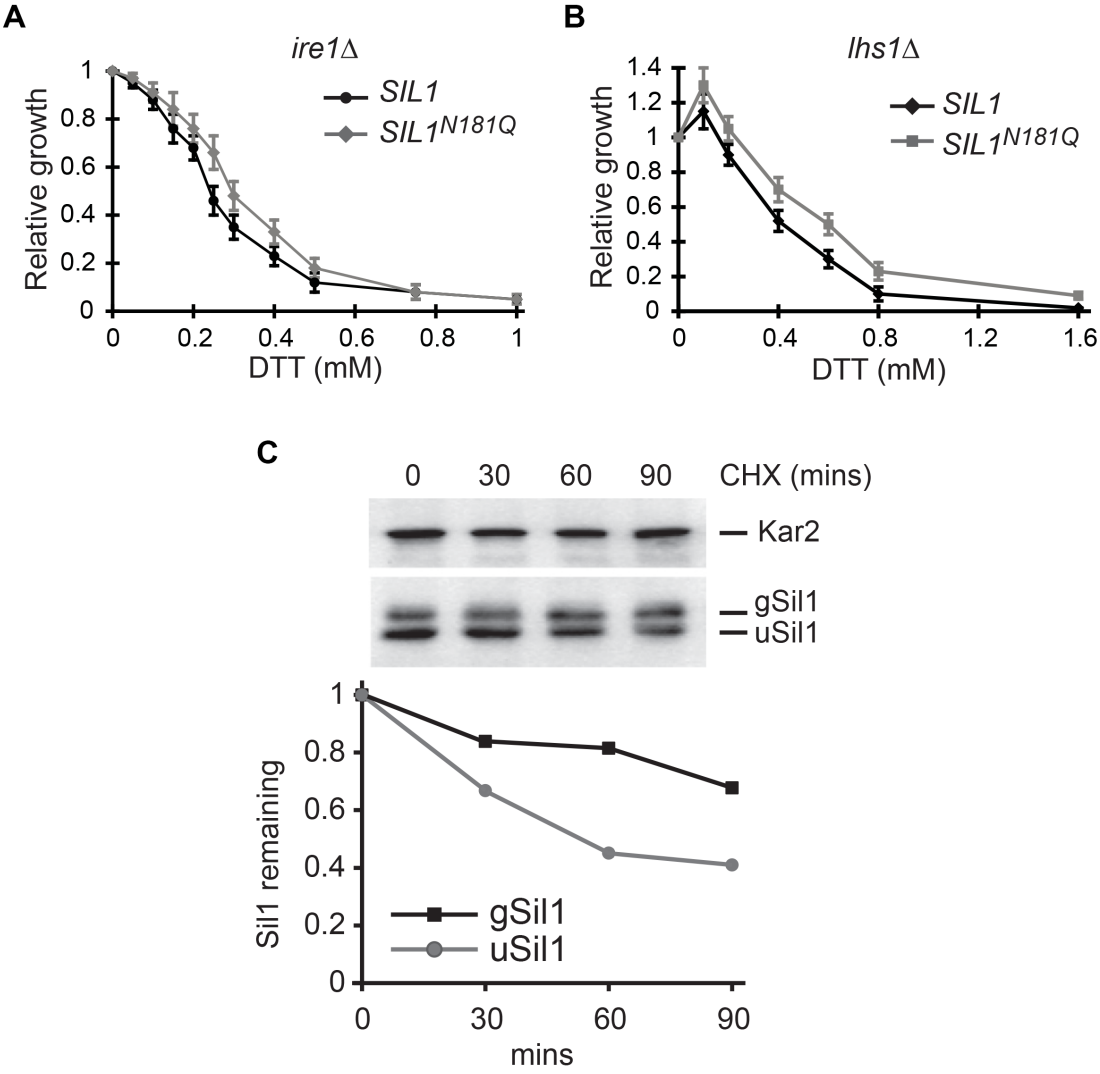

Figure 4.10 Unglycosylated Sil1 is beneficial in reductive stress.

(A) *ire1Δ* cells harboring either YCp *SIL1* or YCp *sil1^{N181Q}* were inoculated at 0.01 OD_{600} and grown until control had reached 1 OD_{600}. The relative growth with DTT (0.05– 1 mM) relative to "no-DTT" control (ddH_2O) are plotted as function of DTT concentration (x axis). Values show mean ± SEM of normalized growth for each DTT concentration from three independent experiments. (B) *SIL1 lhs1Δ* and *sil1^{N181Q} lhs1Δ* cells were inoculated at 0.01 OD_{600} and grown until control had reached 1 OD_{600}. The relative growth with DTT (0.1–1.6 mM) relative to "no-DTT" control (ddH_2O) are plotted as function of DTT concentration (x axis). Values show mean ± SEM of normalized growth for each DTT concentration from three independent experiments. (C) Exponentially growing WT cells grown in the presence of 10 mM DTT for 1 h were pretreated for 20 min with 0.25 mg/ml chx. Afterward, cells were removed at the indicated times and immunoblot analysis of cell lysates was performed and quantified using Image Lab software.

analysed. After 90 minutes, 70% of gSil1 remained, whereas uSil1 had undergone a more severe turnover, with only 40% remaining (Figure 4.10 (C)). This rejects hypothesis that increased stability of uSil1 is the mechanism in which its accumulation benefits cells under reductive stress, instead strengthening the notion that uSil1 is more 'functional' than gSil1.

4.3. Discussion

The ER is a major site of protein biogenesis, coupling protein translation with facilitated transfer into the lumen of the organelle. This provides a unique environment in which proteins are permitted to adopt the final conformations. Assisting this, are multiple, highly regulated pathways linking protein folding with quality control, limiting the generation of misfolded proteins, and rapidly adapting to any fluctuations that are detrimental to these processes. Protein N-glycosylation is one such mechanism co-ordinating both protein folding and degradation. Typically, N-glycosylation occurs co-translocationally, and is therefore poised to respond to subtle changes to the environmental conditions of the ER. Here I demonstrate this to be true, with Ost3 dependent N-glycosylation of Sil1 to be sensitive to ER reductive stress.

Alterations to the glycosylation status of Sil1 have been observed previously following mutation of the essential translocon component Sss1 (personal communication, Carl Mousley). I also observed changes in Sil1 N-glycosylation in response to mutation of sites within Sec63 (Chapter 3) and upon UPR induction following treatment with DTT. These observations provided the initial rationale to investigate this phenomenon in greater detail. As expected, unglycosylated Sil1 accumulated upon induction of the UPR using the reductant DTT. However, it was not known if UPR induction or reductive stress was the progenitor of this response. As accumulation of uSil1 in response to DTT treatment occurred in the absence of *IRE1*, it was confirmed to be independent of the UPR. Furthermore, specifically inhibiting Ero1, the protein responsible for generating the oxidising environment of the ER, demonstrated that Sil1 N-glycosylation was perturbed in direct response to a reduced ER.

The ER Hsp70 protein Kar2 (BiP) has two nucleotide exchange factors, Sil1 and Lhs1, with only one of the two required for viability in yeast. Of the two, Lhs1 is characterised with possessing a greater nucleotide exchange activity *in vitro* than Sil1, with deletion of *LHS1* resulting in more severe phenotypes. This led to the conclusion that Lhs1 is the predominant NEF for Kar2, and that Sil1 provides

additional NEF activity during extended stress conditions. As both Lhs1 and Sil1 are Ost3 dependent substrates, indicating a commonality between their N-glycosylation processes, it is interesting that only Sil1 N-glycosylation is affected in response to reductive stress. This, coupled with the dominant phenotype expression of unglycosylated Sil1 (*Sil1^{N181Q*})* bestows upon cells lacking *LHS1* and *IRE1*, is strongly suggestive of a Sil1 specific activity regulated by N-glycosylation (Figure 4.8).

Supportive of this conclusion was the observed increase in uSil1 accumulation in *ire1Δ lhs1 Δ* cells over expressing WT *SIL1.* In these cells I observe a non-uniform suppression of the *ire1Δ lhs1Δ growth* defect, with larger and smaller colonies present. With increased uSil1 accumulation found to correlate with the larger colonies. These large colonies were able to grow at increased rates, and even at restrictive temperatures indicating they had successfully adapted to the detrimental phenotype characterised by loss of *LHS1* and *IRE1*. Furthermore, the smaller colonies, accumulating predominantly gSil1, would yield both large and small colonies following restreaking, with the large colonies again accumulating uSil1 and rescuing all growth deficits. The opposite was not true, with large colonies consistently producing uniform suppression, never reverting phenotype. The fact that cells rapidly adapt to accumulate uSil1, strongly suggests that unglycosylated Sil1 allows for an increase in 'activity' not afforded by its glycosylated cognate. The exact nature of this adaptation is not known, although the end result would strongly suggest either the glycosylation machinery is altered, or that mutations within Sil1 are perturbing its efficient glycosylation. If the increase in uSil1 accumulation is the result of altered OST functionality, this strain would provide a unique tool in assessing glycoproteins whose glycosylation is sensitive to perturbations in OST dynamics, having the potential to identify additional substrates whose glycosylation status modifies their activity. Currently, I believe this to be the only documented case in which N-glycosylation is able to rapidly alter protein function in a direct response to changes in the cellular environment. It is unlikely that Sil1 is unique in this capacity, and this data provides a novel aspect of N-glycan regulation that requires further investigation.

How N-glycosylation of Sil1 affects its activity is not obvious when just considering the act of glycosylation itself. The attachment of N-glycans is commonly associated with an increase in protein stability, and I do observe gSil1 to possess an increased half-life. This however would not explain the gain in function observed for uSil1, as a higher turnover would presumably reduce the abundance and thus effectiveness of uSil1. It does however indicate that accumulation of uSil1 may be disadvantageous under certain conditions reflected by its increased turnover. N-glycans are also known to aid protein folding by forcing regions of the polypeptide to the protein surface due to their hydrophilic nature, however it is highly unlikely that N-glycosylation is required for correct Sil1 protein folding. I have shown uSil1 to be functional *in vivo*, and characterisation of Sil1 NEF activity was conducted with *SIL1* expressed in *E. coli*, thus unglycosylated (Tyson and Stirling 2000). Furthermore, the site of attachment, N181, is unlikely to affect its NEF activity. Located on the external face of the armadillo repeats, this site does not contact Kar2, nor does it occlude the nucleotide binding pocket required for exchange activity. N-glycosylation could however be responsible for a conformational change within the Sil1 structure, altering its activity, or preventing its interaction with Kar2. Again, I consider this unlikely as gSil1 accumulates equally in WT cells as it does in *lhs1Δ*. If N-glycosylation negatively affected its NEF activity, I would expect loss of *LHS1* to result in a large increase in uSil1. Future work characterising the respective exchange activity of gSil1 and uSil1 *in vitro* is required to confirm this.

I hypothesise the observed increase in 'activity' conferred upon Sil1 under reductive stress is not due directly to the site of N-glycosylation, nor to alterations in its NEF activity. Instead, I postulate one of two scenarios; that the N-glycan of Sil1 is used to bind and sequester Sil1, or that a domain within Sil1 binds and interacts with the N-glycan limiting its functionality. In the first model proposed, I speculate that the attachment of an N-glycan to Sil1 could allow for its interaction with lectin binding proteins, such as Calnexin. This would sequester Sil1, thus limiting its availability to perform its intrinsic NEF activity, and any other functions Sil1 possesses. The extensive modification observed in Sil1 throughout this study is likely mannosylation and provides an alternative scenario for its sequestration.

Glycan trimming and mannosylation are used to identify proteins that have adopted their correct fold. Additional modifications are gained as they traverse the secretory pathway. As Sil1 contains the sequence RDEL (ER retention motif), it is possible that following retrieval, Sil1 would require re-modification of its glycosylation/mannosylation sites. Ergo, undergoing extended chaperone cycling, limiting the overall available pool of Sil1 at any given moment. Backing this statement is the knowledge that uSil1 is turned over far quicker than gSil1, indicating Sil1 is monitored by the ERAD pathway, with glycosylation preventing rapid turnover. Being as both Sil1 and Lhs1 are glycoproteins, why would this repeated retrieval and modification affect Sil1 alone. It is known that Lhs1 has the greater NEF activity *in vitro*, and is involved in both translocation and protein folding, with deletion constitutively inducing the UPR (Craven, Egerton and Stirling 1996; Hale et al. 2010; Saris et al. 1997). The increased severity due to loss of *LHS1* versus *SIL1*, demonstrates the importance of Lhs1 in various stages of protein maturation in the ER. This strengthens the notion that Lhs1 is the dominant NEF for Kar2, as its functions require it to be located proximal to the translocon. Therefore, the interactions of Lhs1 may prevent/reduce its cycling between the ER and cis-golgi. Furthermore, binding of Kar2 by its NEFs has been shown to be mutually exclusive, increasing the probability that Sil1 is excluded from interacting with Kar2, thereby entering the aforementioned cycling (Hale et al. 2010).

The second model I propose involves Sil1 self-interacting with its N-glycan, thus limiting its activity. The rationale for this being the observation that the unstructured N-terminal domain of mammalian Sil1 (Bap) is required for efficient substrate release from BiP, with the N-terminal domain able to act as a pseudo-substrate for BiP (Rosam et al. 2018). If this domain is flexible enough to interact with the lid domain, is it also able to self-interact specifically with its N-glycan? No consensus motif exists for lectin binding, however several software programs have been developed to determine the likelihood of proteins to interact with glycans. I have utilised a program trained to predict carbohydrate binding regions within proteins to investigate the N-terminal domain of Sil1, and as a control the bonified lectin binding protein Calnexin, for both yeast and mammalian proteins (Zhao et al.

2018). Both Calnexin proteins were predicted to have carbohydrate binding activity in the regions corresponding to their known binding site. Interestingly, both yeast and mammalian Sil1 were predicted to possess a region capable of carbohydrate binding with strong significance (Figure 4.11). Furthermore, the regions identified were analogous, with the strongest predicated site R84 (R92 in mammals), a residue known to be mutated in the rare Marinesco-Sjögren syndrome. Yeast and mammalian *SIL1* share only >20% sequence identity and >40% similarity, however the 40 amino acid region surrounding the predicted site shares ~40% identity. The conserved nature of this site strongly predicted to possess carbohydrate binding activity is made all the more credible by the fact it is a known disease causing allele. Mutations within Sil1 are characterised in ~50% of Marinesco-Sjögren syndrome cases, with the majority resulting from loss of Sil1, either through loss of ER retention motifs, or truncated, non-functional variants of Sil1. It is therefore possible that R84 in yeast (and mammals) co-ordinates interaction with its glycosylation site, thus hindering Sil1s ability to effectively interact with Kar2, specifically preventing the N-terminal domain from acting as a pseudo-substrate. Furthermore, if this was the case, reduced Sil1 interaction with Kar2 could again promote its cycling between the ER and golgi and interaction with other lectin binding proteins. Future work would characterise the models previously proposed. With investigation of R84 of Sil1 particularly interesting due to its implication in Marinesco-Sjögren syndrome. A greater understanding of the importance of this residue may provide a clearer understanding of the dynamics N-glycosylation bestows upon Sil1 activity, additional to understanding the negative effect this mutation has in humans.

Unlike the reasons for how N-glycosylation of Sil1 is able to regulate its 'activity', understanding the implications, particularly in the context of reductive stress, are more obvious. Reductive stress in the ER is particularly detrimental as it also negatively effects the entire secretory pathway, as well as having repercussions on mitochondrial function, and cellular physiology as a whole. The initial cause of these deficits is related to an inability to efficiently and correctly fold a broad spectrum of proteins trafficked through the ER, and as this can account for over

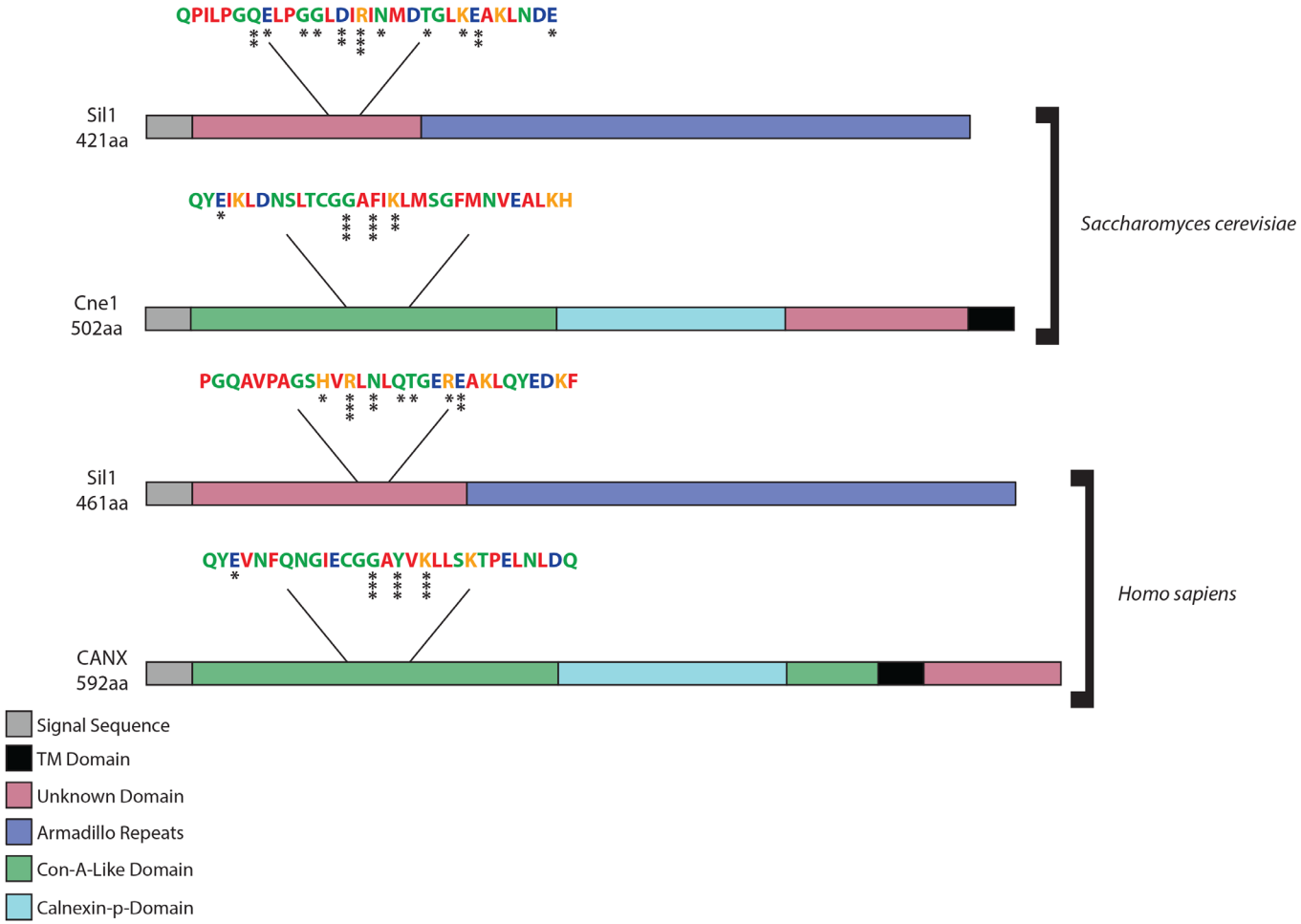

Figure 4.11 Lectin binding prediction of Sil1.

Lectin binding site prediction software program SPRINT-CBH (Zhao et al. 2018), was used to predict if any lectin binding sites exist in *S. cerevisiae* and *H. sapien* Sil1. Calnexin (Cne1 in yeast and CANX in humans) was used as a control for 'bona fide' lectin binding, with the sites predicted corresponding to the actual lectin binding sites of Calnexin. Asterisks indicate sites predicted to possess lectin binding, higher confidence in the prediction is depicted as additional asterisks

30% of the proteome, this is a significant problem. To remedy reductive stress, the UPR is activated, upregulating the expression of a multitude of factors able to increase the folding capacity of the ER and restore ER homeostasis. Included in this upregulation are *KAR2*, *LHS1* and *SIL1*, all factors able to assist in protein folding. However, under conditions of reductive stress, Kar2 alone is likely unable to prevent the aggregation of misfolded proteins alone, with the Hsp70 activity of Lhs1 providing support. Lhs1 is well characterised with having nucleotide independent holdase activity both *in vitro* and *in vivo* following heat stress (Saris et al. 1997). It is also required for the ERAD of specific glycoproteins, therefore under conditions of reductive stress is more likely to be required for preventing inappropriate protein accumulation rather than as a NEF for Kar2 (Buck et al. 2013). I envisage these to be the conditions in which uSil1 accumulation, in response to reductive stress, is able to alleviate the increased requirement for Lhs1 holdase activity. In this hypothesis, the large increase in unfolded/misfolded proteins increases the requirement for Sil1 dependent nucleotide exchange of Kar2, accomplished through the accumulation of uSil1. In such a scenario, there is a conditional need for Lhs1 in limiting protein aggregation and assisting the degradation of terminally misfolded proteins. This idea is supported by my observations that s*il1*^{N181Q} is better able to support loss of Lhs1 in all conditions tested in particular following DTT treatment. Additionally, the natural adaptation towards accumulating uSil1, and the impressive suppression of the growth defect in *ire1Δ lhs1Δ* provided by s*il1*^{N181Q}, shows uSil1 activity to be more effective than gSil1 under conditions in which the UPR is unable to be activated. I also propose that Ost3 acts as a redox sensor, and its position adjacent to the translocon allows for immediate changes to Sil1 N-glycosylation dependent on the redox status of the ER. This is reinforced by the fact that the translocon is the channel responsible for glutathione flux in the ER, with glutathione being the molecule by which redox homeostasis in the ER is maintained. Furthermore, this would explain why uSil1 is more labile than gSil1. Following restoration of ER homeostasis, the requirement for NEF activity is decreased, as is the requirement for Lhs1 holdase activity. Accumulation of uSil1 could be disadvantageous, overly stimulating Kar2s ATPase

cycle, and in low nutrient conditions, lead to excessive consumption of ATP. Therefore, increased turnover of uSil1 would remove the excess of highly active Sil1, whilst maintaining sufficient levels for normal cell function. In this model, Sil1 activity is able to be tuned to the specific requirements of the ER through its N-glycosylation status, representing a novel process in which N-glycosylation is utilised by the cell.

Sil1 Degradation and Response to Oxidative Stress

5.1. Introduction

Protein folding in the ER requires a niche set of environmental conditions, in particular the maintenance of an oxidative environment. This oxidative potential is generated through the coordinated import and oxidation of glutathione, which acts as the electron carrier for oxidative protein folding (Hwang, Sinskey and Lodish 1992; Sevier et al. 2007). Additionally, in higher eukaryotes, the ER is a storage site for Ca^{2+} an important signalling molecule in stress responses, and in the protein folding/quality control pathway of the ER (Ashby and Tepikin 2001). Disruption of ER homeostasis leads to the activation of stress responses such as the UPR (Walter and Ron 2011). I have spoken at length about the consequences of reductive stress in the ER with a particular emphasis on the NEF Sil1 and how the glycosylation machinery is able to tailor Sil1 activity to meet the needs of the major ER chaperone Kar2. Reductive stress is rarely discussed, however oxidative stress has been an area studied in depth, due to the numerous and often severe phenotypes observed following extended exposure to highly oxidising conditions (Sies, Berndt and Jones 2017). The endoplasmic reticulum possesses a uniquely oxidised environment when compared to the majority of the cell, and this oxidising power is maintained to ensure oxidative protein folding is efficiently carried out (Hwang, Sinskey and Lodish 1992). Recent observations have identified that overly oxidising conditions within the ER negatively affect Kar2 function. Specifically, a conserved cysteine residue, C63, within the nucleotide binding pocket of Kar2 inhibits ATPase activity following oxidation by peroxide or glutathione (Wang et al. 2014). Interestingly, oxidation of Kar2 increases the peptide binding activity, but as ATPase activity is inhibited, the substrate is unable to be released, altering the activity of Kar2 to that of a holdase. Furthermore, the authors also found that Kar2 cysteine mutants mimicking a reduced state were detrimental to cell growth in the presence of oxidising agents (Wang et al. 2014). I therefore wished to characterise the effect

of oxidative stress on Sil1 function with the knowledge that its activity is acutely sensitive to changes in the redox environment of the ER. Additionally, through my investigation into the nature of Sil1 regulation, I have identified several anomalies, which have been addressed here. All together, these observations further our knowledge of Sil1, and open several new avenues of research.

5.2. Results

5.2.1. Cysteines within Sil1 regulate its degradation

I have demonstrated that Sil1 is pivotal in responding to the effects of reductive stress, alleviating ER dysfunction, likely through an increased ability to interact with and regulate Kar2. In a reduced environment, the glycosylation status of Sil1 is modulated to meet the needs of the ER. Conversely in oxidative conditions, I found a trend towards decreased Sil1 abundance, with uSil1 being undetectable at higher concentrations of H_2O_2. I have previously seen uSil1 to be degraded at an increased rate compared to gSil1. This would be consistent with my observed decrease in uSil1 abundance in highly oxidising conditions and total Sil1 levels. However, the specific element that regulates Sil1 stability is unclear. During oxidative stress uncontrolled disulfide bond formation is a major cause of dysfunction, with the oxidation status of cysteines often found to regulate multiple aspects of protein biology (Go, Chandler and Jones 2015). The Sil1 protein contains four cysteine residues, being as oxidative stress causes a decrease in abundance of Sil1, do the cysteines within Sil1 coordinate its stability?

My initial characterisation of Sil1 led us to investigate if any of the four cysteines within Sil1 were required for its N-glycosylation. While not required for N-glycosylation cysteine 52 and 57 of Sil1, when mutated to serine, appeared to accumulate a higher molecular weight species. Upon further investigation unlike mutants of C203 and C373, overexpression of *sil1*$^{C52S\ C57S}$ does lead to the accumulation of higher molecular weight species. Specifically, the laddering observed would be consistent with polyubiquitination, as I observed higher molecular weight species with progressive increases of ~8-10kDa, consistent with the size of ubiquitin (Figure 5.1).

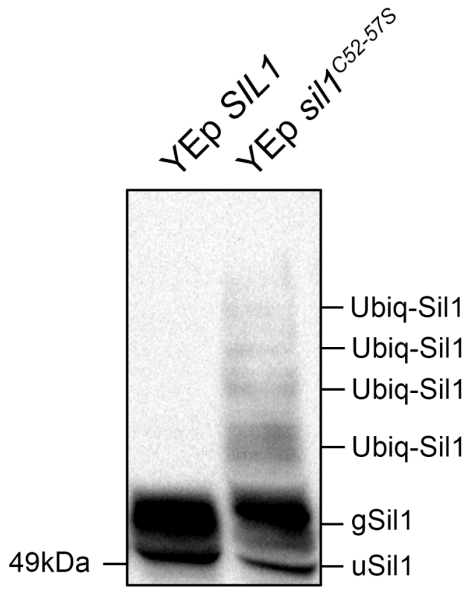

Figure 5.1 Mutation of two cysteines within Sil1 results in the accumulation of a higher molecular weight form.

Immunoblot analysis of whole cell lysates derived from *sil1Δ* cells expressing either YEp *SIL1* or YEp *sil*$^{C52\text{-}57S}$. Indicated are the known unglycosylated Sil1 (uSil1) and glycosylated Sil1 (gSil1), and the presumed ubiquitinated Sil1 (Ubiq-Sil1).

5.2.2. ERAD-dependent degradation of Sil1 is non-classical

The accumulation of ubSil1 at such high levels in cells expressing *sil1*$^{C52S\ C57S}$ strongly indicates that it is indeed being turned over. To investigate if *sil1*$^{C52S\ C57S}$ is an ERAD substrate I assessed the stability of WT *SIL1* and *sil1*$^{C52S\ C57S}$ by cycloheximide chase analysis. Exponentially growing *sil1Δ* cells expressing YEp *SIL1* or YEp *sil1*$^{C52S\ C57S}$ were treated with 0.25 mg/ml of cycloheximide 20 min prior to sampling, with samples taken at 0, 30, 60 and 90 min intervals, then cell lysates prepared and investigated using α-Sil1 antisera (Figure 5.2(A)). As can be seen, WT Sil1 protein levels were unaffected during the 90 min cycloheximide chase. This is juxtaposed to what I observe for *sil1*$^{C52S\ C57S}$, with less than 40% of the protein remaining following the 90 min chase (Figure 5.2(B)). The increased turnover of *sil1*$^{C52S\ C57S}$ and the resulting ubiquitin ladder strongly infer that *sil1*$^{C52S\ C57S}$ is being targeted for ERAD.

Two dominant ERAD pathways exist and they are characterised by the substrates they target. ERAD L/M and C survey the ER for soluble luminal/membrane proteins and ER membrane proteins with cytosolic misfolding respectively. Each pathway requires the activity of a dedicated ubiquitin ligase, Hrd1 is responsible for ERAD L/M with Doa10 targeting ERAD C substrates (Ruggiano, Foresti and Carvalho 2014). Additional components in each pathway further specialise the substrates they recognise. For example, Hrd3 is involved in targeting glycosylated proteins, specifically soluble proteins, in the lumen of the ER. Being as Sil1 is both soluble and glycosylated, it would reason that it is an ERAD L substrate, potentially requiring interaction with Hrd3. To determine which pathway/s were required for Sil1 degradation, the YEp *sil1*$^{C52S\ C57S}$ vector was transformed into KO strains for the two E3 ligases, Doa10 and Hrd1, and additionally into Hrd3 to determine if is degradation was assisted by glycan specific ERAD pathways.

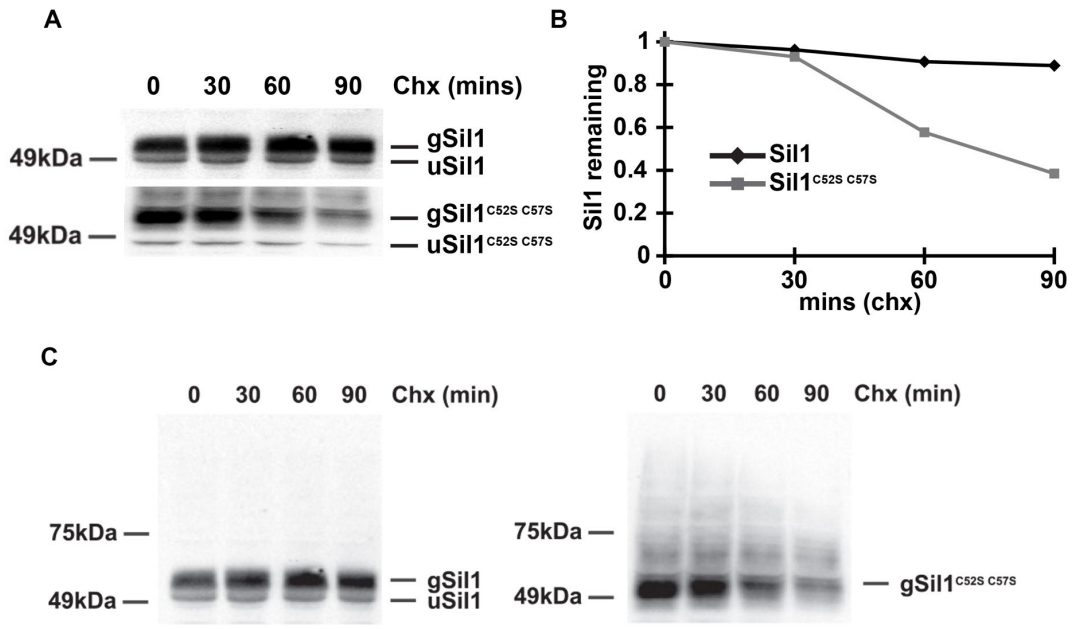

Figure 5.2 Stability of wildtype Sil1 and mutant Sil1$^{C52\text{-}57S}$.

Exponentially growing *sil1Δ* cells expressing either YEp *SIL1* or YEp *sil1$^{C52\text{-}57S}$* were treated with 0.25 mg/ml of cyclohexamide for 20 minutes. Following this incubation, a 'zero' time point sample, and a subsequent sample removed every 30 minutes for a total of 90 minutes. Following sampling, whole cell lysates were made immediately, with samples immunoblotted for Sil1. (A) Shows α-Sil1 immunoblots for both YEp *SIL1* and YEp *sil1$^{C52\text{-}57S}$* at the indicated time points. (B) Densitometry analysis of total Sil1, with values given as a percentage of Sil1 levels at 0 minutes. (C) Expanded image of (A) showing the accumulated higher molecular weight species.

Following transformation, cycloheximide chase assays were performed as before, and immunoblots performed for Sil1, with the rate of degradation compared to that of WT cells (Figure 5.3 (A)). As before, *sil1*$^{C52S\ C57S}$ levels in WT cells after 90 min were below 50%, confirming the elevated degradation rate previously observed for the mutant (Figure 5.3 (B)). Interestingly, the degradation kinetics in *hrd1Δ* and *hrd3Δ* were comparable to those observed in WT cells, and as Sil1 is a soluble luminal protein, it would be predicted to be recognised, and directed through the Hrd1 dependent ERAD-L pathway. Unexpectedly, expression of *sil1*$^{C52S\ C57S}$ in *doa10Δ* cells resulted in its stabilisation, with almost no loss observed within the 90 min chase (Figure 5.3 (B)). Additionally, expression of YEp *sil1*$^{C52S\ C57S}$ in *doa10Δ* cells resulted in a significant growth defect, further supporting the Doa10 dependence of Sil1 degradation (Figure 5.3 (C)). This is the only instance of Doa10 dependent ERAD for a luminal substrate that I am aware of, however Doa10 was found to degrade the translocon component Sbh2, and its degron (peptide that regulates degradation rate) was located within the ER membrane (Habeck et al. 2015). This would suggest that Sil1 is either tethered to, or closely associated with the ER membrane a potential role for the N-glycan of Sil1.

5.2.3. Oxidative stress effects Sil1 abundance

In my initial characterisation of Sil1, the focus was on reductive stress, and H_2O_2 was used only to determine if any changes in the N-glycosylation occurred. Unlike with reductive stress, only a single chemical oxidant was utilised, and the use of H_2O_2 does not adequately simulate an overly oxidised ER as it generates a universal increase in oxidising potential. As with reductive stress, targeting Ero1, the enzyme responsible for maintaining the ERs oxidised environment, would represent the ideal scenario. The use of the hyperactive Ero1* mutant has previously been used to do just this and is known to oxidise Kar2 *in vivo (Sevier et al. 2007)*. However, without access to this mutant an alternative was used to mimic ER oxidative stress.

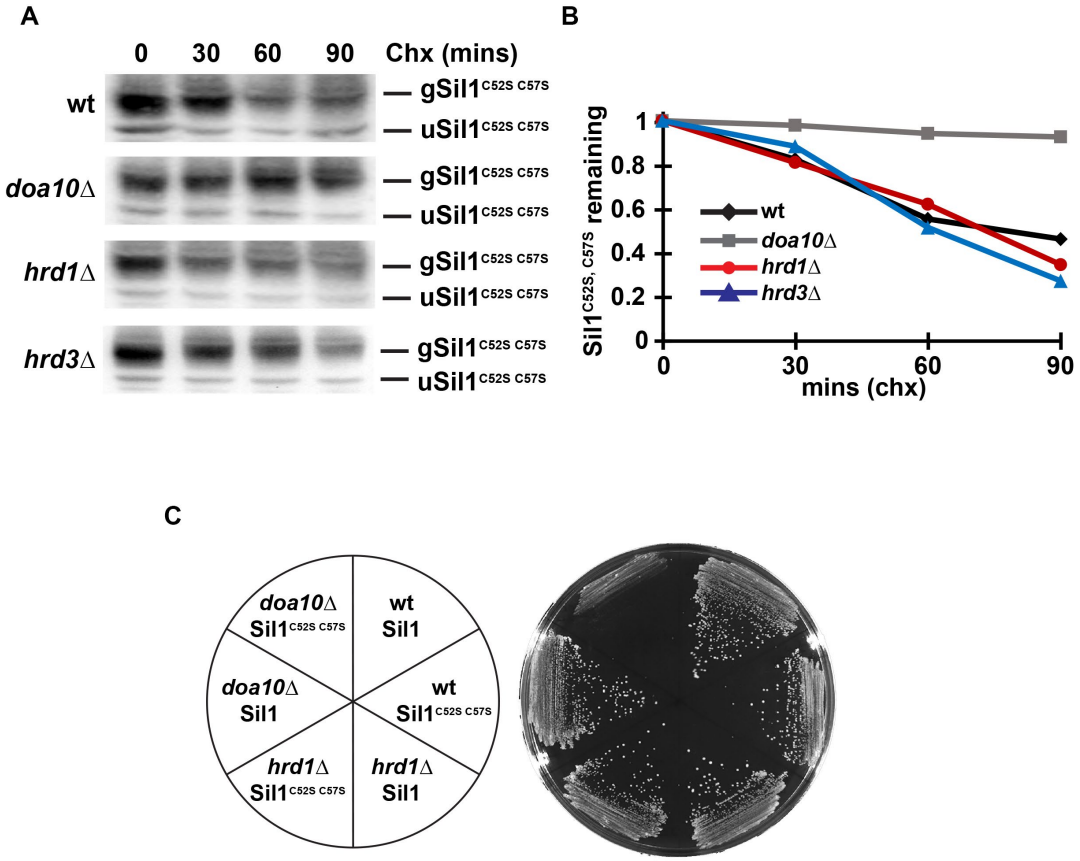

Figure 5.3 Analysis of protein stability and growth of *sil1*$^{C52\text{-}57S}$ in ERAD mutants.

(A) Cells (strains indicated) were transformed with YEp *sil1*$^{C52\text{-}57S}$, following transformation cells were grown to mid-log before being pretreated with 0.25 mg/ml of cyclohexamide for 20 minutes. Following the pre-treatment, samples were taken from the culture every 30 minutes for a total of 90 minutes. Whole cell lysates were prepared immediately following isolation and immunoblots were performed for Sil1. (B) Densitometric analysis of Sil1 levels for the immunoblots performed in (A), with the 0 minute timepoint used as 100% in all cases. (C) Growth at 30°C of the indicated strains transformed with either Yep Sil1 or Yep *sil1*$^{C52\text{-}57S}$.

The sulfhydryl-reagent Diamide (1,1'-Azobis(N,N-dimethylformamide)) has been shown to directly oxidise glutathione, the primary redox agent of the ER, thus replicating the effects of oxidative stress more accurately than H_2O_2 (Kosower et al. 1969). Initial testing using diamide was used to determine if any changes in protein abundance occurred as previously increasing concentrations of H_2O_2 showed a trend towards increased abundance of Sil1. As before, WT cells were either left untreated, or exposed to increasing concentrations of diamide, with Tm and DTT treatments used as controls for glycosylation defects and induction of the UPR. Interestingly, unlike with H_2O_2 exposure, treatment with 2.5 mM diamide not only resulted in an ~1.5 fold increase in total Sil1, but the accumulation of uSil1 in a similar manner to that of DTT treatment (Figure 5.4 (A)). Furthermore, increasing the concentration of diamide to 5 mM resulted in the loss of uSil1 accompanied with a severe reduction in total Sil1, with similar results at 10 mM diamide (Figure 5.4 (A)). This data contradicts my previous observations using H_2O_2, however as diamide is both a more potent oxidising agent, and more likely to directly oxidise the ER, significantly more H_2O_2 may be required to replicate the effect of diamide. I therefore expanded the range of H_2O_2 used to determine if it was able replicate the effects seen when using diamide. However even at concentrations as high as 200 mM, no significant changes to the glycosylation status of Sil1 were observed (Figure 5.4 (A)). Treatment with H_2O_2, even at higher concentrations has a trend towards accumulating gSil1, with little to no uSil1 remaining at 200 mM H_2O_2. Furthermore, at concentrations higher than 25 mM, growth was inhibited, indicating that either the cells are in stasis, or dead. In either case, any changes observed at concentrations above 25 mM would likely not be physiologically relevant. Of note however is the gradual increase in molecular weight of gSil1 as H_2O_2 concentrations increase. While this increase is minimal, it would appear that at 200 mM H_2O_2, the majority of Sil1 accumulates as this higher species. As to the nature of this increase, I propose this is the result of extensive glycosylation modification or mannosylation.

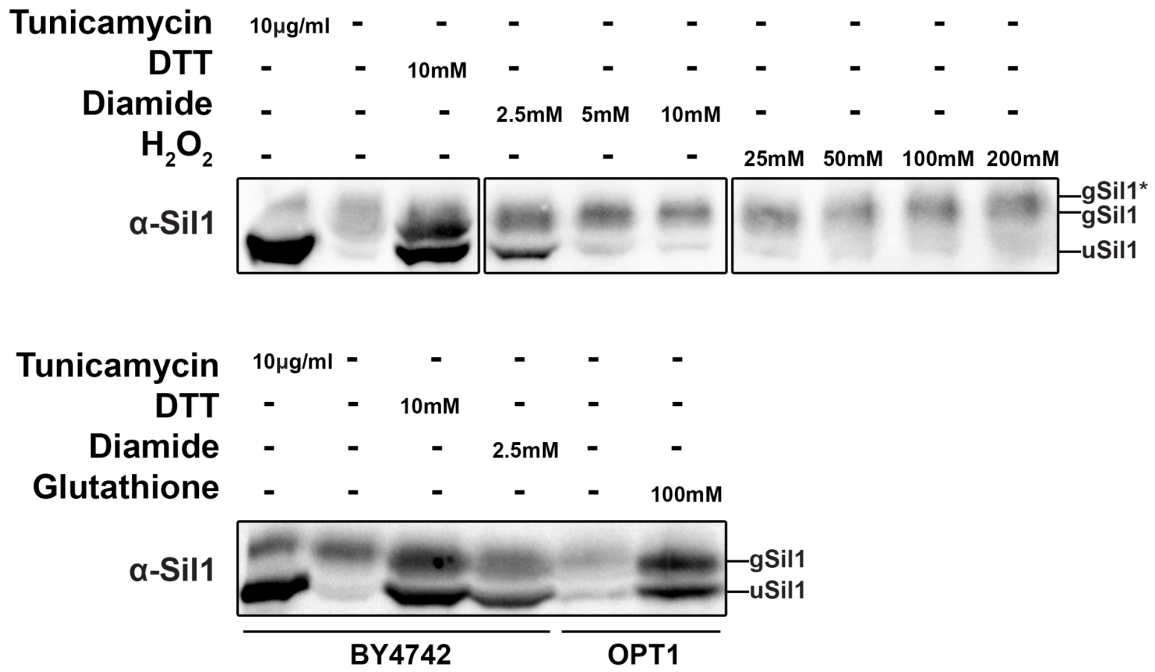

Figure 5.4 The effect of oxidative stress and glutathione of Sil1 glycosylation.

(A) BY4742 cells were grown in YPD at 30^{o}C to mid-log and subsequently treated with the indicated compounds at various concentrations. Cell were incubated with each compound for 60 minutes and whole cell lysates prepared. Shown are immunoblots for Sil1 with the notation gSil1* indicating a potentially higher molecular weight species. (B) BY4742 cells transformed with either vector control (pDR195) or pOPT1 (pDR195 backbone) were cells grown at 30^{o}C in YPD to mid-log and treated with the indicated compounds for 60 minutes. Following treatment, cells were harvested with whole cell lysates prepared and immunoblots performed for Sil1.

Treatments with diamide and H_2O_2 provide contrasting information, which I speculate is due not to their oxidising power, but more their mode of action. With low concentrations of diamide mimicking DTT treated cells, yet at higher concentrations more H_2O_2 like, it would reason that Sil1 glycosylation is perturbed by the communicable redox status of the ER, and not the abundance of redox altering compounds. Therefore, the abundance and ratio of reduced to oxidised glutathione would be the determinant in regulating Sil1 glycosylation. If correct, with the knowledge that diamide is a potent oxidiser of glutathione, I predict that altering the total glutathione flux of the cell may replicate my observations in diamide treated cells. Simply growing yeast in higher concentrations of glutathione would not substantially increase its cellular concentration as it requires active transport into the cell. Therefore, to increase the uptake of glutathione in the cell, overexpression of *OPT1* (oligopeptide transporter 1), a plasma membrane resident transporter of glutathione was utilised. For this, WT cells were transformed with the 2μ vector (pDR195) alone or containing the ORF of *OPT1*. Cells were then grown with or without the addition of 100 mM glutathione. For controls, WT cells were left untreated or exposed to the following; 10 μg/ml Tm, 10 mM DTT, and 2.5 mM diamide. Following treatment, cells were isolated and whole cells lysates prepared before running on SDS page gels and immunoblotting for Sil1. As can be seen, treatment with Tm increased the total Sil1 abundance and specifically uSil1, as does treatment with the reductant DTT (Figure 5.4 (B)). As before, treatment with low levels of diamide also generates a significant amount of uSil1, however Sil1 levels are not increased to the same level as with Tm and DTT. Finally, we can see overexpression of *OPT1* in WT cells alone has no discernible effect on Sil1 glycosylation, whereas *OPT1* overexpression in the presence of 100 mM glutathione produces a Sil1 profile similar to that of DTT and diamide treatment (Figure 5.4 (B)). While not a complete analogue, I believe this supports the notion that diamide treatment, particularly at lower concentrations elicits perturbations to ER glutathione homeostasis. This further indicates the susceptible nature of Sil1 glycosylation to changes in the cellular environment.

5.2.4. Unglycosylated Sil1 is detrimental to cell survival in oxidative stress

Having observed that both differential modification of Sil1 and protein abundance is affected upon treatment with diamide, I wished to assess if Sil1 activity differs in oxidative conditions. In reductive stress uSil1 accumulates to the benefit of the cell. Being as uSil1 generated by *sil1*^{N181Q} was able to alleviate the growth defects of both *ire1Δ* and *lhs1Δ* cells when grown in the presence of DTT, I decided to investigate how uSil1 would function in oxidative conditions. Ideally this test would be conducted in *lhs1Δ* cells, so as to minimise the effects of NEF redundancy, or in the *ire1Δ lhs1Δ* double mutant as uSil1 is highly beneficial in this instance. However, as loss of Lhs1 is associated with increased resistance to H_2O_2, and *ire1Δ* cells are conversely sensitive, any changes observed may be the result of the KO mutants. I therefore chose to observe the differences between WT cells expressing YEp *SIL1* and YEp *sil1*^{N181Q} in response to diamide treatment. Treatment with diamide can elicit total growth inhibition at concentrations as low as 2 mM in WT cells, which lends to the potent oxidising effects of diamide. As my previous experiment saw changes to Sil1 in diamide concentrations ≥2.5 mM, I instead investigated the effect of an acute treatment with a high concentration of diamide. For this, WT cells harbouring either YEp *SIL1* or YEp *sil1*^{N181Q} were grown to midlog, and cells incubated with or without 10 mM diamide for 60 and 120 minutes, before rigorously washing cells twice in ddH_2O (0 min timepoint represents cells left untreated). Cells were then allowed to recover for 8 hours in YPD, before being spotted out in 10-fold serial dilutions onto YPD agar. Cells overexpressing *SIL1* were recovered at all dilutions following treatment with diamide, albeit with reduced numbers following treatment (Figure 5.5). Conversely, cells overexpressing *sil1*^{N181Q} were highly sensitive to the effects of diamide with treatment for 60 min resulting in a recovery rate ~100 fold lower than cells expressing *SIL1*. The effect was even greater for the 120 min time point with ~1000 fold fewer cells recovered. This would suggest that accumulating uSil1 in highly oxidising conditions is acutely toxic, supportive of my previous observations whereby gSil1 accumulates in oxidative stress (Figure 5.4 (A)).

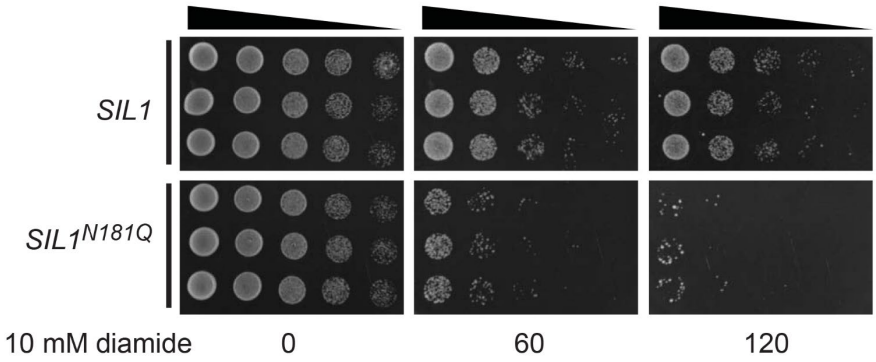

Figure 5.5 The effects on growth for cells expressing either glycosylated or unglycosylated Sil1.

WT cells were transformed with either YEp *SIL1* (glycosylatable) or YEp *sil1*^{N181Q} (unglycosylatable) and grown to mid-log in YNB. Cells were then either left untreated (0) or treated with 10 mM diamide for 60 and 120 minutes. Following treatment, cells were washed and recovered in YPD for 8 hours, then serially spotted onto YPD and grown at 30^{o}C for 2 days. (3 technical replicates are shown here)

5.2.5. Sil1 undergoes additional modifications upon treatment with cyclohexamide

My investigation into Sil1 function has required incubation with various chemical compounds, many of which have given rise to changes in the SDS page mobility of Sil1. In the majority of these cases, this mobility shift has been attributed to the accumulation of two dominant species of Sil1, unglycosylated and glycosylated. During these investigations I have also noted several species intermediate to uSil1 and gSil1. Their exact nature is more difficult to discern, but as Sil1 is glycosylated, and a resident of the secretory pathway, I have considered them to be products of glycan modification/trimming or mannosylation. While these species have yet to be formally identified, their accumulation during the various treatments appears not to follow a trend, and therefore have been considered 'normal' modifications. However, I have observed one change in which the observed increase in molecular weight and the mechanism by which it occurs are unable to be rationalised. Following treatment with cycloheximide, it was observed that Sil1 in WT cells migrated at a slightly increased molecular weight, with the abundance of this higher MW specie increasing over the treatment period. Furthermore, this modification occurs rapidly in response to cycloheximide exposure with samples undergoing an upshift within 1 hour of treatment (Figure 5.6 (A)). As Sil1 is a glycoprotein, my initial assumption was the event was related to extensive glycan modification or the further addition of sugar moieties. I therefore conducted the experiment in *ost3Δ* cells, as I have previously determined Sil1 glycosylation to be Ost3 dependant, and thus would not expect to observe the same change in molecular weight. Surprisingly, upon treatment with cycloheximide, the Sil1 profile in *ost3Δ* cells replicated the results observed in WT cells, albeit to a greater extent with Sil1 observed to migrate with an analogous MW to that of gSil1 (Figure 5.6 (A)). Furthermore, Sil1 levels following exposure to cycloheximide would suggest that this form is relatively stable, with degradation rates comparable between WT and *ost3Δ* cells (Figure 5.6 (B)).

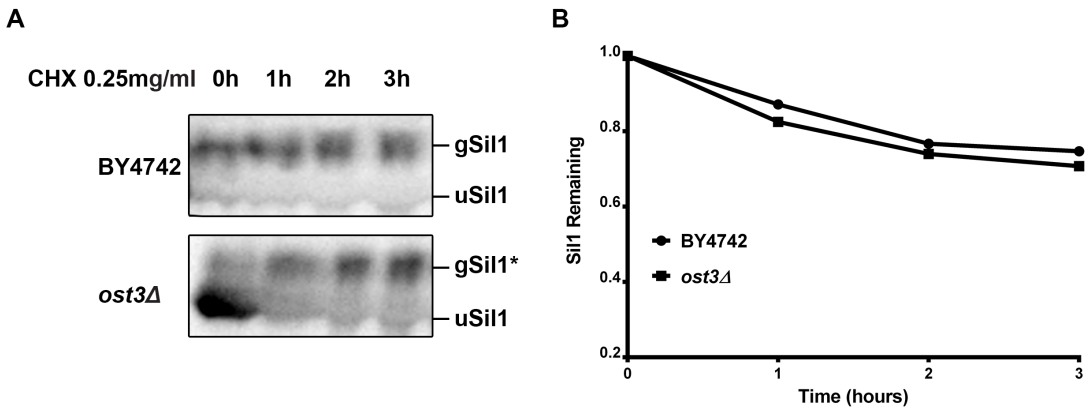

Figure 5.6 Treatment with cycloheximide results in an unknown modification of Sil1.

(A) WT (BY4742) and *ost3Δ* cells were pretreated with 0.25 mg/ml of cyclohexamide for 20 minutes. Following the pre-treatment, samples were taken from the culture every hour for a total of 3 hours. Whole cell lysates were prepared immediately following isolation and immunoblots were performed for Sil1. (B) Densitometric analysis of Sil1 levels for the immunoblots performed in (A), with the 0 minute timepoint used as 100%. gSil1* denotes the unknown upshifted form of Sil1.

While the results in *ost3Δ* cells would suggest this upshift is not the result of N-glycosylation, Sil1 contains several potential sequons, and this event may represent glycosylation of an additional Ost3 independent site. I therefore set out to characterise this modification event in greater detail. One aspect to be considered is the nature in which it occurs, or more specifically, what cellular conditions does cycloheximide treatment mimic besides the direct effect of translation inhibition. I speculate that the physiological consequences of cycloheximide treatment would, to the cell and specifically the ER, represent cellular death, or depletion of sufficient energy stores in which to complete protein translation. In this regard, would treatment with a compound that depletes cellular ATP, and thus indirectly limit translation also elicit modification of Sil1? Exposure of cells to sodium azide (NaN_3) is highly detrimental as it inhibits the activity of cytochrome oxidase, and thus antagonises oxidative phosphorylation, depleting cells of ATP and can also be used as a translation inhibitor (Amesz and van der Zeijst 1972). Consequently, I treated WT and *ost3Δ* cells with 10 mM NaN_3 with samples taken 30 and 60 minutes post incubation, with whole cell lysates prepared, and Sil1 investigated via immunoblot analysis. As before with cycloheximide treatments, exposure of cells to NaN_3 resulted in the same molecular weight increase (Figure 5.7 (A)). This supports my notion that the additional modification of Sil1 occurs in response to severe deleterious stresses within the cell. Potentially indicating that cellular ATP levels are communicated to the ER, and in regard to Sil1, modifications are made presumably to the benefit of the ER and therefore the cell. The large difference in molecular weight change of Sil1 between WT and *ost3Δ* cells treated with cycloheximide and NaN_3 led us to consider why such a difference exists. One possibility is that the unknown modification specifically targets uSil1, either post-translocationally glycosylating Sil1, or mimicking such a modification. I therefore treated *ost3Δ* cells with cycloheximide for 2 hours with samples taken every 30 minutes with whole cell lysates probed with α-Sil1 (Figure 5.7 (B)). As can be seen over the course of this experiment, I see a decrease in uSil1 levels with an increase in Sil1*. Upon further analysis, at the 120 minute time point I see a near

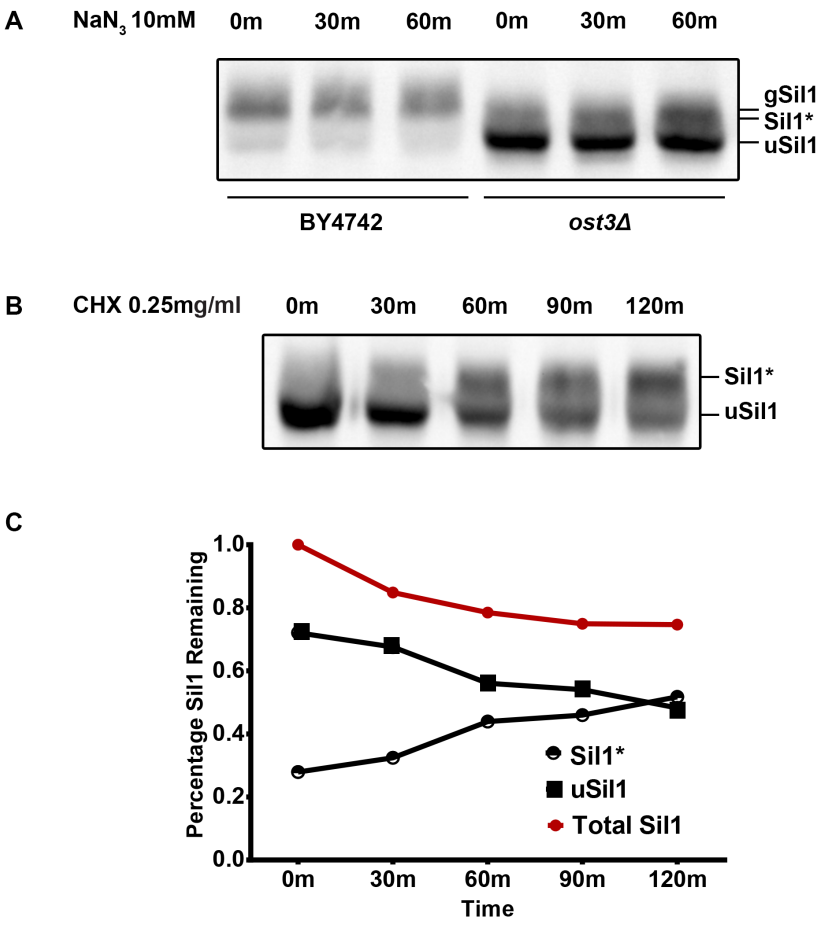

Figure 5.7 Characterisation of Sil1 species accumulating following NaN_3 and cyclohexamide treatment.

(A) Both WT and *ost3Δ* cells were grown to mid-log then pretreated with 10 mM NaN_3 for 20 minutes. Following the pre-treatment, samples were taken from the culture at 0, 30 and 60 minutes. Whole cell lysates were prepared immediately and immunoblots were performed for Sil1. (B) *ost3Δ* cells were grown to mid-log and treated with 0.25 mg/ml of cyclohexamide. Following the treatment, samples were taken from the culture every 30 minutes for a total of 2 hours with whole cell lysates prepared and immunoblots performed for Sil1. (C) Densitometric analysis of Sil1 levels for the immunoblots performed in (B), with the 0 minute timepoint used as 100% with values on the red trace a % of the total at time point zero. The black traces of Sil1* and uSil1 are the ratios of each species at that time point. Sil1* denotes the unknown upshifted form of Sil1.

50/50 ratio of uSil1/Sil1*, while total Sil1 degradation rates are comparable to the previously observed rates (Figure 5.7 (C)). Furthermore, the depletion of uSil1 depicted here supports my previous observation that uSil1 is more labile than gSil1, however I now observe this difference in degradation is likely due to the conversion of uSil1 to a higher molecular weight specie.

I have two instances in which this modification occurs, however the nature of the modification is unknown. While the MW is consistent with N-glycosylation, I find this unlikely, as such I attempted to exclude the possibility. Firstly, I took WT and *ost3Δ* cells and exposed them to either Tm, CHX, or a combination of both, with untreated cells used as controls. In cells treated with both, Tm treatment was performed 1 hour prior to CHX, so as to deplete free dolichol-glycan intermediates and provide the initial pool of uSil1. Immunoblot analysis of both Lhs1 and Sil1 was performed, with Lhs1 being used as a control for appropriate glycosylation, particularly as at least one site has been shown to be Ost3 dependant. Untreated samples are as expected, with WT predominantly accumulating gSil1 and gLhs1, whereas *ost3Δ* cells accumulating uSil1 and an intermediate form of Lhs1 (Figure 5.8 (A)). Again, as expected, Tm treatment causes the increase in abundance of both Lhs1 and Sil1 and the increased accumulation of the unglycosylated forms of both. Cyclohexamide treatment alone produced no changes to the migration of Lhs1 in both WT and *ost3Δ* cells. However, a decreased electrophoretic mobility was seen for Sil1 in WT and *ost3Δ* cells, with this upshifted form the dominant specie in both (Figure 5.8 (A)). When cells were treated with the combination of Tm and CHX, I observed again the increase in apparent molecular weight, and the depletion of uSil1 levels. In this case the size of upshifted Sil1 was comparable in both, and comparable to CHX treatment alone in *ost3Δ* cells (Figure 5.8 (A)). This would indicate that the modification occurs independently of N181 glycosylation. It is also suggestive that the modification is not a further N-glycosylation event, as it occurs in the presence of Tm.

To better resolve the nature of this modification, and more accurately demonstrate that this event is N-glycosylation independent, I performed a PNGase sensitivity assay. The enzyme PNGase F is commonly used to remove the

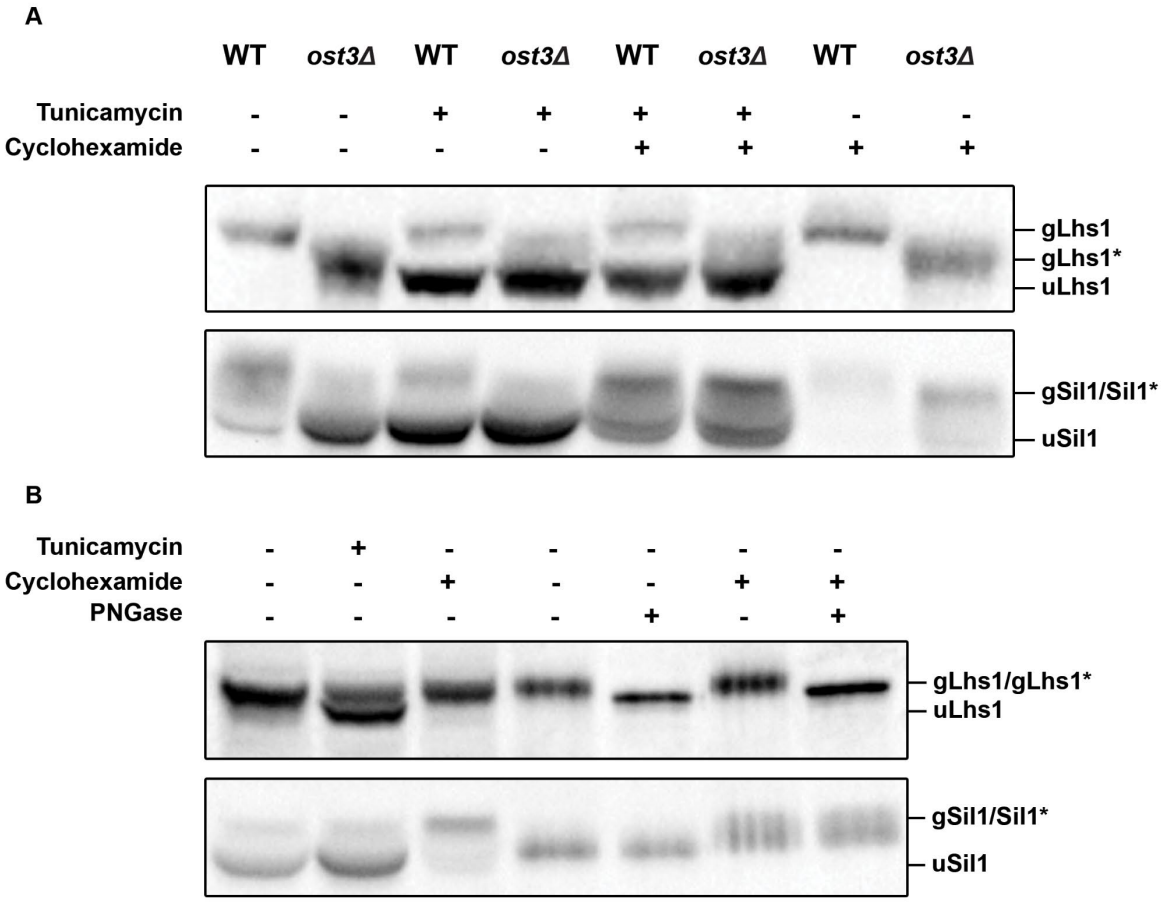

Figure 5.8 Investigating the nature of Sil1 modifications following cyclohexamide treatment.

(A) Both WT and *ost3Δ* cells were grown to mid-log then treated with Tm (10µg/ml), cycloheximide (50µg/ml) or a combination of both as indicated for 1 hour. Following treatment, whole cell lysates were prepared and immunoblot analysis performed for Lhs1 and Sil1. (B) *ost3Δ* cells were grown to mid-log and treated with either Tm (10µg/ml) or cycloheximide (50µg/ml) for 1 hour. Following treatments, membranes were extracted, with samples used directly for controls (solubilised with laemmli buffer) or detergent solubilised using 1% NP-40. Following NP-40 solubilisation, samples were either mock treated, or treated with PNGase F for 1 hour, and finally solubilised in laemmli prior to SDS-PAGE and immunoblot analysis for Lhs1 and Sil1.

majority of N-glycans from proteins, whereby it cleaves the sugar moiety between the innermost GlcNAc and the asparagine residue. Therefore, if the high molecular weight specie found to accumulate following cycloheximide treatment had undergone an additional glycosylation event, I would expect to see a decrease in its molecular weight following the addition of PNGase F. To limit any discrepancies in molecular weight being attributed to N-glycosylation of N181, this experiment was performed in *ost3Δ* cells. Once again Lhs1 was used as a control as its glycosylation is only partially Ost3 dependent, and as I do not observe any changes to its molecular weight following cycloheximide treatment. For this experiment membranes were prepared from *ost3Δ* cells alone, or from cells treated with cycloheximide, with Tm treatment used as a control for molecular weight comparisons. Membranes were then lysed using the detergent NP40, and $1OD_{260}$ units of membranes either mock treated or incubated with PNGase F for 1 hour at 37^{o}C. Samples were then prepared in laemmli buffer and ran on SDS-PAGE gels, followed by immunoblot analysis. As a control, untreated, Tm treated and cycloheximide treated membranes were prepared in laemmli alone and ran alongside. As can be seen in the controls, treatment with tunicamyc0in ablates the remaining N-glycans in Lhs1, and treatment with cycloheximide results in a higher molecular weight specie of Sil1 but not Lhs1 (Figure 5.8 (B)). Interestingly, incubating membranes in the PNGase reaction buffer resulted in an equivalent decrease to the electrophoretic mobility of both Lhs1 and Sil1 compared to the samples prepared in laemmli buffer alone (Figure 5.8 (B)). Treatment with PNGase F alone resulted in a decrease to molecular weight of Lhs1 which is expected as Lhs1 is still glycosylated in *ost3Δ* cells, with no change to the mobility of Sil1. Treatment with cycloheximide alone again results in the accumulation of a higher molecular weight species of Sil1 but not Lhs1 (Figure 5.8 (B)). Incubating cyclohexamide treated cells with PNGase F was unable to revert the molecular weight increase associated with the treatment. Together this data would conclude that the marginal increased molecular weight of Sil1 observed in cells treated with cycloheximide is not due to the covalent attachment of N-glycans.

5.3. Discussion

My characterisation of Sil1 in a reduced ER has elucidated novel regulatory mechanisms in which the restrictions previously imparted by the presence of a N-glycan are removed, allowing for an increase in 'activity'. I propose that N-glycosylation of Sil1 limits the activity of the protein, likely through sequestration. As the covalent attachment of N-glycans occurs cotranslocationally, Sil1 activity can be tailored to the current environmental conditions of the ER. Specifically, I have found that the accumulation of uSil1 during reductive stress to be beneficial, buffering the ER to this deleterious stress. Following recovery from reductive stress the increased protein turnover of uSil1 prevents the inappropriate accumulation of this more 'active' form. As Sil1s regulation during reductive stress is highly specific, I was interested to determine how Sil1 is regulated in oxidative conditions.

During my initial analysis of the factors responsible for the accumulation uSil1, I treated cells with the oxidant H_2O_2 and observed an overall decrease in the abundance of Sil1, with a notable decrease in the abundance of uSil1. To better characterise Sil1 dynamics in oxidative conditions, diamide, a potent oxidiser of glutathione, and therefore highly effective in oxidising the ER was used. Unlike with H_2O_2, cells treated with low concentrations of diamide were found to have elevated levels of Sil1. Unexpectedly, I also found uSil1 to accumulate in a manner akin to treatment with DTT. This seemingly contradicts my previous conclusions that loss of Sil1 glycosylation is specifically a response to reductive stress. Furthermore, the use of high concentrations of H_2O_2 were unable to replicate the effects of diamide, suggestive that this phenotype is not due to oxidation alone. Instead I suspect this is related to the mode of action for these oxidants. As a physiological oxidant, H_2O_2 is directly responsible for the increased abundance of oxygen free radicals, whereby the oxidative potential is equally distributed. In contrast, diamide is an oxidising agent with a particular affinity for oxidising reduced glutathione (GSH), the predominant cellular redox buffer (Kosower et al. 1969). Therefore, diamide treatment would more readily elicit fluctuations to glutathione homeostasis. In agreeance with this are the experiments in which increased GSH (reduced glutathione) transport into the cell through overexpression of Opt1 also results in

the accumulation of uSil1. Together this would indicate that glutathione communicates the redox status of the ER, and in turn regulates Sil1 glycosylation. With low level diamide treatment likely increasing the flux of glutathione into the ER, generating a localised zone of reduced glutathione. Being that the OST complex and glycosylation occur adjacent to the Sec61 translocon, with this channel responsible for the import of GSH into the ER, I predict this to effect the redox sensitive Ost3-dependent glycosylation of Sil1.

I observe the increased accumulation of uSil1 during reductive stress to be beneficial to the cell, with oxidising conditions characterised to preferentially accumulate gSil1 with an overall reduced abundance. Therefore, what are the consequences of accumulating uSil1 during oxidative stress? When *sil1*^{N181Q} is expressed in cells exposed to the glutathione oxidant diamide, viability is significantly decreased. This would suggest that during reductive stress, the rapid change in N-glycosylation preference for Sil1 is targeting it for specific activities, which if left unregulated, would lead to significant damage to the cell. These findings support recent literature in which deletion of *SIL1* was shown to increase the resistance to diamide (Siegenthaler et al. 2017).

The authors also showed that Sil1 was responsible for reducing an oxidised cysteine within Kar2, previously determined to inhibit its ATPase activity (Siegenthaler et al. 2017; Wang et al. 2014). Upon becoming oxidised, inhibition of ATPase activity directs Kar2 to function as a holdase sequestering unfolded proteins, preventing aberrant misfolding due to an excessive oxidative potential. With this, it is clear why overexpression of *sil1*^{N181Q} results in such a detrimental outcome. I propose glycosylation of Sil1 is used to specify its activity in accordance with the current environmental status of the ER. How this is accomplished is uncertain, however I suspect glycosylation endows interaction of Sil1 with an additional factor within the ER, thus limiting its interactions with Kar2. Alternatively, I envisage the N-terminal domain of Sil1 itself to directly bind the glycan, thus preventing activities related to the N-terminus itself. If glycosylation of Sil1 sequesters its 'activity', accumulation of uSil1 in oxidative stress would allow for the unchecked reduction of Kar2, thus re-engaging ATPase activity, ultimately

leading to the accumulation of misfolded proteins, and total dysfunction of the ER. The opposite is true for reductive stress, whereby a large increase in unfolded proteins requires a reciprocal increase in the foldase activity of Kar2. The accumulation of uSil1 during this time would benefit Kar2 foldase activity. As the burden of unfolded proteins increases, so too does the requirement for Lhs1 holdase activity, therefore decreasing the requirement for Kar2 in preventing protein aggregation. Thus, limiting Lhs1s opportunity for NEF activity, with the increased availability of uSil1 then better able to substitute for Lhs1. Additionally, a consequence of repeated folding cycles by Kar2 is the increased potential for oxidation of the key cysteine residue. Preventing Sil1 glycosylation would therefore allow its increased interaction with Kar2, whereby Sil1 is able to reduce C63, maintaining maximal ATPase activity, thus resolving the ensuing stress more efficiently. In this context, I envisage Sil1 to be a direct regulator of Kar2 activity, with Ost3 sensing changes in the redox potential of the ER and co-ordinating Sil1 N-glycosylation to meet the needs of the cell.

Two cysteines with the N terminus of Sil1, C52 and C57, are essential for the reduction of the key cysteine in Kar2 (Siegenthaler et al. 2017). It is therefore interesting that I have found mutation of these residues to serine results in *sil1*$^{C52S\ C57S}$ being targeted for ERAD. This provides greater insight into the exquisite redox sensitivity of Sil1, with the implication being that both Sil1 activity and stability are regulated by redox. I previously determined Sil1 turnover to be faster in cells treated with DTT, additionally, uSil1 is more labile than gSil1. Mutation of cysteine to serine likely mimics the peptide to be in a fully reduced state. Thus, my observation that *sil1*$^{C52S\ C57S}$ is an ERAD substrate supports the notion that reduced Sil1 is more labile. This would be consistent with my model for Sil1, in that its abundance and activity are directly regulated in response to the changing needs of the ER in the context of redox. In highly oxidising conditions, I see a decrease in Sil1 levels, with little uSil1 detected. This would support the observed toxicity of expressing *sil1*^{N181Q} in the presence of diamide. In highly oxidising conditions, Kar2 is directed towards holdase activity through oxidation of C63. As Sil1 can reduce this cysteine in Kar2, restoring the foldase activity, ERAD is employed to reduce Sil1

levels, with uSil1 preferentially targeted. The same applies under conditions of reductive stress, uSil1 is abundant until the stress is alleviated, at which time uSil1 levels are rapidly reduced to prevent any unwanted stimulation of Kar2. I have also seen that at low levels, diamide results in both increased Sil1, and the appearance of uSil1. I hypothesise that low levels of this oxidant stimulates protein folding and results in an influx of reduced glutathione, temporarily generating a localised reduced environment surrounding the translocon. This highly localised reduced environment around the translocon would explain the increase in uSil1, which at such time would benefit Kar2 activity due to the increased oxidative folding potential.

One unexpected observation during these analyses was the accumulation of an additional specie of Sil1 following cycloheximide and sodium azide treatment. This specie while not significantly larger in WT cells, where the predominant specie of Sil1 is glycosylated, is far more obvious in *ost3Δ* cells. This discrepancy initially led us to assume the upshift to be representative of an additional glycosylation event, independent of Ost3, as the specie in *ost3Δ* cells appears similar in molecular weight to WT gSil1. However as cells pre-treated with Tm, followed by incubation with cycloheximide, also displayed this unusual Sil1 phenotype, it is indicative that it is not due to N-glycosylation. Furthermore, following treatment with the N-glycosylation trimming enzyme PNGase F, no decrease in molecular weight was observed, confirming this modification is not due to the attachment of an N-glycan.

During these investigations, I found this modification to be specific for uSil1, with the minor changes observed for gSil1 likely due to glycan modification. As to the role this modification plays, I suspect degradation of Sil1 requires the interaction of Sil1 with the membrane, supported by my observation that Sil1 degradation is non-classical, with it being a Doa10 dependent substrate. As such, uSil1 is able to be targeted for degradation through this observed modification. The identity of this modification is, however, still unknown. I have shown regulation of Sil1 to be extremely sensitive to changes in cellular homeostasis, with N-glycosylation being the primary mode of regulation. It is therefore not unexpected to observe Sil1 again undergoing a rapid modification in response to the current

cellular environment. Future work will require a more detailed investigation into the nature and biological ramifications of this modification. And as with the redox dependent regulation of Sil1 N-glycosylation, this may represent a novel regulatory response. As to the degradation kinetics of Sil1, the differing rates of degradation between uSil1 and gSil1, and Sil1s requirement for the Doa10 pathway, make this a compelling substrate to better our understanding of ERAD.

Collectively, the role of Sil1 in the ER is more substantial than previously believed. Specifically, Sil1 activity is directly responsible for modulating the folding kinetics of the ER in response to changes in redox. It may also help to explain the severe phenotype observed in patients with Marinesco-Sjogren syndrome, a disease in which over 50% of cases are characterised by complete or partial loss of Sil1. Marinesco-Sjogren syndrome is associated with a wide range of symptoms including mental and physical developmental defects, muscle ataxia, and hypogonadism, all of which occur during development, with increasing severity. (Senderek et al. 2005). Interestingly, many of the issues relating to Marinesco-Sjogren syndrome are found within tissues known to generate large amounts of ROS or are highly secretory in nature. Loss of Sil1 may therefore result in these tissues being unable to sufficiently adapt to changes within the redox environment, or efficiently fold and secrete proteins. Increased understanding of the fundamental role of Sil1, and ER function will hopefully elucidate their specific roles in the context of both development and disease.

Conclusion

Approximately 1/3rd of all proteins synthesised are targeted to the secretory pathway, with the translocation of unfolded proteins across the ER membrane being the first step in this pathway. The luminal environment of the ER is sufficiently equipped to deal with the incoming cargo, coordinating folding and maturation of these proteins prior to their continued progression. Together these processes are highly demanding of cellular resources, which poses the question: how is the nutritional status of the cell communicated to the ER?

Eukaryotic cells possess multiple nutritional signalling pathways, with the TOR signalling network regarded as the master regulator of cellular anabolism. The activation of TOR is dependent on the abundance and quality of nutrients, with nitrogen (amino acids) and carbon (glucose) availability communicated to the kinase complex (Loewith and Hall 2011). When the nutritional demands are met, TOR is activated allowing for the upregulation of anabolic processes essential for cellular growth. One key activity intimately linked to TOR activity is protein translation. When active, TOR increases the translational capacity of the cell via two main mechanisms, the first being an increased biosynthesis of ribosomes, thus increasing the total translational capacity of the cell. The significance of this is obvious when considering inhibition of TOR results in a 40-60% reduction of ribosomes in yeast (Jorgensen et al. 2004; Lempiäinen and Shore 2009). The second, and more complex role elicited by TOR on translation is its regulation of the eukaryotic initiation factor complex (eIF), whereby TOR activity stimulates the assembly of the eIF4F complex, which in turn is responsible for the translation initiation of many mRNAs (Berset, Trachsel and Altmann 1998). Therefore, under optimal conditions for growth, TOR activity results in an increased translation of proteins and consequently an increase in proteins being targeted to the ER. Considering the above, I re-pose the question: is TOR responsible for communicating the nutritional status of the cell to the ER?

This is an attractive hypothesis for many reasons, as to date very little has been described correlating TOR activity with the ER, the major exception being

autophagy. In this regard, TOR and autophagy are mutually exclusive in that activation of one requires the repression of the other. The role of the ER during autophagy is complex and multifaceted, with the ER being a major source of membranes for the production of autophagosomes, thus involved early in the process (Lamb, Yoshimori and Tooze 2013; Wilkinson 2019). Autophagy is initiated by Atg1, which requires the interaction of several additional factors, with Atg13 described to be essential for the recruitment of these factors. TOR dependent phosphorylation of Atg13 diminishes these interactions, inactivating autophagy (Jung et al. 2010). The ER has also been demonstrated to undergo a process termed ERphagy, which occurs independently of TOR activity. These activities would suggest the ER is sensitive to the nutritional demands of the cell and is able to respond appropriately. Yet these activities oppose anabolism, and as such are not directly regulated by TOR.

With the rationale that anabolic processes, as directed by TOR activity, impact the secretory pathway, I aimed to establish the existence of a novel regulatory pathway. In doing so, I have identified that Sec63, a key component of the translocation apparatus, is phosphorylated in a TOR dependent manner. Given that phosphorylation of Sec63 in *S. pombe* is also found to be sensitive to TOR phosphorylation, I suspect this may be a conserved feature. Although sequentially diverse, these sites in both organisms are located in the C-terminal portion of the Brl-domain, suggestive of conservation. Regarding higher eukaryotes, human Sec63 is known to be phosphorylated by CK2 at the extreme C-terminus, as with yeast this is required for its interaction with Sec62 (Ampofo et al. 2013). Additional phosphorylation events in human Sec63 have been documented in numerous high throughput investigations of global phosphorylation. Of the <20 sites described, the phosphorylation of T537 in the human orthologue is noteworthy regarding my own observations. Having been documented in 14 separate studies, I can assume this site to be genuine, and abundant enough for detection (Hornbeck et al. 2015). The properties of the amino acids that immediately flank T537 have similar properties to those surrounding the sequence of T467-S468 in *S. cerevisiae*, thus making this site a potential candidate for TOR dependent phosphorylation. While this is highly

speculative, the potential for a corresponding site of phosphorylation in higher eukaryotes provides additional rationale for a more detailed investigation into TOR dependent phosphorylation of Sec63.

I initially aimed to characterise the TOR dependent phosphorylation of Sec63, and the effects this had on its function. The mutagenesis of two phosphorylation sites, found in this study to be sensitive to TOR activity, was the primary method of analysis. In doing so, I was unable to establish any changes in Sec63 activity. Attempts were made to mimic phosphorylation of these sites through aspartic and glutamic acid substitutions. While no changes in function were observed, I was unable to confirm if these mutations successfully mimic phosphorylation, a common difficulty in studies of this nature. Therefore, it can only be concluded that ablation of phosphorylation (alanine substitution) does not affect the proteins function. One observation made during my investigations, was the accumulation of unglycosylated Sil1 in a truncated mutant of Sec63. Although this truncation is not representative of phosphorylation, its proximal location to T467-S468 provided insight into the potential function of this region while establishing the basis for my investigation into the nature of Sil1 glycosylation dynamics. Coupled with the inferences made studying the structure of the posttranslational translocon and my new understandings of Sil1, additional conclusions can be drawn on the function of this domain. As previously stated, the location of T467-S468 and the 20 aa truncation are in close proximity to a domain of Sec63 found to interact with Sec61 (Wu, Cabanos and Rapoport 2019). This interaction has been proposed to anchor Sec63 to the Sec61 translocon, occupying the same region in which the ribosome contacts Sec61, thus preventing its interaction. Additionally, it is proposed this interaction forms the basis for the Sec63 dependent opening of the lateral gate, a process essential for posttranslational translocation (Wu, Cabanos and Rapoport 2019). My observation that Sil1 glycosylation is perturbed in the truncated mutant was initially thought to be a general consequence of ER stress, as elicited by disrupted translocon function. I now understand Sil1 glycosylation to be extremely sensitive to reductive stress, a phenotype which is replicated through increased glutathione flux. Therefore, a

possible explanation of the phenotype observed in my truncated mutant is the increased permeability of the translocon. This would support both my observations, and the insights garnered from the structure, that this region is involved in the opening of the lateral gate. Furthermore, this region may constitute an additional Sec61 interaction site, and direct my investigations into the role of phosphorylation of this domain. My use of Sil1 differential glycosylation as a diagnostic marker for the redox state of the ER, also establishes this as tool for investigations of ER translocon gating/permeability.

Regarding Sil1, my initial observation that it is differentially glycosylated in mutants of Sec63 instigated my interest into understanding this phenomenon. As one of two nucleotide exchange factors in the ER, Sil1 has often been regarded as the lesser of the two. Primarily these assumptions are due to observations that Sil1 is less proficient as a NEF than Lhs1, as determined by the rate of ATP hydrolysis by Kar2 (Tyson and Stirling 2000). Additionally, loss of Lhs1 elicits substantially more deficits, with the constitutive induction of the UPR highly suggestive Lhs1 activity is required for normal ER function (Saris et al. 1997). Yet as I, and in recent times others, have shown, the role of Sil1 is substantially more important than previously thought. Following its discovery and initial characterisation, renewed interest in the protein is likely the result of its association with the developmental disorder Marinesco-Sjögren syndrome (MSS). In MSS, loss of function mutations of Sil1 typically result in its decreased abundance, have been observed in approximately 2/3 of MSS cases (Senderek et al. 2005). Symptomatically, individuals with MSS are characterised with possessing moderate intellectual disability, myopathy, muscle ataxia and among other symptoms, disrupted sexual development (Senderek et al. 2005). The traits associated with MSS would indicate that Sil1 function is important for early development, neurogenesis, and in terminally differentiated tissues. Upon consulting the protein atlas, I find the human Sil1 protein to be highly abundant in brain, endocrine, pancreatic and GI tissues (Uhlen et al. 2015). This is consistent with the dysfunctions associated with MSS and shows Sil1 to be associated with highly secretory tissues.

Outside of MSS, the importance of Sil1 in higher eukaryotes has been demonstrated in multiple studies. Alterations to ER function are often seen in many disease states, in particular neurodegenerative disorders (Roussel et al. 2013; Ozcan and Tabas 2012; Yoshida 2007). It is now evident that disrupted regulation of Sil1 may be a factor in ER associated pathologies. The 'woozy mouse', used as a model for various neuropathies now including MSS, presents with ataxia and Purkinje cell loss in the cerebellum, which was believed to be a result of ER dysfunction and subsequently found to be due to mutation of Sil1 (Zhao et al. 2005). Increased Sil1 has been found in the surviving neurons of Alzheimer's diseased brains during autopsies, indicating Sil1 may have a protective role in the progression of the disease (Liu et al. 2016), while decreased Sil1 has been shown to inhibit the progression of gliomas, suggesting Sil1 may act as an oncogene in certain cancers (Xu et al. 2018). Decreased Sil1 abundance has also been associated with disrupted ER homeostasis, resulting in myopathy, and shown to negatively affect insulin levels and secretion in pancreatic beta cells (Ittner et al. 2014). Together these studies indicate that Sil1 provides an essential role in higher eukaryotes, one that is unable to be covered by Lhs1, with disruption to Sil1 resulting in various pathologies.

In considering these pathologies, my investigations of Sil1 may be of use in understanding their underlying molecular mechanisms. I have now documented regulation of Sil1 to be unique and highly responsive to changes in the environmental conditions of the ER. Specifically, I find Sil1 activity to be altered in accordance with the redox status of the ER, whereby reductive stress induces changes in the glycosylation efficiency of Sil1. The accumulation of uSil1 during reductive stress is beneficial to the cell, bolstering ER function limiting the deleterious effects until homeostasis is restored. Conversely, in oxidative stress Sil1 levels are seen to be diminished, with glycosylated Sil1 preferred. If unglycosylatable Sil1 is allowed to accumulate in oxidative conditions, cell viability is significantly reduced. How Sil1 activity is altered in response to its glycosylation status is not fully understood. I have speculated that glycosylation of Sil1 endows

an unknown interaction, either with an additional ER factor or, as previously discussed a self-interaction.

Together, the findings presented here help to elucidate several previously unknown mechanisms pertaining to ER function. While my characterisation of TOR dependant phosphorylation of Sec63 was unable to determine the exact nature of this relationship, I did establish that Sec63 phosphorylation is differentially regulated in response to TOR inhibition. Furthermore, the location of these phosphorylation sites within a region known to co-ordinate Sec63-Sec61 interaction, may prove highly informative (Wu, Cabanos and Rapoport 2019). The observed accumulation of uSil1 in the *sec63*$^{467/468\text{- AA-Trunc}}$ mutant is of particular interest. As I have now determined, uSil1 accumulation is a direct response to changes in the redox status of the ER. As such I have concluded this mutant potentially disrupts ER permeability, resulting in dysfunction. The importance of this is exemplified by the knowledge that the Sec61 translocon is essential for the transport of small molecules, such as glutathione and Ca^{2+} (Ponsero et al. 2017; Linxweiler, Schick and Zimmermann 2017; Lang et al. 2011; Van Coppenolle et al. 2004). The regulation of this permeability is coordinated by several factors. Primarily, when in a translocation active state, the channel is sealed by the channel binding partner (SRP, Sec62 complex), with the translocating peptide preventing the free flow of solutes. On the luminal side, Kar2 is also found to provide an additional seal, with this activity coordinated by the oxidation /nucleotide status of Kar2, with ADP bound Kar2 forming a strong interaction with Sec61 (Schauble et al. 2012). As such, this work has identified Sec63 to be a potential regulator of translocon gating, as determined by the inappropriate accumulation of uSil1, a phenotype directly reporting the oxidation status of the ER. Furthermore, as Sec63 is a co-chaperone of Kar2, this phenotype may result from multiple aspects of Sec63 activity.

While this work has helped to characterise multiple facets of ER dynamics, in particular the role of glycosylation on the protein folding machinery, it has also generated several further questions. One area requiring more investigation is the role of phosphorylation on Sec63 activity. My initial identification of the sites

responsive to TOR inhibition while informative, is lacking in both detail, and significance. Better experimental design, and higher resolution analysis of the various isoforms present (i.e. single and double phosphorylation at residues T467-S468) would significantly bolster our understanding. Furthermore, the lack of a discernible phenotype is suggestive that more readouts need to be considered. In regards to Sil1, the use of mass spectrometry to better analyse the various modifications occurring under different conditions would be very informative, as would looking to identify additional ER factors whose glycosylation is sensitive to either loss of Ost3 or changes in REDOX. We find it unlikely that this differential glycosylation of Sil1 is unique, thus representing an interesting avenue in which further investigation is required.

As presented herein, the maintenance of ER homeostasis is critically important for its function. The ER is sufficiently able to negate perturbations to various stresses, such as reductive stress, demonstrated by the redox dependent regulation of Sil1 activity through glycosylation. My observations have provided a greater understanding of intricacies involved and provided new avenues for investigation. With more studies detailing the ER, and more specifically, mutation of genes involved in protein translocation and folding, to be responsible for a range of pathologies, understanding how they function is of the upmost importance.

References

Absmeier, Eva, Karine F. Santos, and Markus C. Wahl. 2016. "Functions and Regulation of the Brr2 Rna Helicase During Splicing." *Cell Cycle* 15 (24): 3362-3377. doi: 10.1080/15384101.2016.1249549.

Acosta-Alvear, Diego, G. Elif Karagöz, Florian Fröhlich, Han Li, Tobias C. Walther, and Peter Walter. 2018. "The Unfolded Protein Response and Endoplasmic Reticulum Protein Targeting Machineries Converge on the Stress Sensor Ire1." *eLife* 7: e43036. doi: 10.7554/eLife.43036.

Akiyama, Y, and K Ito. 1987. "Topology Analysis of the Secy Protein, an Integral Membrane Protein Involved in Protein Export in Escherichia Coli." *The EMBO Journal* 6 (11): 3465-3470.

Albuquerque, Claudio P., Marcus B. Smolka, Samuel H. Payne, Vineet Bafna, Jimmy Eng, and Huilin Zhou. **2008a**. "A Multidimensional Chromatography Technology for in-Depth Phosphoproteome Analysis." *Molecular & Cellular Proteomics* 7 (7): 1389-1396. doi: 10.1074/mcp.M700468-MCP200.

———. **2008b**. "A Multidimensional Chromatography Technology for in-Depth Phosphoproteome Analysis." *Molecular & Cellular Proteomics* 7 (7): 1389-1396. doi: 10.1074/mcp.M700468-MCP200.

Alderson, Thomas Reid, Jin Hae Kim, and John Lute Markley. 2016. "Dynamical Structures of Hsp70 and Hsp70-Hsp40 Complexes." *Structure (London, England : 1993)* 24 (7): 1014-1030. doi: 10.1016/j.str.2016.05.011.

Althoff, S., D. Selinger, and J. A. Wise. 1994. "Molecular Evolution of Srp Cycle Components: Functional Implications." *Nucleic Acids Research* 22 (11): 1933-1947. http://www.ncbi.nlm.nih.gov/pmc/articles/PMC308104/.

Amesz, W. J. C., and B. A. M. van der Zeijst. 1972. "Azide as Inhibitor of Protein Synthesis in Yeast Protoplasts." *FEBS Letters* 26 (1): 165-168. doi: https://doi.org/10.1016/0014-5793(72)80565-9.

Ampofo, Emmanuel, Sabrina Welker, Martin Jung, Linda Müller, Markus Greiner, Richard Zimmermann, and Mathias Montenarh. 2013. "Ck2 Phosphorylation of Human Sec63 Regulates Its Interaction with Sec62." *Biochimica et Biophysica Acta (BBA) - General Subjects* 1830 (4): 2938-2945. doi: http://dx.doi.org/10.1016/j.bbagen.2012.12.020.

Apweiler, Rolf, Henning Hermjakob, and Nathan Sharon. 1999. "On the Frequency of Protein Glycosylation, as Deduced from Analysis of the Swiss-Prot Database11dedicated to Prof. Akira Kobata and Prof. Harry Schachter on the Occasion of Their 65th Birthdays." *Biochimica et Biophysica Acta (BBA) - General Subjects* 1473 (1): 4-8. doi: https://doi.org/10.1016/S0304-4165(99)00165-8.

Ashby, Michael C., and Alexei V. Tepikin. 2001. "Er Calcium and the Functions of Intracellular Organelles." *Seminars in Cell and Developmental Biology* 12 (1): 11-17. doi: 10.1006/scdb.2000.0212.

Berg, Bert van den, William M. Clemons, Ian Collinson, Yorgo Modis, Enno Hartmann, Stephen C. Harrison, and Tom A. Rapoport. 2004. "X-Ray

Structure of a Protein-Conducting Channel." *Nature* 427 (6969): 36-44. doi: 10.1038/nature02218.

Berset, C., H. Trachsel, and M. Altmann. 1998. "The Tor (Target of Rapamycin) Signal Transduction Pathway Regulates the Stability of Translation Initiation Factor Eif4g in the Yeast Saccharomyces Cerevisiae." *Proc Natl Acad Sci U S A* 95 (8): 4264-9. doi: 10.1073/pnas.95.8.4264.

Biederer, T., C. Volkwein, and T. Sommer. 1996. "Degradation of Subunits of the Sec61p Complex, an Integral Component of the Er Membrane, by the Ubiquitin-Proteasome Pathway." *EMBO Journal* 15 (9): 2069-2076.

Blobel, G., and B. Dobberstein. 1975. "Transfer of Proteins across Membranes. I. Presence of Proteolytically Processed and Unprocessed Nascent Immunoglobulin Light Chains on Membrane-Bound Ribosomes of Murine Myeloma." *The Journal of Cell Biology* 67 (3): 835-51.

Boisramé, Anita, Jean-Marie Beckerich, and Claude Gaillardin. 1996. "Sls1p, an Endoplasmic Reticulum Component, Is Involved in the Protein Translocation Process in the Yeast Yarrowia Lipolytica." *Journal of Biological Chemistry* 271 (20): 11668-11675. doi: 10.1074/jbc.271.20.11668.

Boisramé, Anita, Mehdi Kabani, Jean-Marie Beckerich, Enno Hartmann, and Claude Gaillardin. 1998. "Interaction of Kar2p and Sls1p Is Required for Efficient Co-Translational Translocation of Secreted Proteins in the Yeastyarrowia Lipolytica." *Journal of Biological Chemistry* 273 (47): 30903-30908. doi: 10.1074/jbc.273.47.30903.

Bordallo, Javier, Richard K. Plemper, Andreas Finger, and Dieter H. Wolf. 1998. "Der3p/Hrd1p Is Required for Endoplasmic Reticulum-Associated Degradation of Misfolded Lumenal and Integral Membrane Proteins." *Molecular Biology of the Cell* 9 (1): 209-222. doi: 10.1091/mbc.9.1.209.

Brachmann, C. B., A. Davies, G. J. Cost, E. Caputo, J. Li, P. Hieter, and J. D. Boeke. 1998. "Designer Deletion Strains Derived from Saccharomyces Cerevisiae S288c: A Useful Set of Strains and Plasmids for Pcr-Mediated Gene Disruption and Other Applications." *Yeast* 14 (2): 115-32. doi: 10.1002/(sici)1097-0061(19980130)14:2<115::Aid-yea204>3.0.Co;2-2.

Braunger, Katharina, Stefan Pfeffer, Shiteshu Shrimal, Reid Gilmore, Otto Berninghausen, Elisabet C. Mandon, Thomas Becker, Friedrich Förster, and Roland Beckmann. 2018. "Structural Basis for Coupling Protein Transport and N-Glycosylation at the Mammalian Endoplasmic Reticulum." *Science (New York, N.Y.)* 360 (6385): 215-219. doi: 10.1126/science.aar7899.

Brodsky, J L, and R Schekman. 1993. "A Sec63p-Bip Complex from Yeast Is Required for Protein Translocation in a Reconstituted Proteoliposome." *The Journal of Cell Biology* 123 (6): 1355-1363. doi: 10.1083/jcb.123.6.1355.

Brodsky, J. L., E. D. Werner, M. E. Dubas, J. L. Goeckeler, K. B. Kruse, and A. A. McCracken. 1999. "The Requirement for Molecular Chaperones During Endoplasmic Reticulum-Associated Protein Degradation Demonstrates That Protein Export and Import Are Mechanistically Distinct." *J Biol Chem* 274 (6): 3453-60. http://www.ncbi.nlm.nih.gov/pubmed/9920890.

Buck, Teresa M., Lindsay Plavchak, Ankita Roy, Bridget F. Donnelly, Ossama B. Kashlan, Thomas R. Kleyman, Arohan R. Subramanya, and Jeffrey L. Brodsky. 2013. "The Lhs1/Grp170 Chaperones Facilitate the Endoplasmic Reticulum-

Associated Degradation of the Epithelial Sodium Channel." *Journal of Biological Chemistry* 288 (25): 18366-18380. doi: 10.1074/jbc.M113.469882.

Bultynck, Geert, Victoria L. Heath, Alia P. Majeed, Jean-Marc Galan, Rosine Haguenauer-Tsapis, and Martha S. Cyert. 2006. "Slm1 and Slm2 Are Novel Substrates of the Calcineurin Phosphatase Required for Heat Stress-Induced Endocytosis of the Yeast Uracil Permease." *Molecular and Cellular Biology* 26 (12): 4729-4745. doi: 10.1128/mcb.01973-05.

Caplan, A J, J Tsai, P J Casey, and M G Douglas. 1992. "Farnesylation of Ydj1p Is Required for Function at Elevated Growth Temperatures in Saccharomyces Cerevisiae." *Journal of Biological Chemistry* 267 (26): 18890-18895. http://www.jbc.org/content/267/26/18890.abstract.

Caplan, Avrom J., Douglas M. Cyr, and Michael G. Douglas. 1992. "Ydj1p Facilitates Polypeptide Translocation across Different Intracellular Membranes by a Conserved Mechanism." *Cell* 71 (7): 1143-1155. doi: 10.1016/S0092-8674(05)80063-7.

Carvalho, Pedro, Veit Goder, and Tom A. Rapoport. 2006. "Distinct Ubiquitin-Ligase Complexes Define Convergent Pathways for the Degradation of Er Proteins." *Cell* 126 (2): 361-373. doi: https://doi.org/10.1016/j.cell.2006.05.043.

Chambers, Joseph E., Kseniya Petrova, Giulia Tomba, Michele Vendruscolo, and David Ron. 2012. "Adp Ribosylation Adapts an Er Chaperone Response to Short-Term Fluctuations in Unfolded Protein Load." *The Journal of cell biology* 198 (3): 371-385. doi: 10.1083/jcb.201202005.

Chapman, Rowan E., and Peter Walter. 1997. "Translational Attenuation Mediated by an Mrna Intron." *Current Biology* 7 (11): 850-859. doi: https://doi.org/10.1016/S0960-9822(06)00373-3.

Chavan, M., A. Yan, and W. J. Lennarz. 2005. "Subunits of the Translocon Interact with Components of the Oligosaccharyl Transferase Complex." *J Biol Chem* 280 (24): 22917-24. doi: 10.1074/jbc.M502858200.

Chen, Wentao, Sebastian Enck, Joshua L. Price, David L. Powers, Evan T. Powers, Chi-Huey Wong, H. Jane Dyson, and Jeffery W. Kelly. 2013. "Structural and Energetic Basis of Carbohydrate-Aromatic Packing Interactions in Proteins." *Journal of the American Chemical Society* 135 (26): 9877-9884. doi: 10.1021/ja4040472.

Chi, An, Curtis Huttenhower, Lewis Y. Geer, Joshua J. Coon, John E. P. Syka, Dina L. Bai, Jeffrey Shabanowitz, Daniel J. Burke, Olga G. Troyanskaya, and Donald F. Hunt. 2007. "Analysis of Phosphorylation Sites on Proteins from <Em>Saccharomyces Cerevisiae</Em> by Electron Transfer Dissociation (Etd) Mass Spectrometry." *Proceedings of the National Academy of Sciences* 104 (7): 2193-2198. doi: 10.1073/pnas.0607084104.

Chirico, William J., M. Gerard Waters, and Gunter Blobel. 1988. "70k Heat Shock Related Proteins Stimulate Protein Translocation into Microsomes." *Nature* 332 (6167): 805-810. http://dx.doi.org/10.1038/332805a0.

Connolly, T., and R. Gilmore. 1989. "The Signal Recognition Particle Receptor Mediates the Gtp-Dependent Displacement of Srp from the Signal Sequence of the Nascent Polypeptide." *Cell* 57 (4): 599-610. doi: 10.1016/0092-8674(89)90129-3.

Connolly, T., P. J. Rapiejko, and R. Gilmore. 1991. "Requirement of Gtp Hydrolysis for Dissociation of the Signal Recognition Particle from Its Receptor." *Science* 252 (5009): 1171-3. doi: 10.1126/science.252.5009.1171.

Corbett, Elaine F., Karolina M. Michalak, Kim Oikawa, Steve Johnson, Iain D. Campbell, Paul Eggleton, Cyril Kay, and Marek Michalak. 2000. "The Conformation of Calreticulin Is Influenced by the Endoplasmic Reticulum Luminal Environment." *Journal of Biological Chemistry* 275 (35): 27177-27185. http://www.jbc.org/content/275/35/27177.abstract.

Corsi, A. K., and R. Schekman. 1997. "The Lumenal Domain of Sec63p Stimulates the Atpase Activity of Bip and Mediates Bip Recruitment to the Translocon in Saccharomyces Cerevisiae." *J Cell Biol* 137 (7): 1483-93. http://www.ncbi.nlm.nih.gov/pubmed/9199165.

Craven, R. A., M. Egerton, and C. J. Stirling. 1996. "A Novel Hsp70 of the Yeast Er Lumen Is Required for the Efficient Translocation of a Number of Protein Precursors." *EMBO J* 15 (11): 2640-50. http://www.ncbi.nlm.nih.gov/pubmed/8654361.

Dardalhon, Michèle, Chitranshu Kumar, Ismail Iraqui, Laurence Vernis, Guy Kienda, Agata Banach-Latapy, Tiantian He et al. 2012. "Redox-Sensitive Yfp Sensors Monitor Dynamic Nuclear and Cytosolic Glutathione Redox Changes." *Free Radical Biology and Medicine* 52 (11-12): 2254-2265. doi: 10.1016/j.freeradbiomed.2012.04.004.

Davila, Sonia, Laszlo Furu, Ali G. Gharavi, Xin Tian, Tamehito Onoe, Qi Qian, Airong Li et al. 2004. "Mutations in Sec63 Cause Autosomal Dominant Polycystic Liver Disease." *Nature Genetics* 36 (6): 575-577. doi: 10.1038/ng1357.

Deshaies, Raymond J., Bruce D. Koch, Margaret Werner-Washburne, Elizabeth A. Craig, and Randy Schekman. 1988. "A Subfamily of Stress Proteins Facilitates Translocation of Secretory and Mitochondrial Precursor Polypeptides." *Nature* 332 (6167): 800-805. http://dx.doi.org/10.1038/332800a0.

Deshaies, Raymond J., Sylvia L. Sanders, David A. Feldheim, and Randy Schekman. 1991. "Assembly of Yeast Sec Proteins Involved in Translocation into the Endoplasmic Reticulum into a Membrane-Bound Multisubunit Complex." *Nature* 349 (6312): 806-808. http://dx.doi.org/10.1038/349806a0.

Deshaies, Raymond J., and Randy Schekman. 1987. "A Yeast Mutant Defective at an Early Stage in Import of Secretory Protein Precursors into the Endoplasmic Reticulum." *The Journal of Cell Biology* 105 (2): 633-645. doi: 10.2307/1612425.

Desilva, Am, We Balch, and A. Helenius. 1990. "Quality-Control in the Endoplasmic-Reticulum - Folding and Misfolding of Vesicular Stomatitis-Virus G-Protein in Cells and Invitro." *J. Cell Biol.* 111 (3): 857-866. doi: 10.1083/jcb.111.3.857.

Dixon, Brian M., Shi-Hua D. Heath, Robert Kim, Jung H. Suh, and Tory M. Hagen. 2008. "Assessment of Endoplasmic Reticulum Glutathione Redox Status Is Confounded by Extensive Ex Vivo Oxidation." *Antioxidants & redox signaling* 10 (5): 963-972. doi: 10.1089/ars.2007.1869.

Dudek, Johanna, Jörg Volkmer, Christiane Bies, Silvia Guth, Anika Müller, Monika Lerner, Peter Feick et al. 2002. "A Novel Type of Co-Chaperone Mediates Transmembrane Recruitment of Dnak-Like Chaperones to Ribosomes." *The EMBO Journal* 21 (12): 2958-2967. doi: 10.1093/emboj/cdf315.

Elston, Timothy C. 2002. "The Brownian Ratchet and Power Stroke Models for Posttranslational Protein Translocation into the Endoplasmic Reticulum." *Biophysical journal* 82 (3): 1239-1253. http://search.proquest.com/docview/71488646?accountid=10382

Esnault, Y, D Feldheim, M O Blondel, R Schekman, and F Képès. 1994. "Sss1 Encodes a Stabilizing Component of the Sec61 Subcomplex of the Yeast Protein Translocation Apparatus." *Journal of Biological Chemistry* 269 (44): 27478-27485. http://www.jbc.org/content/269/44/27478.abstract.

Fahey, Robert, John Hunt, and Gayle Windham. 1977. "On the Cysteine and Cystine Content of Proteins." *Journal of Molecular Evolution* 10 (2): 155-160. doi: 10.1007/BF01751808.

Feldheim, D, and R Schekman. 1994. "Sec72p Contributes to the Selective Recognition of Signal Peptides by the Secretory Polypeptide Translocation Complex." *The Journal of Cell Biology* 126 (4): 935-943. doi: 10.1083/jcb.126.4.935.

Finke, K, Kathrin Plath, Steffen Panzner, S Prehn, T A Rapoport, Enno Hartmann, and Thomas Sommer. 1996a. "A Second Trimeric Complex Containing Homologs of the Sec61p Complex Functions in Protein Transport across the Er Membrane of S. Cerevisiae." *The EMBO Journal* 15 (7): 1482-1494.

Finke, K., K. Plath, S. Panzner, S. Prehn, T. A. Rapoport, E. Hartmann, and T. Sommer. 1996b. "A Second Trimeric Complex Containing Homologs of the Sec61p Complex Functions in Protein Transport across the Er Membrane of S. Cerevisiae." *The EMBO Journal* 15 (7): 1482-1494. doi: 10.1002/j.1460-2075.1996.tb00492.x.

Forte, Gabriella M. A., Martin R. Pool, and Colin J. Stirling. 2011. "N-Terminal Acetylation Inhibits Protein Targeting to the Endoplasmic Reticulum." *PLoS Biol* 9 (5): e1001073. doi: 10.1371/journal.pbio.1001073.

Frand, Alison R., and Chris A. Kaiser. 1999. "Ero1p Oxidizes Protein Disulfide Isomerase in a Pathway for Disulfide Bond Formation in the Endoplasmic Reticulum." *Molecular Cell* 4 (4): 469-477. doi: https://doi.org/10.1016/S1097-2765(00)80198-7.

Freiden, P. J., J. R. Gaut, and L. M. Hendershot. 1992. "Interconversion of Three Differentially Modified and Assembled Forms of Bip." *Embo j* 11 (1): 63-70.

Freymann, Douglas M., Robert J. Keenan, Robert M. Stroud, and Peter Walter. 1997. "Structure of the Conserved Gtpase Domain of the Signal Recognition Particle." *Nature* 385 (6614): 361-364. http://dx.doi.org/10.1038/385361a0.

Gething, Mary-Jane, Karen McCammon, and Joe Sambrook. 1986. "Expression of Wild-Type and Mutant Forms of Influenza Hemagglutinin: The Role of Folding in Intracellular Transport." *Cell* 46 (6): 939-950. doi: 10.1016/0092-8674(86)90076-0.

Go, Young-Mi, Joshua D. Chandler, and Dean P. Jones. 2015. "The Cysteine Proteome." *Free radical biology & medicine* 84: 227-245. doi: 10.1016/j.freeradbiomed.2015.03.022.

Gross, Einav, David B. Kastner, Chris A. Kaiser, and Deborah Fass. 2004. "Structure of Ero1p, Source of Disulfide Bonds for Oxidative Protein Folding in the Cell." *Cell* 117 (5): 601-610. doi: https://doi.org/10.1016/S0092-8674(04)00418-0.

Gundelfinger, Eckart D., Elke Krause, Marialuisa Melli, and Bemhard Dobberstein. 1983. "The Organization of the 7sl Rna in the Signal Recognition Particle." *Nucleic Acids Research* 11 (21): 7363-7374. doi: 10.1093/nar/11.21.7363.

Gupta, R. S., and G. B. Golding. 1993. "Evolution of Hsp70 Gene and Its Implications Regarding Relationships between Archaebacteria, Eubacteria, and Eukaryotes." *J Mol Evol* 37 (6): 573-82. doi: 10.1007/bf00182743.

Habeck, Gregor, Felix A. Ebner, Hiroko Shimada-Kreft, and Stefan G. Kreft. 2015. "The Yeast Erad-C Ubiquitin Ligase Doa10 Recognizes an Intramembrane Degron." *The Journal of cell biology* 209 (2): 261-273. doi: 10.1083/jcb.201408088.

Hale, Sarah J., Simon C. Lovell, Jeanine de Keyzer, and Colin J. Stirling. 2010. "Interactions between Kar2p and Its Nucleotide Exchange Factors Sil1p and Lhs1p Are Mechanistically Distinct." *Journal of Biological Chemistry* 285 (28): 21600-21606. doi: 10.1074/jbc.M110.111211.

Halic, Mario, Thomas Becker, Martin R. Pool, Christian M. T. Spahn, Robert A. Grassucci, Joachim Frank, and Roland Beckmann. 2004. "Structure of the Signal Recognition Particle Interacting with the Elongation-Arrested Ribosome." *Nature* 427 (6977): 808-814. doi: http://www.nature.com/nature/journal/v427/n6977/suppinfo/nature02342_S1.html.

Hamman, Brian D., Linda M. Hendershot, and Arthur E. Johnson. 1998. "Bip Maintains the Permeability Barrier of the Er Membrane by Sealing the Lumenal End of the Translocon Pore before and Early in Translocation." *Cell* 92 (6): 747-758. doi: 10.1016/S0092-8674(00)81403-8.

Hampton, R. Y., R. G. Gardner, and J. Rine. 1996. "Role of 26s Proteasome and Hrd Genes in the Degradation of 3-Hydroxy-3-Methylglutaryl-Coa Reductase, an Integral Endoplasmic Reticulum Membrane Protein." *Molecular Biology of the Cell* 7 (12): 2029-2044. doi: 10.1091/mbc.7.12.2029.

Hampton, R. Y., and J. Rine. 1994. "Regulated Degradation of Hmg-Coa Reductase, an Integral Membrane Protein of the Endoplasmic Reticulum, in Yeast." *The Journal of Cell Biology* 125 (2): 299. http://jcb.rupress.org/content/125/2/299.abstract.

Hartl, F. U., and M. Hayer-Hartl. 2002. "Molecular Chaperones in the Cytosol: From Nascent Chain to Folded Protein." *Science* 295 (5561): 1852-8. doi: 10.1126/science.1068408.

Hatahet, Feras, and Lloyd W. Ruddock. 2009. "Protein Disulfide Isomerase: A Critical Evaluation of Its Function in Disulfide Bond Formation." *Antioxidants & redox signaling* 11 (11): 2807. doi: 10.1089/ARS.2009.2466.

Hendershot, L. M., J. Ting, and A. S. Lee. 1988. "Identity of the Immunoglobulin Heavy-Chain-Binding Protein with the 78,000-Dalton Glucose-Regulated Protein and the Role of Posttranslational Modifications in Its Binding Function." *Mol Cell Biol* 8 (10): 4250-6. doi: 10.1128/mcb.8.10.4250.

Heritage, D., and W. F. Wonderlin. 2001. "Translocon Pores in the Endoplasmic Reticulum Are Permeable to a Neutral, Polar Molecule." *The Journal of biological chemistry* 276 (25): 22655-22662. doi: 10.1074/jbc.M102409200.

High, Stephen, and Bernhard Dobberstein. 1991. "The Signal Sequence Interacts with the Methionine-Rich Domain of the 54-Kd Protein of Signal Recognition

Particle." *The Journal of Cell Biology* 113 (2): 229-233. doi: 10.2307/1614477.
Hinnebusch, Alan G. 2005. "Translational Regulation of Gcn4 and the General Amino Acid Control of Yeast." *Annual Review of Microbiology* 59 (1): 407-450. doi: doi:10.1146/annurev.micro.59.031805.133833.
Holt, Liam J., Brian B. Tuch, Judit Villén, Alexander D. Johnson, Steven P. Gygi, and David O. Morgan. 2009. "Global Analysis of Cdk1 Substrate Phosphorylation Sites Provides Insights into Evolution." *Science* 325 (5948): 1682-1686. doi: 10.1126/science.1172867.
Hornbeck, P. V., B. Zhang, B. Murray, J. M. Kornhauser, V. Latham, and E. Skrzypek. 2015. "Phosphositeplus, 2014: Mutations, Ptms and Recalibrations." *Nucleic Acids Res* 43 (Database issue): D512-20. doi: 10.1093/nar/gku1267.
Hsu, Peggy P., Seong A. Kang, Jonathan Rameseder, Yi Zhang, Kathleen A. Ottina, Daniel Lim, Timothy R. Peterson et al. 2011. "The Mtor-Regulated Phosphoproteome Reveals a Mechanism of Mtorc1-Mediated Inhibition of Growth Factor Signaling." *Science* 332 (6035): 1317-1322. doi: 10.1126/science.1199498.
Huyer, Gregory, Wachirapon F. Piluek, Zoya Fansler, Stefan G. Kreft, Mark Hochstrasser, Jeffrey L. Brodsky, and Susan Michaelis. 2004. "Distinct Machinery Is Required in Saccharomyces Cerevisiae for the Endoplasmic Reticulum-Associated Degradation of a Multispanning Membrane Protein and a Soluble Luminal Protein." *Journal of Biological Chemistry* 279 (37): 38369-38378. doi: 10.1074/jbc.M402468200.
Hwang, C, AJ Sinskey, and HF Lodish. 1992. "Oxidized Redox State of Glutathione in the Endoplasmic Reticulum." *Science* 257 (5076): 1496-1502. doi: 10.1126/science.1523409.
Ittner, A. A., J. Bertz, T. Y. Chan, J. van Eersel, P. Polly, and L. M. Ittner. 2014. "The Nucleotide Exchange Factor Sil1 Is Required for Glucose-Stimulated Insulin Secretion from Mouse Pancreatic Beta Cells in Vivo." *Diabetologia* 57 (7): 1410-9. doi: 10.1007/s00125-014-3230-z.
Jan, Calvin H., Christopher C. Williams, and Jonathan S. Weissman. 2014. "Principles of Er Cotranslational Translocation Revealed by Proximity-Specific Ribosome Profiling." *Science* 346 (6210): 1257521. doi: 10.1126/science.1257521.
Jermy, Andrew J., Martin Willer, Elaine Davis, Barrie M. Wilkinson, and Colin J. Stirling. 2006. "The Brl Domain in Sec63p Is Required for Assembly of Functional Endoplasmic Reticulum Translocons." *Journal of Biological Chemistry* 281 (12): 7899-7906. doi: 10.1074/jbc.M511402200.
Jorgensen, Paul, Ivan Rupeš, Jeffrey R. Sharom, Lisa Schneper, James R. Broach, and Mike Tyers. 2004. "A Dynamic Transcriptional Network Communicates Growth Potential to Ribosome Synthesis and Critical Cell Size." *Genes & Development* 18 (20): 2491-2505. doi: 10.1101/gad.1228804.
Jung, Chang Hwa, Seung-Hyun Ro, Jing Cao, Neil Michael Otto, and Do-Hyung Kim. 2010. "Mtor Regulation of Autophagy." *FEBS Letters* 584 (7): 1287-1295. doi: 10.1016/j.febslet.2010.01.017.
Kamada, Yoshiaki, Yuko Fujioka, Nobuo N. Suzuki, Fuyuhiko Inagaki, Stephan Wullschleger, Robbie Loewith, Michael N. Hall, and Yoshinori Ohsumi. 2005. "Tor2 Directly Phosphorylates the Agc Kinase Ypk2 to Regulate Actin

Polarization." *Molecular and Cellular Biology* 25 (16): 7239-7248. doi: 10.1128/mcb.25.16.7239-7248.2005.

Keenan, Robert J., Douglas M. Freymann, Peter Walter, and Robert M. Stroud. 1998. "Crystal Structure of the Signal Sequence Binding Subunit of the Signal Recognition Particle." *Cell* 94 (2): 181-191. doi: http://dx.doi.org/10.1016/S0092-8674(00)81418-X.

Kitao, Y., K. Ozawa, M. Miyazaki, M. Tamatani, T. Kobayashi, H. Yanagi, M. Okabe et al. 2001. "Expression of the Endoplasmic Reticulum Molecular Chaperone (Orp150) Rescues Hippocampal Neurons from Glutamate Toxicity." *J Clin Invest* 108 (10): 1439-50. doi: 10.1172/jci12978.

Knauer, Roland, and Ludwig Lehle. 1999. "The Oligosaccharyltransferase Complex from Saccharomyces Cerevisiae : Isolation of the Ost6 Gene, Its Synthetic Interaction with Ost3, and Analysis of the Native Complex." *Journal of Biological Chemistry* 274 (24): 17249-17256. doi: 10.1074/jbc.274.24.17249.

Knop, M., A. Finger, T. Braun, K. Hellmuth, and D. H. Wolf. 1996. "Der1, a Novel Protein Specifically Required for Endoplasmic Reticulum Degradation in Yeast." *The EMBO Journal* 15 (4): 753-763. doi: 10.1002/j.1460-2075.1996.tb00411.x.

Kosower, Nechama S., Edward M. Kosower, Bilha Wertheim, and Walter S. Correa. 1969. "Diamide, a New Reagent for the Intracellular Oxidation of Glutathione to the Disulfide." *Biochemical and Biophysical Research Communications* 37 (4): 593-596. doi: https://doi.org/10.1016/0006-291X(69)90850-X.

Kozlov, Guennadi, Pekka Määttänen, David Y. Thomas, and Kalle Gehring. 2010. 'A Structural Overview of the Pdi Family of Proteins.' Oxford, UK.

Kurzchalia, T. V., M. Wiedmann, A. S. Girshovich, E. S. Bochkareva, H. Bielka, and T. A. Rapoport. 1986. "The Signal Sequence of Nascent Preprolactin Interacts with the 54k Polypeptide of the Signal Recognition Particle." *Nature* 320 (6063): 634-636. http://dx.doi.org/10.1038/320634a0.

Lakkaraju, Asvin K. K., Ratheeshkumar Thankappan, Camille Mary, Jennifer L. Garrison, Jack Taunton, and Katharina Strub. 2012. "Efficient Secretion of Small Proteins in Mammalian Cells Relies on Sec62-Dependent Posttranslational Translocation." *Molecular Biology of the Cell* 23 (14): 2712-2722. doi: 10.1091/mbc.E12-03-0228.

Lamb, C. A., T. Yoshimori, and S. A. Tooze. 2013. "The Autophagosome: Origins Unknown, Biogenesis Complex." *Nat Rev Mol Cell Biol* 14 (12): 759-74. doi: 10.1038/nrm3696.

Lang, Sven, Frank Erdmann, Martin Jung, Richard Wagner, Adolfo Cavalie, and Richard Zimmermann. 2011. "Sec61 Complexes Form Ubiquitous Er Ca2+ Leak Channels." *Channels* 5 (3): 228-235. doi: 10.4161/chan.5.3.15314.

Lauffer, Leander, Pablo D. Garcia, Richard N. Harkins, Lisa Coussens, Axel Ullrich, and Peter Walter. 1985. "Topology of Signal Recognition Particle Receptor in Endoplasmic Reticulum Membrane." *Nature* 318 (6044): 334-338. doi: 10.1038/318334a0.

Ledford, Barry E., and Gregory H. Leno. 1994. "Adp-Ribosylation of the Molecular Chaperone Grp78/Bip." *Molecular and Cellular Biochemistry* 138 (1): 141-148. doi: 10.1007/BF00928456.

Lee, Hui Sun, Yifei Qi, and Wonpil Im. 2015. "Effects of N-Glycosylation on Protein Conformation and Dynamics: Protein Data Bank Analysis and Molecular Dynamics Simulation Study." *Scientific reports* 5: 8926-8926. doi: 10.1038/srep08926.

Lempiäinen, Harri, and David Shore. 2009. "Growth Control and Ribosome Biogenesis." *Current Opinion in Cell Biology* 21 (6): 855-863. doi: http://dx.doi.org/10.1016/j.ceb.2009.09.002.

Li, Xue, Scott A. Gerber, Adam D. Rudner, Sean A. Beausoleil, Wilhelm Haas, Judit Villén, Joshua E. Elias, and Steve P. Gygi. 2007. "Large-Scale Phosphorylation Analysis of A-Factor-Arrested Saccharomyces Cerevisiae." *Journal of Proteome Research* 6 (3): 1190-1197. doi: 10.1021/pr060559j.

Liberek, K., J. Marszalek, D. Ang, C. Georgopoulos, and M. Zylicz. 1991. "Escherichia Coli Dnaj and Grpe Heat Shock Proteins Jointly Stimulate Atpase Activity of Dnak." *Proc Natl Acad Sci U S A* 88 (7): 2874-8. http://www.ncbi.nlm.nih.gov/pubmed/1826368.

Linxweiler, Maximilian, Bernhard Schick, and Richard Zimmermann. 2017. "Let's Talk About Secs: Sec61, Sec62 and Sec63 in Signal Transduction, Oncology and Personalized Medicine." *Signal Transduction and Targeted Therapy* 2 (1): 17002. doi: 10.1038/sigtrans.2017.2.

Linxweiler, Maximilian, Stefan Schorr, Nico Schäuble, Martin Jung, Johannes Linxweiler, Frank Langer, Hans-Joachim Schäfers, Adolfo Cavalié, Richard Zimmermann, and Markus Greiner. 2013. "Targeting Cell Migration and the Endoplasmic Reticulum Stress Response with Calmodulin Antagonists: A Clinically Tested Small Molecule Phenocopy of Sec62 Gene Silencing in Human Tumor Cells." *BMC cancer* 13: 574-574. doi: 10.1186/1471-2407-13-574.

Liu, Z. C., J. Chu, L. Lin, J. Song, L. N. Ning, H. B. Luo, S. S. Yang et al. 2016. "Sil1 Rescued Bip Elevation-Related Tau Hyperphosphorylation in Er Stress." *Mol Neurobiol* 53 (2): 983-994. doi: 10.1007/s12035-014-9039-4.

Llewelyn Roderick, H., D. H. Llewellyn, A. K. Campbell, and J. M. Kendall. 1998. "Role of Calreticulin in Regulating Intracellular Ca2+ Storage and Capacitative Ca2+ Entry in Hela Cells." *Cell Calcium* 24 (4): 253-62. doi: 10.1016/s0143-4160(98)90049-5.

Lloyd, D. J., M. C. Wheeler, and N. Gekakis. 2010. "A Point Mutation in Sec61alpha1 Leads to Diabetes and Hepatosteatosis in Mice." *Diabetes* 59 (2): 460-70. doi: 10.2337/db08-1362.

Loayza, Diego, Amy Tam, Walter K. Schmidt, Susan Michaelis, and Peter Walter. 1998. "Ste6p Mutants Defective in Exit from the Endoplasmic Reticulum (Er) Reveal Aspects of an Er Quality Control Pathway Insaccharomyces Cerevisiae." *Molecular Biology of the Cell* 9 (10): 2767-2784. doi: 10.1091/mbc.9.10.2767.

Loewith, Robbie, and Michael N. Hall. 2011. "Target of Rapamycin (Tor) in Nutrient Signaling and Growth Control." *Genetics* 189 (4): 1177-1201. doi: 10.1534/genetics.111.133363.

Luirink, J, CM ten Hagen-Jongman, CC van der Weijden, B Oudega, S High, B Dobberstein, and R Kusters. 1994. "An Alternative Protein Targeting

Pathway in Escherichia Coli: Studies on the Role of Ftsy." *The EMBO Journal* 13 (10): 2289.

Marcus, Gutscher, Pauleau Anne-Laure, Marty Laurent, Brach Thorsten, H. Wabnitz Guido, Samstag Yvonne, J. Meyer Andreas, and P. Dick Tobias. 2008. "Real-Time Imaging of the Intracellular Glutathione Redox Potential." *Nature Methods* 5 (6): 553. doi: 10.1038/nmeth.1212.

Matheson, Kinnari, Lance Parsons, and Alison Gammie. 2017. "Whole-Genome Sequence and Variant Analysis of W303, a Widely-Used Strain of Saccharomyces Cerevisiae." *G3 (Bethesda, Md.)* 7 (7): 2219-2226. doi: 10.1534/g3.117.040022.

Matlack, K. E., B. Misselwitz, K. Plath, and T. A. Rapoport. 1999a. "Bip Acts as a Molecular Ratchet During Posttranslational Transport of Prepro-Alpha Factor across the Er Membrane." *Cell* 97 (5): 553-64. http://www.ncbi.nlm.nih.gov/pubmed/10367885.

Matlack, Kent E. S., Benjamin Misselwitz, Kathrin Plath, and Tom A. Rapoport. 1999b. "Bip Acts as a Molecular Ratchet During Posttranslational Transport of Prepro-A Factor across the Er Membrane." *Cell* 97 (5): 553-564. doi: http://dx.doi.org/10.1016/S0092-8674(00)80767-9.

Mayer, Matthias P., Hartwig Schröder, Stefan Rüdiger, Klaus Paal, Thomas Laufen, and Bernd Bukau. 2000. "Multistep Mechanism of Substrate Binding Determines Chaperone Activity of Hsp70." *Nature Structural Biology* 7 (7): 586-593. doi: 10.1038/76819.

Mezghrani, Alexandre, Anna Fassio, Adam Benham, Thomas Simmen, Ineke Braakman, and Roberto Sitia. 2001. "Manipulation of Oxidative Protein Folding and Pdi Redox State in Mammalian Cells." *The EMBO Journal* 20 (22): 6288. http://emboj.embopress.org/content/20/22/6288.abstract.

Miller, J. D., H. Wilhelm, L. Gierasch, R. Gilmore, and P. Walter. 1993. "Gtp Binding and Hydrolysis by the Signal Recognition Particle During Initiation of Protein Translocation." *Nature* 366 (6453): 351-4. doi: 10.1038/366351a0.

Milstein, C., G. G. Brownlee, T. M. Harrison, and M. B. Mathews. 1972. "A Possible Precursor of Immunoglobulin Light Chains." *Nat New Biol* 239 (91): 117-20.

Mohd Yusuf, Siti N. H., Ulla-Maja Bailey, Nikki Y. Tan, Muhammad Fairuz Jamaluddin, and Benjamin L. Schulz. 2013. "Mixed Disulfide Formation in Vitro between a Glycoprotein Substrate and Yeast Oligosaccharyltransferase Subunits Ost3p and Ost6p." *Biochemical and Biophysical Research Communications* 432 (3): 438-443. doi: https://doi.org/10.1016/j.bbrc.2013.01.128.

Monk, Kelly R., Matthew G. Voas, Clara Franzini-Armstrong, Ian S. Hakkinen, and William S. Talbot. 2013. "Mutation of Sec63 in Zebrafish Causes Defects in Myelinated Axons and Liver Pathology." *Disease Models & Mechanisms* 6 (1): 135-145. doi: 10.1242/dmm.009217.

Morgan, Bruce, Daria Ezerina, Theresa N. E. Amoako, Jan Riemer, Matthias Seedorf, and Tobias P. Dick. 2013. "Multiple Glutathione Disulfide Removal Pathways Mediate Cytosolic Redox Homeostasis." *Nature Chemical Biology* 9 (2): 119-25. doi: http://dx.doi.org/10.1038/nchembio.1142.

Mothes, W., S. Prehn, and T A. Rapoport. 1994. "Systematic Probing of the Environment of a Translocating Secretory Protein During Translocation through the Er Membrane." *EMBO Journal* 13 (17): 3973-82.

Müller, Linda, Maria Diaz de Escauriaza, Patrick Lajoie, Melanie Theis, Martin Jung, Anika Müller, Carsten Burgard et al. 2010. "Evolutionary Gain of Function for the Er Membrane Protein Sec62 from Yeast to Humans." *Molecular Biology of the Cell* 21 (5): 691-703. doi: 10.1091/mbc.e09-08-0730.

Ng, Davis T. W., Jeremy D. Brown, and Peter Walter. 1996. "Signal Sequences Specify the Targeting Route to the Endoplasmic Reticulum Membrane." *The Journal of Cell Biology* 134 (2): 269-278. doi: 10.2307/1617644.

Nilsson, I M, and G von Heijne. 1993. "Determination of the Distance between the Oligosaccharyltransferase Active Site and the Endoplasmic Reticulum Membrane." *Journal of Biological Chemistry* 268 (8): 5798-801. http://www.jbc.org/content/268/8/5798.abstract.

Nishikawa, S. I., S. W. Fewell, Y. Kato, J. L. Brodsky, and T. Endo. 2001. "Molecular Chaperones in the Yeast Endoplasmic Reticulum Maintain the Solubility of Proteins for Retrotranslocation and Degradation." *J Cell Biol* 153 (5): 1061-70. http://www.ncbi.nlm.nih.gov/pubmed/11381090.

Nishikawa, Shuh-ichi, Jeffrey L. Brodsky, and Kunio Nakatsukasa. 2005. "Roles of Molecular Chaperones in Endoplasmic Reticulum (Er) Quality Control and Er-Associated Degradation (Erad)." *Journal of Biochemistry* 137 (5): 551-555. doi: 10.1093/jb/mvi068.

Osborne, Andrew R., Tom A. Rapoport, and Bert van den Berg. 2005. "Protein Translocation by the Sec61/Secy Channel." *Annual Review of Cell and Developmental Biology* 21: 529-50. http://search.proquest.com/docview/217949377?accountid=10382

Ozcan, Lale, and Ira Tabas. 2012. "Role of Endoplasmic Reticulum Stress in Metabolic Disease and Other Disorders." *Annual review of medicine* 63: 317-328. doi: 10.1146/annurev-med-043010-144749.

Panzner, Steffen, Lars Dreier, Enno Hartmann, Susanne Kostka, and Tom A. Rapoport. 1995. "Posttranslational Protein Transport in Yeast Reconstituted with a Purified Complex of Sec Proteins and Kar2p." *Cell* 81 (4): 561-570. doi: http://dx.doi.org/10.1016/0092-8674(95)90077-2.

Parlati, F., M. Dominguez, J. J. Bergeron, and D. Y. Thomas. 1995. "Saccharomyces Cerevisiae Cne1 Encodes an Endoplasmic Reticulum (Er) Membrane Protein with Sequence Similarity to Calnexin and Calreticulin and Functions as a Constituent of the Er Quality Control Apparatus." *J Biol Chem* 270 (1): 244-53. doi: 10.1074/jbc.270.1.244.

Pedruzzi, Ivo, Frédérique Dubouloz, Elisabetta Cameroni, Valeria Wanke, Johnny Roosen, Joris Winderickx, and Claudio De Virgilio. 2003. "Tor and Pka Signaling Pathways Converge on the Protein Kinase Rim15 to Control Entry into G₀." *Molecular Cell* 12 (6): 1607-1613. doi: 10.1016/S1097-2765(03)00485-4.

Plath, Kathrin, and Tom A. Rapoport. 2000. "Spontaneous Release of Cytosolic Proteins from Posttranslational Substrates before Their Transport into the Endoplasmic Reticulum." *The Journal of Cell Biology* 151 (1): 167-178. doi: 10.2307/1620012.

Ponsero, Alise J., Aeid Igbaria, Maxwell A. Darch, Samia Miled, Caryn E. Outten, Jakob R. Winther, Gael Palais, Benoit D'Autréaux, Agnès Delaunay-Moisan, and Michel B. Toledano. 2017. "Endoplasmic Reticulum Transport of Glutathione by Sec61 Is Regulated by Ero1 and Bip." *Molecular Cell* 67 (6): 962-973.e5. doi: https://doi.org/10.1016/j.molcel.2017.08.012.

Ponting, C P. 2000. "Proteins of the Endoplasmic-Reticulum-Associated Degradation Pathway: Domain Detection and Function Prediction." *Biochem. J.* 351 (2): 527-535. http://www.biochemj.org/bj/351/bj3510527.htm.

Pool, Martin R. 2005. "Signal Recognition Particles in Chloroplasts, Bacteria, Yeast and Mammals (Review)." *Molecular Membrane Biology* 22 (1-2): 3-15. doi: doi:10.1080/09687860400026348.

Poritz, Mark A., Harris D. Bernstein, Katharina Strub, Dieter Zopf, Heike Wilhelm, and Peter Walter. 1990. "An E. Coli Ribonucleoprotein Containing 4.5s Rna Resembles Mammalian Signal Recognition Particle." *Science* 250 (4984): 1111-1117. doi: 10.2307/2878284.

Powers, Ted, Sofia Aronova, and Brad Niles. 2010. "10 - Torc2 and Sphingolipid Biosynthesis and Signaling: Lessons from Budding Yeast." In *The Enzymes*, eds N. Hall Michael and Tamanoi Fuyuhiko, 177-197. Academic Press.

Powers, Ted, and Peter Walter. 1997. "Co-Translational Protein Targeting Catalyzed by the Escherichia Coli Signal Recognition Particle and Its Receptor." *EMBO J* 16 (16): 4880-4886. http://dx.doi.org/10.1093/emboj/16.16.4880.

Rosam, Mathias, Daniela Krader, Christina Nickels, Janine Hochmair, Katrin C. Back, Ganesh Agam, Anders Barth et al. 2018. "Bap (Sil1) Regulates the Molecular Chaperone Bip by Coupling Release of Nucleotide and Substrate." *Nature Structural & Molecular Biology* 25 (1): 90-100. doi: 10.1038/s41594-017-0012-6.

Roussel, Benoit D., Antonina J. Kruppa, Elena Miranda, Damian C. Crowther, David A. Lomas, and Stefan J. Marciniak. 2013. "Endoplasmic Reticulum Dysfunction in Neurological Disease." *The Lancet Neurology* 12 (1): 105-118. doi: https://doi.org/10.1016/S1474-4422(12)70238-7.

Rüdiger, S., L. Germeroth, J. Schneider-Mergener, and B. Bukau. 1997. "Substrate Specificity of the Dnak Chaperone Determined by Screening Cellulose-Bound Peptide Libraries." *EMBO Journal* 16 (7): 1501-1507. doi: 10.1093/emboj/16.7.1501.

Ruggiano, Annamaria, Ombretta Foresti, and Pedro Carvalho. 2014. "Er-Associated Degradation: Protein Quality Control and Beyond." *The Journal of Cell Biology* 204 (6): 869-879. doi: 10.1083/jcb.201312042.

Sadler, I, A Chiang, T Kurihara, J Rothblatt, J Way, and P Silver. 1989. "A Yeast Gene Important for Protein Assembly into the Endoplasmic Reticulum and the Nucleus Has Homology to Dnaj, an Escherichia Coli Heat Shock Protein." *The Journal of Cell Biology* 109 (6): 2665-2675. doi: 10.1083/jcb.109.6.2665.

Saris, Nina, Heidi Holkeri, Rachel A. Craven, Colin J. Stirling, and Marja Makarow. 1997. "The Hsp70 Homologue Lhs1p Is Involved in a Novel Function of the Yeast Endoplasmic Reticulum, Refolding and Stabilization of Heat-Denatured Protein Aggregates." *The Journal of Cell Biology* 137 (4): 813-824. doi: 10.1083/jcb.137.4.813.

Schauble, N., S. Lang, M. Jung, S. Cappel, S. Schorr, O. Ulucan, J. Linxweiler et al. 2012. "Bip-Mediated Closing of the Sec61 Channel Limits Ca2+ Leakage from the Er." *Embo j* 31 (15): 3282-96. doi: 10.1038/emboj.2012.189.

Schmelzle, Tobias, and Michael N. Hall. 2000. "Tor, a Central Controller of Cell Growth." *Cell* 103 (2): 253-262. doi: http://dx.doi.org/10.1016/S0092-8674(00)00117-3.

Schmid, D, A Baici, H Gehring, and P Christen. 1994. "Kinetics of Molecular Chaperone Action." *Science* 263 (5149): 971-973. doi: 10.1126/science.8310296.

Schonthal, A. H. 2012. "Endoplasmic Reticulum Stress: Its Role in Disease and Novel Prospects for Therapy." *Scientifica (Cairo)* 2012: 857516. doi: 10.6064/2012/857516.

Schulz, B. L., C. U. Stirnimann, J. P. Grimshaw, M. S. Brozzo, F. Fritsch, E. Mohorko, G. Capitani, R. Glockshuber, M. G. Grutter, and M. Aebi. 2009. "Oxidoreductase Activity of Oligosaccharyltransferase Subunits Ost3p and Ost6p Defines Site-Specific Glycosylation Efficiency." *Proc Natl Acad Sci U S A* 106 (27): 11061-6. doi: 10.1073/pnas.0812515106.

Senderek, J., M. Krieger, C. Stendel, C. Bergmann, M. Moser, N. Breitbach-Faller, S. Rudnik-Schoneborn et al. 2005. "Mutations in Sil1 Cause Marinesco-Sjogren Syndrome, a Cerebellar Ataxia with Cataract and Myopathy." *Nat Genet* 37 (12): 1312-4. doi: 10.1038/ng1678.

Sevier, C. S., H. Qu, N. Heldman, E. Gross, D. Fass, and C. A. Kaiser. 2007. "Modulation of Cellular Disulfide-Bond Formation and the Er Redox Environment by Feedback Regulation of Ero1." *Cell* 129 (2): 333-44. doi: 10.1016/j.cell.2007.02.039.

Sevier, Carolyn S., and Chris A. Kaiser. 2008. "Ero1 and Redox Homeostasis in the Endoplasmic Reticulum." *Biochimica et Biophysica Acta (BBA) - Molecular Cell Research* 1783 (4): 549-556. doi: https://doi.org/10.1016/j.bbamcr.2007.12.011.

Siegel, Vivian, and Peter Walter. 1985. "Elongation Arrest Is Not a Prerequisite for Secretory Protein Translocation across the Microsomal Membrane." *The Journal of Cell Biology* 100 (6): 1913-1921. doi: 10.2307/1611309.

Siegel, Vivian, and Peter Walter. **1988a**. "Binding Sites of the 19-Kda and 68/72-Kda Signal Recognition Particle (Srp) Proteins on Srp Rna as Determined by Protein-Rna ``Footprinting''." *Proceedings of the National Academy of Sciences of the United States of America* 85 (6): 1801-1805. doi: 10.2307/31393.

———. **1988b**. "Each of the Activities of Signal Recognition Particle (Srp) Is Contained within a Distinct Domain: Analysis of Biochemical Mutants of Srp." *Cell* 52 (1): 39-49. doi: http://dx.doi.org/10.1016/0092-8674(88)90529-6.

Siegenthaler, K. D., K. A. Pareja, J. Wang, and C. S. Sevier. 2017. "An Unexpected Role for the Yeast Nucleotide Exchange Factor Sil1 as a Reductant Acting on the Molecular Chaperone Bip." *Elife* 6. doi: 10.7554/eLife.24141.

Sies, Helmut, Carsten Berndt, and Dean P. Jones. 2017. "Oxidative Stress." *Annual Review of Biochemistry* 86 (1): 715-748. doi: 10.1146/annurev-biochem-061516-045037.

Sikorski, R. S., and P. Hieter. 1989. "A System of Shuttle Vectors and Yeast Host Strains Designed for Efficient Manipulation of DNA in Saccharomyces Cerevisiae." *Genetics* 122 (1): 19-27.

Simons, J. F., S. Ferro-Novick, M. D. Rose, and A. Helenius. 1995. "Bip/Kar2p Serves as a Molecular Chaperone During Carboxypeptidase Y Folding in Yeast." *J Cell Biol* 130 (1): 41-9. http://www.ncbi.nlm.nih.gov/pubmed/7790376.

Song, Weiqun, David Raden, Elisabet C. Mandon, and Reid Gilmore. 2000. "Role of Sec61α in the Regulated Transfer of the Ribosome–Nascent Chain Complex from the Signal Recognition Particle to the Translocation Channel." *Cell* 100 (3): 333-343. doi: https://doi.org/10.1016/S0092-8674(00)80669-8.

Soulard, Alexandre, Alessio Cremonesi, Suzette Moes, Frédéric Schütz, Paul Jenö, and Michael N. Hall. 2010. "The Rapamycin-Sensitive Phosphoproteome Reveals That Tor Controls Protein Kinase a toward Some but Not All Substrates." *Molecular biology of the cell* 21 (19): 3475-3486. doi: 10.1091/mbc.E10-03-0182.

Spiro, R. G. 2002. "Protein Glycosylation: Nature, Distribution, Enzymatic Formation, and Disease Implications of Glycopeptide Bonds." *Glycobiology* 12 (4): 43r-56r. doi: 10.1093/glycob/12.4.43r.

Steel, G. J., D. M. Fullerton, J. R. Tyson, and C. J. Stirling. 2004. "Coordinated Activation of Hsp70 Chaperones." *Science* 303 (5654): 98-101. doi: 10.1126/science.1092287.

Stella, M. Hurtley, G. Bole David, Hoover-Litty Helana, Helenius Ari, and S. Copeland Constance. 1989. "Interactions of Misfolded Influenza Virus Hemagglutinin with Binding Protein (Bip)." *The Journal of Cell Biology* 108 (6): 2117-2126. doi: 10.1083/jcb.108.6.2117.

Stevens, Kofi L. P., Amy L. Black, Kelsi M. Wells, K. Y. Benjamin Yeo, Robert F. L. Steuart, Colin J. Stirling, Benjamin L. Schulz, and Carl J. Mousley. 2017. "Diminished Ost3-Dependent N-Glycosylation of the Bip Nucleotide Exchange Factor Sil1 Is an Adaptive Response to Reductive Er Stress." *Proceedings of the National Academy of Sciences* 114 (47): 12489-12494. doi: 10.1073/pnas.1705641114.

Stirling, C. J., J Routhblatt, M Hosobuchi, Raymond J. Deshaies, and R Schekman. 1992. "Protein Translocation Mutants Defective in the Insertion of Integral Membrane Proteins into the Endoplasmic Reticulum." *Molecular Biology of the Cell* 3 (2): 129-142.

Stracka, D., S. Jozefczuk, F. Rudroff, U. Sauer, and M. N. Hall. 2014. "Nitrogen Source Activates Tor (Target of Rapamycin) Complex 1 Via Glutamine and Independently of Gtr/Rag Proteins." *J Biol Chem* 289 (36): 25010-20. doi: 10.1074/jbc.M114.574335.

Swanson, Robert, Martin Locher, and Mark Hochstrasser. 2001. "A Conserved Ubiquitin Ligase of the Nuclear Envelope/Endoplasmic Reticulum That Functions in Both Er-Associated and Matα2 Repressor Degradation." *Genes & Development* 15 (20): 2660-2674. doi: 10.1101/gad.933301.

Szabo, A., T. Langer, H. Schroder, J. Flanagan, B. Bukau, and F. U. Hartl. 1994. "The Atp Hydrolysis-Dependent Reaction Cycle of the Escherichia Coli Hsp70 System Dnak, Dnaj, and Grpe." *Proc Natl Acad Sci U S A* 91 (22): 10345-9. http://www.ncbi.nlm.nih.gov/pubmed/7937953.

Thomas, Sommer, and Jentsch Stefan. 1993. "A Protein Translocation Defect Linked to Ubiquitin Conjugation at the Endoplasmic Reticulum." *Nature* 365 (6442): 176. doi: 10.1038/365176a0.

Travers, Kevin J., Christopher K. Patil, Lisa Wodicka, David J. Lockhart, Jonathan S. Weissman, and Peter Walter. 2000. "Functional and Genomic Analyses Reveal an Essential Coordination between the Unfolded Protein Response and Er-Associated Degradation." *Cell* 101 (3): 249-258. doi: http://dx.doi.org/10.1016/S0092-8674(00)80835-1.

Tyson, J. R., and C. J. Stirling. 2000. "Lhs1 and Sil1 Provide a Lumenal Function That Is Essential for Protein Translocation into the Endoplasmic Reticulum." *EMBO J* 19 (23): 6440-52. doi: 10.1093/emboj/19.23.6440.

Uhlen, M., L. Fagerberg, B. M. Hallstrom, C. Lindskog, P. Oksvold, A. Mardinoglu, A. Sivertsson et al. 2015. "Proteomics. Tissue-Based Map of the Human Proteome." *Science* 347 (6220): 1260419. doi: 10.1126/science.1260419.

Van Coppenolle, F., F. Vanden Abeele, C. Slomianny, M. Flourakis, J. Hesketh, E. Dewailly, and N. Prevarskaya. 2004. "Ribosome-Translocon Complex Mediates Calcium Leakage from Endoplasmic Reticulum Stores." *J Cell Sci* 117 (Pt 18): 4135-42. doi: 10.1242/jcs.01274.

van Nues, Rob W., and Jean D. Beggs. 2001. "Functional Contacts with a Range of Splicing Proteins Suggest a Central Role for Brr2p in the Dynamic Control of the Order of Events in Spliceosomes of Saccharomyces Cerevisiae." *Genetics* 157 (4): 1451-1467. http://www.genetics.org/content/157/4/1451.abstract.

von Heijne, Gunnar. 1985. "Signal Sequences: The Limits of Variation." *Journal of Molecular Biology* 184 (1): 99-105. doi: http://dx.doi.org/10.1016/0022-2836(85)90046-4.

Voth, Warren P., Yi Wei Jiang, and David J. Stillman. 2003. "New 'Marker Swap' Plasmids for Converting Selectable Markers on Budding Yeast Gene Disruptions and Plasmids." *Yeast* 20 (11): 985-993. doi: 10.1002/yea.1018.

Walter, P, and G Blobel. 1981. "Translocation of Proteins across the Endoplasmic Reticulum Iii. Signal Recognition Protein (Srp) Causes Signal Sequence-Dependent and Site-Specific Arrest of Chain Elongation That Is Released by Microsomal Membranes." *The Journal of Cell Biology* 91 (2): 557-561. doi: 10.1083/jcb.91.2.557.

Walter, Peter, and David Ron. 2011. "The Unfolded Protein Response: From Stress Pathway to Homeostatic Regulation." *Science* 334 (6059): 1081-1086. doi: 10.1126/science.1209038.

Wang, J., K. A. Pareja, C. A. Kaiser, and C. S. Sevier. 2014. "Redox Signaling Via the Molecular Chaperone Bip Protects Cells against Endoplasmic Reticulum-Derived Oxidative Stress." *Elife* 3: e03496. doi: 10.7554/eLife.03496.

Wang, Xian, and Nils Johnsson. 2005. "Protein Kinase Ck2 Phosphorylates Sec63p to Stimulate the Assembly of the Endoplasmic Reticulum Protein Translocation Apparatus." *Journal of Cell Science* 118 (4): 723-732. doi: 10.1242/jcs.01671.

Ward, Cristina L., Satoshi Omura, and Ron R. Kopito. 1995. "Degradation of Cftr by the Ubiquitin-Proteasome Pathway." *Cell* 83 (1): 121-127. doi: 10.1016/0092-8674(95)90240-6.

Wild, Rebekka, Julia Kowal, Jillianne Eyring, Elsy M. Ngwa, Markus Aebi, and Kaspar P. Locher. 2018. "Structure of the Yeast Oligosaccharyltransferase Complex

Gives Insight into Eukaryotic N-Glycosylation." *Science* 359 (6375): 545-550. doi: 10.1126/science.aar5140.

Wilkinson, Barrie M., John R. Tyson, and Colin J. Stirling. 2001. "Ssh1p Determines the Translocation and Dislocation Capacities of the Yeast Endoplasmic Reticulum." *Developmental Cell* 1 (3): 401-409. doi: https://doi.org/10.1016/S1534-5807(01)00043-0.

Wilkinson, Simon. 2019. "Er-Phagy: Shaping up and Destressing the Endoplasmic Reticulum." *The FEBS Journal* 286 (14): 2645-2663. doi: 10.1111/febs.14932.

Willer, Martin, Andrew J. Jermy, Gregor J. Steel, Helen J. Garside, Stephanie Carter, and Colin J. Stirling. 2003. "An in Vitro Assay Using Overexpressed Yeast Srp Demonstrates That Cotranslational Translocation Is Dependent Upon the J-Domain of Sec63p†." *Biochemistry* 42 (23): 7171-7177. doi: 10.1021/bi034395l.

Williams, David B. 2006. "Beyond Lectins: The Calnexin/Calreticulin Chaperone System of the Endoplasmic Reticulum." *Journal of Cell Science* 119 (4): 615-623. doi: 10.1242/jcs.02856.

Winzeler, Elizabeth A., Daniel D. Shoemaker, Anna Astromoff, Hong Liang, Keith Anderson, Bruno Andre, Rhonda Bangham et al. 1999. "Functional Characterization of the ≪Em≫S. Cerevisiae≪/Em≫ Genome by Gene Deletion and Parallel Analysis." *Science* 285 (5429): 901. doi: 10.1126/science.285.5429.901.

Wittke, Sandra, Martin Dünnwald, and Nils Johnsson. 2000. "Sec62p, a Component of the Endoplasmic Reticulum Protein Translocation Machinery, Contains Multiple Binding Sites for the Sec-Complex." *Molecular Biology of the Cell* 11 (11): 3859-3871. doi: 10.1091/mbc.11.11.3859.

Wu, Xudong, Cerrone Cabanos, and Tom A. Rapoport. 2019. "Structure of the Post-Translational Protein Translocation Machinery of the Er Membrane." *Nature* 566 (7742): 136-139. doi: 10.1038/s41586-018-0856-x.

Xu, H., S. Xu, R. Zhang, T. Xin, and Q. Pang. 2018. "Sil1 Functions as an Oncogene in Glioma by Akt/Mtor Signaling Pathway." *Onco Targets Ther* 11: 3775-3783. doi: 10.2147/ott.S167552.

Yang, Jiao, Melesse Nune, Yinong Zong, Lei Zhou, and Qinglian Liu. 2015. "Close and Allosteric Opening of the Polypeptide-Binding Site in a Human Hsp70 Chaperone Bip." *Structure (London, England : 1993)* 23 (12): 2191-2203. doi: 10.1016/j.str.2015.10.012.

Yoshida, H. 2007. "Er Stress and Diseases." *Febs j* 274 (3): 630-58. doi: 10.1111/j.1742-4658.2007.05639.x.

Young, B. P., R. A. Craven, P. J. Reid, M. Willer, and C. J. Stirling. 2001. "Sec63p and Kar2p Are Required for the Translocation of Srp-Dependent Precursors into the Yeast Endoplasmic Reticulum in Vivo." *EMBO journal.* 20 (1-2): 262-271. http://search.proquest.com/docview/49265568?accountid=10382

Zhang, Qing, and Russell D. Salter. 1998. "Distinct Patterns of Folding and Interactions with Calnexin and Calreticulin in Human Class I Mhc Proteins with Altered <Em>N</Em>-Glycosylation." *The Journal of Immunology* 160 (2): 831-837. https://www.jimmunol.org/content/jimmunol/160/2/831.full.pdf.

Zhao, H., G. Taherzadeh, Y. Zhou, and Y. Yang. 2018. "Computational Prediction of Carbohydrate-Binding Proteins and Binding Sites." *Curr Protoc Protein Sci* 94 (1): e75. doi: 10.1002/cpps.75.

Zhao, Lihong, Chantal Longo-Guess, Belinda S. Harris, Jeong-Woong Lee, and Susan L. Ackerman. 2005. "Protein Accumulation and Neurodegeneration in the Woozy Mutant Mouse Is Caused by Disruption of Sil1, a Cochaperone of Bip." *Nature Genetics* 37 (9): 974-979. doi: 10.1038/ng1620.

Zheng, Ning, and Lila M. Gierasch. 1997. "Domain Interactions in E. Coli Srp: Stabilization of M Domain by Rna Is Required for Effective Signal Sequence Modulation of Ng Domain." *Molecular Cell* 1 (1): 79-87. doi: http://dx.doi.org/10.1016/S1097-2765(00)80009-X.

Zhou, Jie, Laura Lancaster, John Paul Donohue, and Harry F. Noller. 2014. "How the Ribosome Hands the a-Site Trna to the P Site During Ef-G-Catalyzed Translocation." *Science (New York, N.Y.)* 345 (6201): 1188-1191. doi: 10.1126/science.1255030.

Zimmer, Jochen, Yunsun Nam, and Tom A. Rapoport. 2008. "Structure of a Complex of the Atpase Seca and the Protein-Translocation Channel." *Nature* 455 (7215): 936-943. doi: 10.1038/nature07335.

Zopf, D., Harris D. Bernstein, Arthur E. Johnson, and P Walter. 1990. "The Methionine-Rich Domain of the 54 Kd Protein Subunit of the Signal Recognition Particle Contains an Rna Binding Site and Can Be Crosslinked to a Signal Sequence." *EMBO Journal* 9 (13): 4511-7.

Appendix

8.1. First Author Publication

Presented below is the manuscript which was prepared, and accepted for publication in 2017 featuring much of the work I generated for chapters 4 and 5. While those chapters provide a greater volume of data, and some further developments, the information as presented in the paper may be of use, and provide greater clarity, due to the succinctness of such a manuscript.

Diminished Ost3-dependent N-glycosylation of the BiP nucleotide exchange factor Sil1 is an adaptive response to reductive ER stress

Kofi L. P. Stevens[a,b], Amy L. Black[a,b], Kelsi M. Wells[a,b], K. Y. Benjamin Yeo[c], Robert F. L. Steuart[b], Colin J. Stirling[d,1], Benjamin L. Schulz[c], and Carl J. Mousley[a,b,2]

[a]School of Biomedical Sciences, Faculty of Health Sciences, Curtin University, Bentley, WA 6102, Australia; [b]Curtin Health Innovation Research Institute and Faculty of Health Sciences, Curtin University, Bentley, WA 6102, Australia; [c]School of Chemistry and Molecular Biosciences, Faculty of Science, University of Queensland, Brisbane St Lucia, QLD 4072, Australia; and [d]Faculty of Life Sciences, University of Manchester, Manchester M13 9PT, United Kingdom

Edited by Armando Parodi, Fundacion Instituto Leloir, Buenos Aries, Argentina, and approved October 3, 2017 (received for review May 10, 2017)

BiP (Kar2 in yeast) is an essential Hsp70 chaperone and master regulator of endoplasmic reticulum (ER) function. BiP's activity is regulated by its intrinsic ATPase activity that can be stimulated by two different nucleotide exchange factors, Sil1 and Lhs1. Both Sil1 and Lhs1 are glycoproteins, but how N-glycosylation regulates their function is not known. Here, we show that N-glycosylation of Sil1, but not of Lhs1, is diminished upon reductive stress. N-glycosylation of Sil1 is predominantly Ost3-dependent and requires a functional Ost3 CxxC thioredoxin motif. N-glycosylation of Lhs1 is largely Ost3-independent and independent of the CxxC motif. Unglycosylated Sil1 is not only functional but is more effective at rescuing loss of Lhs1 activity than N-glycosylated Sil1. Furthermore, substitution of the redox active cysteine pair C52 and C57 in the N terminus of Sil1 results in the Doa10-dependent ERAD of this mutant protein. We propose that reductive stress in the ER inhibits the Ost3-dependent N-glycosylation of Sil1, which regulates specific BiP functions appropriate to the needs of the ER under reductive stress.

N-glycosylation | redox | Sil1 | Ost3 | ERAD

The endoplasmic reticulum (ER) is a major site of protein and lipid biogenesis. Proteins that function within the secretory pathway, or are secreted, are translocated into the ER as unfolded polypeptide chains where they can be N-glycosylated or form disulphide bonds to adopt their mature structures. Fully matured proteins are subsequently transported from the ER to their appropriate destinations. These processes are closely monitored by the ER quality control apparatus to prevent protein aggregation and maintain homeostasis.

The Hsp70 ortholog BiP (Kar2 in yeast) is essential for ER homeostasis, where it acts as a chaperone to promote productive protein folding (1–5). Kar2 activity is regulated by two classes of coregulators; Hsp40/DnaJ-like proteins stimulate ATP hydrolysis, whereas nucleotide exchange factors (NEFs) promote ADP release (6, 7). Together they promote Kar2 activity by allowing it to undergo multiple cycles of substrate binding and release. Cells possess several mechanisms that regulate Kar2 activity to buffer against fluctuations in the ER folding capacity and prevent protein misfolding during ER stress.

ER function relies on the maintenance of an appropriate redox balance. Upon increased ER oxidation, a highly conserved cysteine residue, C63, within the ATPase domain of BiP becomes oxidized (8, 9). This alters BiP/Kar2 chaperone activity to limit polypeptide aggregation during suboptimal redox conditions for ER protein folding (9–11). Reductive stress also gives rise to the accumulation of misfolded proteins. However, little is known regarding the mechanisms that exist to regulate BiP activity during reductive stress, for instance during extensive oxidative protein folding in secretory cells such as pancreatic acinar cells (12).

Here, we show that reductive ER stress diminishes N-glycosylation of the Kar2 NEF Sil1, but not of Lhs1. N-glycosylation of Sil1 is entirely Ost3-dependent and requires a functional CxxC thioredoxin motif. N-glycosylation of Lhs1 is partially Ost3-dependent and independent of the CxxC motif. The unglycosylated Sil1 variant (uSil1) retains functionality and is able to substitute for Lhs1 activity more effectively than its cognate N-glycosylated derivative. We propose that the N-glycosylation status of Sil1 directs the NEF to coordinate specific Kar2-regulated activities to suit the needs of the ER when in a state of reductive stress.

Results

N-Linked Glycosylation of the Sil1 Nucleotide Exchange Factor, but Not of Lhs1, Is Diminished by Reductive Stress. Environmental stress can vary the load of unfolded or misfolded proteins in the ER, so BiP/Kar2 and its effectors must be available and appropriately active in times of need to maintain ER homeostasis. In yeast, treatment with the reductant DTT or the N-glycosylation inhibitor tunicamycin (Tm) increases expression of Kar2 and its NEFs Lhs1 and Sil1 (13). This correlates with an increase in both Sil1 and Lhs1 at the protein level (Fig. 1A). Both Lhs1 and Sil1 are N-glycosylated in vegetative cells, and their N-glycosylation is perturbed in cells treated with Tm (Fig. 1A). However, we also observed accumulation of unglycosylated Sil1 (uSil1) in cells treated with DTT (Fig. 1A). Protease protection analysis ruled out the possibility that cytoplasmic pre-Sil1, rather than uSil1, accumulates in DTT-treated cells (Fig. S1A). Also, the predominant form of Sil1 that accumulates upon DTT treatment was not a substrate for the N-glycan–binding lectin Con A (Fig. S1B). In

Significance

Endoplasmic reticulum (ER) function relies on the maintenance of an appropriate redox balance. We observe that ER reductive stress is sensed through the oligosaccharyltransferase subunit Ost3 and acts to inhibit glycosylation of Sil1. Misfolded proteins accumulate within the ER under reductive stress and may sequester Lhs1 and limit the pool of free Lhs1 that can function as a BiP nucleotide exchange factor. Furthermore, unglycosylated Sil1 can compensate for the loss of Lhs1 activity more readily than glycosylated Sil1. Accumulation of unglycosylated Sil1 upon reductive stress may therefore be an adaptive mechanism that allows Sil1 to compensate for loss of Lhs1 NEF activity under these conditions.

Author contributions: C.J.S. and C.J.M. designed research; K.L.P.S., A.L.B., K.M.W., and C.J.M. performed research; K.Y.B.Y. and B.L.S. contributed new reagents/analytic tools; K.L.P.S., R.F.L.S., and C.J.M. analyzed data; and K.L.P.S., R.F.L.S., B.L.S., and C.J.M. wrote the paper.

The authors declare no conflict of interest.

This article is a PNAS Direct Submission.

[1] Present address: Office of Vice-Chancellor, Flinders University, Bedford Park, SA 5043, Australia.

[2] To whom correspondence should be addressed. Email: carl.mousley@curtin.edu.au.

This article contains supporting information online at www.pnas.org/lookup/suppl/doi:10.1073/pnas.1705641114/-/DCSupplemental.

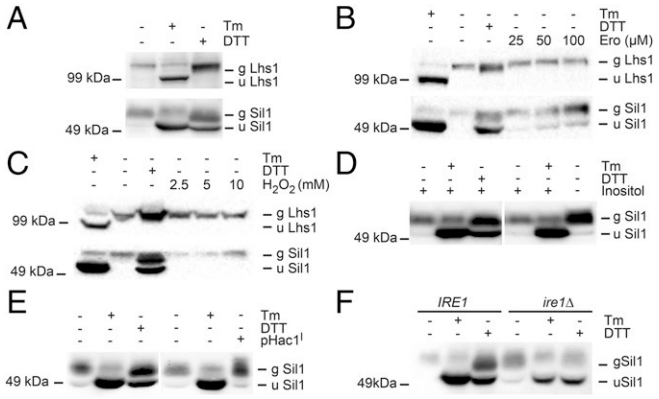

Fig. 1. N-glycosylation of Sil1 is redox sensitive and independent of the UPR. (A) Cell extracts derived from WT cells that were either untreated or treated with 10 μg/mL tunicamycin (Tm) or 10 mM DTT for 2 h were immunoblotted with anti-Lhs1 or anti-Sil1 antibodies. (B) As A but with the inclusion of whole-cell lysates derived from cells treated with the indicated concentrations of erodoxin. (C) As A but with the inclusion of whole-cell lysates derived from cells treated with the indicated concentrations of H_2O_2. (D) Immunoblot analysis of cell extracts derived from WT cells grown in the presence and absence of inositol. For control, cells were untreated or treated with either 10 μg/mL Tm or 10 mM DTT for 2 h. (E) Immunoblot analysis of cell lysates derived from WT cells transformed with either pHac1^{I} or vector control. For control, cells were untreated or treated with either 10 μg/mL Tm or 10 mM DTT for 2 h. (F) Cell extracts derived from WT and ire1Δ cells that were untreated or treated with either 10 μg/mL Tm or 10 mM DTT for 2 h were immunoblotted with anti-Sil1 antibodies.

contrast to Sil1, treatment with DTT did not affect glycosylation of Lhs1 (Fig. 1A). This suggested that uSil1 specifically accumulated upon DTT-induced ER stress.

As a reductant, DTT disrupts the redox balance of the ER. The essential Ero1 protein is a thiol oxidase that maintains the ER redox balance required to promote oxidative protein folding in this organelle (14–16). To confirm that Sil1 N-glycosylation is perturbed as a consequence of general ER reductive stress rather than by DTT alone, we investigated Sil1 glycosylation in cells treated with the Ero1 inhibitor 1-bromo-5-methoxy-2,4-dinitrobenzene (Erodoxin) (17). We observe a similar N-glycosylation profile of Sil1 and Lhs1 in cells treated with Erodoxin to that observed in cells treated with DTT, with accumulation of uSil1 but maintenance of efficiently glycosylated Lhs1 (Fig. 1B). In contrast to treatments that induce reductive stress, treatment of cells with hydrogen peroxide to impose oxidative stress had no effect on glycosylation of Sil1 or Lhs1 (Fig. 1C).

The burden of reductive stress induces the unfolded protein response (UPR). We therefore investigated whether Sil1 N-glycosylation is perturbed in cells in which the UPR is induced by other means. For this, we starved cells of inositol and/or constitutively overexpressed Hac1^{I}. Inositol depletion activates the UPR by disrupting phospholipid homeostasis, while Hac1^{I} is the direct transcriptional activator of the UPR (18, 19). Independent or concurrent inositol depletion or Hac1^{I} overexpression strongly induced the UPR (Fig. S1C). Consistent with UPR induction, Sil1 protein levels were substantially increased in inositol-starved cells (Fig. 1D) or cells expressing Hac1^{I} (Fig. 1E) compared with control cells. However, Sil1 N-glycosylation was not perturbed by either inositol starvation (Fig. 1D) or Hac1^{I} expression (Fig. 1E). We next tested if inhibition of Sil1 N-glycosylation by reductive stress required a functional UPR. uSil1 accumulated in cells treated with DTT with or without the UPR activator Ire1 (ire1Δ) (Fig. 1F). Therefore, Sil1 N-glycosylation is not perturbed by general ER stress, but instead is specifically hypersensitive to the redox potential of the ER lumen.

N-Glycosylation of Sil1 Is Ost3-Dependent. Oligosaccharyltransferase (OST) acts at the confluence of protein modification and protein folding. Yeast OST is comprised of eight protein subunits: Ost1, Ost2, Ost4, Ost5, Stt3, Swp1, Wbp1, and either Ost3 or Ost6 (20–23). Ost3 and Ost6 are paralogues, each with distinct substrate specificities, and the incorporation of either into OST defines two isoforms of the enzyme (24). The lumenal domain of both Ost3 and Ost6 possesses a CxxC thioredoxin-like motif, and their redox-dependent peptide binding activities increase the glycosylation efficiency of distinct sites in protein substrates (24). We sought to determine the dependence of Lhs1 and Sil1 N-glycosylation on OST with either Ost3 or Ost6. N-glycosylation of both Lhs1 and Sil1 was not affected in Ost6deficient cells (ost6Δ) (Fig. 2A). In contrast, Sil1 was essentially completely unglycosylated in ost3Δ cells, indicating that N-glycosylation of Sil1 was predominantly Ost3-dependent (Fig. 2A). ost3Δ cells also accumulated a form of Lhs1, termed g* Lhs1, with a greater electrophoretic mobility than WT but less than that in cells treated with Tm (Fig. 2A). Importantly, no further reduction in glycosylation of Lhs1 was observed in ost3Δ cells treated with DTT. This indicated that while N-glycosylation of at least one site in Lhs1 is Ost3-dependent, only Sil1 N-glycosylation is Ost3-dependent and redox sensitive.

The redox sensitivity of Sil1 N-glycosylation suggested the involvement of the Ost3 CxxC thioredoxin-like motif. To test this, we investigated Sil1 N-glycosylation in ost3Δ cells expressing Ost3 or a redox inactive variant of Ost3 in which both cysteine residues of the CxxC motif were replaced with serines (ost3$^{C\to S}$). N-glycosylation of Sil1 in ost3Δ cells was effectively restored by expression of OST3 but not with ost3$^{C\to S}$ (Fig. 2B). In contrast, N-glycosylation of Lhs1 was restored in cells expressing either OST3 or ost3$^{C\to S}$ (Fig. 2B). This confirms that Sil1 N-glycosylation requires the oxidoreductase activity of the Ost3-containing OST in vivo and that Sil1 N-glycosylation is exquisitely sensitive to the redox status of the ER lumen.

The transient binding of nascent polypeptide to Ost3 and Ost6 proceeds noncovalently or through mixed disulphides and is necessary to inhibit local protein folding to increase N-glycosylation efficiency of substrates (24, 25). The Sil1 protein possesses four cysteine residues (C52, 57, 203, and 373) and six potential Nglycosylation sites (N105, 181, 215, 233, 315, and 333). Sil1 Nglycosylation was not affected by substitution of either C52, C57, C203, or C373 with either alanine or serine (Fig. 2C). This was surprising given that Sil1 N-glycosylation is perturbed by reductive stress. Furthermore, the accumulation of uSil1 observed following

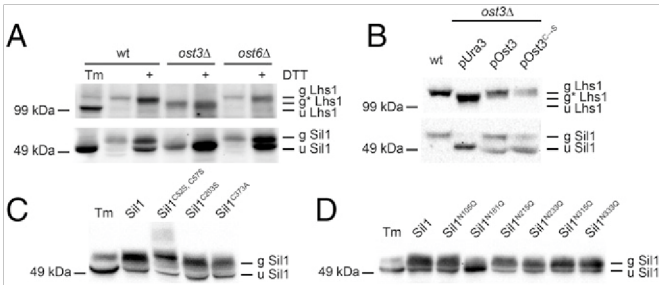

Fig. 2. N-glycosylation of Sil1 is Ost3-dependent. (A) Immunoblot analysis of cell extracts derived from either WT, ost3Δ, or ost6Δ cells that were untreated or treated with either 10 μg/mL Tm or 5 mM DTT for 2 h. (B) Immunoblot analysis of cell lysates derived from either WT or ost3Δ cells transformed with either vector alone, YCp OST3, or YCp ost3$^{C\to S}$. (C) Immunoblot analysis of cell lysates derived from sil1Δ cells expressing either SIL1, SIL1$^{C52S, C57S}$, SIL1^{C203S}, or SIL1^{C373S}. For control, cells were treated with 10 μg/mL Tm. (D) Immunoblot analysis of cell lysates derived from sil1Δ cells expressing either SIL1, SIL1N105Q, SIL1N181Q, SIL1N215Q, SILN233Q, SIL1N315Q, or SIL1^{N333Q}. For control, cells were treated with 10 μg/mL Tm.

DTT treatment was not diminished by substitution of either C52, C57, C203, or C373 with either alanine or serine (Fig. S2A). Therefore, the Ost3-dependence of Sil1 N-glycosylation is not bypassed by elimination of a cysteine in Sil1. Glutamine scanning mutagenesis of each potential sequon identified that Sil1 Nglycosylation was only disrupted following substitution of N181 (Fig. 2D). Previous studies have shown that disruption of the Ost3 thioredoxin motif only affects the N-glycosylation of a small subset of substrates (24). That no cysteine residue within Sil1 is necessary for N-glycosylation rules out the possibility that reductive stress ablates formation of a mixed disulphide between Ost3 and Sil1. Rather, our data best supports a model in which the substrate-binding domain of Ost3 undergoes a sufficient redoxdependent structural change so that the Sil1 nascent polypeptide is no longer recognized as being a substrate, as has been reported in vitro for model Ost3/Ost6 substrates (24, 25).

Upon further inspection, we realized that Sil1$^{C52S\ C57S}$ had undergone a series of posttranslational modification giving rise to protein laddering (Fig. S2B). Such "laddering" is a hallmark of protein polyubiquitination and occurs when ER resident proteins are targeted for ER-associated degradation (ERAD). To investigate whether Sil1$^{C52S\ C57S}$ is turned over, we investigated the stability of Sil1$^{C52S\ C57S}$ and WT Sil1 in cells by cycloheximide (chx) chase analysis. Sil1 protein levels remained constant throughout the 90-min chx chase (Fig. 3 A and B). In contrast, the Sil1$^{C52S\ C57S}$ protein was more labile as levels diminished throughout the chx chase (Fig. 3 A and B). We next investigated whether Sil1$^{C52S\ C57S}$ is degraded via ERAD. DOA10, and HRD1/DER3 encode for the two major ER resident E3 ligases Doa10 and Hrd1 in yeast (26–28). Deletion of DOA10 (doa10Δ) led to an almost complete stabilization of the Sil1$^{C52S\ C57S}$ protein (Fig. 3 C and D). Furthermore, expression of SIL1$^{C52S\ C57S}$ severely diminished the growth of doa10Δ yeast (Fig. 3E). In contrast, deletion of HRD1 (hrd1Δ) had no detectable effect on Sil1$^{C52S\ C57S}$ protein stability (Fig. 3 C and D), and expression of SIL1$^{C52S\ C57S}$ did not affect hrd1Δ cellular growth (Fig. 3E). Deletion of the HRD3 (hrd3Δ) structural gene, which encodes for the Hrd3 component of the HRD complex, also had no detectable effect on Sil1$^{C52S\ C57S}$ protein stability (Fig. 3 C and D). A role for Doa10 in the degradation of ERAD-L substrates has not been described previously.

However, Doa10 has been shown to be required for the degradation of the ERAD-M substrate Sbh2 (29). Given that Sil1$^{C52S\ C57S}$ ERAD is Doa10-dependent, we speculate that Sil1 can associate with the lumenal face of the ER membrane, a hypothesis supported by a previous study showing that the Yarrowia lipolytica Sil1 ortholog, Sls1, can be coimmunoprecipitated with Sec61 (30).

Unglycosylated Sil1 Is Functional. Individual deletions of SIL1 (sil1Δ) or LHS1 (lhs1Δ) in yeast are viable (31–33), while the double deletion (sil1Δ lhs1Δ) is lethal, indicating that Kar2dependent nucleotide exchange is an essential cellular activity (33). We tested if expression of the unglycosylatable variant SIL1^{N181Q} could sustain cell viability in sil1Δ lhs1Δ cells. YCp SIL1 and YCp

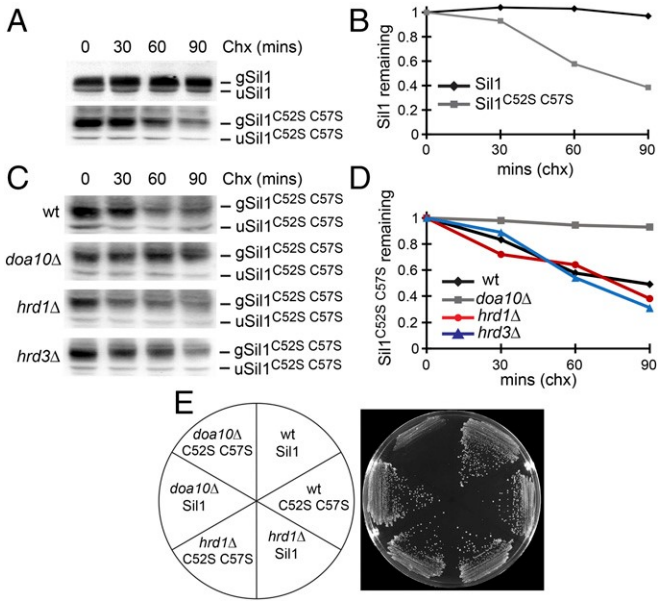

Fig. 3. Sil1$^{C52S,\ C57S}$ is a Doa10 ERAD substrate. (A) Exponentially growing sil1Δ cells expressing either SIL1 or SIL1$^{C52S,\ C57S}$ were pretreated for 20 min with 0.25 mg/mL chx. Afterward cells were removed at the indicated times and immunoblot analysis of cell lysates performed. (B) Densitometric analysis of A using Image Lab software (Bio-Rad). (C) Exponentially growing WT, doa10Δ, hrd1Δ, and hrd3Δ cells expressing SIL1$^{C52S,\ C57S}$ were pretreated for 20 min with 0.25 mg/mL chx. Afterward, cells were removed at the indicated times and immunoblot analysis of cell lysates performed. (D) Densitometric analysis of C using Image Lab software (Bio-Rad). (E) WT, doa10Δ, and hrd1Δ yeast harboring either YEp SIL1 or YEp SIL1$^{C52S,\ C57S}$ were streaked onto –Leu selective medium and incubated at 30 °C for 2 d.

kanMX4 [pJT40 (LHS1, ADE3, URA3)]} and tested the ability of these strains to grow after loss of pJT40 on 5-FOA medium. Again, we observed that overexpression of SIL1 partially suppresses the severe growth defect of ire1Δ lhs1Δ double mutant cells. Surprisingly, overexpression of SIL1^{N181Q} allowed a more impressive suppression of this growth defect (Fig. S3A). This suggested that under these conditions, uSil1 may compensate for the loss of Lhs1 activity more readily than gSil1. Next, we tested if only modest overexpression of unglycosylatable SIL1^{N181Q} was sufficient to rescue the growth defect of ire1Δ lhs1Δ cells. This was indeed the case, with low copy expression of SIL1^{N181Q} from centrimeric plasmid YCp sufficient to promote growth of JTY62 yeast after induced loss of plasmid-borne LHS1 expression on 5-FOA medium (Fig. S3B). Expression of SIL1 in the same system only allowed poor growth (Fig. S3B). Given the extent to which low copy expression of SIL1^{N181Q} was able to promote growth of JTY62 yeast after induced loss of plasmidborne LHS1 expression on 5-FOA medium, we tested if expression of SIL1^{N181Q} as the only source of SIL1 was sufficient to rescue the growth defect of ire1Δ lhs1Δ cells. A SIL1^{N181Q} integration cassette containing the LEU2 selectable marker was integrated into the SIL1 genetic locus by homologous recombination, and successful substitution was confirmed by sequencing and immunoblot (Fig. S3 C and D). Genomic substitution of SIL1 with SIL1^{N181Q}::LEU2 was sufficient to promote growth of JTY62 yeast after induced loss of plasmid-borne LHS1 expression on 5-FOA medium (Fig. 4B). Together, this shows that unglycosylated Sil1 can compensate for the loss of Lhs1 activity more readily than glycosylated Sil1.

The accumulation of unglycosylated Sil1 upon reductive stress may be necessary to protect cells from this deleterious stress. To test this, we investigated whether low copy expression of SIL1^{N181Q} would reduce the hypersensitivity of ire1Δ cellular growth to DTT. The rationale for this is that in ire1Δ cells, the

SIL1^{N181Q} were transformed into JTY65 {sil1Δ::kanMX4 lhs1Δ:: kanMX4 [pRC43 (LHS1, URA3)]} (33) and tested for the ability of these strains to grow after loss of pRC43 on 5-fluoroorotic acid (5-FOA) medium. Strains harboring either SIL1 or SIL1^{N181Q} produced viable colonies, whereas cells transformed with vector alone could not (Fig. 4A). This confirmed that unglycosylated Sil1 was functional.

Overexpression of SIL1 suppresses the severe growth defect of ire1Δ lhs1Δ double mutant cells (33). We therefore tested whether overexpression of the SIL1^{N181Q} N-glycosylation mutant was able to suppress this growth defect. We transformed YEp SIL1 and YEp SIL1^{N181Q} into JTY62 {ire1Δ::kanMX4 lhs1Δ::

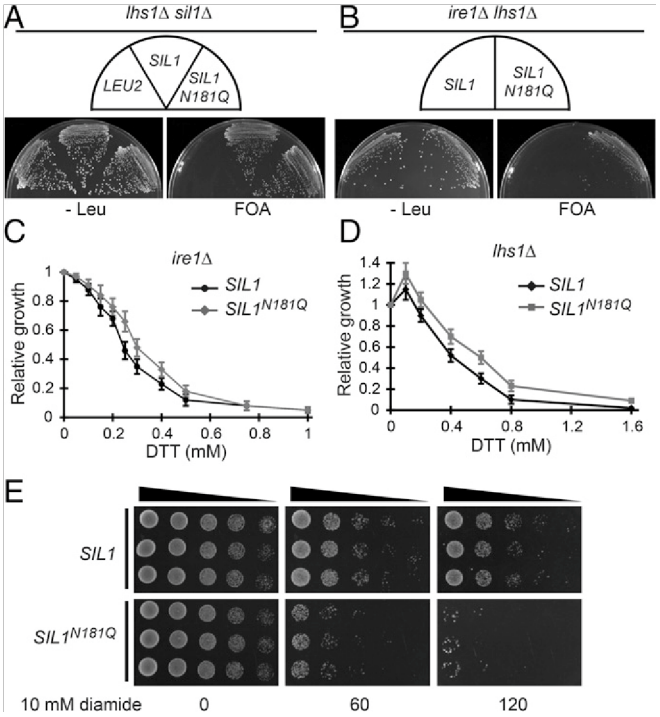

Fig. 4. uSil1 functionally compensates lhs1Δ better than gSil1. (A) JTY65 yeast harboring either YCp LEU2, YCp SIL1, or YCp SIL1^{N181Q} were streaked onto –Leu selective medium and medium containing FOA and incubated at 30 °C for 2 d. (B) JTY62 yeast in which the SIL1 genetic locus has been substituted with a SIL1^{N181Q}::LEU2 integration cassette and JTY62 parental cells harboring YCp LEU2 were streaked onto –Leu selective medium and medium containing FOA and incubated at 30 °C for 2 d. (C) ire1Δ cells harboring either YCp SIL1 or YCp SIL1^{N181Q} were inoculated at 0.01 OD_{600} and grown until control had reached 1 OD_{600}. The relative growth with DTT (0.05– 1 mM) relative to "no-DTT" control (ddH_2O) are plotted as function of DTT concentration (x axis). Values show mean ± SEM of normalized growth for each DTT concentration from three independent experiments. (D) SIL1 lhs1Δ and SIL1^{N181Q} lhs1Δ cells were inoculated at 0.01 OD_{600} and grown until control had reached 1 OD_{600}. The growth with DTT (0.1–1.6 mM) relative to "no-DTT" control (ddH_2O) are plotted as function of DTT concentration (x axis). Values show mean ± SEM of normalized growth for each DTT concentration from three independent experiments. (E) WT cells harboring either YEp SIL1 or YEp SIL1^{N181Q} were grown to midlog phase. One OD_{600} of cells were incubated with and without 10 mM diamide for 60 and 120 min. Afterward, cells were isolated and washed twice with 5 mL ddH_2O and then recovered in YPD for 8 h. Cells were spotted in a 10-fold dilution series and grown at 30 °C for 2 d.

UPR cannot be induced, and cellular growth is sensitive to concentrations of DTT that negligibly affect Sil1 N-glycosylation. This is important as SIL1 expression is highly elevated upon UPR induction and would likely mask any beneficial effects of SIL1^{N181Q} expression. The relative growth of ire1Δ cells transformed with either YCp SIL1 or YCp SIL1^{N181Q} was determined in growth medium containing increasing concentrations of DTT (0.05–1 mM). We observed YCp SIL1^{N181Q} to bestow modest suppression of ire1Δ DTT hypersensitivity compared with YCp SIL1 (Fig. 4C). We find the growth fitness of ire1Δ cells that express SIL1^{N181Q} to be ≅1.5× greater than those expressing SIL1 when exposed to 0.25–0.5 mM DTT (Fig. 4C).

lhs1Δ cellular growth is also sensitive to concentrations of DTT that negligibly affect Sil1 N-glycosylation. Given that uSil1 can compensate for the loss of Lhs1 activity more readily than glycosylated Sil1, we were interested to determine whether expression of SIL1^{N181Q} would also reduce the hypersensitivity of lhs1Δ cellular growth to DTT. We observed SIL1^{N181Q} expression to

partially suppress lhs11Δ DTT hypersensitivity as lhs1Δ SIL1^{N181Q} cell growth was greater than lhs1Δ SIL1 cells at all concentrations of DTT (0.1–1.6 mM) (Fig. 4D).

Cells under reductive stress may benefit from uSil accumulation simply because it is more stable than gSil1. We tested this by chx chase analysis in cells that had been acutely challenged with DTT for 1 h. We observed a steady decline in gSil1 protein levels, with ⍰70% gSil1 remaining after 90-min chase (Fig. S4 A and B). However, the decline in uSil1 protein levels over this time course was even more pronounced, with ⍰40% uSil1 remaining after 90-min chase (Fig. S4 A and B). uSil1 is therefore more labile than gSil1 under these conditions. As such, the increased ability of uSil1 to rescue the growth defect of ire1Δ lhs1Δ cells and to improve the fitness of ire1Δ grown in the presence of DTT is not due to its increased stability.

It has previously been shown that a sil1Δ strain exhibits improved survival in the presence of the cysteine oxidant diamide due in part due to the loss of Sil1 NEF activity allowing BiP to reside longer in an ADP/peptide-bound state, thus enhancing BiP's holdase activity (8, 9). Given this, we hypothesized that overexpression of uSil1 would render cells hypersensitive to acute cysteine oxidation evoked by exposure to diamide. To test this, cells overexpressing either SIL1 or SIL1^{N181Q} were either mock treated or exposed to 10 mM diamide for either 1 or 2 h and cell viability was determined following an 8-h recovery in rich media. Indeed, SIL1^{N181Q} overexpressing cells were more sensitive to the deleterious effects of diamide, as after 1- or 2-h exposure to 10 mM diamide, ⍰100× or 1,000× fewer SIL1^{N181Q} overexpressing cells were recovered relative to cells overexpressing SIL1 (Fig. 4E).

Discussion

N-Glycosylation Enables Sil1 Functional Specialization. N-glycosylation and protein folding are intimately linked in the ER. Here, we show that ER reductive stress sensed through Ost3 acts to inhibit glycosylation of Sil1, which increases Sil1's activity as a suppressor of loss of Lhs1. Efficient N-glycosylation under nonstressed conditions is therefore a negative regulator of some aspects of Sil1 function. Genetic or chemical inhibition of N-glycosylation results in widespread underglycosylation of diverse proteins, generally resulting in loss of protein folding efficiency, stability, and function. In contrast, loss of glycosylation of Sil1 results in a gain of function whereby uSil1 is a better Lhs1 substitute than its cognate glycosylated derivative.

It is not obvious how loss of N-glycosylation would alter Sil1 function. The crystal structure of Sil1 shows that N181 is located on the opposite face of Sil1 to the surface that mediates interaction with Kar2 (34). Lack of glycosylation would therefore be unlikely to directly impact interactions between Sil1 and Kar2. However, loss of glycosylation could alter Sil1 structure, flexibility, or dynamics in ways that alter this interaction or that regulate Sil1's NEF activity. It is also possible that loss of glycosylation at N181 specifically impacts interactions between Sil1 and other proteins.

Although Sil1 and Lhs1 are functionally related, they are not entirely interchangeable, as some mutant phenotypes remain upon cross-complementation even with high levels of overexpression. Genetic interaction networks are distinct for lhs1Δ and sil1Δ cells (17, 35–45), further suggesting Lhs1 and Sil1 have some specialized function(s). We consider the N-glycosylation of Sil1 to be an important factor that enables regulation of such functional specialization. For example, Lhs1 can also act as an ATP-independent holdase, binding to misfolded proteins to prevent them from aggregating (46–48). The accumulation of misfolded proteins in the ER under reductive stress may sequester Lhs1 and limit the pool of free Lhs1 that can function as a NEF. Given that uSil1 is a better substitute for Lhs1, accumulation of unglycosylated Sil1 upon reductive stress may allow Sil1 to either compensate for loss of Lhs1 NEF activity or to bolster NEF activity in ER functions coordinated by Lhs1 under these conditions.

Sil1, a Redox-Dependent ERAD Substrate? It is the accepted model that ERAD-L substrates are exclusively recognized by the Hrd1 complex, and ERAD-C substrates by the Doa10 complex (29, 49–53). As Sil1 does not possess a transmembrane domain, we predicted Sil1$^{C52S\ C57S}$ would be a Hrd1-dependent ERAD-L substrate. However, the supposition that ERAD-L and ERAD-C substrates are exclusively recognized by the Hrd1 complex and Doa10 complex, respectively, is derived from analysis of a limited number of ERAD substrates. Our observation that ERAD of Sil1$^{C52S\ C57S}$ is Doa10-dependent suggests that this model is incomplete, and there may well be more unidentified Doa10dependent ER lumenal substrates. Another possibility is that membrane association of lumenal proteins can drive Doa10dependent ERAD. It has recently been shown that Doa10 is required for degradation of the ERAD-M substrate Sbh2 (29). Sbh2 is the first characterized Doa10 substrate for which its TM domain and short ER-lumenal domain can target the protein for Doa10-dependent degradation (29). It is possible that Sil1 associates predominantly with the lumenal face of the ER membrane, and it is this association that enables Sil1$^{C52S\ C57S}$ to be a Doa10 ERAD substrate. We attempted to test if N-glycosylation is necessary for Doa10-dependent ERAD of Sil1$^{C52S\ C57S}$, but the pool of uSil1$^{C52S\ C57S}$ that accumulates upon tunicamycin treatment undergoes rapid additional posttranslational modification, making analysis impossible (Fig. S2C). However, uSil1 turnover is faster than gSil1 in DTT-treated cells, showing that N-glycosylation is not required for Sil1 turnover.

Residues C52 and C57 of Sil1 have recently been shown to form a redox-active cysteine pair that facilitates the reduction of C63 in the ATPase domain of Kar2 (8). Oxidation of C63 impairs Kar2's ATPase activity, altering its chaperone function to cope with the suboptimal folding conditions that arise during oxidative stress (8–11). Sil1 can then reduce the oxidized cysteine residue in the BiP ATPase domain to restore ATPase activity and chaperone function once the levels of oxidative stress in the ER have subsided. Inappropriate reduction of Kar2 C63 by Sil1 under oxidative stress would therefore be undesirable. Our observation that Sil1$^{C52S,\ C57S}$ is an ERAD substrate suggests that Sil1 degradation is redox-dependent, with the Sil1$^{C52S,\ C57S}$ variant simulating the Sil1 N terminus in its fully reduced state. In addition, we frequently observe Sil1 turnover to be more pronounced in DTTtreated cells relative to control. The redox-dependent degradation of Sil1 may therefore appropriately limit the amount of Sil1 that has the potential to reduce C63 in the ATPase domain of Kar2/ BiP, such as when Kar2 is required to function as a holdase.

Concluding Remarks

With their ER-lumenal thioredoxin-like domains, the Ost3 and Ost6 subunits of OST integrate protein modification and protein folding of diverse substrates across the cellular glycoproteome. Our discovery that the redox status of Ost3 controls the Nglycosylation of the ER lumenal Sil1 nucleotide exchange factor also places this OST subunit at the heart of ER protein folding homeostasis. Based on our data, we propose a model in which ER reductive stress reduces the Ost3 CxxC motif, inhibiting N-glycosylation of Sil1 to modulate its activity such that Kar2 function can be tailored to suit the needs of the ER. Furthermore, the apparent hypersensitivity of Sil1 N-glycosylation to reductive stress may provide a simple assay to monitor the redox environment of the ER.

Materials and Methods

Strain and Growth Conditions. Saccharomyces cerevisiae strains are listed in Table S1, and plasmids are listed in Table S2. Yeast strains were grown routinely at 30 °C in YP medium (2% peptone, 1% yeast extract) containing 2% glucose (YPD) or in minimal medium (0.67% yeast nitrogen base; YNB) with 2% glucose plus appropriate supplements for selective growth. All media were from Difco Laboratories. Yeast transformations and 5-FOA counterselection of URA3 cells were carried out as described previously (54). Cell density in liquid culture was monitored by A_{600} using an Eppendorf Biophotometer.

Immunoblotting. Whole yeast extracts were prepared byglass bead lysis in SDS sample buffer from cultures grown to mid-log phase, resolved by SDS/PAGE, transferred to a nitrocellulose membrane (Bio-Rad), and probed with either αLhs1, αKar2, or αSil1 antiserum whose production has been described previously (33). These antibodies were used at the dilutions indicated in parentheses for immunoblotting: Lhs1 (sheep, 1:10000), Kar2 (sheep, 1:10000), Sil1 (sheep, 1:5000) peroxidase-conjugated goat anti-sheep IgG (1:10000; Sigma). Immunoreactive species were visualized using Clarity (Bio-Rad), and protein degradation rates were determined using a ChemiDoc imaging system (Bio-Rad) and Image Lab software (Bio-Rad).

Chx Chase Analyses. Chx chase analyses were performed according to Habeck et al. (29). Briefly, 0.25 mg/mL chx was added to log-phase yeast cultures, and cell aliquots were removed at the indicated times after addition. Cells were harvested by centrifugation and resuspended in ice cold 10 mM NaN_3. After preparation of lysates, proteins were separated by SDS/PAGE and immunodetection was performed as described above.

ACKNOWLEDGMENTS. This work was supported by a Curtin University Faculty of Health Sciences start-up fund (to C.J.M.).

1. Brodsky JL, et al. (1999) The requirement for molecular chaperones during endoplasmic reticulum-associated protein degradation demonstrates that protein export and import are mechanistically distinct. J Biol Chem 274:3453–3460.
2. Corsi AK, Schekman R (1997) The lumenal domain of Sec63p stimulates the ATPaseactivity of BiP and mediates BiP recruitment to the translocon in Saccharomyces cerevisiae. J Cell Biol 137:1483–1493.
3. Matlack KE, Misselwitz B, Plath K, Rapoport TA (1999) BiP acts as a molecular ratchetduring posttranslational transport of prepro-alpha factor across the ER membrane. Cell 97:553–564.
4. Nishikawa SI, Fewell SW, Kato Y, Brodsky JL, Endo T (2001) Molecular chaperones inthe yeast endoplasmic reticulum maintain the solubility of proteins for retrotranslocation and degradation. J Cell Biol 153:1061–1070.

5. Simons JF, Ferro-Novick S, Rose MD, Helenius A (1995) BiP/Kar2p serves as a molecularchaperone during carboxypeptidase Y folding in yeast. J Cell Biol 130:41–49.
6. Liberek K, Marszalek J, Ang D, Georgopoulos C, Zylicz M (1991) Escherichia coli DnaJand GrpE heat shock proteins jointly stimulate ATPase activity of DnaK. Proc Natl Acad Sci USA 88:2874–2878.
7. Szabo A, et al. (1994) The ATP hydrolysis-dependent reaction cycle of the Escherichiacoli Hsp70 system DnaK, DnaJ, and GrpE. Proc Natl Acad Sci USA 91:10345–10349.
8. Siegenthaler KD, Pareja KA, Wang J, Sevier CS (2017) An unexpected role for the yeastnucleotide exchange factor Sil1 as a reductant acting on the molecular chaperone BiP. Elife 6:e24141.
9. Wang J, Pareja KA, Kaiser CA, Sevier CS (2014) Redox signaling via the molecularchaperone BiP protects cells against endoplasmic reticulum-derived oxidative stress. Elife 3:e03496.
10. Wang J, Sevier CS (2016) Formation and reversibility of BiP protein cysteine oxidationfacilitate cell survival during and post oxidative stress. J Biol Chem 291:7541–7557.
11. Xu M, Marsh HM, Sevier CS (2016) A conserved cysteine within the ATPase domain ofthe endoplasmic reticulum chaperone BiP is necessary for a complete complement of BiP activities. J Mol Biol 428:4168–4184.
12. Maity S, et al. (2016) Oxidative homeostasis regulates the response to reductive endoplasmic reticulum stress through translation control. Cell Rep 16:851–865.
13. Travers KJ, et al. (2000) Functional and genomic analyses reveal an essential coordination between the unfolded protein response and ER-associated degradation. Cell 101:249–258.
14. Frand AR, Kaiser CA (1998) The ERO1 gene of yeast is required for oxidation ofprotein dithiols in the endoplasmic reticulum. Mol Cell 1:161–170.
15. Pollard MG, Travers KJ, Weissman JS (1998) Ero1p: A novel and ubiquitous proteinwith an essential role in oxidative protein folding in the endoplasmic reticulum. Mol Cell 1:171–182.
16. Sevier CS, et al. (2007) Modulation of cellular disulfide-bond formation and the ERredox environment by feedback regulation of Ero1. Cell 129:333–344.
17. Costanzo M, et al. (2010) The genetic landscape of a cell. Science 327:425–431.
18. Gaspar ML, Aregullin MA, Jesch SA, Henry SA (2006) Inositol induces a profound alteration in the pattern and rate of synthesis and turnover of membrane lipids in Saccharomyces cerevisiae. J Biol Chem 281:22773–22785.
19. Kelley MJ, Bailis AM, Henry SA, Carman GM (1988) Regulation of phospholipid biosynthesis in Saccharomyces cerevisiae by inositol. Inositol is an inhibitor of phosphatidylserine synthase activity. J Biol Chem 263:18078–18085.
20. Karaoglu D, Kelleher DJ, Gilmore R (1995) Functional characterization of Ost3p. Lossof the 34-kD subunit of the Saccharomyces cerevisiae oligosaccharyltransferase results in biased :evens et al. underglycosylation of acceptor substrates. J Cell Biol 130:567–577.
21. Kelleher DJ, Gilmore R (2006) An evolving view of the eukaryotic oligosaccharyltransferase. Glycobiology 16:47R–62R.
22. Schwarz M, Knauer R, Lehle L (2005) Yeast oligosaccharyltransferase consists of twofunctionally distinct sub-complexes, specified by either the Ost3p or Ost6p subunit. FEBS Lett 579:6564–6568.
23. Spirig U, Bodmer D, Wacker M, Burda P, Aebi M (2005) The 3.4-kDa Ost4 protein isrequired for the assembly of two distinct oligosaccharyltransferase complexes in yeast. Glycobiology 15:1396–1406.
24. Schulz BL, et al. (2009) Oxidoreductase activity of oligosaccharyltransferase subunitsOst3p and Ost6p defines site-specific glycosylation efficiency. Proc Natl Acad Sci USA 106:11061–11066.
25. Jamaluddin MF, Bailey UM, Schulz BL (2014) Oligosaccharyltransferase subunits bindpolypeptide substrate to locally enhance N-glycosylation. Mol Cell Proteomics 13: 3286–3293.
26. Bordallo J, Plemper RK, Finger A, Wolf DH (1998) Der3p/Hrd1p is required for endoplasmic reticulum-associated degradation of misfolded lumenal and integral membrane proteins. Mol Biol Cell 9:209–222.
27. Hampton RY, Gardner RG, Rine J (1996) Role of 26S proteasome and HRD genes in thedegradation of 3-hydroxy-3-methylglutaryl-CoA reductase, an integral endoplasmic reticulum membrane protein. Mol Biol Cell 7:2029–2044.
28. Swanson R, Locher M, Hochstrasser M (2001) A conserved ubiquitin ligase of thenuclear envelope/endoplasmic reticulum that functions in both ER-associated and Matalpha2 repressor degradation. Genes Dev 15:2660–2674.
29. Habeck G, Ebner FA, Shimada-Kreft H, Kreft SG (2015) The yeast ERAD-C ubiquitinligase Doa10 recognizes an intramembrane degron. J Cell Biol 209:261–273.
30. Boisramé A, Beckerich JM, Gaillardin C (1996) Sls1p, an endoplasmic reticulum component, is involved in the protein translocation process in the yeast Yarrowia lipolytica. J Biol Chem 271:11668–11675.
31. Craven RA, Egerton M, Stirling CJ (1996) A novel Hsp70 of the yeast ER lumen is required for the efficient translocation of a number of protein precursors. EMBO J 15: 2640–2650.
32. Steel GJ, Fullerton DM, Tyson JR, Stirling CJ (2004) Coordinated activation ofHsp70 chaperones. Science 303:98–101.
33. Tyson JR, Stirling CJ (2000) LHS1 and SIL1 provide a lumenal function that is essentialfor protein translocation into the endoplasmic reticulum. EMBO J 19:6440–6452.
34. Yan M, Li J, Sha B (2011) Structural analysis of the Sil1-Bip complex reveals themechanism for Sil1 to function as a nucleotide-exchange factor. Biochem J 438: 447–455.
35. Sharifpoor S, et al. (2012) Functional wiring of the yeast kinome revealed by globalanalysis of genetic network motifs. Genome Res 22:791–801.
36. Jonikas MC, et al. (2009) Comprehensive characterization of genes required forprotein folding in the endoplasmic reticulum. Science 323:1693–1697.
37. Schuldiner M, et al. (2005) Exploration of the function and organization of the yeastearly secretory pathway through an epistatic miniarray profile. Cell 123:507–519.
38. Bircham PW, et al. (2011) Secretory pathway genes assessed by high-throughputmicroscopy and synthetic genetic array analysis. Mol Biosyst 7:2589–2598.
39. Hoppins S, et al. (2011) A mitochondrial-focused genetic interaction map reveals ascaffold-like complex required for inner membrane organization in mitochondria. J Cell Biol 195:323–340.
40. Krogan NJ, et al. (2006) Global landscape of protein complexes in the yeast Saccharomyces cerevisiae. Nature 440:637–643.
41. Wang Y, et al. (2012) Coiled-coil networking shapes cell molecular machinery. Mol Biol Cell 23:3911–3922.
42. Ho Y, et al. (2002) Systematic identification of protein complexes in Saccharomycescerevisiae by mass spectrometry. Nature 415:180–183.
43. McClellan AJ, et al. (2007) Diverse cellular functions of the Hsp90 molecular chaperone uncovered using systems approaches. Cell 131:121–135.
44. Batisse J, Batisse C, Budd A, Böttcher B, Hurt E (2009) Purification of nuclear poly(A)binding protein Nab2 reveals association with the yeast transcriptome and a messenger ribonucleoprotein core structure. J Biol Chem 284:34911–34917.
45. Tarassov K, et al. (2008) An in vivo map of the yeast protein interactome. Science 320: 1465–1470.
46. Behnke J, Hendershot LM (2014) The large Hsp70 Grp170 binds to unfolded proteinsubstrates in vivo with a regulation distinct from conventional Hsp70s. J Biol Chem 289:2899–2907.
47. Buck TM, et al. (2013) The Lhs1/GRP170 chaperones facilitate the endoplasmicreticulum-associated degradation of the epithelial sodium channel. J Biol Chem 288: 18366–18380.
48. de Keyzer J, Steel GJ, Hale SJ, Humphries D, Stirling CJ (2009) Nucleotide binding byLhs1p is essential for its nucleotide exchange activity and for function in vivo. J Biol Chem 284:31564–31571.
49. Zattas D, Hochstrasser M (2015) Ubiquitin-dependent protein degradation at theyeast endoplasmic reticulum and nuclear envelope. Crit Rev Biochem Mol Biol 50: 1–17.
50. Ruggiano A, Foresti O, Carvalho P (2014) Quality control: ER-associated degradation: Protein quality control and beyond. J Cell Biol 204:869–879.
51. Rubenstein EM, Kreft SG, Greenblatt W, Swanson R, Hochstrasser M (2012) Aberrantsubstrate engagement of the ER translocon triggers degradation by the Hrd1 ubiquitin ligase. J Cell Biol 197:761–773.
52. Brodsky JL, Skach WR (2011) Protein folding and quality control in the endoplasmicreticulum: Recent lessons from yeast and mammalian cell systems. Curr Opin Cell Biol 23:464–475.
53. Hirsch C, Gauss R, Horn SC, Neuber O, Sommer T (2009) The ubiquitylation machineryof the endoplasmic reticulum. Nature 458:453–460.
54. Wilkinson BM, Tyson JR, Reid PJ, Stirling CJ (2000) Distinct domains within yeastSec61p involved in post-translational translocation and protein dislocation. J Biol Chem 275:521–529.
55. Rothblatt JA, Meyer DI (1986) Secretion in yeast: Reconstitution of the translocationand glycosylation of alpha-factor and invertase in a homologous cell-free system. Cell 44:619–628.

56. Winzeler EA, et al. (1999) Functional characterization of the S. cerevisiae genome bygene deletion and parallel analysis. Science 285:901–906.
57. Chapman RE, Walter P (1997) Translational attenuation mediated by an mRNA intron. Curr Biol 7:850–859.